

**AN INVESTIGATION OF COPPER RECOVERY FROM A
SULPHIDE OXIDE ORE WITH A MIXED COLLECTOR SYSTEM**

by

Morgan Sarah Davidson

A thesis submitted to the Department of Mining Engineering
in conformity with the requirements for
the degree of Master of Science in Engineering

Queen's University

Kingston, Ontario, Canada

(August, 2009)

Copyright ©Morgan Sarah Davidson, 2009

For Daddy.

Abstract

Current copper deposits contain significant amounts of secondary non-sulphide minerals and newly discovered deposits are increasingly complex. As a result, research into the improvement of sulphide-oxide copper ores processing through the use of mixed collector systems has surged. The flotation of a natural porphyry copper ore with bornite and malachite was investigated via fundamental work with pure minerals and a bench-scale testing regime. The processing of the test ore was problematic due to a mineral assemblage that caused prevalent slime generation.

Fundamental adsorption, micro-flotation and Eh-pH tests were conducted on pure minerals to investigate mineral-collector behaviours. PAX and hydroxamate form multiple collector layers on malachite and bornite, with malachite and hydroxamate exhibiting the highest adsorption density. The effective pH range of the collectors was pH 8-10 where the collector species, according to equilibrium species distribution diagrams, were Cu(HXM)₂ (aq) and CuEX (s) for hydroxamate and xanthate respectively.

A Box-Behnken response surface design was used to determine collector dosages that provide an optimum flotation response for the natural ore. The collectors were: potassium amyl xanthate (PAX), Cytec Promoter 6494 hydroxamate and DETA. The copper recovery, malachite recovery, minor copper recovery and copper grade responses were optimized using JMP statistical software. Indicators of model inadequacies were noted but since the models predicted sensible solutions, inaccurate test ratios and un-modeled effects were hypothesized to be the source of the inadequacies. The model predicted 98 % copper recovery using 202.7g/t PAX, 674.99 g/t hydroxamate and 61.9 g/t DETA. The copper grade model predicted an the overall copper grade of 19% using with 0 g/t PAX, 167 g/t hydroxamate and 101 g/t DETA .

Acknowledgements

I would like to thank my supervisor, Dr. Sadan Kelebek, for his help throughout my time as a graduate student. Both as my professor and my supervisor, his knowledge, expertise and hours spent during this study were greatly appreciated.

Thank you to Coban Resources for generously providing the test ore used in this thesis.

I would like to say a big thank you to Maritza Bailey. She allowed me to draw on her experience to develop solutions to problems both in and out of the laboratory. Tina, Kate and Wanda in the office also deserve a special thank you. Their guidance and gossip were critical to keeping a good attitude while working through the stress of a tight deadline. I am grateful to Peter Auchincloss and Ayman. Without them, this thesis would have remained in softcopy format.

My friends Aynsley, Allison, Jesse, Sarah, Lauren and Adrienne supported me through all parts of my undergraduate and graduate education. Alisa, Natalie, Tom, Mallory, Bryce and everyone else at Clark Hall Pub were a source of professional and non-professional direction. Ryan, Mark, Mike, Tina, Kristen, Erin and many others that have been here through my post graduate work were fellow commiserates, and celebrators of the joys and struggles of being a Master's student. I could count on all these friends whenever I needed them, for this, I offer them a great many thanks and a debt of gratitude.

I must thank my Mother, and acknowledge the direction she has given me from the beginning until now. She has a unique ability to put things into perspective; though, it can be as frustrating as it is fulfilling.

Finally, thank you Mikhail. For everything else.

Table of Contents

Abstract.....	iii
Acknowledgements.....	iv
List of Figures	vii
List of Tables	xii
Chapter 1 Introduction	1
Chapter 2 Literature Review	6
2.1 Geology.....	9
2.2 Sulphidization	12
2.2.1 Kinetics	16
2.2.2 pH.....	17
2.2.3 Dosage.....	19
2.2.4 Oxidation Reactions.....	20
2.3 Chelating Agents.....	21
2.3.1 pH.....	25
2.3.2 Substituents.....	26
2.3.3 Octyl Hydoxamate	27
2.4 Summary	33
Chapter 3 Materials and Methods	34
3.1 Adsorption.....	34
3.2 Micro-flotation and Eh-pH.....	36
3.3 Bench Scale Flotation	38
4.3.1 Exploratory Work	42
4.3.2 Preliminary Testing.....	42
4.3.3 Box-Behnken Design	43
3.3.4 N-phenylbenzohydroxamic acid	47
Chapter 4 Results and Analysis	49
4.1 Adsorption.....	49
4.1.1 Malachite-PAX	49
4.1.2 Malachite-Hydroxamate.....	52
4.1.3 Bornite-PAX	54

4.1.4	Bornite-Hydroxamate	56
4.2	Micro-flotation and Eh-pH.....	58
4.2.1	PAX Micro-flotation.....	59
4.2.2	Hydroxamate Micro-flotation	61
4.2.3	N-benzoyl Micro-flotation	62
4.2.4	Bornite Micro-flotation	64
4.2.5	Eh-pH.....	65
4.3	Bench Scale Flotation	71
4.3.1	Exploratory Work	75
4.3.2	Preliminary Investigation.....	76
4.3.3	Box-Behnken	82
4.3.3.1	<i>Copper Recovery</i>	84
4.3.3.2	<i>Malachite Recovery</i>	96
4.3.3.3	<i>Minor Copper</i>	106
4.3.3.4	<i>Copper Grade</i>	116
4.3.4	<i>N-Benzoyl</i>	126
Chapter 5 Discussion	131	
5.1	Adsorption, Micro-flotation and Eh-pH Results.....	131
5.2	Bench Scale Flotation	135
5.2.1	Statistical Models.....	136
Chapter 6 Conclusions and Future Work	143	
6.1	Adsorption, Micro-flotation and Eh-pH.....	143
6.2	Bench Scale Flotation	147
6.3	Box-Behnken	148
6.4	Future Work.....	152
6.5	Concluding Remarks.....	154
References.....	156	
Appendix A	165	
Appendix B	169	
Appendix C	177	
Appendix D	183	
Appendix E	195	

List of Figures

Figure 2.1: Equilibrium copper species at a total copper concentration of 1.5x10-4 mol/L.....	8
Figure 2.2 : World copper production.....	10
Figure 2.3 : Idealized vertical section of a copper porphyry deposit	12
Figure 2.4 : Malachite treated with sodium hydrosulphide and sodium tetrasulphide	13
Figure 2.5- Schematic of the primary and secondary sulphidization layers on a malachite surface	14
Figure 2.6- Residual tetrasulphide ion concentration versus time in the sodium tetrasulphide-malachite system (Zhou and Chander, 1993).....	16
Figure 2.7- The effect of pH on potassium amyl xanthate uptake on chrysocolla.....	18
Figure 2.8- pH effect on the activation of chrysocolla and subsequent recovery with sodium sulphide and collected with xanthate..	18
Figure 2.9- Structures of typical chealate forming collectors (Fuerstenau et al, 2000).	22
Figure 2.10- Schematic representation of chemisorption, surface reaction and bulk precipitation of copper oxides (Fuerstenau et al, 2000)	23
Figure 2.11- A chemisorbed chelating reagent on a copper oxide surface.	24
Figure 2.12- Structures of 8-hydroxyquinoline, potassium octyl hydroxamate, dithizone, dithiocarbamate and diethylenetriamine fom left to right.....	24
Figure 2.13: Tautomers of hydroxamic acid, hydroxyamide and hydroxyoxime	27
Figure 2.14 : Mechanism by which hydroxamic acids form metal complexes.....	28
Figure 2.15 : Adsorption isotherm of octyl hydroxamate on malachite	29
Figure 2.16: Infrared spectra of octyl hydroxamate on malachite	30
Figure 2.17: Possible hydroxylation reactions.....	31
Figure 2.18: Mechanisms for multi-layer formation :	33
Figure 3.1 : Schmatic of the modified Hallimond tube used for micro flotation.....	37
Figure 3.2: Cumulative passing size of the bench-scale flotation charges.....	40
Figure 3.3: Bench scale flotation apparatus.....	41
Figure 3.4: Structure of N-phenylbenzohydroxamic acid.....	47
Figure 4.1 : The kinetics of PAX adsorption on malachite.....	50
Figure 4.2 : The effect of pH on PAX adsorption density on malachite.....	51
Figure 4.3 : The kinetics of hydroxamate adsorption on malachite.....	53

Figure 4.4 : The effect of pH on the adsorption of hydroxamate on malachite.....	54
Figure 4.5: The kinetics of PAX adsorption on bornite.....	55
Figure 4.6 : The effect of pH on the adsorption and the uptake of PAX on bornite.....	56
Figure 4.7 : The kinetics of hydroxamate adsorption on bornite.....	57
Figure 4.8: The effect of pH on hydroxamate adsorption and collector uptake on bornite.....	58
Figure 4.9 : The relationship between the flotation recovery of pure malachite and bornite with PAX.....	60
Figure 4.10 : The relationship between the flotation recovery of pure malachite and bornite with hydroxamate.....	61
Figure 4.11 : The relationship between the flotation recovery of pure malachite and bornite with N-benzoyl.....	63
Figure 4.12 : Comparison between collectorless bornite flotation and flotation with PAX, hydroxamate and N-benzoyl.....	65
Figure 4.13: Distribution diagram for cupric ions and malachite	67
Figure 4.14 : Species distribution diagram for a benzohydroxamate (BHMA)	69
Figure 4.15: Species distribution diagram showing xanthate, cuprous xanthate (CuEX).....	71
Figure 4.16 : Cumulative Cu grade versus cumulative Cu recovery for T1 and T2.....	74
Figure 4.17 : Kinetics of metal recovery for T1 and T2. T1 is indicated by the open markers.	74
Figure 4.18 : Kinetics of metal grade for T1 and T2. T1 is indicated by the open markers.	75
Figure 4.19 : Copper grade versus recovery for preliminary tests T4 through T8.....	77
Figure 4.20 : Cumulative copper grade for preliminary tests T4 through T8.....	78
Figure 4.21 : Cumulative copper recovery for preliminary tests T4 through T8.....	79
Figure 4.22 : Cumulative mineral recovery for preliminary tests T4 through T8.....	80
Figure 4.23: Schematic illustrating the contours obtained with a quadratic response surface.....	84
Figure 4.24: Copper recovery versus run number for the Box-Behnken experimental design.....	85
Figure 4.25 : Principal component analysis output from JMP.....	86
Figure 4.26: Actual by predicted and residual by predicted plot or a linear model.....	88
Figure 4.27: Scatterplot matrix for a linear model for copper recovery.	88
Figure 4.28: Scatterplot matrix for the full quadratic model for copper recovery	90
Figure 4.29: Actual by predictedand residual by predicted plot for the response surface model with no interaction effects.	93
Figure 4.30: Scatterplot matrix for the response surface model with no interaction effects.....	94

Figure 4.31 : JMP surface profile for the interaction effects between the explanatory variables for the copper recovery model.....	95
Figure 4.32: Malachite recovery versus run number for the Box-Behnken experiments.	96
Figure 4.33: Principal component analysis output from JMP.....	97
Figure 4.34: Actual by predicted and residual by predicted plot for the linear model of malachite recovery.	98
Figure 4.35: Scatterplot matrix for the linear model of malachite recovery.....	99
Figure 4.36 : Scatterplot matrix for the full response surface model for malachite recovery.....	100
Figure 4.37: Actual by predicted and residual by predicted plot for the final model of malachite recovery.	103
Figure 4.38: Scatterplot matrix for the final model for malachite recovery.	103
Figure 4.39: JMP surface profile for the interaction effects between the explanatory variables	105
Figure 4.40 : Minor copper recovery vs. run number.	106
Figure 4.41 : Principal component analysis for the minor copper recovery model.	107
Figure 4.42: Actual vs. predicted and residual vs. predicted plots for the linear model for minor copper recovery.....	108
Figure 4.43 : Scatterplot matrix of the residuals vs. the explanatory variables in for the linear minor copper recovery model.	109
Figure 4.44: Actual vs. predicted and residual vs. predicted plots for the full quadratic response surface model for minor copper recovery.	110
Figure 4.45 : Scatterplot matrix of the residuals vs. the explanatory variables for the full quadratic response surface model of minor copper recovery.	111
Figure 4.46 : Actual vs. predicted and residual by predicted plots for the final minor copper recovery model.	113
Figure 4.47 : Scatterplot matrix of the residuals vs. the explanatory variables for the full quadratic response surface model of minor copper recovery.	114
Figure 4.48 : JMP surface profile for the interaction effects between the explanatory variables in the final minor copper recovery model.	115
Figure 4.49 : Copper grade versus run number for the Box-Behnken experiments.....	116
Figure 4.50 : Principal component analysis for the copper grade model.	117
Figure 4.51: Actual vs. predicted and residual vs. predicted plots for the linear copper grade model.	118

Figure 4.52 : Scatterplot matrix for the linear copper recovery model.....	119
Figure 4.53 : Actual by predicted and residual by predicted plots for the full quadratic response surface model of copper grade.	120
Figure 4.54 : Scatterplot matrix for the full quadratic response model for copper grade.	121
Figure 4.55 : Actual vs. predicted and residual vs. predicted plot for the final copper grade model.	123
Figure 4.56 : Scatterplot matrix for the final response model for copper grade.	124
Figure 4.57 : JMP surface profile for the interaction effects between the explanatory variables in the final copper grade model.	125
Figure 4.58: Copper recovery versus grade for tests BZ1 and BZ2.....	127
Figure 4.59: Copper recovery for tests BZ1 and BZ2.....	128
Figure 4.60: Cumulative grade for tests BZ1 and BZ2.....	128
Figure A.1 : XRD report for a combined sulphide concentrate.....	165
Figure A.2 : XRD report for a combined oxide concentrate.....	166
Figure A.3 : Tailings XRD report.	167
Figure A.4 : XRD report for the slime fraction.....	168
Figure B.1 : PAX calibration curve.	169
Figure B.2 : Hydroxamate calibration curve.....	169
Figure C.1 : Cu grade vs. Cu recovery for B1-B5 of the Box-Behnken experiments.....	177
Figure C.2 : Cu recovery vs. time for B1-B5 of the Box-Behnken experiments.....	177
Figure C.3 : Cu grade vs. time for B1-B5 of the Box-Behnken experiments.....	178
Figure C.4 : Mineral recovery vs. time for B1-B5 of the Box-Behnken experiments.....	178
Figure C.5 : Cu grade vs. Cu recovery for B6-B10 of the Box-Behnken experiments.....	179
Figure C.6 : Cu recovery vs. time for B6-B10 of the Box-Behnken experiments.....	179
Figure C.7: Cu grade vs. time for B6-B10 of the Box-Behnken experiments.	180
Figure C.8 : Mineral recovery vs. time for B6-B10 of the Box-Behnken experiments.....	180
Figure C.9: Cu grade vs. Cu recovery for B11-B15 of the Box-Behnken experiments.....	181
Figure C.10 : Cu recovery vs. time for B11-B15 of the Box-Behnken experiments.	181
Figure C.11 : Cu grade vs. time for B11-B15 of the Box-Behnken experiments.	182
Figure C.12 : Mineral recovery vs. time for B11-B15 of the Box-Behnken experiments.	182
Figure D.1: JMP output for the linear copper recovery model.	183
Figure D.2: JMP output for the full quadratic response surface model of copper recovery.	184

Figure D.3: JMP output for final copper recovery model.....	185
Figure D.4: JMP output for the linear model of malachite recovery.	186
Figure D.5 : JMP output for the full quadratic response surface for malachite recovery.	187
Figure D.6: JMP output for the final malachite recovery model.	188
Figure D.7 : JMP output for the linear minor copper recovery model.....	189
Figure D.8: JMP output for the full quadratic model for minor copper recovery.....	190
Figure D.9: JMP output for the final minor copper recovery model.	191
Figure D.10 : JMP output for the linear model of copper grade.	192
Figure D.11 : JMP output for the full quadratic response surface model of copper grade	193
Figure D.12 : JMP output for the final model of copper grade.....	194

List of Tables

Table 2.1- Effects of initial sodium tetrasulphide concentrations on thickness of the sulphidized layer and the specific rate constant	17
Table 2.2: Comparison of bond energy magnitudes and their associated adsorption mechanism.	32
Table 3.1: Specific surface areas (m^2/g) of the mineral samples by mesh size.....	34
Table 3.2: Experimental design for bench-scale Box-Behnken design.	46
Table 4.1: The results of the Box Behnken bench-scale flotation experiments.....	83
Table 4.2: Correlation table between explanatory variables.....	86
Table 4.3: Akaike Information Criterion (AIC) for potential models.....	92
Table 4.4: Correlation table for the explanatory variables in the malachite recovery model.	97
Table 4.5: AIC values calculated for the malachite recovery models.....	101
Table 4.6 : Correlation table for the explanatory variables used in the minor copper recovery model.....	107
Table 4.7 : AIC values calculated for the minor recovery models.....	112
Table 4.8 : Correlation table between the explanatory variables.....	117
Table 4.9: AIC values calculated for the copper grade models.	122
Table B.1 : Absorbance values for the PAX-Malachite system.....	171
Table B.2 : Absorbance data for the Hydroxamate-Malachite system.	171
Table B.3 : Absorbance data for the PAX-Bornite system.	171
Table B.4 : Absorbance data for the Hydroxamate-Bornite system.	171
Table B.5 : Micro-flotation and Eh-pH data for the PAX-malachite system.....	172
Table B.6 : Micro-flotation and Eh-pH data for the Hydroxamate-malachite system.	172
Table B.7 : Micro-flotation and Eh-pH data for the N-Benzoyl-malachite system.	173
Table B.8 : Micro-flotation and Eh-pH data for the PAX-bornite system.	173
Table B.9 : Micro-flotation and Eh-pH data for the Hydroxamate-bornite system.	174
Table B.10 : Micro-flotation and Eh-pH data for the N-Benzoyl-bornite system.	174
Table B.11 : Micro-flotation and Eh-pH data for the collectorless bornite system.	175
Table B.12 : Thermodynamic data for species distribution diagrams.	176
Table E.1 : Flotation report for T1 of the exploratory work.	195
Table E.2 : Flotation results spreadsheet for T1 of the exploratory work.....	196
Table E.3 : Flotation Report for T2 of the exploratory work.....	197

Table E.4 : Flotation results spreadsheet for T2 of the exploratory work.....	198
Table E.5 : Flotation report for T4 of the preliminary investigations.....	199
Table E.6: Flotation results spreadsheet for T4 of the preliminary work.	200
Table E7 : Flotation report for T5 of the preliminary investigations.....	201
Table E.8 : Flotation results spreadsheet for T5 of the preliminary work.	202
Table E.9: Flotation report for T6 of the preliminary investigations.....	203
Table E.10 : Flotation results spreadsheet for T6 of the preliminary investigations.	204
Table E.11: Flotation report for T7 of the preliminary investigations.....	205
Table E.12 : Flotation results spreadsheet for T7 of the preliminary testing.....	206
Table E.13: Flotation report for T8 of the preliminary investigations.....	207
Table E.14: Flotation results spreadsheet for T8 of the preliminary testing.....	208
Table E.15: Flotation report for B1 of the Box-Behnken.	209
Table E.16: Flotation results spreadsheet for B1 of the Box-Behnken experiments.	210
Table E.17: Flotation report for B2 of the Box-Behnken.	211
Table E.18: Flotation results spreadsheet for B2 of the Box-Behnken experiments.	212
Table E.19: Flotation report for B3 of the Box-Behnken.	213
Table E.20: Flotation results spreadsheet for B3 of the Box-Behnken experiments.	214
Table E.21: Flotation report for B4 of the Box-Behnken experiments.	215
Table E.22: Flotation results spreadsheet for B4 of the Box-Behnken experiments.	216
Table E.23: Flotation report for B5 of the Box-Behnken experiments.	217
Table E.24: Flotation results spreadsheet for B5 of the Box-Behnken experiments.	218
Table E.25: Flotation report for B6 of the Box-Behnken experiments.	219
Table E.26: Flotation results spreadsheet for B6 of the Box-Behnken experiments.	220
Table E.27: Flotation report for B7 of the Box-Behnken experiments.	221
Table E.28: Flotation results spreadsheet for B7 of the Box-Behnken experiments.	222
Table E.29: Flotation report for B8 of the Box-Behnken experiments.	223
Table E.30: Flotation results spreadsheet for B8 of the Box-Behnken experiments.	224
Table E.31: Flotation report for B9 of the Box-Behnken experiments.	225
Table E.32: Flotation results spreadsheet for B9 of the Box-Behnken experiments.	226
Table E.33: Flotation report for B10 of the Box-Behnken experiments.	227
Table E.34: Flotation results spreadsheet for B10 of the Box-Behnken experiments.	228
Table E.35: Flotation report for B11 of the Box-Behnken experiments.	229

Table E.36: Flotation results spreadsheet for B11 of the Box-Behnken experiments	230
Table E.37: Flotation report for B12 of the Box-Behnken experiments.....	231
Table E.38:Flotation results spreadsheet for B12 of the Box-Behnken experiments	232
Table E.39: Flotation report for B13 of the Box-Behnken experiments.....	233
Table E.40: Flotation results spreadsheet for B13 of the Box-Behnken experiments	234
Table E.41: Flotation report for B14 of the Box-Behnken experiments.....	235
Table E.42: Flotation results spreadsheet for B14 of the Box-Behnken experiments	236
Table E.43: Flotation report for B15 of the Box-Behnken experiments.....	237
Table E.44:Flotation results spreadsheet for B15 of the Box-Behnken experiments	238
Table E.45: Flotation report for BZ1 investigation of N-benzoyl.	239
Table E.46: Flotation results spreadsheet for BZ1 of the N-benzoyl investigation.....	240
Table E.47: Flotation report for BZ2 of the N-Benzoyl investigation.....	241
Table E.48: Flotation results spreadsheet for BZ2 of the N-Benzoyl investigation.....	242

Chapter 1

Introduction

Global economic growth drives consumption and depletion of natural resources. This drive for natural resources has led to a dwindling supply, increased demand and significant environmental degradation. Currently, as much as 10% of the global economy, 50 % of global resources and 40 % of global energy is dedicated to the construction industry (Roodman and Lenseen, 1994; Price Waterhouse Cooper, 2008). For the first time in modern history, developing nations like India and China are the leaders of world growth (Callen, 2007).

Copper is an integral component in many industries, but is most used in construction. Modern homes, offices, and manufacturing plants require massive amounts of copper. Copper is used everywhere in structural components, wiring and piping, HVAC systems and aesthetic features (ICASEA, 2009). Half the copper demand in the United States, nearly 538,000 tonnes a year, ends up in buildings (Roodman and Lenseen, 1994). The construction of a typical house in the United States consumes 450 lbs of copper (Reuters, 2008).

Many of the copper mines around the world contain copper oxide ore associated with sulphide ore reserves. Copper oxide reserves contain economic quantities of copper in the form of secondary copper minerals such as malachite ($\text{Cu}_2(\text{OH})_2\text{CO}_3$), azurite ($\text{Cu}_3(\text{CO}_3)_2(\text{OH})_2$), cuprite (Cu_2O) and tenorite(CuO). Large amounts of copper oxides go un-recovered due to a focus on sulphide recovery and problematic oxide processing (Zhou and Chander, 1993). Most mines will either have part of their copper oxides report to tailings or will stockpile them appropriately for future processing; a majority chooses the former. A study by Aplan and Fuerstenau (1984) found that U.S copper tailings contained, on average, 0.7 kg of copper per tonne. Even when copper

prices rose to an 8000\$/t in 2008 (Infomine, 2008), copper oxide recovery remained overlooked.

In 2009, the global economy has experienced a recession. The economic slowdown was particularly tough on the mining industry; metal prices fell and operating costs rose.

The capital and operating costs of a mine are enormous. Costs begin with an exploration program and continue through construction, operation and mine closure. Exploration begins with the discovery of a mineral deposit and is followed by a feasibility study. If it is determined commercially viable, a mine is developed. At this stage, the mine infrastructure is put in place. Once completed, mining and mineral processing begin. As the mine reaches the end of its life, a closure management plan is put in place (Moon et al, 2006).

While the exploration costs and timeline can be large, as much as 1440 USD/t of increased resources over an average span of 12 years, comminution is reputedly the most energy and cost intensive part of mining (Moon et al, 2006). The comminution, or size-reduction, process takes ore from an average size of 40 cm to a final product of 270 to 325 mesh. This is the most energy intensive and costly step in a mining operation. It was estimated by Schoenert (1986) that in 1976 approximately 3.3 % of the global electrical energy was devoted to crushing and grinding. With more mines in operation today, this number is assumed to be larger (Fuerstenau and Abouzeid, 2002). An example of mine operating costs by unit operation outlined by Workman and Eloranta (2003) shows that grinding is by far the greatest operating expense, followed closely by crushing and blasting.

Once a mine is operating, its copper oxides are sunk costs. It has paid for the copper contained in the secondary minerals in every stage of its mine development. Although the recovery of copper oxides can be un-economical due to reagent costs, in the current economy it seems intuitive to attempt to collect as much of the copper as possible. With a renewed push to recover copper oxides due to economic constraints and diminishing sulphide supplies, recovery techniques that have been laboratory curiosities for over 50 years are being studied and improved.

Several techniques have been developed to float copper oxide minerals, but none have been implemented on an industrial scale. The current conventional technique for floating copper oxide minerals is to use a sulphidizing pre-treatment. Another technique requires acid leaching of the copper oxides followed by solvent extraction and electrowinning (SX/EW). Although this technique has proven successful (Kordorsky, 2002), it requires capital expenditure to construct a dedicated leaching plant. It is possible that many mining companies could afford such a capital investment, but it makes practical and economic sense to extract the copper oxides simultaneously alongside the sulphides.

Prior to flotation, sulphidizing re-surfacing the oxides with a copper-sulphide layer to allow collection by xanthates (Zhang, 1994). This process has many disadvantages which prevents it from being implemented industry-wide, as discussed in Chapter 2. Widely used in analytical chemistry, chelating agents have been proposed as an alternative reagent since the 1920s because of their highly specific adsorbate-adsorbent interactions. In theory, this allows them to selectively float only ore minerals by complexing with their metal cations. Chelating agents form durable complexes with copper sites (Barbaro et al, 1997) and can provide a higher degree of selectivity during the flotation process (Fuerstenau et al, 2000). After nearly half a century of study, chelating agents have shown more promise as universal collectors of copper oxides that need no pre-treatment (Fuerstenau and Pradip, 1984).

The first objective of this thesis is to gain insight into the behaviour of malachite and bornite with two types of collectors: a chelating agent, alkyl hydroxamate and a conventional collector, potassium amyl xanthate. This is done by performing fundamental adsorption and micro-flotation work using pure minerals and laboratory grade reagents. In particular, the behaviour of the minerals and collectors is investigated on a flotation time scale to determine the potential effectiveness of a mixed-collector system.

The second objective of this thesis is to propose an effective collector regime to improve copper recovery from a mixed sulphide-oxide copper ore with bornite and malachite as the economic minerals. To do this, a statistical Box-Behnken experimental design is used to create a model quantifying the effects of collector dosages on copper, malachite and bornite recoveries. A response surface experimental methodology is used with the hopes of determining the collector dosages that deliver optimum copper recovery, as discussed in Chapter 4.

Chapter 2 presents a review of existing literature on the flotation of copper oxide minerals, with a specific focus on chelating agents and their interactions with malachite. This chapter also outlines the theory and disadvantages of sulphidizing, the current industrial technique for the collection of copper oxides. Chelating agents are discussed with respect to applicability, type and form. The adsorption of octyl hydroxamate, a chelating agent, on malachite is reviewed with an emphasis on flotation.

Chapter 3 presents a detailed description of the experimental techniques used for the adsorption, micro-flotation and bench-scale flotation. In addition, it outlines the details and reasoning behind the choice of experimental design and variable levels in the statistical modeling of a rougher concentrate stage with the raw ore.

Chapter 4 presents the results of the fundamental work and bench-scale flotation testing described in Chapter 3. The results of the exploratory and preliminary testing of the raw sulphide-oxide ore are presented to show effects of various reagent levels and combinations. Response surface models are created to describe copper recovery, malachite recovery and bornite recovery and their adequacy is assessed.

Chapter 5 is a discussion of the results presented in Chapter 4: an understanding of the fundamental behaviour of collectors and minerals as well as the flotation characteristics of mixed collector flotation.

Chapter 6 presents the conclusions of this thesis with respect to the improved copper recovery from a sulphide-oxide copper ore and a mixed collector flotation system. This chapter also outlines potential areas of future investigations to improve copper recovery and grade from this type of ore.

In this thesis, the terms “copper oxides” and “copper sulphides” are used interchangeably with “oxides” and “sulphides”. The former term includes carbonates and silicates due to the presence of oxygen in both cases. These terms are meant to describe the economic ore minerals that occur in porphyry copper deposits

Chapter 2

Literature Review

Current copper deposits contain significant amounts of secondary non-sulphide minerals in the form of oxide ore. Secondary minerals, such as malachite, $\text{Cu}_2(\text{OH})_2\text{CO}_3$ and chrysocolla, $(\text{Cu},\text{Al})_2\text{H}_2\text{Si}_2\text{O}_5(\text{OH})_4 \cdot n(\text{H}_2\text{O})$ contain economic quantities of copper (57.5% and 33.9% respectively). These minerals often go un-recovered because they are not easily amenable to conventional thiol collection techniques effective for sulphide minerals. Aside from copper oxide recovery, there are also sulphide ores with poor conventional recovery. These are ores with very fine-grained economic minerals or ones that are finely intergrown with gangue minerals.

An important factor in the problematic recovery of copper oxides is their surface properties (Marabini et al, 1991). Oxides are prone to dissolution, lack mechanical strength and possess strongly hydrophilic surfaces that cannot be transformed into hydrophobic ones (Barbaro et al, 1997). Conventional sulphide copper collectors fail to adhere to the oxide, resulting in excessive collector consumption, limited selectivity and poor recovery. The mineral assemblage in oxidized copper zones contains gangue that creates slimes detrimental to recovery, grade and frothing conditions (Poling, 1973).

Copper sulphides behave differently in flotation cells than copper oxides. Copper oxide minerals are generally porous with little mechanical strength. They occur in a conglomerate matrix or thin fracture fillings and end up in the slimes fraction of the ground ore feed (Poling, 1973). Flotation behaviour of the copper oxides is dependent on mineral composition, crystal structure and the ionic composition of the pulp.

The solubility of copper oxides is substantially different from copper sulphides. They are more soluble. The log solubility product of copper oxides and copper sulphides average

around -20 and -40 respectively. Additionally, copper oxides possess a narrower band of pH stability than sulphides. Copper oxides such as malachite and cuprite perform poorly in regions of high E_H and will dissolve easily in a pH range of 6 to 7. In fact, for many oxide copper minerals, significant dissolution can occur in near neutral waters. Dissolved copper ion concentrations of 10^{-4} to 10^{-6} mol/L have been observed. Both the solubility product and the narrow pH stability range indicate that non-sulphide copper minerals dissolve readily; it is difficult for collector coatings to remain stable (Poling, 1973).

Crystal structures affect the floatability of copper oxides. Mechanical strength, dissolution rate, hydration and copper ion accessibility are derivatives of a mineral's crystal structure. The lack of mechanical strength of copper oxide surfaces has been demonstrated by floating malachite with only xanthate. This was only possible when turbulence and attrition within the flotation cell were minimized. If agitated, the collector coatings were readily removed and formed putty-like balls of copper xanthate. Copper oxides consist of an infinite three dimensional array of Cu^{2+} , OH^- and CO_3^{2-} . The fracturing of copper oxide minerals often leaves the copper ions buried; this hinders the formation of a hydrophobic coating. Most collectors are designed to complex only with copper atoms (Poling, 1973).

The ionic composition of the pulp affects the chemical composition and the electrical characteristics of the copper oxide surfaces. An equilibrium diagram (Figure 2.1) showing the abundance of different copper-hydroxy species at different pH levels indicates that the most surface active species at near-neutral pH is $Cu_2(OH)_2^{2+}$. This cationic species has been attributed with the ability to reverse the negative zeta potential of copper oxides. Optimum copper oxide flotation has been linked to the near neutral pH range indicating that $Cu_2(OH)_2^{2+}$ is a flotation activator.

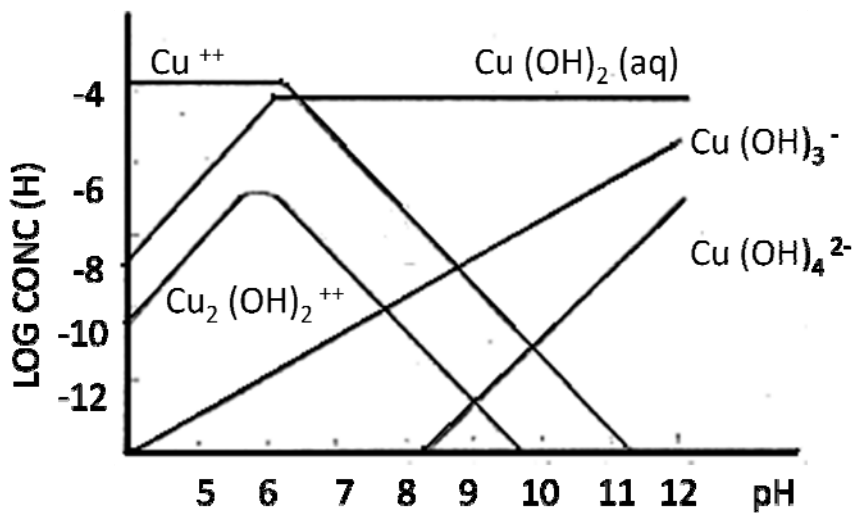
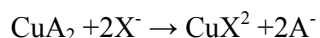


Figure 2.1: Equilibrium copper species at a total copper concentration of 1.5×10^{-4} mol/L
 (Poling, 1973)

Newly discovered ore bodies are becoming increasingly complex and lower in grade.

These ores require smaller grinding sizes for liberation. According to Takahashi and Wakamatsu (1984), flotation is still the superior technique for the industrial separation of fine particles. It is important to develop a technique that will successfully and economically float copper oxides.

Flotation depends on the conversion of hydrophilic sites to insoluble hydrophobic surfaces. This is done by the adsorption of organic reagents known as collectors. To float copper oxides, the collector system must also reduce the rate of surface dissolution (Poling, 1973). The reaction between a copper oxide mineral and a xanthate collector can be seen in the following where A represents either OH^- or a silicate ion and X is a xanthate ion (Castro et al, 1976).



Secondary copper minerals are well known for their poor response to xanthates (Fuerstenau et al, 2000). Xanthate collectors are not effective enough to make the strongly

hydrophilic oxide surfaces amenable to flotation. The xanthate attack on the particle surfaces form precipitates instead of acting as a collector. Colloidal dispersions indicate precipitation of dissolved copper and particles released from the mineral surface (Castro et al, 1976). Collectors will therefore interact chemically with dissolved copper ions rather than form stable coatings; collector requirements are very costly (Barbaro et al, 1997).

Aplan and Fuerstenau (1984) and Zhou and Chander (1993) outlined some general methods for recovering oxidized minerals: sulphidization-flotation, soap flotation, leaching, carboxylic acid processes, chelating agents and mercaptans. The first three methods have been used commercially. The use of carboxylic acids is not applicable in the case of carbonaceous copper oxides and leaching processes are ineffective due to significant losses of sulphide components. The application of chelating agents is a laboratory curiosity leaving the sulphidization-flotation as the most applied industrial method.

2.1 Geology

The most common source of mixed sulphide-oxide copper ores is from porphyry deposits. These deposits are large low to medium grade deposits in which hypogene ore minerals are structurally controlled. Porphyry deposits are a type of magmatic hydrothermal ore deposit formed due to interactions of briny hydrothermal fluids in the roots of andesitic stratovolcanoes (Kirkham and Sinclair, 1996). Porphyry copper deposits are very common in the Western hemisphere (Bartlett, 1998). They are the world's most important source of copper (Sinclair, 2007), which can be seen in Figure 2.2.

Porphyry copper deposits occur in continental or island arc settings. Continental arc settings occur at the convergence of oceanic and continental plates while island arc settings occur at the convergence of two oceanic plates. For an ore deposit to form, there are three required components: a metal source, a conduit and a depositional site. At the meeting of two plates,

magma is pushed upwards towards the surface from the mantle. As the magma journeys upwards through previously deposited magmatic rocks, it melts them and re-mobilises the metals contained within them. This magma upwelling is the source of the metals that will eventually be concentrated in the ore deposit.

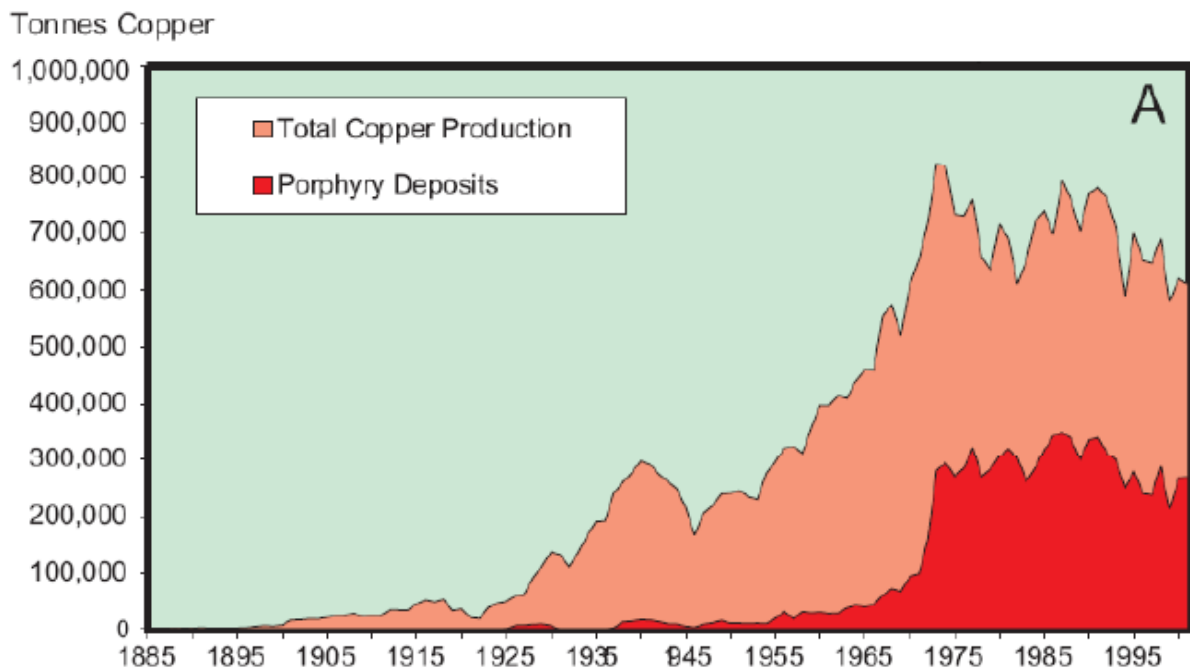


Figure 2.2 : World copper production (Sinclair, 2007)

There must be an easy route for the magma to reach the depositional site. This conduit is generally through regional structures or faults. The rocks above the magma upwelling will begin to crack and fracture, allowing the magma to continue upwards. The magma will begin to cool as it rises upwards and start to exolve magmatic water from the melt. This water would be rich in copper metal and chloride ions as copper is transported as complex chloride or sulphide ions. This saline brine is capable of transporting metals from the magma melt because it minimizes losses to crystallization. Once the fluids reach the depositional site, and begin to cool, they precipitate.

Several mechanisms govern the precipitation of ore minerals. Barnes (1997) states that wall rock interactions are crucial to mineral precipitation. The briny hydrothermal fluids are weak acids, but when they come into contact with wall rock, they begin to extract hydrogen atoms. This increases the acidity of the waters, which reduces the stability of the chloride complexes and begins sulphide mineral precipitation. This form of sulphide precipitation from chloride complexes will stop as soon as all sulphide ions are consumed. Interactions with the wall rock will also introduce reduced sulphur species into the melt that allow continued sulphide precipitation (Barnes 1997). Typical primary sulphide ore minerals are chalcopyrite, bornite and covellite.

An idealized cross-section of a porphyry copper deposit is seen in Figure 2.3. It can be seen that the primary sulphidic ore is present at depth. Above this zone is an intermediate secondary enrichment zone and at the top, there exists an oxidized and a naturally weathered zone. Copper oxide minerals are found mainly in the oxidation zone which is directly above the water table. The oxidized zone cannot delve below the water table, at least how it existed during deposit genesis, as water flooding excludes air and prevents oxidation. Purely oxidized zones are generally void of economic minerals due to leaching by supergene that percolates copper downwards. This soluble copper can precipitate below the water table as the oxidation potential drops. This is the mechanism for secondary copper enrichment which commonly produces further sulphide minerals. Valuable copper oxide minerals will not form if acidic conditions are not maintained in the oxidation zone (Bartlett, 1998).

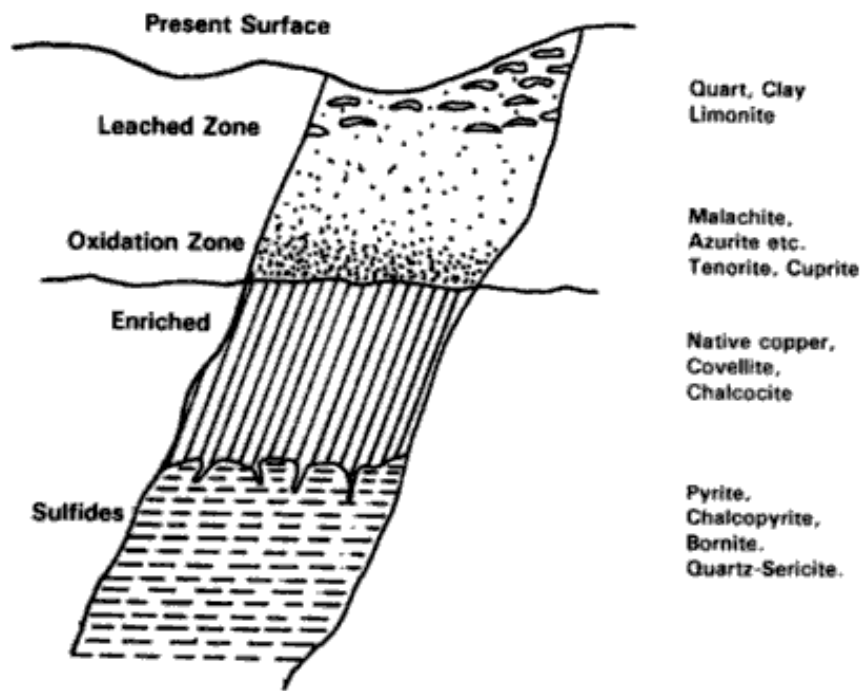


Figure 2.3 : Idealized vertical section of a copper porphyry deposit (Bartlett, 1998)

2.2 Sulphidization

Sulphidization is a process where oxidized minerals are treated in an aqueous sulphide solution prior to being floated. This pre-treatment promotes the formation of a copper-sulphide layer on the copper oxide surface. This is crucial to flotation as it creates a hydrophobic surface that will respond economically to conventional collectors (Barbaro et al, 1997).

Copper oxides have been found to respond well to xanthate collectors after sulphidization. X-ray diffraction techniques have confirmed the presence of copper sulphide coatings on minerals. Scanning electron micrographs taken of malachite after sulphidization, shown below in Figure 2.4, exhibit hydrophobic precipitates and layers. The surfaces have also been confirmed to be hydrophobic by contact angle measurements (Zhou and Chander, 1993).

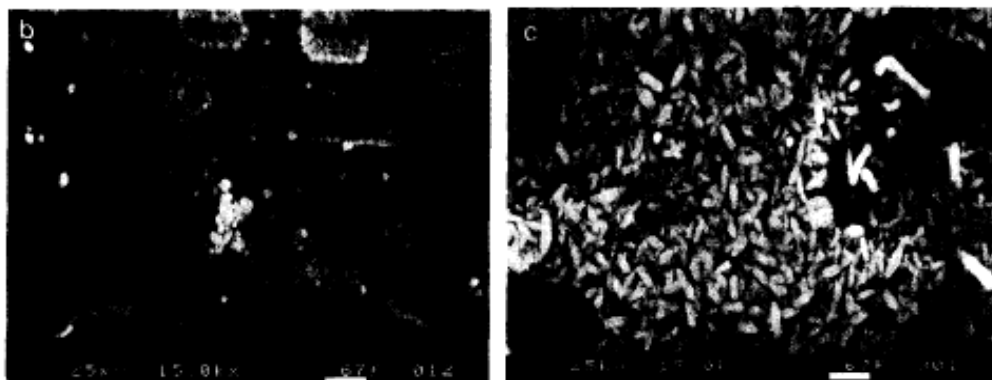


Figure 2.4 : Malachite treated with sodium hydrosulphide (right) and sodium tetrasulphide (left) (Zhou and Chander, 1993)

Different sulphidizing reagents are used, but there are commonalities present in all sulphidizing processes. The sulphidization reaction appears to be a heterogeneous reaction with two secondary reactions. Initially, a primary sulphidized layer is formed. The adsorption of sulphur to form the primary sulphidized layer occurs rapidly. This layer is formed as sulphide ions come into contact with CuO and react to form copper sulphide; this layer is crucial in xanthate flotation. The secondary sulphidization processes includes the formation of a secondary copper sulphide layer and the formation of oxysulphide species. The formation of the secondary sulphidized layer takes place as copper ions diffuse through cracks in the primary sulphidized layer. Figure 2.5 shows a schematic of these two layers for two different sulphidizing reagents (Zhou and Chander, 1993).

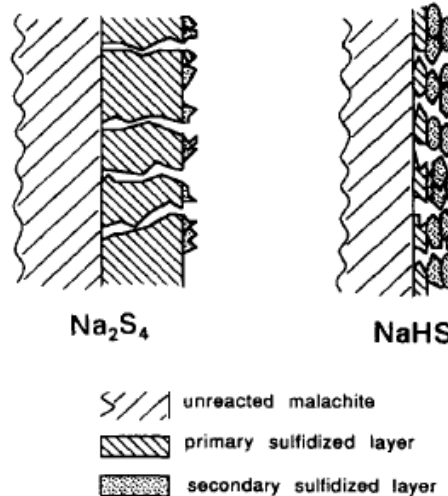
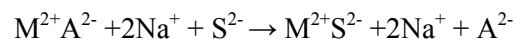


Figure 2.5- Schematic of the primary and secondary sulphidization layers on a malachite surface (Zhou and Chander, 1993).

Aqueous methods are not the only way to sulphidize copper oxides. Sulphidization has been confirmed by differential thermoanalysis by Martinez and Hollander (1964). This alternate process involves heating mixtures of copper oxides and sulphur over 225 °C to form a copper sulphide coating. This temperature is required to vapourize the sulphur.

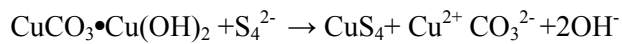
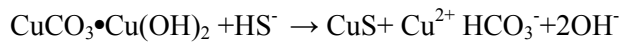
Sulphidizing agents are typically a variety of sodium sulphide. Sodium sulphide has shown the ability to enhance the flotation of oxidized copper minerals with xanthate collectors by stabilizing the collector film. Below is an example of the net sulphidization reaction where M^{2+} is the surface metal ion and A^{2-} is the anion resulting from sulphidization (Clark et al, 2006) :



The reaction above demonstrates the conversion of the surface metal ion into a metal sulphide, which is inherently hydrophobic. The adsorption of a collector particle on a mineral

surface requires the surface to be hydrophobic. If it is hydrophilic, as in the case of copper oxides, the non-polar xanthates will have to replace water molecules in order to collect the particle. For hydrophobic sites, the displacement of water will be spontaneous due to hydrophobic bonding contributions (Castro et al, 1976).

The selection of a sulphidizing agent is usually dependent on cost and local availability since most reactants produce the same surface active ions (Poling, 1973). Sodium sulphide is most commonly used in sulphidization-flotation (Zhou and Chander, 1993). Flotation conditions using sodium sulphide must be exact; the coating is delicate and detaches readily. Other potential reagents are sodium hydrosulphide (NaHS) and sodium tetrasulphide (Na_2S_4). Sodium tetrasulphide has shown particular promise as a replacement for sodium sulphide as it forms a thick and stable primary sulphidization layer. This makes it more amenable to flotation and it is resistant to agitation. The mechanisms between these two reagents and malachite are shown respectively below (Zhou and Chander, 1993):



Ammonium sulphide, (NH_4S), is a promising modifier because of its ammonium ion (Ser et al, 1970). NH_4^+ could speed up the conversion of non-sulphide surfaces. The ammonium ion disperses carbonate gangue minerals by increasing their solubility and improves selectivity by dissolving elemental sulphur (Poling, 1973).

Sulphidization is a more complicated process than the conversion of a non-sulphide surface to a sulphide one. The action of the sulphidizing agent is dependent on the kinetics, solution pH, dosage, particle size and secondary oxidation reactions.

2.2.1 Kinetics

The initial concentration of the sulphidizing agent was studied by Zhou and Chander (1993) to determine its effect on the extent of sulphidization. It was found that smaller rate constants were associated with high initial concentrations. A small rate constant is indicative of a greater extent of primary sulphidization that causes a larger primary sulphidized layer. Figure 2.6 shows that there is a rapid initial drop in sulphur species concentration associated with the formation of the primary sulphidized layer. The formation of the secondary sulphidized layer follows first order kinetics and is controlled by the diffusion of copper ions through the cracks in the primary sulphidized layer. Table 2.1 demonstrates that higher initial concentrations lead to a greater extent of sulphidization and the formation of a thicker primary sulphidized layer.

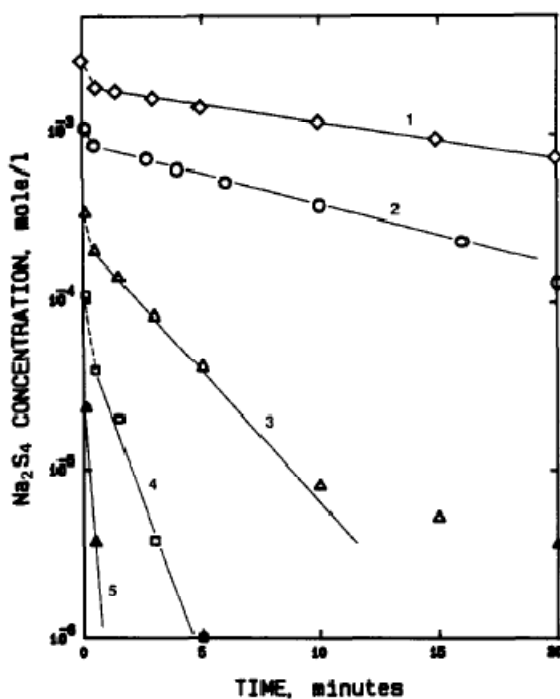


Figure 2.6- Residual tetrasulphide ion concentration versus time in the sodium tetrasulphide-malachite system (Zhou and Chander, 1993).

Table 2.1- Effects of initial sodium tetrasulphide concentrations on thickness of the sulphidized layer and the specific rate constant (Zhou and Chander, 1993)

S ₄ ²⁻ concentration		Calculated thickness of the primary sulfidized layer, Å	Specific rate constant, k l/sec
Initial conc., mole/l	Initial consumption ^a mole/g malachite		
2.3×10 ⁻⁵	b	b	b
1.15×10 ⁻⁴	5.35×10 ⁻⁶	9	0.0185
3.45×10 ⁻⁴	1.06×10 ⁻⁵	17	0.00565
1.15×10 ⁻³	2.47×10 ⁻⁵	40	0.00142
2.3×10 ⁻³	4.10×10 ⁻⁵	66	0.00075

2.2.2 pH

Castro et al (1974) determined that the pH of sulphidization was more important than the pH of flotation. The pH of the conditioning stage affects the sulphur uptake at the surface. If too little sulphur is adsorbed by the oxide minerals, the hydrophobic layer will not form. Figure 2.7 shows the influence of pH on xanthate uptake and Figure 2.8 shows how the recoveries in the flotation stage are affected by the pH of the conditioning stage. At high pH levels, the extent of sulphidization is small; the amount of sulphidizing agent consumed is minimal. If the pH is above 6.0, the reagent uptake rate decreases rapidly. If no reactant is consumed to form the copper-sulphide layer, flotation will not be possible. Higher pH in the conditioning stage corresponds to poor flotation recoveries.

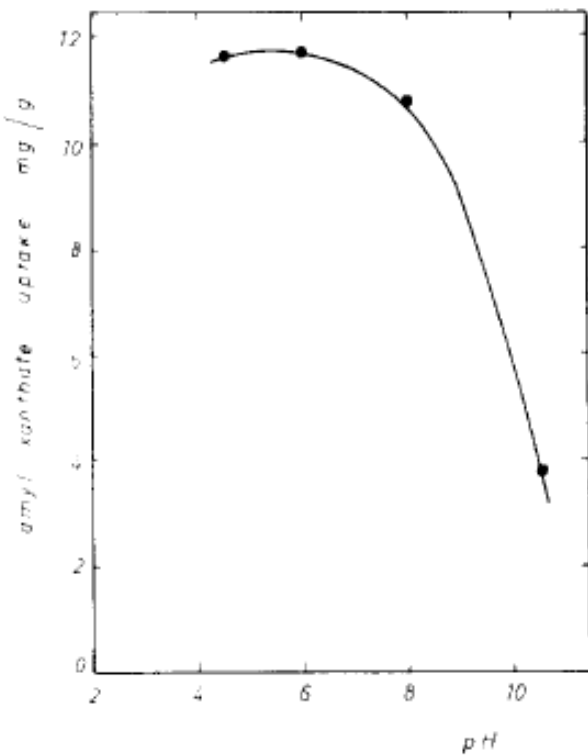


Figure 2.7- The effect of pH on potassium amyl xanthate uptake on chrysocolla (Castro et al, 1976)

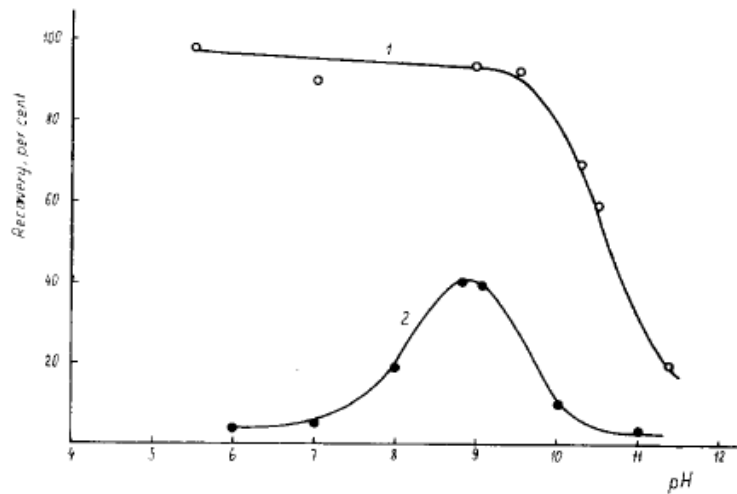


Figure 2.8- pH effect on the activation of chrysocolla and subsequent recovery with sodium sulphide and collected with xanthate. Curves 1 and 2 represent a sulphidization concentration of 200 mg/L and 960 mg/L respectively.

2.2.3 Dosage

The dosage of the sulphidizing reagent is important because when overdosing occurs, hydrophobicity is lost. Castro et al (1974) noted that for copper oxide minerals like chrysocolla, an overdose of sulphidizing agent would result in little or no recovery. A careful balance must be achieved as 1 g/L of sulphidizing agent can cause an irreversible depression, as seen in curve 2 in Figure 2.8. This depression is attributable to an increase in secondary reactions (Zhou and Chander, 1993).

Sulphidizing agents react fastest with the fine non-sulphide fractions. Fast flotation of the finest sulphidized particles occurs. Coarse particles and middlings are starved of sulphidizer. Successive concentrate fractions contain higher portions of coarser copper oxides and require longer contact times.

Ser et al (1970) found that multistage sulphidizer additions always yielded higher copper recoveries. Multistage addition of sulphidizer ensures that higher proportions of the oxides are sulphidized and minimizes overdosing. Critical overdose is avoided; adequate ion concentration is maintained to sulphidize size fractions that require longer contact times.

Floc flotation is a method proposed by Rubio and Phil (1978). Fine particles are agglomerated with high concentrations of K-amyl xanthate at high stirring speeds. The flocs formed are hydrophobic and float successfully. Pre-conditioning at high shear rates results in increased aggregation of ultrafine malachite particles. The mechanisms behind this experimental method are still undetermined. Increased recovery of fines at higher grades was noted.

Monitoring techniques were developed in order to characterize the level of sulphidization. Dielectric analysis can monitor and characterize mineral pulps in flotation cells. Activation, deactivation and collector adsorption changes the superficial conductivity of the mineral pulp. Copper oxide minerals become conductive after activation processes like sulphidization. The adsorption of collector molecules leads to a strong decrease in the dielectric

constant. Both phenomena are detectable with the use of high frequency dielectric measurements. Dielectric analysis measurements are rapid and non-destructive. Measurements are normally acquired in less than a minute and only small amounts of pulp are required for accurate results. This method is promising for copper oxide flotation. It provides rapid and accurate in-situ results. This would help to avoid overdosing on sulphidizing reagents and collectors. Dielectric analysis helps determine optimal processing parameters (Bessiere et al, 1991).

Ion selective electrodes (ISE) are also used for the continuous monitoring of sulphide residuals during sulphidization. The electrodes are solid-state types with silver-sulphide impregnated silicone rubber membranes. They respond rapidly to changes in sulphide ions in solution, have low detection limits over a wide pH range and are robust enough to be used in the mineral pulp. Jones and Woodcock (1978) demonstrated that a sulphide ISE could be used in the laboratory to optimize flotation conditions. .

2.2.4 Oxidation Reactions

The sulphur contained in the sulphidizing agents should be totally consumed to form the sulphide layers, but parallel oxidation reactions occur. Oxidation reactions take place with the sulphidizing agent, the adsorbed HS^- or with the newly formed copper sulphide layer. Sulphidizing agents oxidize to form oxysulphide species S_2O_3^- and SO_3^- . These processes are undesirable; they consume the sulphidizer, inhibit the formation of the copper sulphide layer (Zhou and Chander, 1993) and form oxysulphide species detrimental to flotation. To reduce the effects of these unwanted anions, some processes wash the minerals with distilled water to remove oxysulphide ions prior to flotation (Castro et al, 1974). It has been suggested by Castro et al (1976) that if no oxidization takes place, anions with greater depressant qualities, such as HS^- , will exist. HS^- is a strong reducing agent for copper oxides and sulphides.

The sulphidization-flotation method has proven that it can collect copper oxide minerals. The process is expensive, difficult to control and time consuming. Different flotation stages for oxides and sulphides result in copper sulphide losses. All oxide minerals respond differently. These issues frequently amount to unacceptable recoveries. A variety of different collectors have been proposed, but none have been implemented on an industrial scale.

Monitoring the mineral pulp during flotation allows operators to track changes brought on by reagent additions. Calorimetry, IR spectrometry and electrokinetical monitoring are examples of measurements used for process control. The disadvantage of these methods is that they require treatment of the mineral sample. Sample analysis requires large equipment and is time consuming. Flotation control would benefit from rapid in-situ analysis (Bessiere et al, 1993). In-line dielectric analysis and ion selective electrodes are methods of real time monitoring of copper oxide flotation.

2.3 Chelating Agents

Widely used in analytical chemistry for their abilities to selectively complex metal cations, chelating agents have the potential to process oxidized copper ores. Chelating agents can specifically interact with the copper ion site in copper oxide minerals and separate them without the need for activation (Fuerstenau et al, 2000). They convert the mineral surfaces to either oleophilic or hydrophobic conditions. Chelating agents also have the added ability to collect sulphide and non-sulphide minerals in a single flotation stage (Poling, 1973).

Chelating agents have been studied for mineralogical applications since the early 20th century. In 1927, cassiterite was flotated using ammonium nitrosophenyl hydroxylamine. Only a few years later, Holman began collecting nickel oxide ores with dimethylglyoxime. It wasn't until

1946 that the first detailed study on the applicability of chelating agents in flotation was written by Gutzeit. The trend continued with many other researchers trying different combinations of minerals and chelating agents over the next half century. Finally, Nagaraj and Somasundaran (1979) proposed hydroxy oximes in copper flotation.

Chelate-forming collectors must contain at least two donor atoms capable of forming bonds with a single metal atom. Elements capable of doing this are the electronegative elements such as sulphur, nitrogen, oxygen and phosphorus. Chelating agents can be subdivided into two basic functional groups: acidic and basic. Acidic groups coordinate with the metal cations through the loss of a proton. Basic groups coordinate atoms with lone pairs. Only chelating reagents that form metal chelates are appropriate for flotation. They must have suitable functional groups located in the ligands so that the formation of a ring structure including the metal cation is sterically possible (Fuerstenau et al, 2000). Typical structures of chelate-forming collectors applicable to flotation are shown in Figure 2 9.

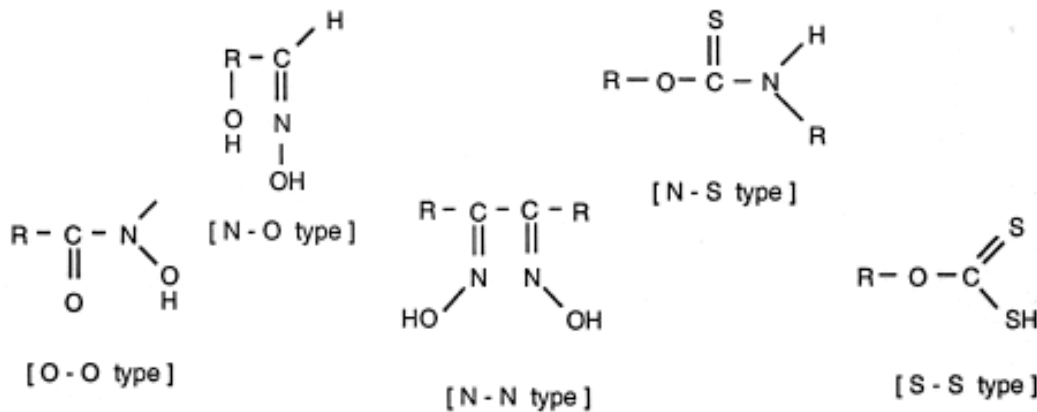


Figure 2 9- Structures of typical chealate forming collectors (Fuerstenau et al, 2000).

Depending on the chemistry of the flotation system, copper chelates can react with the copper ion via chemisorption, surface reaction and bulk precipitation. A schematic representation three of these processes is shown in Figure 2.10:

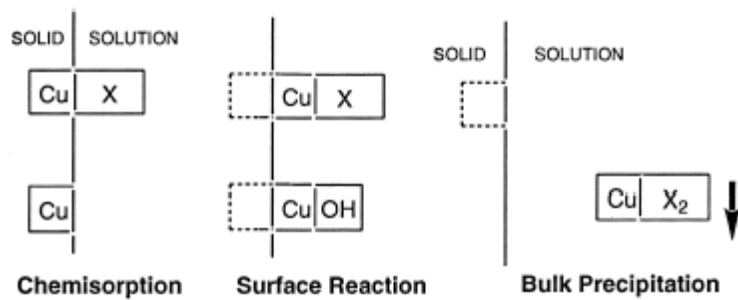


Figure 2.10- Schematic representation of chemisorption, surface reaction and bulk precipitation of copper oxides (Fuerstenau et al, 2000)

Chemisorption involves both coordinate and covalent bonding with the surface copper cations fixed in the crystal lattice. Since the cations remain in the crystal lattice, chemisorption forms only monolayers. A schematic of the monolayer is shown in Figure 2.11, where Y is the chelate functional group. The structure at the left of Figure 2.11 indicates the chelate structure formed during bulk precipitation. When copper cations are removed from the crystal lattice, a surface chemical reaction is occurring. This process moves the cations directly adjacent to the mineral surface and promotes the formation of multiple layers. Bulk precipitation occurs when the flotation system dissolves the mineral surface. Chelating collectors react with the copper cations in solution and form undesirable precipitates. As pointed out by Fuerstenau et al, (2000) chemisorption is the preferred mechanism for mineral processing. It minimizes collector consumption by forming a monolayer.



Figure 2.11- A chemisorbed chelating reagent on a copper oxide surface. Typical monolayer formation (Fuerstenau et al, 2000)

Significant research has been placed into chelating reagents. There are five types of chelating reagents N-O, O-O, N-N, S-S and S-N. An example of each is shown in Figure 2.12 from left to right respectively.

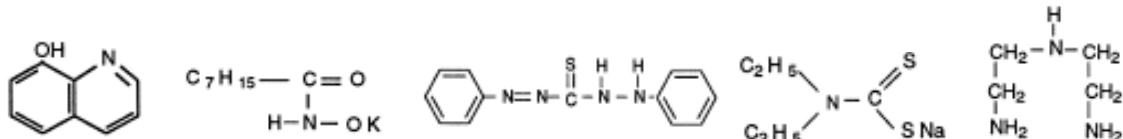


Figure 2.12- Structures of 8-hydroxyquinoline, potassium octyl hydroxamate, dithizone, dithiocarbamate and diethylenetriamine from left to right (Fuerstenau et al, 2000).

N-O type chelating collectors have at least one aromatic ring and have a tendency to adsorb by surface reaction. Hydroxamates are the most important O-O type chelating reagent. Hydroxamates form strong copper complexes under surface reaction conditions. S-N type reagents are important for metal complexation with oxidized metal surfaces. These reagents are thought to chemisorb onto minerals with high solubility and sulphide minerals. The presence of oxygen in the S-S type chelating collector molecule has an electropulling effect on sulphur; this makes it less electron-rich. This tendency reduces the favorability of an S-S chelation with copper cations (Fuerstenau et al, 2000).

Everard and De Cuyper (1975) found that co-operation between hydroxamates and xanthates increased recoveries in copper bearing ores. Co-adsorption will occur if the copper

atoms are structural or adsorbed. The degree of the mineral surface coated with collector was increased with both hydroxamate and xanthate. Hydroxamate adsorption on mineral surfaces gives the surfaces a positive zeta potential, indicating that the surface is more charged post adsorption (Palmer et al, 1975).

Monoalkyldithiocarbamates were found to be efficient collectors of unactivated copper carbonates. Dosages of 0.2 kg/tonne recovered all the pure copper carbonate minerals and reduced the oxides in the tailings to near zero. In the same class, octyldithiocarbamate proved to be extremely selective in trials with sliming problems (Werneke and Jones, 1976).

Chelating flotation reagents are promising. They do not require copper oxide minerals to be activated or sulphidized before flotation. There are still factors affecting the performance of chelating reagents that must be addressed.

2.3.1 pH

pH levels affect the process of metallic surface chelation. Hydrogen cations compete with surface metallic sites to complex with collector anions. Hydroxide anions compete with the collector for surface metallic sites. pH levels affect the dissolution of the copper oxides. Hydrogen ions force copper ions into solution by exchanging into the crystal lattice. Copper ions, now in solution, are quickly chelated by the collector. This process depletes the collector and effectively ends the flotation process. Hydrophilic silica-rich surfaces are also attributed to the leaching of copper ions out of the lattice by hydrogen. It has been recommended by Barbaro et al (1997) that the pH level should be kept above a value where mineral solubility is constant. This allows bulky chelate collector molecules enough time to displace the hydroxide ions from the copper sites.

Dithiocarbamates convert to their unstable acid form as pH decreases. As pH decreases, reagent decomposition accelerates and decreases recovery (Werneke and Jones, 1976). The

adsorption of hydroxamates is directly related to metal ion hydrolysis. It is important to achieve the correct pH range where the metals will hydrolyze to their hydroxide form (Palmer et al, 1975).

2.3.2 Substituents

Many chelating reagents are insoluble in water; it is a disadvantage to industrial applications. In mineral flotation, the formation of a copper chelate does not guarantee a good flotation response. The chelates must be able to attach well to air bubbles. Good air bubble attachment only occurs if the surface metal chelate contains a hydrophobic non-polar part. This is normally achieved by the presence of a long hydrocarbon chain in the non-polar structure of the collector molecule (Fuerstenau et al, 2000).

Studies done by Marabini et al (1991) created three main criteria for efficient chelate collector substituent formations. The position of the alkyl group should be diametrically opposite to the electron donor heteroatom. The para position allows the chain to be perpendicular to the surface for air attachment, while allowing the maximum reactivity between the surface and the functional group.

Straight chains increase the collecting power of a chelate whereas branched or unsaturated chains have adverse effects. The hydrophobicity and affinity for air of a metal chelate increases with the use of straight chains. Steric hindrance is the cause of lower recoveries of branched molecules. The increased cross sectional area of the collector molecule will block neighboring surface adsorption sites and reduce collector adsorption (Werneke and Jones, 1976). The ideal alkyl chain length is between three and six carbons. Straight chain alkyl groups are best when they are attached to aromatic rings with an ether oxygen group.

The presence of etheric oxygen allows for chain fluidity which directly affects the solubility of the reagent in water. An increase in carbons linked with oxygen, increases the

collecting power (Marabini et al, 1991). Water solubility can also be improved by the inclusion of groups with an affinity towards water molecules. Groups with this ability are the amino, the hydroxyl, the carboxyl, the carbonyl, the sulphonic and the phosphoric (Gutzeit, 1946).

2.3.3 Octyl Hydroxamate

Hydroxamic acids are a family of chelating agents that have undergone extensive testing for mineralogical applications. The first hydroxamate patent was obtained by a German scientist, Popperle. He proposed the used of hydroxamic acids or their salts as collectors in ore flotation (Fuerstenau and Pradip, 1983). This sparked many other scientists to explore hydroxamates further. Octyl hydroxamate in particular was first proposed by Peterson et al (1965), when they presented promising results with the use of octyl hydroxamate on chrysocolla. In 1969, a hydroxamate collector, NM-50, was developed by Gorlovski for the flotation of wolframite, cassiterite and rare-earth metal ores. De Cuyper (1975) began floating African copper-cobalt ores with alkyl hydroxamates. Plant-level studies with mixed collector systems involving alkyl hydroxamates and xanthates were conducted in China by Dekun et al (1984). Most recently in 2008, a Canadian mixed sulphide-oxide ore containing chalcopyrite, bornite and ore was successfully floated on a laboratory scale (Lee, et al, 2008).

Hydroxamic acid exists in two tautomeric forms Figure 2.13: hydroxyamide and hydroxyoxime. Infrared studies and UV spectral investigations have shown that metal complexes are only formed using hydroxyamide (Pradip and Fuerstenau, 1983).



Figure 2.13: Tautomers of hydroxamic acid, hydroxyamide (left) and hydroxyoxime (right)
(Pradip and Fuerstenau, 1983)

This structure has one replaceable hydrogen atom that substitutes for a metal cation. Ring closure occurs via the carbonyl oxygen. The mechanism for the formation of a metal complex is shown in Figure 2.14 (Fuerstenau and Pradip, 1984).

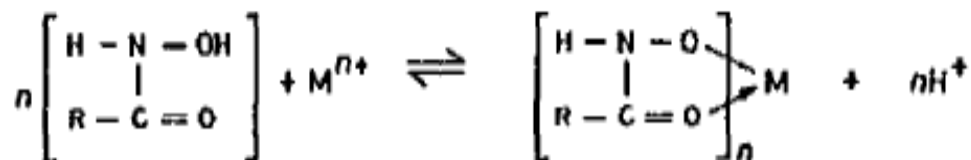


Figure 2.14 : Mechanism by which hydroxamic acids form metal complexes (Fuerstenau and Pradip, 1984).

The pKa of hydroxamic acids lies in the range of 7-9, indicating that they are weak donors (Pradip and Fuerstenau, 1983). The stability constants for different metal-hydroxamic metal complexes vary. The weakest complexes are formed with alkaline earth metals such as Ca^{2+} and Ba^{2+} . Transition metals form slightly stronger complexes, but the strongest complexes are formed with highly charged rare-earth elements, copper and iron. It has been suggested that the stability constants for metal complexes with lattice cations are greater for hydroxamates than they are for carboxylic acids (Fuerstenau and Pradip, 1984).

The mechanism for the adsorption of alkyl hydroxamate on mineral surfaces has been hypothesized to be a combination of chemisorption and surface reactions. Higher adsorption and flotation response has been found in the region of pH 8.5-9; the pK of the collector. (Peterson et al, 1965; Lenormand et al, 1979; Pradip and Fuerstenau, 1983; Fuerstenau and Pradip, 1984).

The chemisorption of potassium octyl hydroxamate on malachite has been proven by Lenormand et al (1979) using UV and IR analysis. The adsorption isotherm shown in Figure 2.15 has a large initial slope, indicating that it is a high-affinity type isotherm. According to the Giles

classification of isotherms, this indicates that the solid phase has a high affinity for the adsorbate (Hinz, 2001). Infrared spectra of malachite contacted with potassium octyl hydroxamate (Figure 2.16) shows the characteristic copper octyl hydroxamate band at $1,520\text{ cm}^{-1}$ although it is partly masked by malachite's carbonate peak at $1,498\text{ cm}^{-1}$.

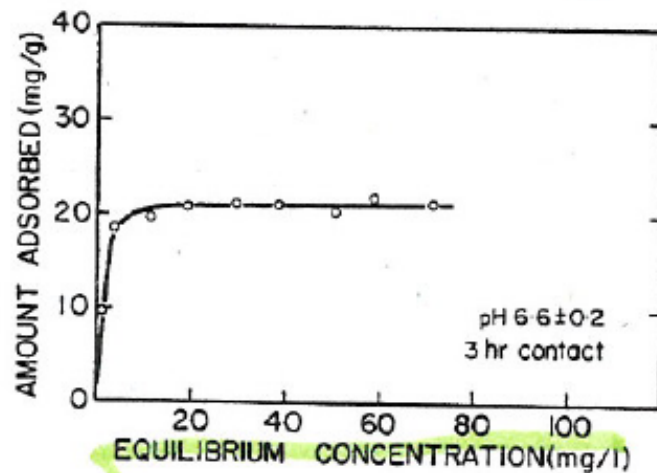


Figure 2.15 : Adsorption isotherm of octyl hydroxamate on malachite (Lenormand et al, 1979)

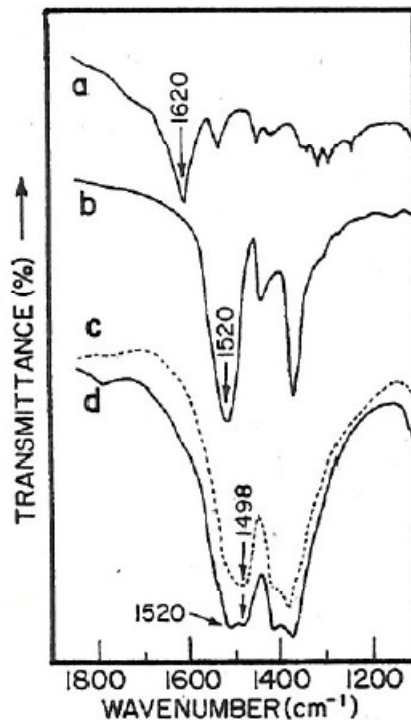


Figure 2.16: Infrared spectra of (a) potassium octyl hydroxamate, (b) copper octyl hydroxamate, (c) malachite and (d) malachite contacted with hydroxamate solution (Lenormand et al, 1979).

Despite the evidence that octyl hydroxamate is capable of chemisorbing onto a mineral surface, there are indications that mineral/collector interactions may also take place via surface reaction. The adsorption and flotation maximums occur around the pK of octyl hydroxamate independent of the mineral that is being collected. Interactions of hydroxamates with mineral surfaces are dependent on the physio-chemical characteristics of the mineral-water interface. Two different phenomena are thought to dictate mineral/hydroxamate interactions: hydrolysis of lattice cations and collector ionization.

The adsorption of anionic collectors like alkyl hydroxamates can be characterized using a mechanism of hydrolysable cationic species proposed by Fuerstenau and Pradip (1984). This mechanism takes place when the cations on the mineral surface hydrolyze in solution into a

variety of hydroxy complexes. These complexes then re-adsorb at the interface and assist in collector adsorption. A schematic of various hydroxylation methods is presented in Figure 2.17. The dotted line indicates the mineral surface; a cation is hydrolyzed if it has moved to the right (Pradip and Fuerstenau, 1983).

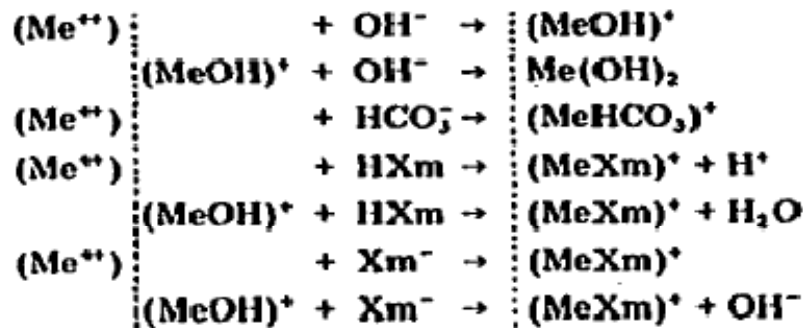


Figure 2.17: Possible hydroxylation reactions (Pradip and Fuerstenau, 1983).

A distinct drop in pH after adsorption has been noted. Similar to hydroxylation, collector ionization plays a role in adsorption. In the alkaline pH range, hydroxamate anions will dominate whereas in acidic ranges, neutral hydroxamic species play an important role. The neutral undissociated hydroxamate molecules contribute to adsorption. Trihydroxamate complexes form when a reaction with neutral hydroxamic species releases H^+ (Pradip and Fuerstenau, 1983).

Flotation using chemisorbing collectors is effective in the pH region where metal hydroxy-complexes predominate and can be further explained by bond energies (E) of copper ions. The following bond energies were outlined by Fuerstenau and co-workers (2000) :

$E_{lattice}$ = Bond energy of copper ions in the crystal lattice

$E_{chemisorption}$ = Bond energy of chelated surface copper ions

$E_{hydrolysis}$ = Bond energy of hydrolysed copper ions

$E_{chelate}$ = Bond energy of chelated copper in solution

By comparing the magnitude of these bond energies, the mechanism by which the collector adsorption would take place can be determined. This data is tabulated in Table 2.2.

Table 2.2: Comparison of bond energy magnitudes and their associated adsorption mechanism (Fuerstenau et al, 2000).

IF Bond Energy of	+ Bond Energy of	> Energy of	Then
Copper ions in the Mineral Lattice		Chelated Copper Ions in Solution	There is no chelating reagent adsorption or interaction with copper ions.
	Chelated Surface Copper Ions	Chelated Copper Ions in Solution	Chemisorption of the chelating reagent at copper surface sites takes place
Hydrolyzed Copper Ions		Copper Ions in the Mineral Lattice	Copper ions might be pulled out of the crystal lattice to form copper hydroxo complex at the interface; hydrolysis of the interfacial copper ions might then lead to surface chemical reaction
		Chelated Copper Ions in Solution	Copper hydroxide may precipitate
< Bond Energy of		Then	
Copper Ions in the Mineral Lattice	Chelated Surface Copper Ions	Chelated Copper Ions in Solution	Formation of a copper chelate precipitate in the solution adjacent to the surface may take place

Chemisorption allows for mono-layer coverage of a mineral surface. Since hydroxamates do not only interact via chemisorption, multi-layer formation is possible through hydrogen bonding or hydrophobic bonding between hydrocarbon chains as shown in Figure 2.18. Multi-layer formation will generally only occur after the initial chemisorbed mono-layer is formed.

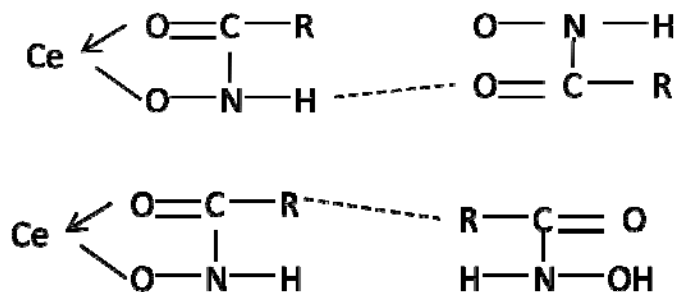


Figure 2.18: Mechanisms for multi-layer formation : hydrogen bonding (top) and hydrophobic bonding (bottom) (Pradip and Fuerstenau, 1983).

2.4 Summary

The above section is a general overview of copper oxide flotation. It encompasses the genesis of mixed sulphide-oxide copper ore and collection techniques. Sulphidization-flotation is outlined to show that it is a process in need of improvement. Chelating agents have been proposed as an alternative to collect both sulphides and oxides more economically and effectively.

The mixed copper ore that is to be studied has been found to contain predominantly bornite and malachite. Chelating reagents have shown promise in fundamental lab work to collect malachite. Hydroxamates seem to be the most promising form of chelating collector due to its solubility in water and its ability to form stable chelates with copper oxides. Factorially designed experiments will be performed to determine the statistical significance of various copper oxide flotation parameters.

Chapter 3

Materials and Methods

Investigations on chelating agents and mixed collector systems for the recovery of sulphide-oxide copper ores have been restricted to a limited amount of laboratory work. Although studies have been performed since the early 1920s, the behaviour of many minerals with chelating agents is not fully understood. Bornite and malachite are among the minerals for which the applicability of a mixed collector system has not been extensively investigated. This study incorporates fundamental adsorption and micro-flotation work with pure minerals to gauge the interactions between the minerals and the collectors on a flotation timescale. A factorial experiment design was also applied to bench-scale flotation to show the statistical significance of the flotation reagents on the recovery and grade of a raw bornite-malachite copper ore. The intent of this combination of pure mineral and natural ore studies is to obtain a deeper understanding of the mineral-collector interactions and collector effects. This understanding will be applied to propose flotation conditions towards optimization of the copper recovery and grade for a rougher stage concentrate of the raw ore.

3.1 Adsorption

The malachite and bornite samples used in the adsorption studies were obtained from Grenville Minerals in Kingston. The minerals had purities of 96.2% and 95.4 % respectively. The mineral samples were washed in ethanol before being pulverized to -200 mesh. The samples were wet screened into three size fractions: -200 +400 mesh, -400 + 635 mesh and -635 mesh. The malachite fractions were allowed to dry in an oven while the bornite samples were dried at 80 °C under argon. The bornite was stored in tightly sealed plastic bags in a freezer to minimize or to prevent oxidation. To determine the adsorption density of the collectors on malachite and

bornite, the surface area of each mineral size fraction was measured. This was done using the BET surface area technique with nitrogen which works on the basis of the adsorption of a N₂-He mixture on the mineral sample and its subsequent desorption. The specific surface area of the minerals is shown in Table 3.1.

Table 3.1: Specific surface areas (m²/g) of the mineral samples by mesh size.

	-200+400	-400+635	-635
Malachite	1.0647±0.0014	1.2201±0.0016	4.0124±0.0107
Bornite	0.1299±0.0016	0.2256±0.0011	0.7474±0.0012

Potassium amyl xanthate (PAX) was purified from a commercial grade reagent by dissolving it in acetone and re-crystallizing it in petroleum ether. The purified PAX crystals were stored in petroleum ether in the dark to avoid adverse effects of oxidation and of light exposure. The hydroxamate was Cytec Promoter 6494 provided by Cytec Industries Inc, located in Stamford, Connecticut, USA. According to this supplier, this is an un-diluted form of the commercial hydroxamate collector, Cytec Promoter 6494. The primary active ingredient is octyl hydroxamate; the reagent is a synthesized mixture with the alkyl chains ranging from 6-10 carbons. The reagent had a waxy consistency that required gentle heating to liquefy. Cytec Promoter 6494 had low solubility in water so a stock solution of 5 g/L in ethanol was prepared as described by Rao and Finch (2008). PAX and hydroxamate collectors were prepared to initial concentrations of 4×10^{-4} mol/L and 10^{-3} mol/L solutions respectively in de-ionized water. For pH adjustment of the collector solutions, a moderately concentrated solution of sodium hydroxide was used prior to contact with the mineral sample.

Adsorption measurements were conducted at ambient temperature in 50 mL Pyrex vials containing mineral samples with a surface area of 0.53 m². Depending on the surface area of the

mineral size fraction, the charges ranged from 0.50 g-0.71 g. The vials were then hand shaken at a constant rate for 15s, 30 s, 60s or 90s to approximate the conditioning time frame in a flotation cell. At the end of the contact period, the samples were quickly filtered via a vacuum assisted filtration system using a Millipore unit and a 0.45 micron membrane filter. A 5 mL sample of the filtrate was taken for UV analysis. This procedure was repeated for all combinations of both collectors and both minerals for the pH range of 5.5-11.5. Tests were performed at 1 pH increments. Analysis of the remaining collector in solution was carried out using a Cary 500 UV-Vis spectrophotometer at 301 nm and 190.5 nm (Lenormand et al, 1979; Rao and Finch, 2008) for PAX and hydroxamate respectively.

3.2 Micro-flotation and Eh-pH

The micro-flotation tests were performed in a 50 mL modified Hallimond tube (Partridge and Smith, 1971). The shaft of the flotation cell is approximately 19 cm long that opens up into a rounded conical section for concentrate collection. A short piece of Tygon tubing was located at the bottom of the rounded section in order to rinse out the concentrate. A fritted glass disk with 20 micron pores was located at the bottom of the flotation cell approximately 1 cm above the gas inlet. The cell was agitated using a Teflon coated magnetic bar and a laboratory stirrer from Fisher Scientific. Nitrogen gas via a pressurized cylinder was used to produce bubbles and was regulated to a constant flow rate of 65 mL/min using a flow meter. A schematic of the micro-flotation cell is shown in Figure 3.1.

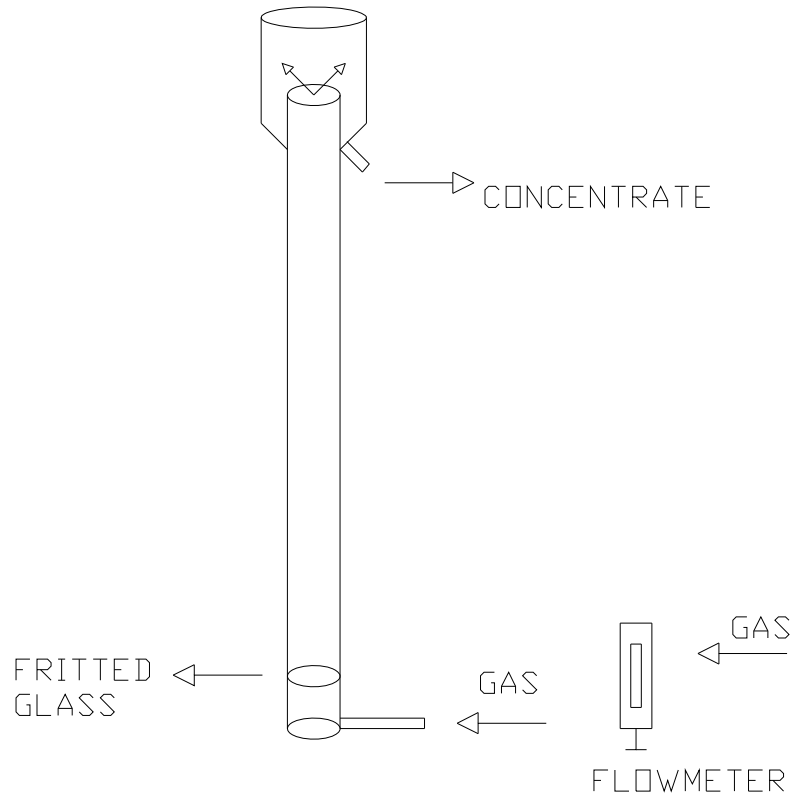


Figure 3.1 : Schematic of the modified Hallimond tube used for micro flotation.

The flotation charges were 0.5g of the -200+400 mesh fraction of the malachite and bornite prepared for the adsorption testing. PAX and the hydroxamate Cytec Promoter 6494 were prepared to a concentration of 4×10^{-4} mol/L using de-ionized water. This collector concentration is in accordance with micro-flotation studies done with chrysocolla by Peterson et al (1965). A third collector, N-phenylbenzohydroxamic acid (Agrawal and Tandon, 1973) was also prepared to the same concentration. Throughout this thesis, N-phenylbenzohydroxamic acid, shown in Figure 3.4, will be referred to as the “N-benzoyl” collector. The Cytec Promoter and N-benzoyl experienced solubility problems in water. These collectors were prepared 6 hours before the

micro-flotation tests and were set to stir on a magnetic stir plate. A 0.1 wt% amyl alcohol solution was used as a frother. HCl and NaOH solutions were used for pH adjustments.

The mineral charge was added to the flotation cell with approximately 20 mL of de-ionized water and stirred as the pH was adjusted to the desired level. The minerals were conditioned with the collector for 3 minutes followed by 30 s conditioning with amyl alcohol. The pH was re-adjusted after the collector addition to ensure that flotation occurred at the target pH. The flotation time was 2 minutes after which the concentrate and tailings fractions were washed into beakers and gravity filtered. They were dried on filter paper at room temperature. Once dry, the concentrate and tailings were weighed and the fractional flotation recovery was calculated. This procedure was repeated for the pH range of 5.5-11.5 with flotation tests occurring at intervals of about 1 pH unit.

To obtain the Eh-pH data readings, the redox potential in the cell was measured at three points. The redox of the mineral in DI water was measured at the target pH before collector addition; after collector addition; and, after the flotation was completed. This data was analysed using a computer program, SOLGASWATER. This program was developed in order to calculate the equilibrium compositions in multi-phase systems using the free-energy minimization technique (Eriksson, 1976).

3.3 Bench Scale Flotation

Flotation of a sulphide-oxide copper ore was performed on a laboratory bench scale basis. The economic copper minerals in the ore are bornite (Cu_5FeS_4) and malachite ($\text{Cu}_2(\text{OH})_2\text{CO}_3$). The ore is from an oxidized copper deposit in Sivas province of Turkey and was provided courtesy of Coban Resources.

An XRD analysis was performed on the ore sample. Bornite and malachite were found to be the economic copper minerals in the ore. The mineral assemblage of the matrix was a typical porphyry copper makeup. Gangue minerals were: quartz (SiO_2), albite ($\text{NaAlSi}_3\text{O}_8$), muscovite ($\text{KAl}_2(\text{AlSi}_3\text{O}_{10})(\text{F},\text{OH})_2$), calcite (CaCO_3) and clinochlore ($(\text{Mg},\text{Fe}^{++})_5\text{Al}(\text{Si}_3\text{Al})\text{O}_{10}(\text{OH})_8$). These minerals form as a result of hydrothermal metamorphism during the formation of a porphyry copper deposit. These minerals all possess the ability to generate slimes. Each of the minerals originates in a different alteration zone of a porphyry copper deposit. The albite forms in the potassic alteration zone of a porphyry copper deposit and the quartz and muscovite form in the proximal phyllitic zone. These two zones are most closely associated with the ore deposit. Further away, the calcite and the clinochlore form in the propylitic and argillic alteration zones. The argillic region is the most distal to the ore body and is characterized with clay minerals, such as clinochlore. They are all seen together because the crushed flotation feed was studied as opposed to hand samples.

A study of polished sections revealed that there are occurrences of other copper minerals such as: covellite (CuS), chalcocite (Cu_2S), chalcopyrite (CuFeS_2) and azurite ($\text{Cu}_3(\text{CO}_3)_2(\text{OH})_2$) and chrysocolla ($(\text{Cu},\text{Al})_2\text{H}_2\text{Si}_2\text{O}_5(\text{OH})_4 \cdot n\text{H}_2\text{O}$). The minor sulphides often occur in conjunction with bornite; sometimes replacing it. The minor oxides occur together and are often intergrown. The oxides and sulphides can be observed cross cutting the gangue minerals. Since no hand samples were available to study the mineral relationships, further analysis of mineral habits cannot be determined.

The natural ore sample was crushed to less than 10 mesh using a gyratory crusher. 4 kg of crushed silica (SiO_2) was added to the 21 kg of sample to create a test ore that had a copper head grade of approximately 5 %. The sample was then split into 885 g charges using a rotary splitter and stored in the freezer in tightly closed plastic bags to prevent oxidation. Prior to flotation, each charge was ground with 477 mL of tap water (65 w/w % solids) in a Denver laboratory rod

mill. The total weight of the mild steel rods was 14 kg. Grinding times ranged between 10 minutes for the exploratory work and 12 minutes for the preliminary testing and factorial experiment. Figure 3.2 shows the particle size distribution of each grinding time. Bench scale flotation was carried out in a 2 L Denver cell using a Denver flotation machine, Kingston, Ontario tap water and air. Flotation tests were carried out at about 20 °C and a constant impeller speed of 1200 rpm. A schematic of the bench scale flotation can be seen below in Figure 3.3.

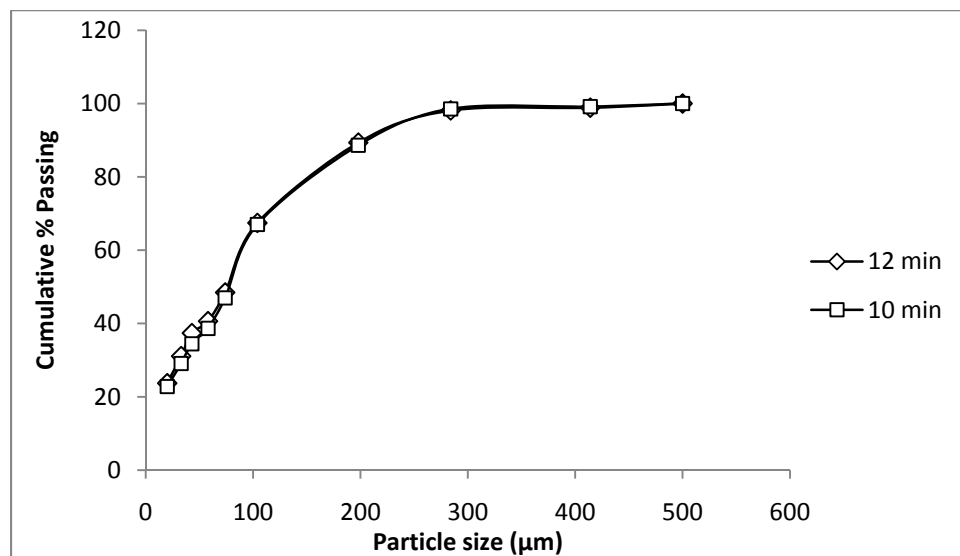


Figure 3.2: Cumulative passing size of the bench-scale flotation charges.

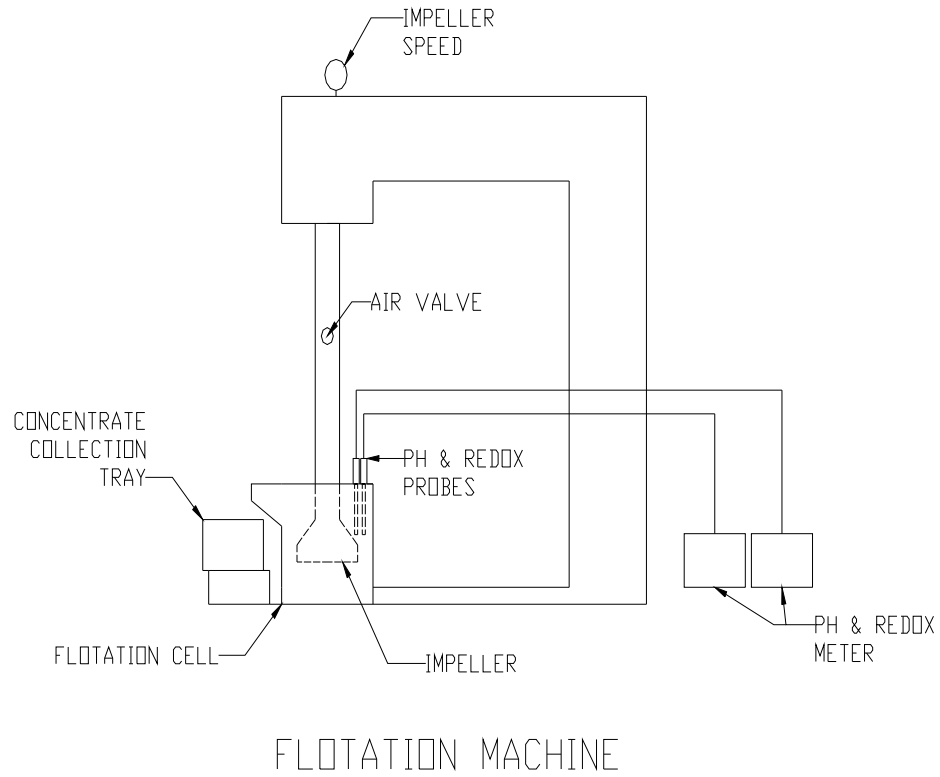


Figure 3.3: Bench scale flotation apparatus.

Four stages of bench scale flotation took place:

1. Exploratory work
2. Preliminary investigations
3. Box-Behnken factorial experiment
4. Limited amount of work using N-phenylbenzohydroxamic acid

The results of the bench scale flotation are presented in Chapter 4.

3.3.1 Exploratory Work

The exploratory work was performed in order to get a sense of how the natural ore behaved during flotation and responded to collectors. The charge was ground for 10 minutes in the rod mill and promptly transferred to the Denver cell for flotation. A 0.1 wt % PAX solution was used as the collector along with a 0.1 wt % DowFroth 250 frother. The reagents were prepared with commercial grade products and Kingston tap water. Other reagents used were sodium silicate, Cytec Promoter 6494 and DETA. Flotation times for the exploratory work ranged from 20-22 minutes with varying collector dosages and reagents. The metal assays of the flotation products were performed using a Perkin-Elmer Model 2380 Atomic Adsorption spectrophotometer. Sulphur and carbon analysis were performed using a LECO SC-444DR sulphur and carbon analyser. It was assumed that the sulphur and carbon present were only due to bornite and malachite. Thus, the mineral recoveries could be calculated using the S and C recoveries.

Due to the discovery of some sliming problems in the exploratory work, the original 885g charges were de-slimed after the 12 minute grinding cycle for the preliminary investigations. Each charge was de-slimed for 55 minutes using a vibrating 20 micron (635 mesh) screen and cold tap water. Both the over and under size fractions from the de-sliming process were filtered using a pressure filter. The oversize fraction became the new flotation charge and was stored slightly damp in the freezer until required. The slime fraction filter cake was allowed to dry at ambient temperature for several days. It was weighed to determine the weight of the flotation charge by difference.

3.3.2 Preliminary Testing

The preliminary investigations consisted of 4 tests to determine reasonable levels of reagent for the Box-Behnken factorial design. Collector levels from literature were used as

guidance. Lee et al (2008) and Dekun et al (1984) were two groups of investigators that had attempted a mixed collector system for the flotation of a sulphide-oxide copper ore. In the current investigation, varying dosages of Cytec Promoter 6494, a 0.1 % commercial PAX solution and DETA were investigated. The metal, sulphur and carbon analysis was performed identically to the exploratory work.

3.3.3 Box-Behnken Design

A goal of this thesis was to propose flotation conditions for the natural ore to optimize copper recovery, copper grade and malachite recovery. In order to do this, response surface methodology was used. Response surface methodology is a combination of statistical and mathematical methods useful for the modeling and analysis of engineering problems (Aslan and Cebeci, 2007). This area of experimental design is used to construct a two-dimensional model called a response surface. This surface is the response plotted based on two explanatory variables that allow for a maximum or minimum response to be pinpointed should it exist within the experimental region (Sall et al, 2005). Response surface experiments also allow for the characterization of the response functions in the region of interest of the experiment and allow for statistical inferences about the sensitivity of the response to the explanatory variables (Mason et al, 1989).

An experimental technique for finding optimum responses is to change one variable at a time. This one-factor-at-a-time strategy is where each factor is individually increased or decreased in order to find the optimum response. This technique not only often fails to find the optimum response; it does not take into account any factor interaction effects (Mason et al, 1989). The technique fails in dynamic multivariate systems where more than one response is significant (Aslan and Fidan, 2008). Two significant responses of froth flotation are to achieve the highest

possible recovery and at an acceptable metal grade. Froth flotation is a dynamic process governed by many sub-processes and interactions that can make it difficult to interpret the effects of explanatory variables in a classical experiment design (Aslan and Fidan (2008); Nanthakumar and Kelebek, (2007); Santana et al (2008)). Statistical methods have not been applied to mineral processing systems to the extent that they have been applied to chemical engineering processes; though, some researchers have successfully characterised and modeled flotation systems. A factorial experiment design performed by Martinez et al (2003) explored the effects of pH, depressant concentration and mineral grade on the floatability of celestite. Aslan and Cebeci (2007) used response surface methodology and a Box-Behnken design to model and optimise processing of some Turkish coals. It has been used to perform stage wise analysis of oxidized pentlandite and pyrrhotite (Nanthakumar and Kelebek, 2007) and to quantify the effect of particle size and reagent dosages on apatite flotation (Santana et al, 2008).

Response surface designs typically begin with a series of experiments designed to find the path of steepest ascent. This initial stage features small areas of interest and usually involves standard two-level factorial designs fitted with first-order models. These equations derived from the first-order models provide the direction toward the surface optimum (Mason et al, 1989). The standard two-level factorial designs are only useful for quantifying the variable effects and finding the path of steepest ascent. Three distinct values for each factor are required to fit a quadratic function; so, these two level designs cannot detect curvature (Sall et al, 2005). There are several different ways to fit response surfaces. Three-level factorial designs (3^k) can be used, but become impractical as the number of factors increase. Regardless of the exponential growth in the number of observations required, these models are not rotatable. Rotatability refers to the property where variance in fitted responses is a function of the distance from the center of the factor space. Rotatability is a desirable property as the orientation of the design with respect to the response surface is unknown (Mason et al, 1989).

There are alternatives to the 3^k factorial design. The most popular response surface design is the central composite design (CCD). This rotatable design augments an ordinary two-level factorial design with center points and axial points. The CCD disadvantage is that axial points require extreme values that may be unrealistic due to engineering considerations (Sall et al, 2005). For example, if collector addition were to be an explanatory variable for a froth flotation process, the axial points would represent either very high or very low collector dosage. In the case of high collector dosage, gangue minerals would be activated, resulting in poor grades. Situations like this are not only undesirable, but unrealistic to practical application.

The Box-Behnken design combines a fractional factorial design with an incomplete block design (Sall et al, 2005). This design places points at the mid-points of the edges of the process space with none on the vertices. If the process space was pictured as a sphere inside of the cube described by a 3^k factorial design, the design points of the Box-Behnken would all be located on the sphere or at its center. The Box-Behnken design is advantageous over the CCD design because it requires fewer runs, avoids the unrealistic axial points and is rotatable.

For the study of the raw bornite-malachite ore, the number of samples was a limiting factor. After the exploratory work and the preliminary investigations, only 18 samples remained. With a limited amount of samples, no initial testing to determine the path of steepest ascent was possible. This meant that the process region would have to be fairly large in order to include an optimum. The explanatory variables chosen to model a rougher concentrate stage for the raw ore were PAX, hydroxamate and DETA dosages. The coded levels of the variables can be seen in Table 3.2. The flotation runs of the Box-Behnken design were run in a random order to minimize systematic errors.

Table 3.2: Experimental design for bench-scale Box-Behnken design.

Std. Order	Run Order	Coded Variables			Actual Level of Variables		
		PAX (x_1)	Cytec 6494 (x_2)	DETA (x_3)	PAX (g/t)	Cytec 6494 (g/t)	DETA (g/t)
1	7	-1	-1	0	0	0	53
2	1	1	-1	0	71	0	53
3	6	-1	1	0	0	408	53
4	2	1	1	0	71	408	53
5	11	-1	0	-1	0	204	0
6	9	1	0	-1	71	204	0
7	4	-1	0	1	0	204	106
8	10	1	0	1	71	204	106
9	12	0	-1	-1	35	0	0
10	3	0	1	-1	35	408	0
11	14	0	-1	1	35	0	106
12	8	0	1	1	35	408	106
13	15	0	0	0	35	204	53
14	5	0	0	0	35	204	53
15	13	0	0	0	35	204	53

The thawed, de-slimed charges were washed into the Denver cell and allowed to heat to 20 °C before flotation. The pH of the pulp for flotation was the natural pH of the ground ore, which was approximately pH 7.85. The rougher flotation was conducted over six concentrate stages with equal reagent dosages. PAX and DETA were added as 0.1 wt % solutions and Cytec Promoter 6494 and the pine oil frother were added drop-wise from 10cc syringes. The first concentrate was allowed 2 minutes conditioning time followed by 1 minute flotation time. The subsequent concentrates all had 1 minute conditioning times. Concentrates 2 and 3 were collected for 2 minutes each while concentrates 4 and 5 were collected for 3 minutes. Concentrate 6 was collected for 4 minutes. The low level was set as 0 g/t in order to investigate the collectorless flotation of the raw ore. The metal, sulphur and carbon analysis was performed identically to the exploratory work and preliminary investigations.

JMP 7, a statistical software program, was used to analyse the data to fit models, perform canonical analysis and interpret the response surfaces to determine optimal operating conditions. Four models were constructed to examine copper recovery, copper grade, malachite recovery and bornite recovery.

3.3.4 N-phenylbenzohydroxamic acid

As a final investigative test, the N-benzoyl collector, shown in Figure 3.4, was used on the natural bornite-malachite ore at the same collector concentration as the mid and high level hydroxamate additions. To be precise, tests B6 and B10 from Table 3.2 were re-run with the alternative N-benzoyl hydroxamate collector.

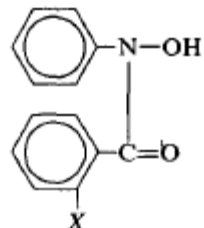


Figure 3.4: Structure of N-phenylbenzohydroxamic acid (Agrawal and Tandon, 1973).

Barbaro et al (1997) studied a synthetic reagent with an alkyl chain as well as an aminothiophenol chelating group on the flotation of chrysocolla. The potential benefit of collectors with aromatic ligands is their hydrophobicity. The formation of a surface copper-chelate is only half of the requirement for effective flotation. The chelate must have a hydrophobic constituent capable of attaching to air bubbles (Fuerstenau et al, 2000). The benzene rings present in the N-benzo collector are strongly hydrophobic. It was found that chrysocolla responded to this aliphatic-aromatic compound in a pH range of 5.5 to 6. The N-benzoyl was initially added in powder form, but encountered significant solubility issues. The higher collector dosage was dissolved in 250 mL of de-ionized water so that the collector could be added in

solution. To dissolve the solid, it was heated to approximately 70 °C on a hot plate and measured just before addition to the flotation cell.

Chapter 4

Results and Analysis

This chapter presents the results of the experimental work outlined in Chapter 3. Section 4.1 describes the results of the adsorption testing of PAX and hydroxamate on pure malachite and bornite. The results of the micro flotation are presented in Section 4.2 along with the speciation diagrams developed in SOLGASWATER. Through a Box-Behnken response surface design, statistical models were developed for copper recovery, malachite recovery, minor copper recovery and copper grade. The results were modeled with the statistical software, JMP, to determine the significant effects and possible optimum flotation conditions. Section 4.3 presents the models as well as an assessment of their adequacy. The results of the investigation into an aromatic chelating collector, N-benzoyl, are presented in Section 4.4.

4.1 Adsorption

Four different adsorption systems were investigated: malachite-PAX, bornite-PAX, malachite-hydroxamate and bornite-hydroxamate. For each system, the adsorption density was analyzed both in terms of adsorption kinetics and pH effects. The raw adsorption data can be seen in Appendix B.

4.1.1 Malachite-PAX

The adsorption behaviour of hydroxamate on malachite as a function of time is shown in Figure 4.1. The initial concentration of PAX is 4×10^{-4} mol/L in each case. The time scale is limited to 90s, which is representative of a typical flotation conditioning time. At 90s, the malachite and PAX system has not achieved an equilibrium state. Adsorption density is

continuing to rise at every pH level. In the range of pH 7.5-10.5, the adsorption density curves are beginning to level off, indicating that the system equilibrium could be close. This plateau also indicates that there is a faster approach to equilibrium in the pH 7.5-10.5 range and this may be related to mineral solubility. The cross-sectional area of a PAX molecule is 29 \AA^2 , giving it a vertical monolayer at $5 \mu\text{mol}/\text{m}^2$. The mechanism by which PAX adsorbs onto a mineral surface has been studied by Mielczarki and coworkers (1989). They determined that PAX begins to chemisorb onto mineral surfaces to a certain degree. The hydrophobic collector layers formed by PAX have been described as amorphous and un-even; this results in un-even distribution of layer thicknesses across the mineral surface. If the system is indicating the formation of 6 collector layers, it is not likely that they are 6 complete and uniform layers. It should also be noted that these are calculated values corresponding to hypothetical layers. Results of these calculations provide no information on physical state of collector layers. A surface analytical method such as ToF-SIMS should provide some details on this matter (Hart et al, 2009). Furthermore, the presence of so many collector layers on the surface of malachite is not necessarily an indicator of good flotation. This is due to the fact that xanthate collector coatings are known to be unstable on oxide surfaces and have a tendency to slough off in the flotation cell.

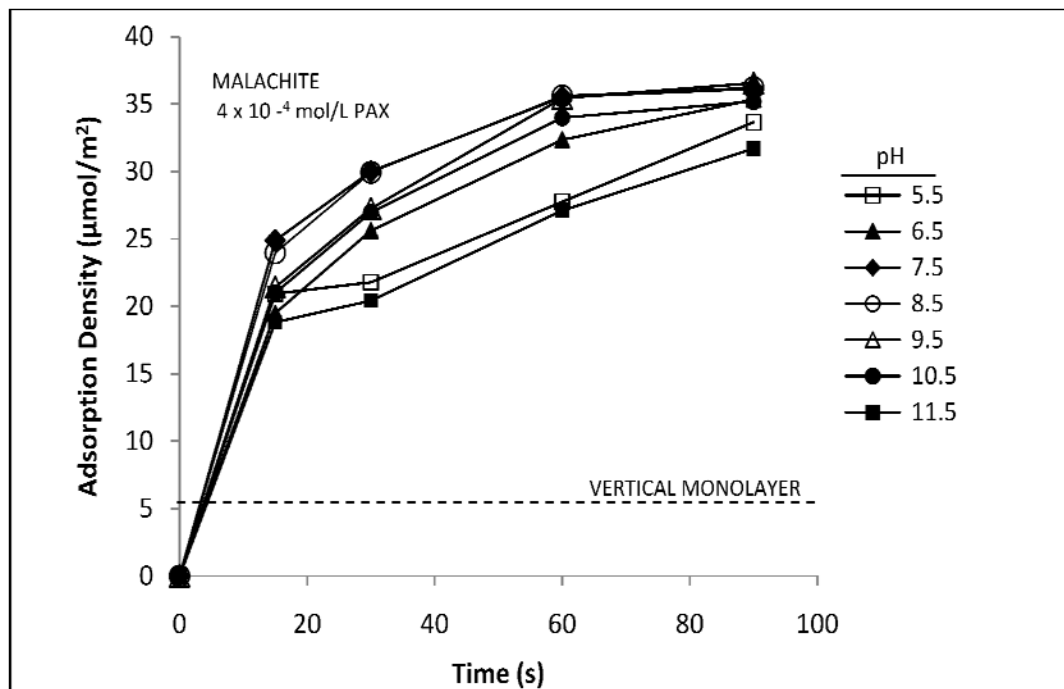


Figure 4.1 : The kinetics of PAX adsorption on malachite.

The effect of pH on adsorption density can be seen in Figure 4.2. The highest adsorption density was $36.56 \mu\text{mol}/\text{m}^2$. This value is achieved at pH 9.5. There is a slight peak at pH 7.5 at 30s, but decreases as contact time increases. The drop in adsorption density to either side of the peak is close to symmetric, with a sharper decline on the alkaline side. There is also a decrease in collector layers towards the alkaline range. At pH 9.5, where the highest adsorption density was achieved, there were 6.4 collector layers. At the most alkaline pH of 11.5, the sixth collector layer was incomplete. This behaviour was consistent with the micro-flotation behaviour, which will be discussed in Section 4.2.

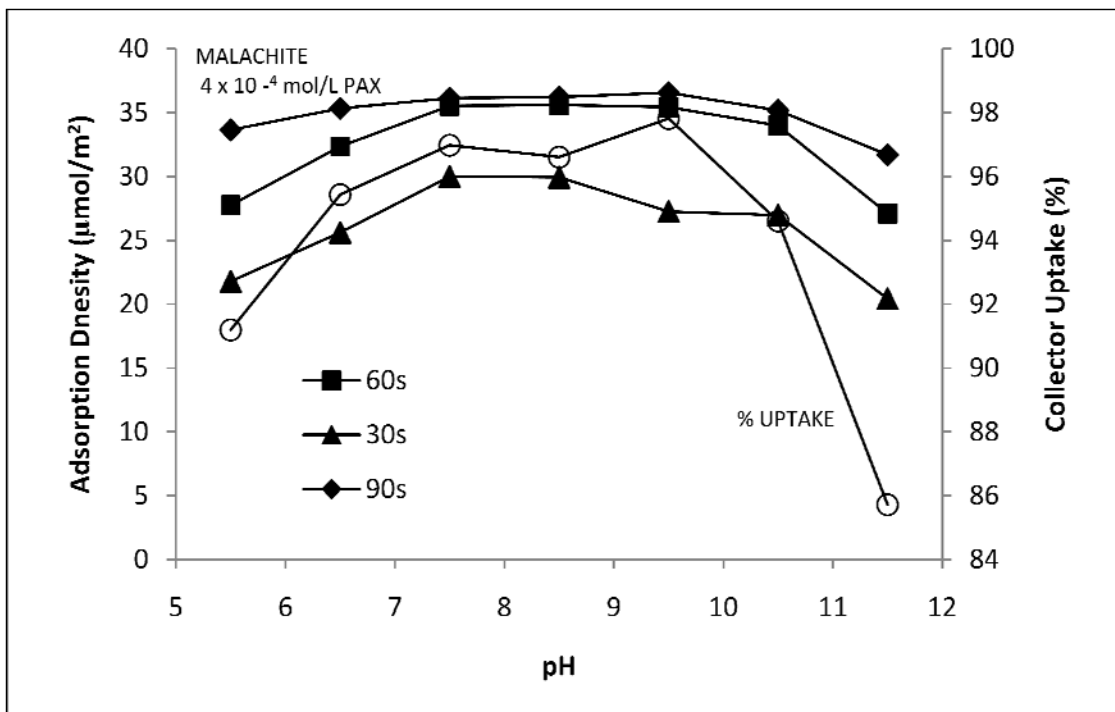


Figure 4.2 : The effect of pH on PAX adsorption density on malachite.

4.1.2 Malachite-Hydroxamate

The malachite-hydroxamate system was investigated using an initial collector concentration of 10^3 mol/L in order to remain in the linear calibration zone. The uptake of hydroxamate on the malachite surface is shown in Figure 4.3. A feature of these adsorption density curves is that equilibrium is reached on a scale of 15 s. The collector solution was a cloudy milky white. After 15 s, the filtrate was considerably clearer. The system achieves a horizontal monolayer (55 \AA^2), and the higher energy vertical monolayer, (20.5 \AA^2) almost instantaneously upon collector contact with the mineral. These monolayers correspond to adsorption densities of $8 \mu\text{mol}/\text{m}^2$ and $3 \mu\text{mol}/\text{m}^2$ respectively. Significant multi-layer adsorption occurs by either hydrogen bonding or hydrophobic bonding through the hydrocarbon chains (Pradip and Fuerstenau, 1983). At the end of the 90s adsorption time, there were calculated to be

9 layers of hydroxamate. This confirms reports by several researchers that hydroxamate adsorption occurs through chemisorption as well as a surface reaction. The chemisorbed monolayers occur within the first 15 s of contact time. The adsorption mechanism then switches to the surface reaction mechanism.

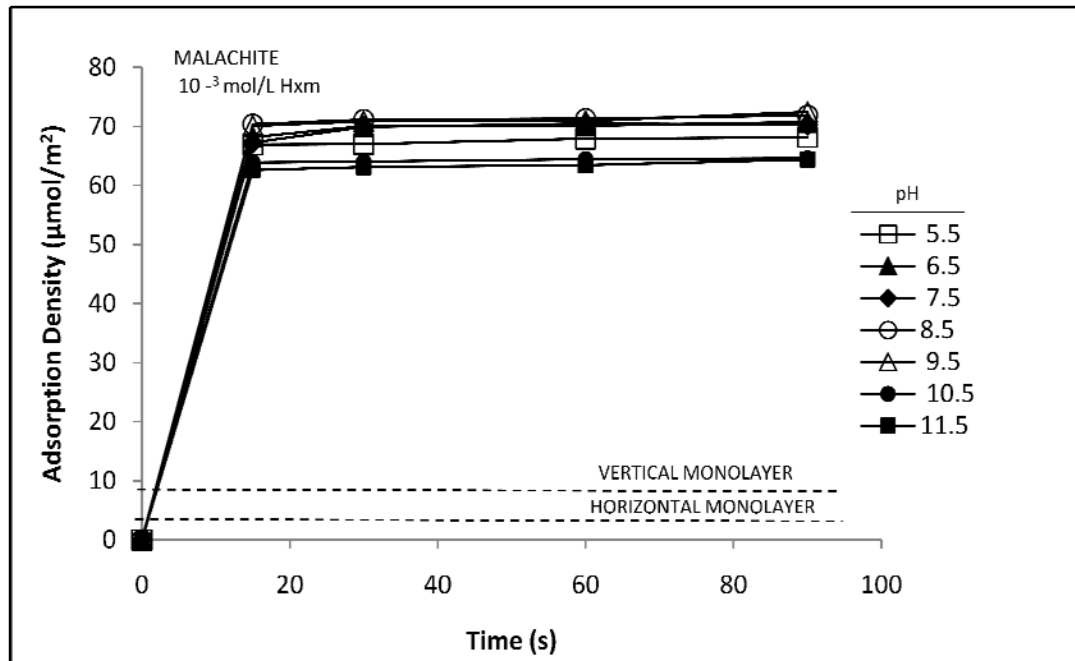


Figure 4.3 : The kinetics of hydroxamate adsorption on malachite.

The effect of pH on the adsorption of hydroxamate on malachite can be seen in Figure 4.4. The characteristic adsorption peak at pH 9.5 is present corresponding to a maximum adsorption density of $72.44 \mu\text{mol}/\text{m}^2$. In general, there is a trend towards a peak around pH 9.5. There is a dip in adsorption density at pH 7.5 which could correspond to the solubility of malachite in near-neutral water noted by Poling (1973). It was found that malachite has a tendency to dissolve in this pH range. The peak around pH 9.5 is not symmetrical. In the lower pH range, hydroxamate appears to be adsorbing better than in the alkaline region. This effect is also mirrored by the number of collector layers deposited on the mineral surface. At the pH of

maximum adsorption, 9 collector layers were deposited. Above pH 10.5, only 8 collector layers were deposited. In the acidic region, the 9th collector layer was incomplete. The flotation recoveries corresponding with pH 5.5 are poor, indicating that true adsorption did not take place. Instead, precipitation of copper hydroxamate is occurring; the concentration of Cu²⁺ ions in solution is high below pH 6 (Lenormand et al., 1979). The right hand portion of the curves drops more sharply due to a greater competition by adsorption of OH⁻ ions and possible repulsion between the hydroxamate anions and the negatively charged malachite surface.

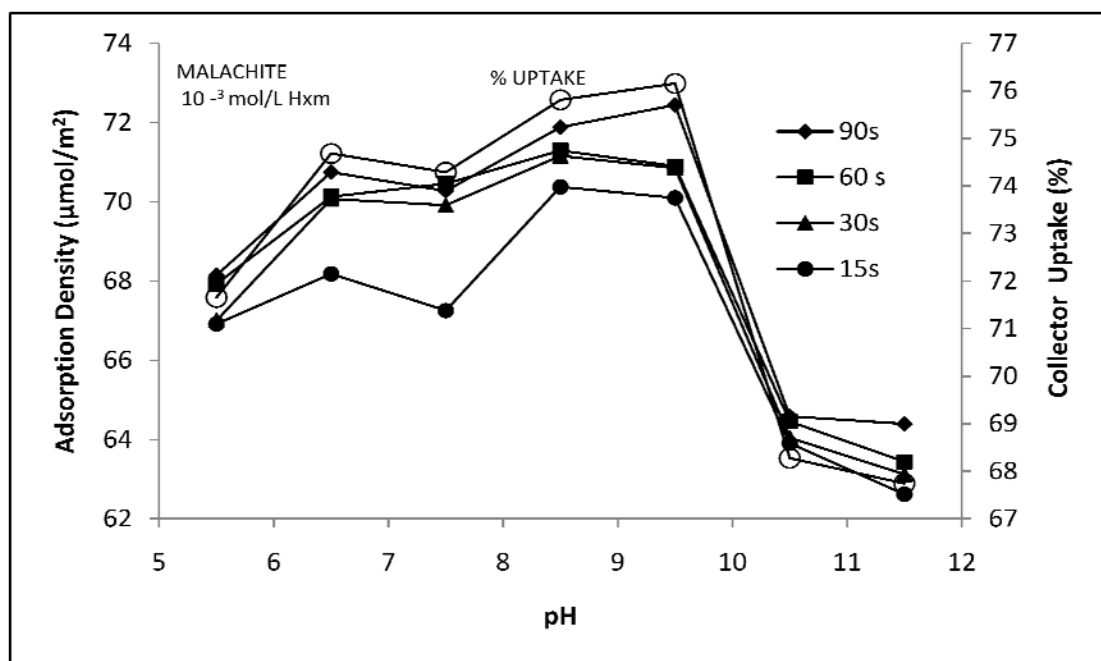


Figure 4.4 : The effect of pH on the adsorption of hydroxamate on malachite.

4.1.3 Bornite-PAX

The adsorption of bornite on PAX as a function of time is shown in Figure 4.5. The bornite-PAX system behaved in a surprising manner. PAX is a conventional thiol collector commonly used for sulphide collection. It was assumed that PAX would adsorb readily onto the

bornite surface. The bornite showed negligible adsorption on PAX in the 90s contact time used for malachite. This was odd because high bornite flotation recoveries are achieved with PAX. When the time was increased to 120 s, it showed some adsorption. When given a 360s contact time, it showed no further adsorption indicating that it had reached equilibrium. The final adsorption density reached was $17.5 \mu\text{mol}/\text{m}^2$. Despite the low PAX adsorption density, there was formation of a monolayer. The monolayer was formed in approximately 40 s, almost twice the time it took to establish a monolayer on the malachite surface. When the system reached equilibrium, 3 layers of collector were deposited on the bornite surface.. This is half the number of collector layers than were deposited on the surface of malachite.

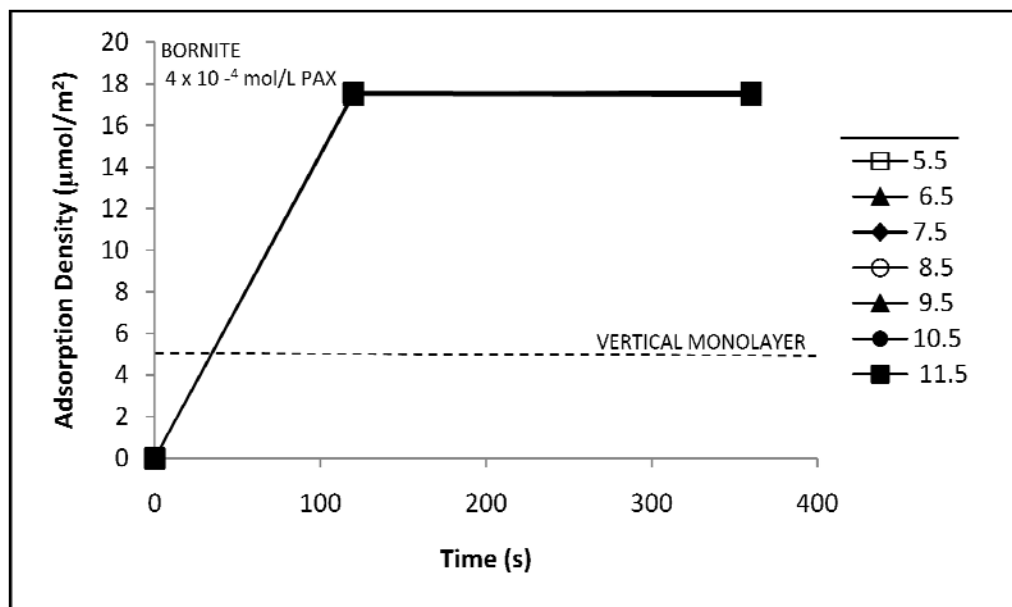


Figure 4.5: The kinetics of PAX adsorption on bornite.

The effect of pH on the adsorption of PAX on bornite was negligible. This is demonstrated below in Figure 4.6. The adsorption density stays close to constant across the entire pH range. Fluctuations are mostly likely caused by experimental or measurement error; the collector uptake remains constant across the entire range. The micro-flotation behaviour of

bornite with PAX corresponds to the adsorption behaviour presented here. There is a similarity in pH independence in the adsorption and micro-flotation, which will be presented in the next section. The small amount of adsorption suggests that the bornite surface was possibly pre-coated by elemental sulphur. This might have blocked the metal sites on bornite and adversely affected xanthate adsorption. The amount of elemental sulphur on pyrrhotite was quantified by Kelebek and Nanthakumar (2007). It is known that elemental sulphur or polysulphide formation is preceded by an iron deficient sulphur rich surface which eventually transforms itself into a hydrophobic state (Buckley et al, 1985).

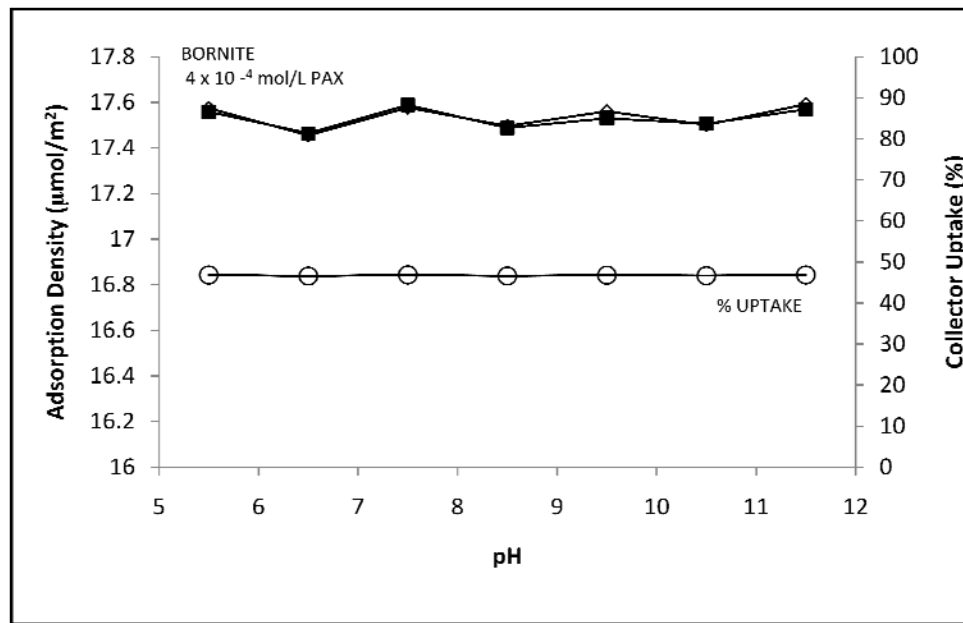


Figure 4.6 : The effect of pH on the adsorption and the uptake of PAX on bornite.

4.1.4 Bornite-Hydroxamate

An initial collector dosage of 10^{-3} mol/L was used for the bornite adsorption tests.

Figure 4.7 shows the kinetics of the adsorption of hydroxamate on bornite. Similar to malachite, hydroxamate adsorbs onto bornite very rapidly. A horizontal mono layer is formed almost instantaneously and followed by a vertical mono layer. The former is consistent with a sulphur

rich bornite surface, which probably has a patchy characteristic with a partial exposure of metal sites (Chander, 1991). It should also be noted that such a surface structure is subject to change by attrition during agitation. Equilibrium is established in 15 s across the entire pH range. A colour change in the adsorption filtrate was noted after 15 s. The adsorption density achieved by bornite is comparable to the adsorption density of hydroxamate with malachite. After the formation of the high-energy vertical monolayer, approximately 8 more collector layers are deposited via surface reaction. The number of collector layers deposited decreases as pH increases. At the highest adsorption density, a 9th collector layer is over half complete. At pH range of 10.5-11.5, there are 7.5 layers of collector.

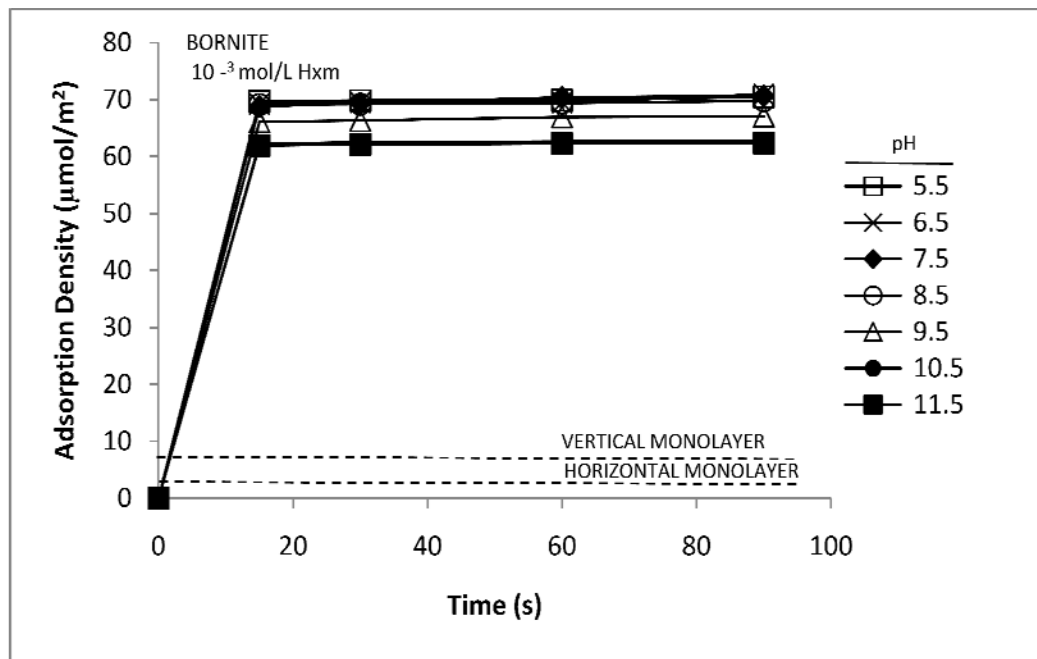


Figure 4.7 : The kinetics of hydroxamate adsorption on bornite.

Figure 4.8 presents the effect of pH on hydroxamate uptake by bornite. The characteristic peak at pH 9 is not seen with bornite; instead a maximum adsorption density is reached at pH 6.5. Studies on the oxidation of bornite done by Fullston et al (1999) have shown that copper hydroxide begins to form on the bornite surface at pH values above pH 6. This could indicate

why the adsorption density of hydroxamate on bornite begins to drop after pH 6. The hydroxamate collector molecules have less copper sites to chelate; copper sites are increasingly transformed to copper hydroxide. The surface of bornite is negatively charged in alkaline regions so that hydroxamate anions must overcome repulsive forces. The adsorption behaviour between bornite and hydroxamate is mirrored in the micro-flotation results presented in Section 4.2.

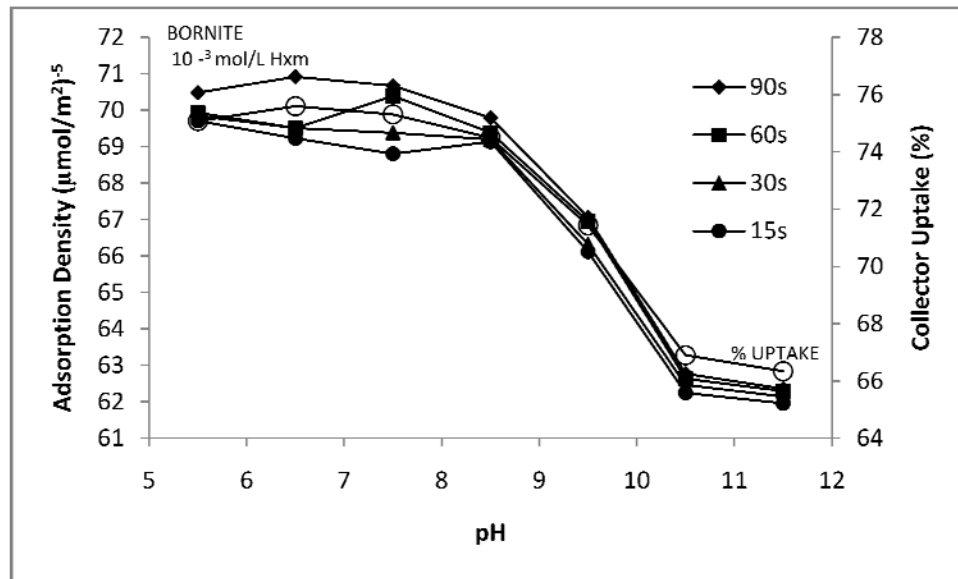


Figure 4.8: The effect of pH on hydroxamate adsorption and collector uptake on bornite.

4.2 Micro-flotation and Eh-pH

The micro-flotation behaviour of pure mineral systems was investigated to study the effect of pH and collector type. The micro-flotation experiments were carried out using 0.5 g chargers in a modified Hallimond tube with a constant collector concentration of 4×10^{-4} mol/L. The results for the micro-flotation of malachite and bornite with PAX, hydroxamate and N-benzoyl are reported in Section 4.2.1, Section 4.2.2 and Section 4.2.3 respectively. Eh

measurements were taken in order to examine collector behaviour. The raw micro-flotation and Eh-pH data can be seen in Appendix B.

4.2.1 PAX Micro-flotation

The effect of pH on the flotation of malachite and bornite with PAX is shown in Figure 4.9. This figure represents the fractional weight recovery of the mineral with respect to pH.

Bornite is more effectively floated than malachite despite lower collector uptake and adsorption density. The presence of elemental sulphur can contribute to this flotation behaviour of bornite since elemental sulphur is strongly hydrophobic. This is also likely due to the fact that the xanthate coating on malachite is easily sloughed off during flotation. Castro et al (1976) reported that PAX can attack oxide surfaces and react with dissolving metal species. Once the mineral begins to dissolve, PAX will react to form a precipitate instead of acting as a collector. Malachite floats relatively well in the narrow pH range of 7.5-9.5. The recovery peaked at 98 %. The flotation rate for malachite in this pH range was rapid; most of the malachite was collected within the first 15 s of the 2 minute collection time. The lowest malachite recoveries occurred in the extreme pH regions. At high and low pH, the flotation rate was considerably slower and the liquid in the cell became slightly yellowish. At high pH values, the liquid in the cell was only slightly yellow while at pH 5.5, the liquid in the cell became distinctly yellow after collector addition. This is indicative of dissolved copper in solution reacting with the PAX to form a precipitate. The lowest recovery was at pH 5.5 due to copper precipitation.

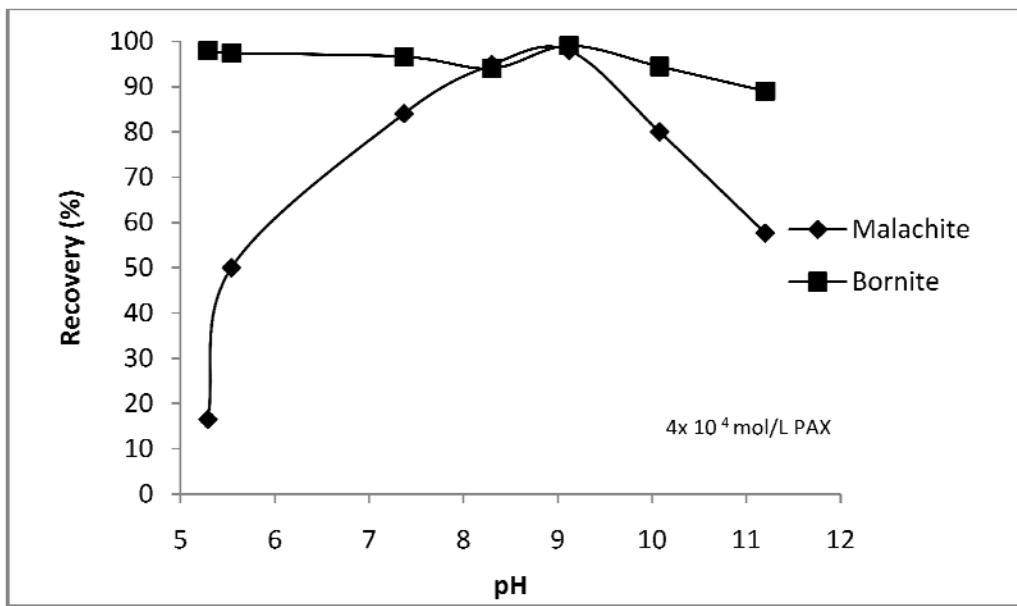


Figure 4.9 : The relationship between the flotation recovery of pure malachite and bornite with 4×10^{-4} mol/L PAX.

The pH level of collection had little effect on the recovery of bornite. Recovery levels above 90% were achieved for all pH levels. The flotation rate was very rapid with collection taking less than 15s in all cases. A persistent, steady froth was obtained across the pH range. While this may have been contributed by elemental sulphur on its surface, it is also possible that the collector dosage was too high for the amount of bornite in the cell. The surface area of bornite is less than the surface area of malachite. Results of collector overdosing overwhelm pH dependent flotation behaviour; however, the adsorption tests conducted with PAX and bornite indicate that collector uptake is only 40 % after 6 minutes of contact time regardless of pH. It is more likely that the bornite micro-flotation results are not due to collector overdosing, but are of bornite flotation behaviour assisted by elemental sulphur.

4.2.2 Hydroxamate Micro-flotation

The micro-flotation results of malachite and bornite with 4×10^{-4} mol/L hydroxamate are shown in Figure 4.10. A strong froth was present for all tests. Frothing characteristics were present prior to frother addition, indicating that hydroxamate has inherent frothing properties.

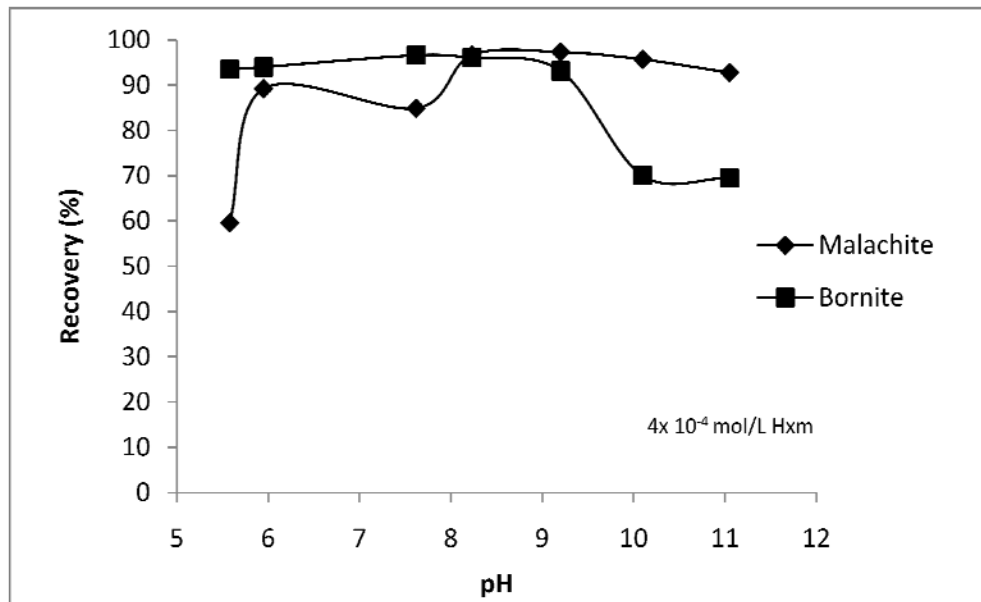


Figure 4.10 : The relationship between the flotation recovery of pure malachite and bornite with 4×10^{-4} mol/L hydroxamate.

The malachite flotation rate was rapid. Collection occurred in less than 10 s across the pH range except at the extreme values of pH 5.5 and 11.5. The recovery peaked at 97 %. This occurred at pH 9.5, which is the characteristic maximum of hydroxamate flotation and adsorption. A slight dip occurs at pH 7.5, which corresponds to the drop in adsorption density observed during the adsorption testing. Again, this is likely due to the tendency of malachite to dissolve in near neutral waters. Once the mineral begins to dissolve, the collector will chelate copper ions in solution rather than contributing to hydrophobicity and flotation. Mineral dissolution is likely the case at pH 5.5 as well. The adsorption density was lower, indicating that the collector was

complexing with copper cations in solution instead of coating the mineral surface. At high pH, hydroxamate adsorption density on malachite was lower; 8 collector layers were deposited. This did not result in significant drop in mineral recovery. The chelates formed between the collector and the copper cations in the malachite surface are more stable than those formed by PAX. This means that once the collector adsorbs onto the surface of the mineral, it will contribute to collection. This is probably why there is not a significant drop in flotation recovery.

Bornite behaved in an opposite manner to malachite. It performed well in acidic regions and poorly in alkaline regions. Sulphides traditionally respond better in regions of low pH due to their stability in this region. This is consistent with thermodynamic stability of elemental sulphur in the acidic pH range. In the low pH range, extensive frothing was present with quick flotation rates. The flotation rate with bornite was slightly slower than with malachite, but collection was still complete within 30 s. The highest flotation recovery was 96 % at pH 7.5. This is at lower than the characteristic hydroxamate peak of pH 9.5. Bornite recovery dropped off significantly at pH 10.5. Sulphides do not perform well in regions of high pH due to the precipitation of hydroxides. The main precipitate is ferric hydroxides. Hydroxamate is an anionic collector. It forms the ring-like copper chelate with a negatively charged oxygen atom. The bornite surface is negatively charged at high pH, resulting in repulsive forces with the hydroxamate collector. The lower adsorption density, hydroxide precipitation and the repulsive effects between the bornite surface and hydroxamate all contribute to the low recovery of bornite at high pH.

4.2.3 N-benzoyl Micro-flotation

Collectors with aromatic substituents have shown promise as effective mineral collectors. The behaviour of N-benzoyl with respect to pH is reported in Figure 4.11.

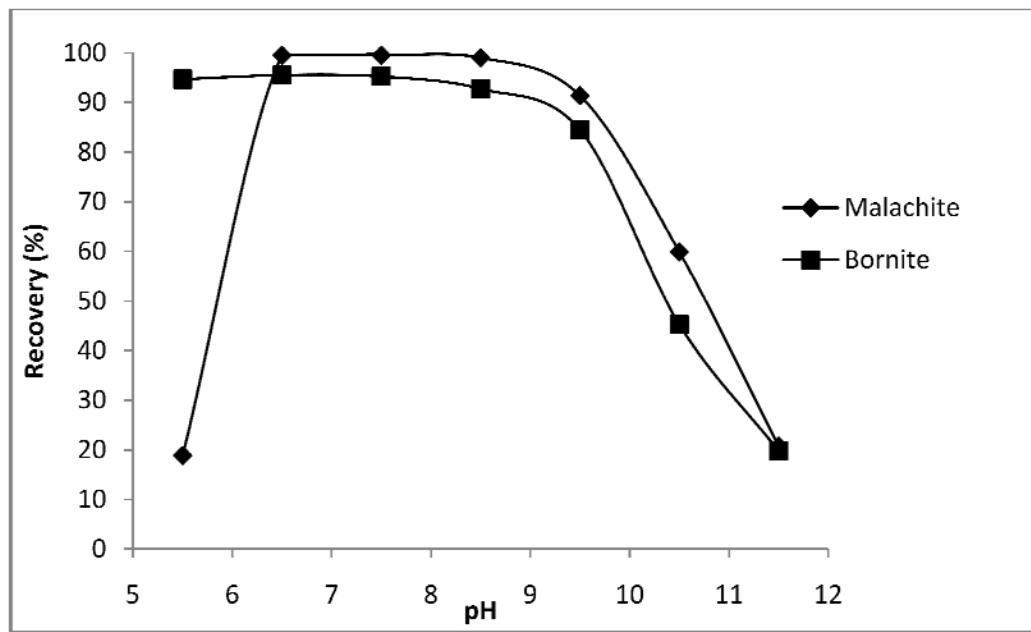


Figure 4.11 : The relationship between the flotation recovery of pure malachite and bornite with 4×10^{-4} mol/L N-benzoyl.

N-benzoyl had a marked effect on malachite behaviour. Immediately after collector addition, the malachite particles agglomerated. The liquid in the cell, which normally appeared milky green, became clear. The agglomerated malachite particles could be seen spinning halfway up the flotation cell. This behaviour was visible at all pH levels, although it was not as pronounced at pH 5.5 and pH 11.5. The agglomeration behaviour and flotation recovery are dependent on pH. In the range of pH 6.5-8.5, 99 % recovery was achieved. Flotation rate was almost instantaneous. Full collection was obtained in 5-10 s, faster than both hydroxamate and PAX. At pH 5.5, poor recovery was achieved, confirming that N-benzoyl has high pH dependence. Agglomeration was not as marked as it was for the mid-pH range, although it did show slightly. The liquid in the flotation cell was not clear, but a translucent green. Flotation rate was slower, taking approximately 40 s for complete collection. The drop in recovery in the alkaline range was not as sudden. At pH 9.5, the agglomeration behaviour was not as effective;

the liquid in the flotation cell remained greenish. Agglomerated particles could still be seen rotating low in the flotation cell due to their increased weight. The N-benzoyl-malachite system produced a very persistent froth. One inch deep froth was clearly visible in the flotation cell, particularly at pH 10.5 and 11.5. Collection took approximately the same time in the alkaline range as it did for pH 5.5. The low recoveries at high and low pH are not only due to the pH dependence of the collector, but also to mineral solubility as outlined in Sections 4.1.1 and 4.1.2.

Bornite did not show the same agglomeration tendency as malachite. The liquid in the cell remained black, although heavy flocs could be seen at certain pH levels. The bornite flocs proved to be too heavy to be lifted by the bubbles and could be seen remaining in the cell after the 2 minute collection time. As expected, bornite recovered well in the acidic pH range. The highest flotation recovery of 95 % occurred at pH 6.5. The froth depth was clearly visible in the flotation cell, except at high pH. From pH 10.5-11.5, there was no visible froth formation. The fact that little to no agglomeration was present with bornite indicates that the pH dependence of N-benzoyl was not a major factor in bornite flotation.

4.2.4 Bornite Micro-flotation

The adsorption behaviour of bornite deviated from what was expected from its flotation response. The collectorless flotation behaviour of bornite was investigated. The results for the collectorless flotation of bornite are shown in Figure 4.12.

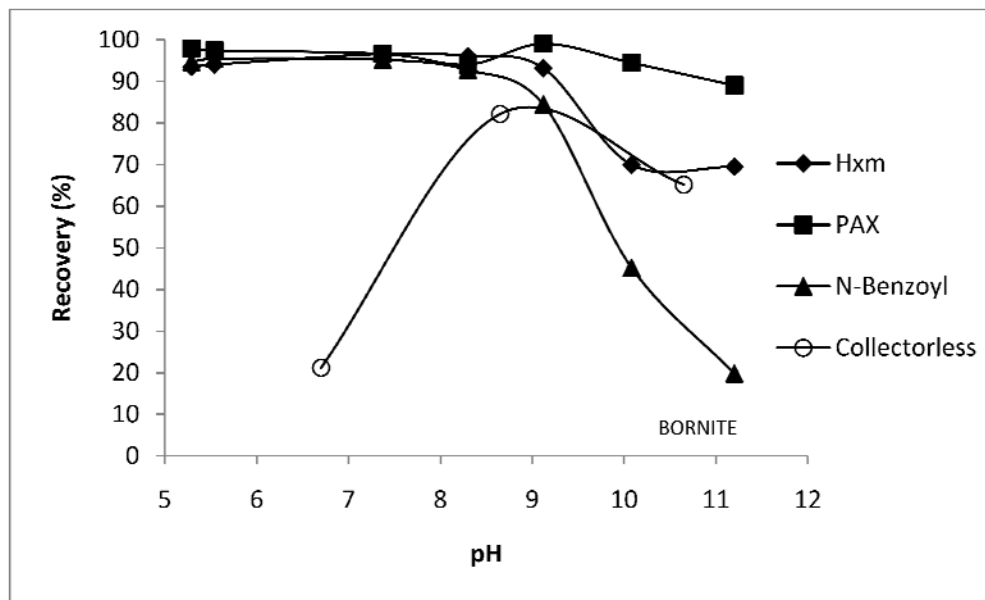


Figure 4.12 : Comparison between collectorless bornite flotation and flotation with PAX, hydroxamate and N-benzoyl.

It can be seen that bornite possesses self-induced floatability. At pH 8.5, bornite recovery was 82 %. It is sensitive to a pH change in acidic and alkaline directions. This is similar to the behaviour of chalcopyrite observed by Tukel (2002). With a small addition of collector in the acidic range, bornite recovery was almost complete. This indicated that the metal ions were highly reactive with the collector added. At high pH, bornite will begin to produce stable metal hydroxides on its surface. The collectorless flotation recovery drops off after pH 8.5. It is apparent from Figure 4.12 that N-benzoyl is a depressant to bornite flotation at higher pH; its recovery curve dips below that of the collectorless flotation.

4.2.5 Eh-pH

The Eh measurements taken during the micro-flotation tests were analysed using SOLGASWATER. This program, developed by Eriksson (1979) at Umea University, uses the free-energy minimization technique. This technique applies to systems containing aqueous

solutions with a solvent of unit activity, a constant volume gas phase and a solid phase with invariant stoichiometry. The components of the system are the smallest number of pure substances required to state the composition. These species are defined at the beginning. Then, SOLGASWATER runs iterations to test which combination of phases delivers the lowest free energy. The free energy of a system is minimized when it is at equilibrium.

A species distribution diagram showing the distribution of copper ions and malachite in solution is shown in Figure 4.13. According to this diagram, malachite begins to dissolve at pH 4.2. At equilibrium, malachite will be completely dissolved at pH 3.3. It should be noted that thermodynamic equilibrium would not be attained during the flotation period. Chemical reactions are unlikely to proceed to completion on the conditioning and flotation timescale. Even slight malachite solubility is likely to release enough cupric ions near pH 4.2 to interact with the collector species. This will cause collector precipitation and decrease the amount of collector available to adsorb onto a mineral surface. As a result, flotation response will decrease.

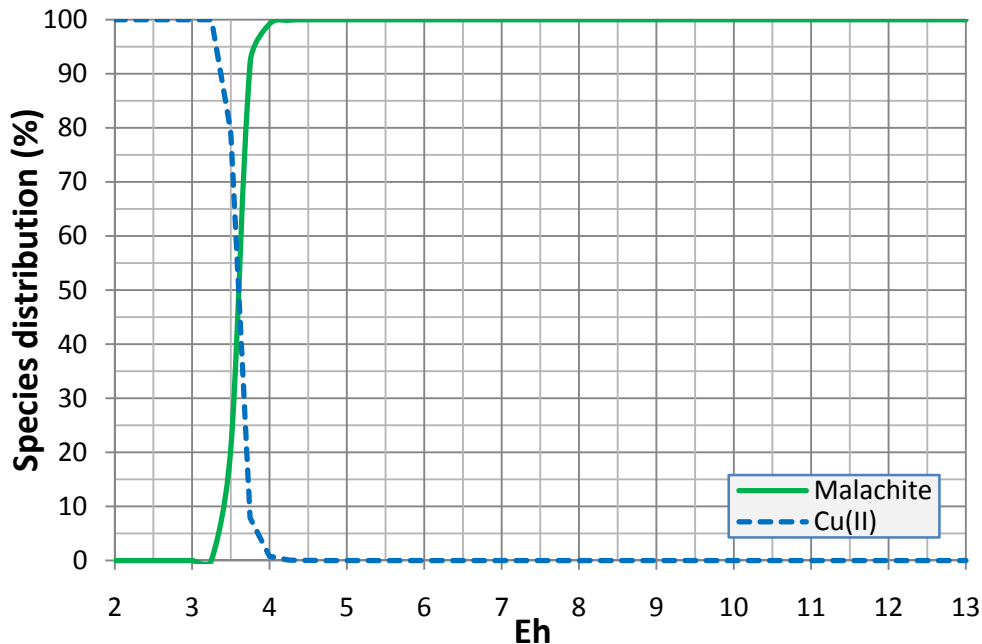


Figure 4.13: Distribution diagram for cupric ions and malachite at 118 mV in the absence of collector species. Total copper concentrations are : $[Cu^{2+}] = CO_3^{2-} = 1 \text{ mM}$.

The reactivity of malachite is dependent on the availability of reagents that have an affinity towards the copper ions in the solution. A species distribution diagram (Figure 4.14) was constructed to investigate the relative stability of the hydroxamate and the xanthate species. The stability constants could not be found for the Cytec 6494 Promoter hydroxamate. For the purposes of this thesis, the stability constants of a benzohydroxamate were used as given by Agrawal and Tandon (1973). Ethyl xanthate was used due to the availability of its thermodynamic data in the literature (Forssberg and coworkers, 1984). Two oxidation levels were considered based on experimental observation: 0 mV and 118 mV. SOLGASWATER defined oxidation levels as pe , which relates to Eh through the equation below, where $F=23061$, $T=298.15 \text{ K}$, $R=1.987 \text{ cal K}^{-1} \text{ mol}^{-1}$. Thus 118 mV, SHE corresponds to a pe value of 2.

$$pe = EhF / (2.303RT \times 1000)$$

It was assumed for the sake of the construction of Figure 4.14 that malachite is the only copper carbonate mineral. Additionally, the formation of Cu₂O was ignored due to the short flotation timescale. If these assumptions were not made, malachite appeared unstable. This was known not to be the case because malachite could be seen in the flotation concentrates. From Figure 4.14, it can be seen that the distribution of BHMA in the alkaline range is independent of the oxidation level as Curve 1 and 5 are superimposed. In acidic solutions, BHMA requires lower pH values for protonation as compared to the higher redox level. This is indicated by Curves 2 and 6 of the figure.

The hydroxamate species form chelates with cupric ions over a majority of the pH spectrum. Cu(BHMA)₂ and Cu(BHMA) are indicated by Curves 4-8 and Curves 3-7. Cu(BHMA)₂ appears to be the more stable chelate as Curve 4 and Curve 8 indicate a species distribution of over 40 % in the range of pH 8 to pH 11. Due to an increase in redox potential, Cu(BHMA)₂ destabilizes more for protonation. This is demonstrated by Curve 8. The maximum distribution for Cu(BHMA) at low redox potential occurs at pH 6.5 as seen in Curve 3. Curve 7 depicts Cu(BHMA) for 118 mV. The maximum distribution is seen at pH 7.5, but it amounts to only 1-2 % of the total concentration.

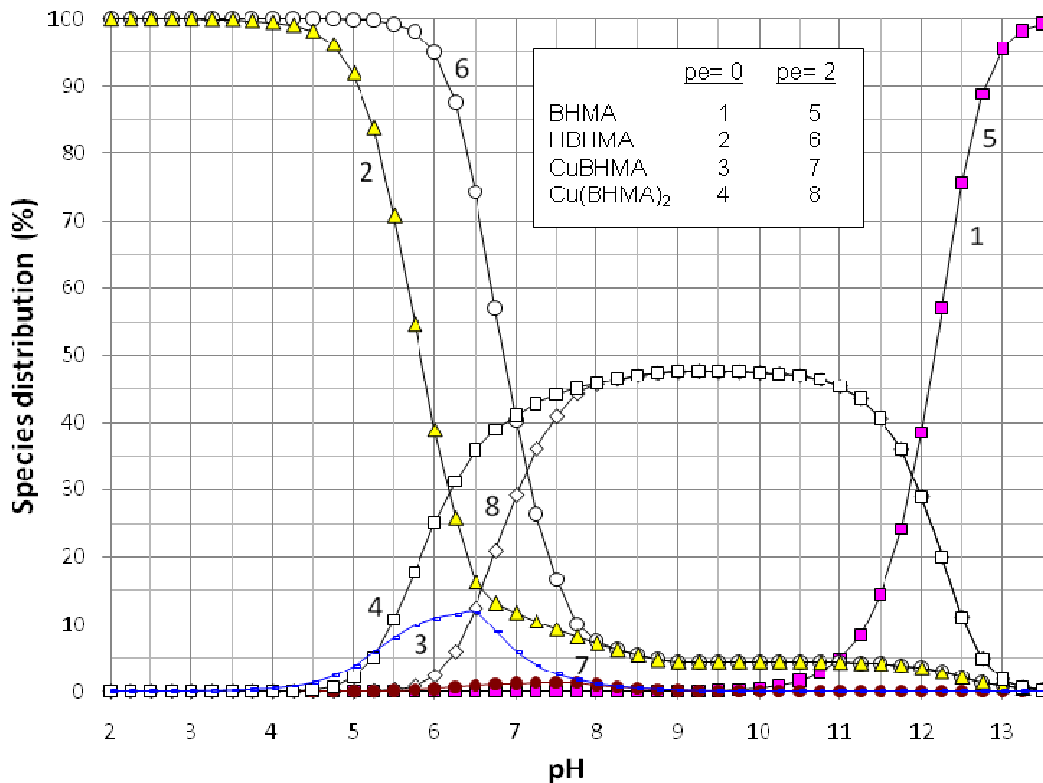


Figure 4.14 : Species distribution diagram for a benzohydroxamate (BHMA), its protonated form (HBHMA) and the copper chelates corresponding to two oxidation levels of 0 mV (pe=0) and 118 mV (pe=2). Total concentrations are: [HBHMA] = [Cu²⁺] = CO₃²⁻ = 1 mM.

The impact of xanthate was investigated by comparing the species distribution for 0.01 mM, 0.1mM and 0.5mM xanthate at 0mV. The species distribution diagram is seen in Figure 4.15. Since the total concentration of Cu(BHMA) was very small, it was not plotted in Figure 4.15. It can be seen that cuprous xanthate forms independently of pH until pH 12. Above this value, it destabilizes and releases xanthate ions. Higher concentrations of xanthate yielded smaller releases of xanthate ions at high pH as shown by the EX⁻ curves. This phenomenon can be explained by the greater hydrophobicity at high xanthate concentrations. Formation appears to be unaffected by fluctuations in xanthate concentration as EX⁻ was formed in all three cases.

The concentration of the hydrophobic entity, CuEX is shown for the three xanthate concentrations in Figure 4.15. The results based on xanthate concentration were: 1 % at 0.01 mM, 10% at 0.1 mM and 50 % at 0.5 mM. These results are amounts relative to the total concentration of the other components at 1 mM. It was observed that the amount of reacting malachite decreased with increased xanthate concentration. The 0.01 mM xanthate reacted with 0.01 mM cuprous ions to form CuEX indicating that nearly 100 % of the xanthate contributes to the formation of CuEX. The chemical reactions involving xanthate indicate that it has a high affinity towards copper. From a thermodynamic point of view, this means that there is a large driving force for xanthate to react with copper oxides. In comparison to hydroxamate, xanthate has a larger driving force to react with copper. During the flotation tests, hydroxamate was observed to collect malachite better than xanthate. The superior performance of the hydroxamate is likely related to its selectivity towards malachite as well as kinetic reactions. From an equilibrium point of view, both xanthate and hydroxamate are reactive towards malachite. Although the reaction of PAX compared to that of hydroxamate is very dominant, the reaction product formed probably does not stay at the malachite surface persistently. This is evident from results of micro-flotation tests in Figures 4.9 and 4.10.

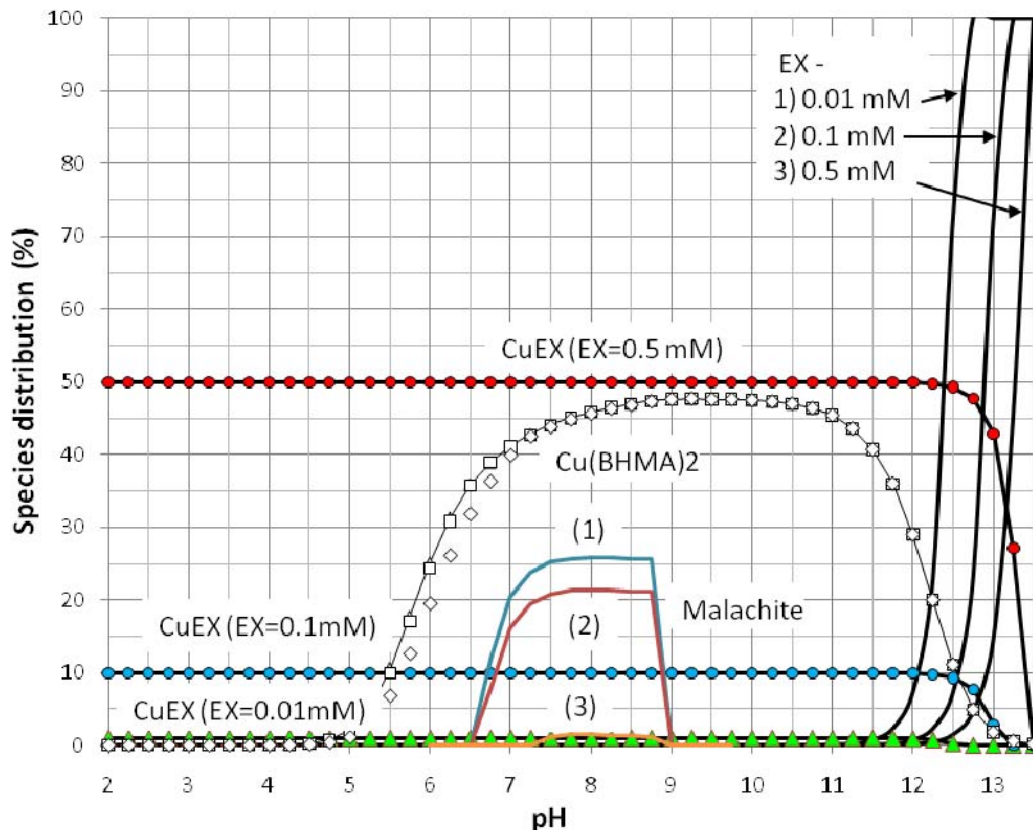


Figure 4.15: Species distribution diagram showing xanthate, cuprous xanthate (CuEX) and malachite and as a function of pH at $Eh = 0$ mV. Total concentrations: $[BHMA]=[Cu^{2+}]=CO_3^{2-} = 1$ mM. Xanthate concentration varied from 10^{-5} M to 5×10^{-4} M.

4.3 Bench Scale Flotation

A natural sulphide-oxide copper ore was studied at laboratory bench scale. The samples received from Ward's Natural Science Establishment (Rochester, New York) were in poor condition and in insufficient amount for a bench scale investigation. A natural ore sample was acquired from a porphyry copper deposit in the Central Eastern region of Turkey. The ore contains bornite and malachite as its copper sulphide and carbonate/hydroxide minerals, respectively. Collector type and dosage were investigated to determine their effects on the

primary flotation or behaviour without cleaning or regrinding stages. The end goal of the bench scale flotation tests was to propose optimum collector dosages that would result in high grade and recovery performance. This was done via a Box-Behnken response surface methodology experiment. Before the Box-Behnken design could be performed, the range of collector levels needed to be determined. Initially, exploratory work was performed to gain insight into the flotation of the raw ore. Next, preliminary tests were performed to define the process space of the Box-Behnken design. The goal of the preliminary investigation was to provide a region in which a likely flotation optimum was present. Finally, N-benzoyl was investigated for its application to bench scale flotation of a raw ore.

4.3.1 Exploratory Work

Two exploratory tests were performed with the raw ore: T1 and T2. Each test had unique collectors and dosages in order to explore the flotation behaviour of the ore. Graphs of cumulative grade versus cumulative recovery as well as the kinetics of metal recovery and grade can be seen in Figure 4.16, Figure 4.17 and Figure 4.18, respectively. The flotation reports and results spreadsheet for the exploratory work can be found in Appendix E.

T1 was performed with an 885 g charge that had been ground for 10 minutes with 0.5 g of Na_2CO_3 . The flotation was performed in a 2L flotation cell at room temperature. The first three concentrates were performed with 0.1% PAX and 0.1% DowFroth. These concentrates had rich froths laden with black bornite particles. It was apparent even before flotation that bornite recovery would not be an issue. During the first conditioning stage, black particles were seen floating to the surface. This could be attributed to the self-induced floatability of bornite as well as how easily it responds to collector addition. After the 3rd concentrate, an attempt was made to disperse the slimes to collect the malachite. Sodium silicate, a common dispersant was added to the cell. It did not appear help the malachite collection. The collection of bornite was still

occurring, but at a much slower rate. The concentrates appeared to be collecting mainly slime particles. Sodium silicate addition ceased after the 6th concentrate as it was not helpful in dispersing the slimes. The collection of slimes can be seen in Figure 4.16. There is a discontinuity in the T1 curve as the copper grade drops due to increased slime recovery and no recovery of copper minerals. The PAX dosage was increased for the 6th concentrate to see if a higher dosage had any effect on malachite. No effect was seen, and the concentrates continued to be slime particles. An oily yellow colour was apparent in the cell. This is indicative that xanthate overdosing had occurred. It was obvious that high dosages of PAX would not illicit malachite collection. At this point, DETA was added to the 9th concentrate. One drop was added and it was found to be too powerful. It changed the structure of the froth and collected only slimes. Cytec 6494 was added for the 10th concentrate along with xanthate. The malachite began to respond at this point. The froth became distinctly green, but became almost barren before the end of the 2 minute collection time. The addition of the hydroxamate collector can be seen in the sudden upwards trend of the cumulative copper recovery curve in Figure 4.17. This is malachite being collected.

From T1, it was clear that the ore possessed a sliming problem. After 10 minutes of grinding time, there was a significant amount of slime production. These slime particles were likely formed by slime-producing gangue minerals. Flotation behaviour can be significantly altered by slime content. Slimes coat mineral particles and prevent or minimize their interactions with minerals. They also consume considerable amounts collector. Regardless of the large collector dosage for T1, the copper recovery was only 61 % with a grade of 25 %.

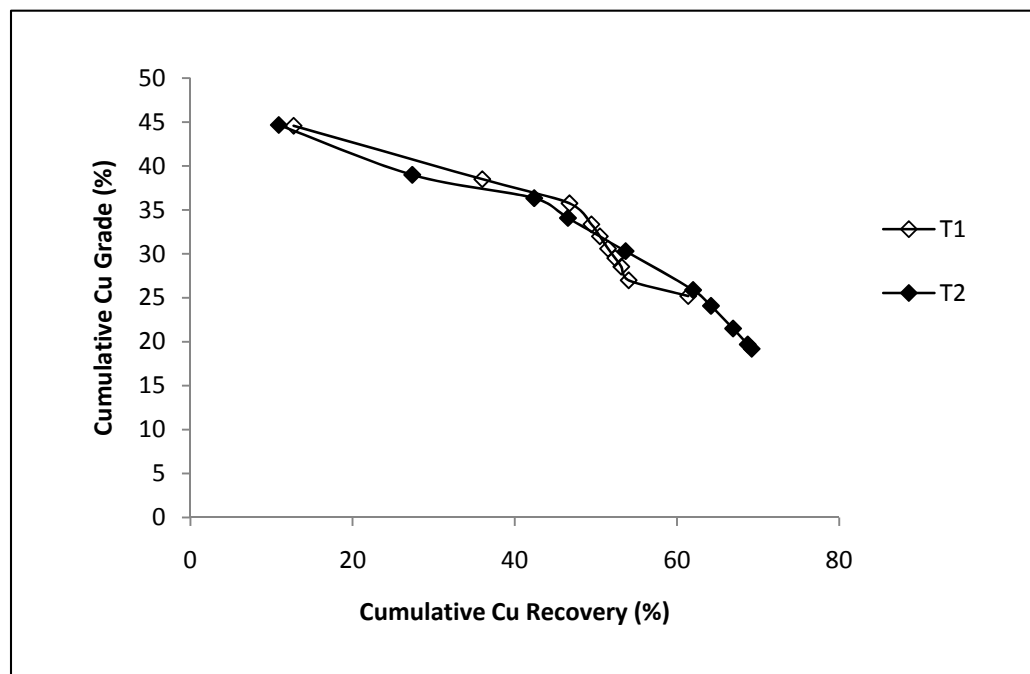


Figure 4.16 : Cumulative Cu grade versus cumulative Cu recovery for T1 and T2.

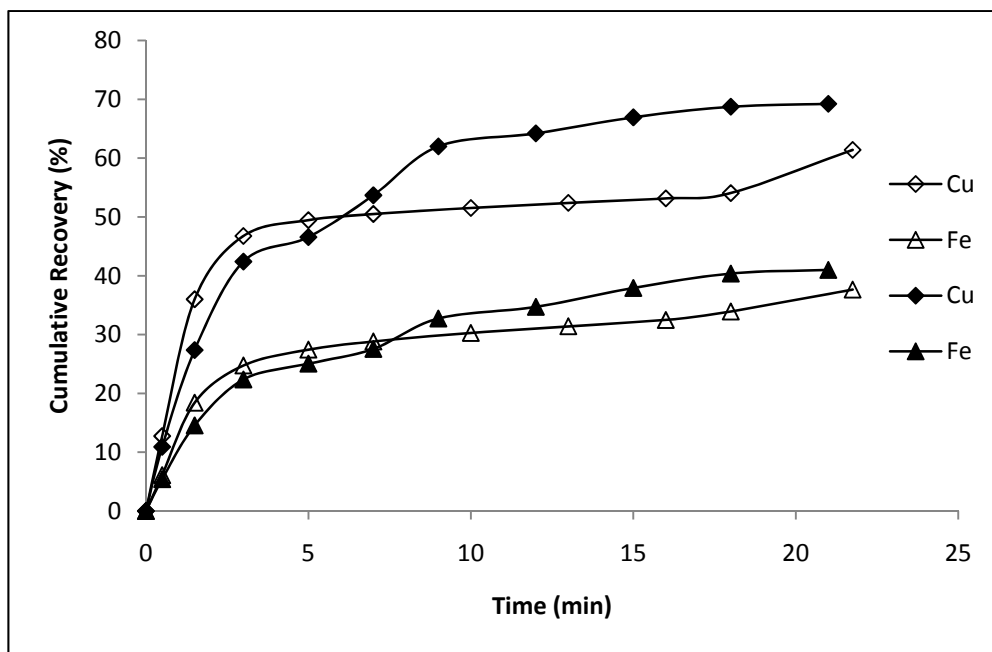


Figure 4.17 : Kinetics of metal recovery for T1 and T2. T1 is indicated by the open markers.

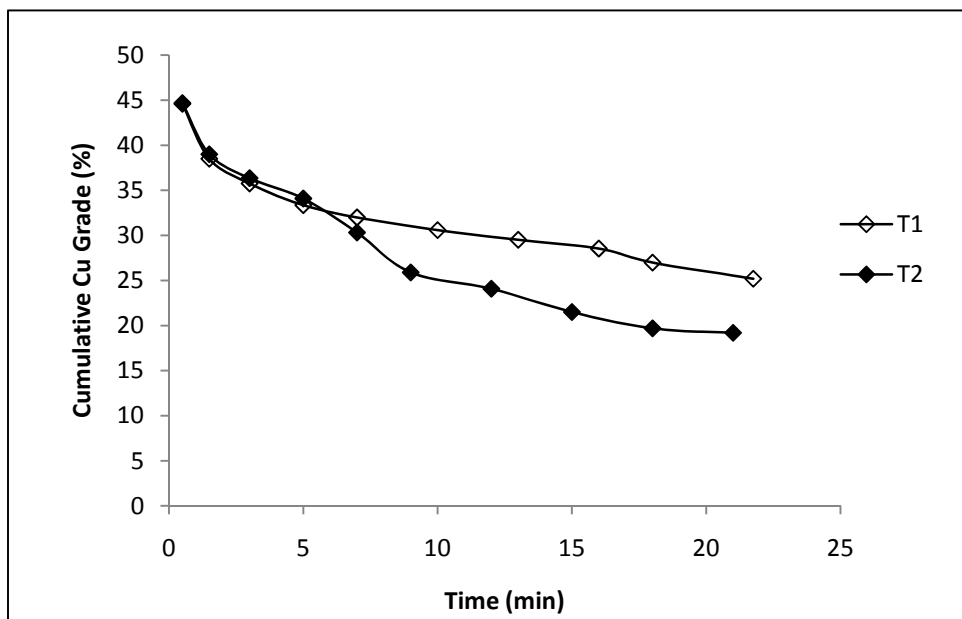


Figure 4.18 : Kinetics of metal grade for T1 and T2. T1 is indicated by the open markers.

T2 was performed with a second 885g charge ground for 10 minutes without any reagent addition to the grinding mill. No sodium silicate was added to the flotation cell and only PAX was used for the first 3 concentrates. Cytec 6494 was added instead of PAX at the 4th concentrate. The discontinuity at 7 minutes in the kinetics of copper recovery curve (Figure 4.17) is caused by the hydroxamate. In T1, the slimes in the ore presented a significant barrier to effective collection. Before the 5th concentrate was pulled, flotation was stopped. The contents of the flotation cell were passed through a -635 (20 micron) sieve. The plus size was returned to the flotation cell and the slime fraction was dried and weighed. After de-sliming, the froth was white and showed no signs of the previous muddiness. Collection was continued for 5 more concentrates using only 3 drops of hydroxamate as a collector. The froth for each following collector appeared white and barren, but copper minerals were still being collected as demonstrated by the copper cumulative recovery curve.

The final copper recovery for T2 was 69 % with a grade of 19 %. The higher recovery for T2 came with a sacrifice in copper grade, which was expected. T2 demonstrated conclusively that the slimes in the ore were detrimental to copper recovery and that a de-sliming step should be a part of the flotation process. This is confirmed in literature by Lee and co-workers (1998) of Cytec Industries, the makers of Cytec 6494. They suggest that if an ore has gangue species that readily generate slimes, a de-sliming step or the use of a dispersant are possible solutions. It was chosen to include a de-sliming step as opposed to relying on a dispersant as slime removal is a guaranteed solution. If a dispersant was used, it would add another reagent to the chemical makeup of the flotation whose dosage would need to be determined and monitored. The natural ore proved problematic enough without an additional variable.

T3 was an incomplete flotation test conducted for the purposes of mineralogical testing only. Its conditions had no bearing no further testing.

4.3.2 Preliminary Investigation

Five tests were performed during the preliminary investigation stage: T4, T5, T6, T7 and T8. These tests were performed with natural ore that had been ground for 12 minutes and deslimed to produce 680 g charges. The goal of this testing phase was to determine appropriate hydroxamate collector dosages for the Box-Behnken experiment. In conventional response surface design, the program begins with two-level factorial designs in order to determine the path of steepest ascent. This path is the direction to the optimum value. Once the region in which the optimum lies is found, a design capable of detecting curvature is applied to that region. In this case, there was a limited amount of samples available for a more detailed testing program, so the process space could not be defined using the path of steepest ascent method. Instead, five tests were performed at varying collector levels in order to determine an appropriate process space.

The flotation reports and results spreadsheet for the preliminary investigations can be found in Appendix E.

The effects of PAX dosage have been well researched. During the exploratory phase, excessive PAX dosages showed negligible effect on malachite recovery. Since the ultimate goal is to improve non-sulphide copper recovery, the main variable that was studied during the preliminary investigation was hydroxamate dosage. Hydroxamate dosages ranged from 229 g/t to 470 g/t with 6 to 9 concentrates. The recovery versus grade curves for the preliminary tests can be seen in Figure 4.19.

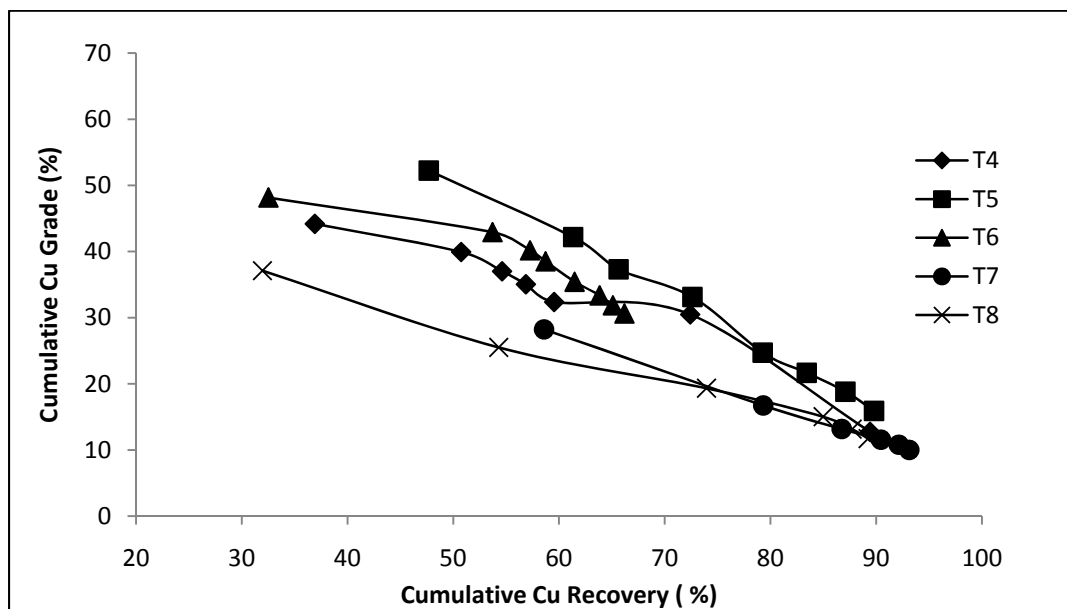


Figure 4.19 : Copper grade versus recovery for preliminary tests T4 through T8.

T4 was performed with 379 g/t hydroxamate. The first three concentrates were pulled using 15 g/t each of hydroxamate. The froth was noticeably greener after concentrate 3. After the third concentrate, the bulk of the bornite is collected, so malachite content can be easily observed. As the hydroxamate dosage was increased to 30 g/t in a later concentrate, there was a large amount of frother activity. The Cytec 6494 hydroxamate possesses an inherent frothing capability.

Frother amounts were decreased or skipped for further concentrates to avoid excess frothing. The last concentrate pulled in T4 was intentionally overdosed with hydroxamate to maximize recovery. The concentrate was very muddy, indicating gangue activation. Due to the gangue activation, flooding occurred and a large amount of material was collected. This can be seen in the copper grade and recovery curves seen in Figure 4.20 and Figure 4.21 respectively. The T4 curve drops sharply in Figure 4.20 as the recovery rises in Figure 4.21. T4 illustrated that malachite recovery is collector dependent. Malachite recovery can be seen to rise steeply in the last few concentrates of T4, as illustrated in Figure 4.22. It collects well when there is sufficient collector, but quickly drops off during the collection time. Since flooding occurs when the hydroxamate dosage is too high, the ideal method would be frequent smaller doses of hydroxamate.

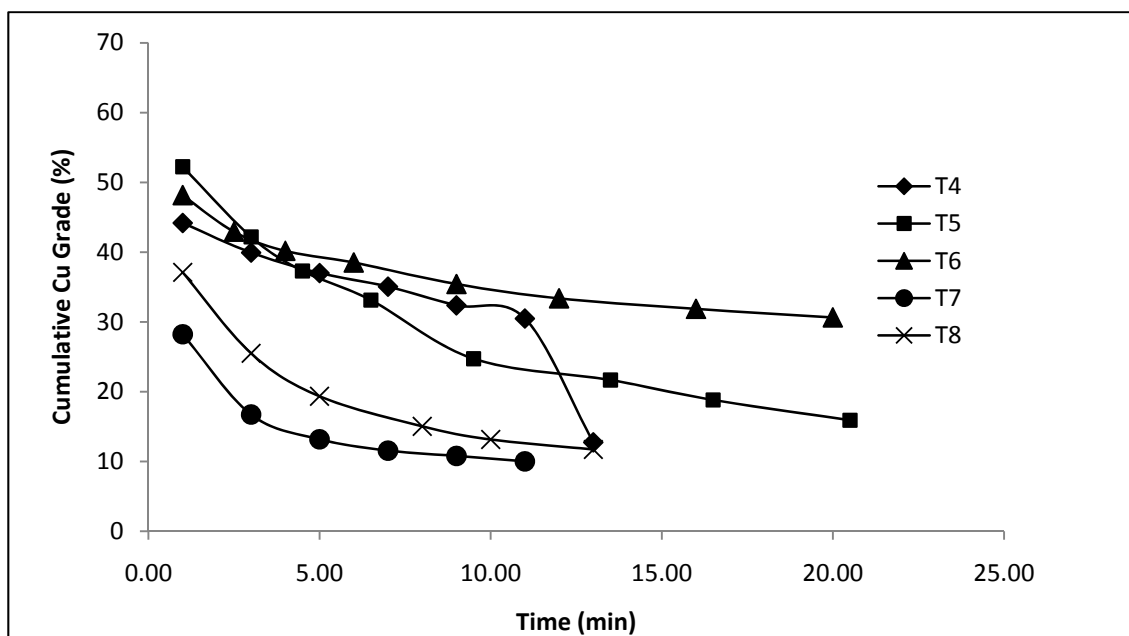


Figure 4.20 : Cumulative copper grade for preliminary tests T4 through T8.

T5 was performed with the highest hydroxamate collector dosage: 470 g/t. It was added in increasing increments from 15 g/t in the first concentrate to 90.6 g/t in 6th, 7th and 8th

concentrates. Bornite collected as expected within the first 2 concentrates. Surprisingly, malachite was observed in the 2nd concentrate, indicating that most of the bornite had been collected in the first concentrate. As the dosage of hydroxamate rose, the frothing activity was sufficient enough that frother only needed to be added twice during the 20.5 minute flotation time. Flooding behaviour was noted as the hydroxamate dosage became higher. Due to the flooding in T5, the grade of the concentrates drops as the dosage gets higher. T5 was one of the most successful preliminary tests as it achieved 89% copper recovery and 78 % malachite recovery as shown in Figure 4.21 and Figure 4.22 respectively.

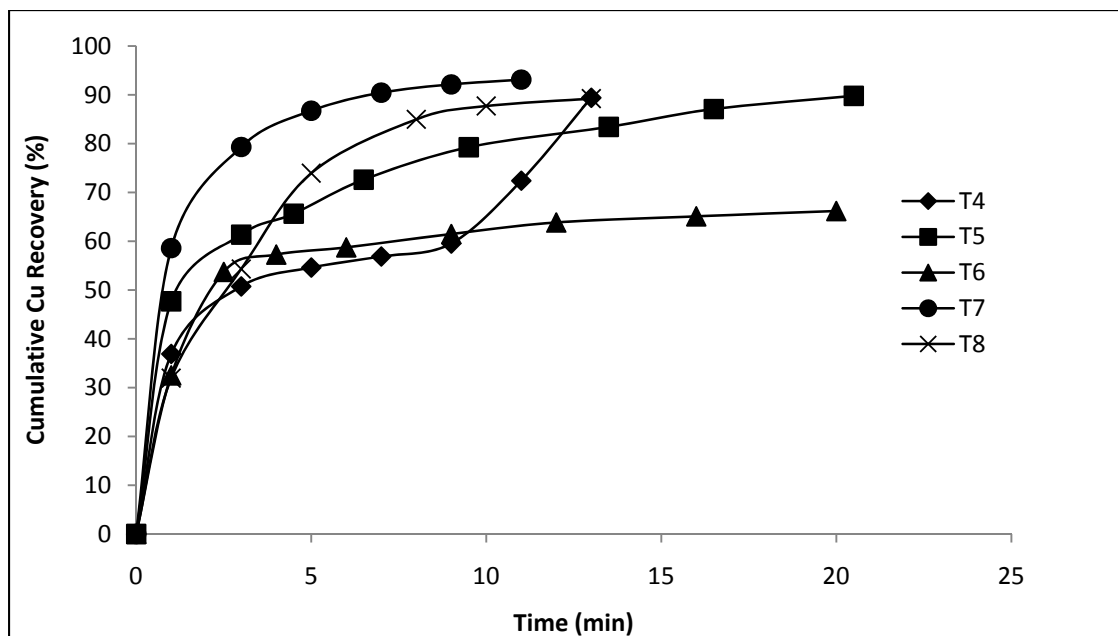


Figure 4.21 : Cumulative copper recovery for preliminary tests T4 through T8.

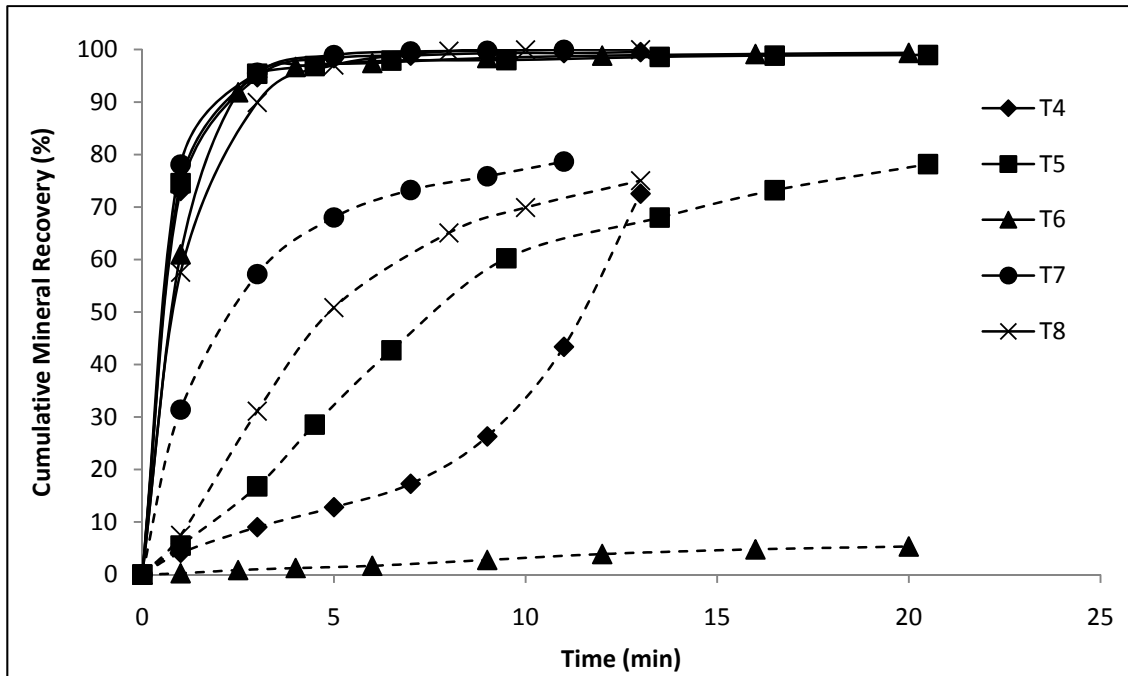


Figure 4.22 : Cumulative mineral recovery for preliminary tests T4 through T8. Solid lines indicate bornite recovery, dashed lines indicate malachite recovery.

T6 was conducted at the opposite end of the dosage scale from T5. It had the lowest hydroxamate dosage of the preliminary tests at 226 g/t. The collector dependence of malachite has already been demonstrated in T4 and T5. Copper recovery was the lowest for T6 with the highest copper grade. After concentrate 3, the froth appeared brownish and quickly turned a barren white colour. Once the bornite had been collected, there was no characteristic green colour to indicate that any malachite was being recovered. Bornite was unaffected by the low doses of hydroxamate, but malachite recovery suffered. From Figure 4.22, the malachite recovery can be seen to be only 5 % after 20 minutes of flotation. Both the copper and the malachite recovery were unacceptable for T6, indicating that the process space starts at a higher hydroxamate dosage.

T7 had the highest copper and malachite recovery of all the preliminary tests. It was conducted at 459 g/t with 6 concentrates. The hydroxamate dosages were weighted more heavily

towards the beginning and then tapered off. This was done to avoid activating gangue. The first concentrate pulled was not the usual pure black, but slightly green. This indicated that even malachite was being collected in the first concentrate alongside the very floatable bornite. Copper grade is not as high for T7 as it is for the rest of the preliminary tests; it achieved the highest copper and malachite recovery even with half the flotation time of the previous tests. This indicates that higher collector doses up front allow for higher recovery of copper minerals with limited gangue activation.

T8 was performed with a similar structure to T7 but with a total hydroxamate dosage of 401 g/t. DETA and sodium metasilicate were added in later concentrates. T8 was an attempt to have a flotation run similar to one that would be used in the Box-Behnken design. The collectors were added in roughly equal dosages across all the concentrates. The initial concentrates were high in bornite, but with some malachite recovery. It was noted in the second and third concentrates that they were initially greenish, but once the malachite slowed down within the concentrate, bornite particles were seen to be still coming. The DETA was added in concentrate 4. It decreased the froth bubble size and some flooding behaviour was seen. The air flow rate was cut back until halfway through the flotation time to avoid excessive flooding. The concentrate was very green and persisted through until the end of the floating time. The copper and malachite recovery were very good for T8. Although they were lower than T7, the recoveries were comparable with T5 regardless of a lower collector dosage and flotation time. This indicates that the equal addition of hydroxamate across all the concentrates produces good copper oxide recoveries and should be implemented for the Box-Behnken design. DETA also appeared to give favorable results. It is even possible that lower collector dosages can be used when DETA is employed.

From the preliminary investigations several key observations were made. Malachite is very collector dependent. With adequate doses, it collects sufficiently well. If this collector dose

is too low, malachite recovery tapers off during the collection time. If the hydroxamate dose is too high, gangue activation and flooding occur. This results in high recoveries, but unacceptable copper grades. Equal doses of hydroxamate for each concentrate provide good malachite recovery as seen in T7 and T8. Hydroxamate aids in the frothing behaviour, so frother doses can be minimized. DETA appeared to have a synergistic effect with hydroxamate and the concentrates with DETA addition appears not only greener, but to sustain malachite collection throughout the flotation time.

4.3.3 Box-Behnken

Three models were constructed from the Box-Behnken experimental design: copper recovery, malachite recovery and minor copper recovery. Bornite recovery was not modeled; its recovery was consistently over 99 %. The results of the Box-Benken experimental design can be seen below in Table 4.1. The graphical results for the Box-Behnken trials can be found in Appendix C. The flotation reports and calculated results can be seen in Appendix E.

Table 4.1: The results of the Box Behnken bench-scale flotation experiments.

PAX (x ₁)	Cytec 6494 (x ₂)	DETA (x ₃)	Cu Recovery (%)	Minor Cu Recovery (%)	Malachite Recovery (%)	Bornite Recovery (%)	Copper Grade (%)	
1	-1	-1	11.20	3.80	4.81	24.78	37.70	
2	1	-1	62.36	37.79	8.45	99.16	12.18	
3	-1	1	90.12	84.42	69.85	99.74	12.30	
4	1	1	91.24	86.50	79.05	99.87	32.54	
5	-1	0	64.33	37.71	17.03	99.60	33.74	
6	1	0	-1	76.01	62.37	43.28	99.60	26.56
7	-1	0	1	80.80	69.12	51.90	99.30	22.68
8	1	0	1	87.09	80.51	67.05	99.64	40.16
9	0	-1	-1	61.45	35.54	8.76	99.33	22.79
10	0	1	-1	85.76	76.92	69.58	99.65	38.09
11	0	-1	1	55.37	29.50	10.87	99.21	8.72
12	0	1	1	89.56	81.39	58.56	99.76	22.14
13	0	0	0	82.94	70.96	57.53	99.33	23.74
14	0	0	0	76.27	58.98	42.93	99.30	28.28
15	0	0	0	81.64	70.42	41.76	99.24	28.28

The creation of a model for a particular system is a subjective and iterative process. A number of graphical and correlation methods are used to assess model adequacy, but no one test is decisive. Given a particular data set, there are a number of possible models that could be fit to the data. The final model is one that is formulated with the aid of statistical tests, the use of engineering judgment and performs the task it was designed for.

In this thesis, these models were created with the goal of proposing collector conditions that produced optimum flotation response. This involved response surface methodology to model curvature in the process space. The use of response surface methodology does not inherently produce an optimum value. If an optimum quadratic response is pictured as a mountain, the foot hills of the mountain would appear quite linear. Only near the top of the mountain would curvature be noted and be significant enough to be modeled. This is seen in Figure 4.23. The

contours of the quadratic surface are shown at each stage. The straight contour lines depict a hillside. This indicates that the optimum is far from the process space. As the contours begin to curve, the surface is classified as a rising ridge. At this point, the optimum is close. When the optimum is in the process space, the contours show a peak. The models produced for this thesis were fit to both a linear and quadratic model to assess the location of the process space.

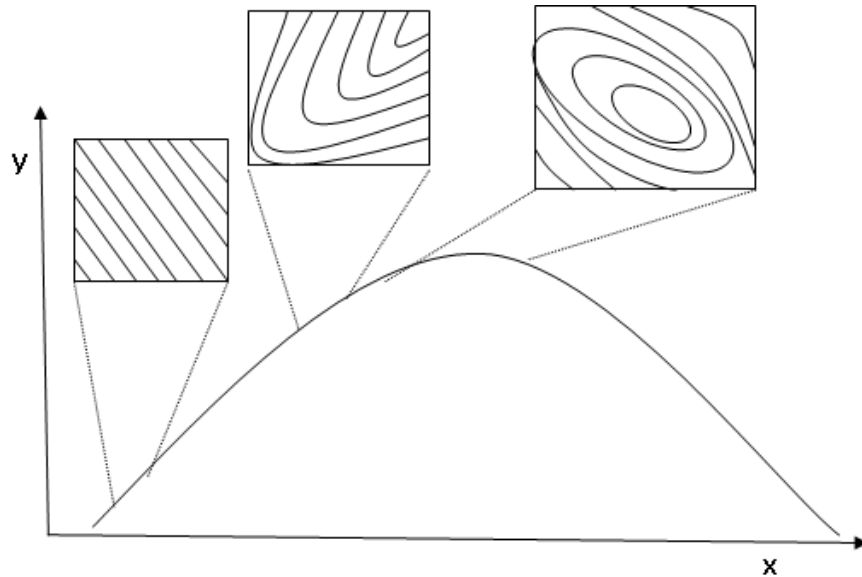


Figure 4.23: Schematic illustrating the contours obtained with a quadratic response surface.
From left to right : hillside, rising ridge and peak.

Below are the descriptions of the models used to describe copper recovery, malachite recovery and minor copper recovery. Along with the models, the iterative process and reasoning for their construction is outlined.

4.3.3.1 Copper Recovery

The overall copper recovery was modeled using response surface methodology. The data was analysed using the standard least squares method. This method is effective in assessing model fits, but is sensitive to outliers in data sets. If there is an outlier, its distance to the model line is taken and then squared. This can skew the data and cloud the interpretation of the results.

The overall copper recovery was plotted with respect to run number in Figure 4.24. The first run of the Box-Behnken experiment was performed collectorless with only DETA addition. This run was included to maintain the structure, symmetry and rotatability of the Box-Behnken design. Running a flotation circuit with no collector addition makes no physical or economic sense. The omission of the first data point makes both statistical and physical sense.

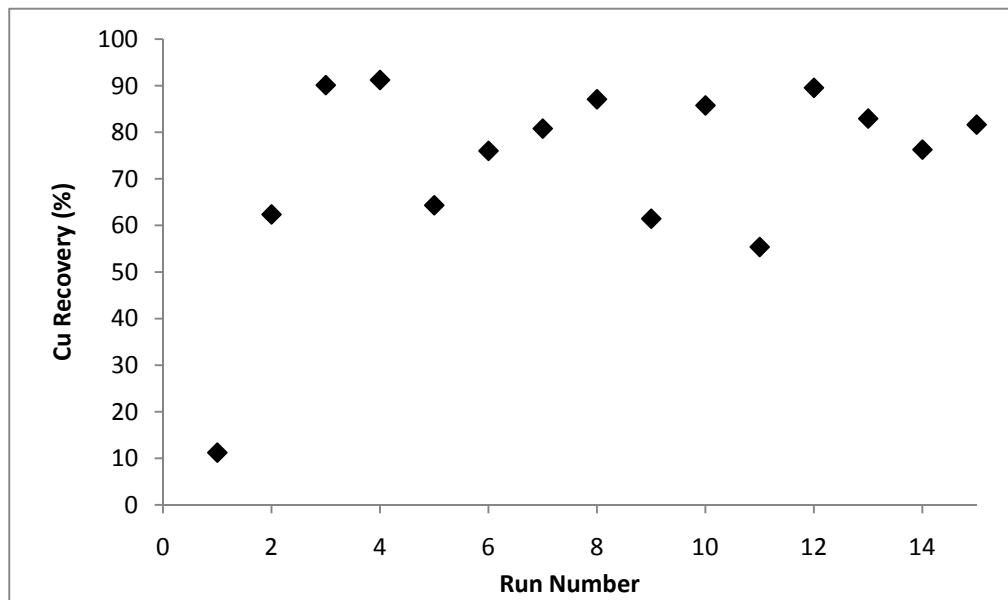


Figure 4.24: Copper recovery versus run number for the Box-Behnken experimental design.

A principal component analysis was performed on the data. Principal component analysis (PCA) is the mathematical transformation of the data to a new coordinate system. This transforms a number of potentially correlated variables into a smaller number of un-correlated variables called principal components. The first principal component accounts for the most variability in the data, meaning that it corresponds to a line that passes through the data and minimizes the sum squared errors of those points (Mason et al, 1989). The principal component analysis performed for the copper recovery can be seen in Figure 4.25. From the PCA, it can be seen that PAX accounts for the majority of the variance in the data. According to the PCA, PAX accounts for

nearly 40 % of the trend present. Hydroxamate follows closely behind PAX, so that combined, PAX and hydroxamate account for over 70 % of the variance present. DETA was the least significant principal component.

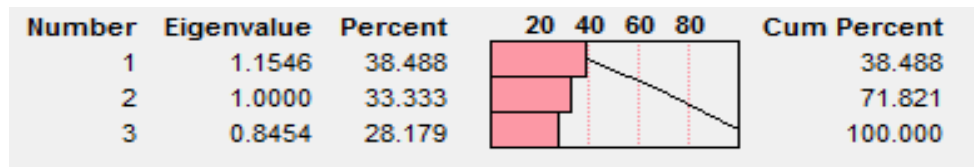


Figure 4.25 : Principal component analysis output from JMP. The components are PAX (1), hydroxamate (2) and DETA (3).

The correlation between the explanatory variables was investigated and shown in Table 4.2. The table indicates that there is a very small correlation between PAX and hydroxamate and no correlation is present with DETA. The variables were considered to be independent of one another.

Table 4.2: Correlation table between explanatory variables.

	PAX	HYDROX	DETA
PAX	1.0000	-0.1546	-0.0000
HYDROX	-0.1546	1.0000	0.0000
DETA	-0.0000	0.0000	1.0000

Despite the fact that the bench-scale experiments were designed with a higher order model in mind, the possibility that a linear model fits is not excluded. As shown in Figure 4.23, the process space might still be in the hillside region. The data was modeled using a full factorial design which includes: the main effect; the two factor interaction effects; and, the three factor interaction effect. The JMP output for this model can be seen in Figure D.1 in Appendix D.

To assess model adequacy, quantitative and graphical diagnostics were analysed. The quantitative diagnostics of the linear model indicated that the model was adequate. The R^2 and adjusted R^2 values were good at 0.86 and 0.74 respectively. The MSR/MSE ratio is statistically significant meaning that significant trend was picked up. The lack of fit test confirms that there is no significant lack of fit. The only significant effect was the hydroxamate main effect. An ideal model is the simplest model possible that contains only significant effects. With some of the insignificant effects removed from the model, the R^2 adjusted value improves slightly. The R^2 adjusted value is a modified R^2 value which adjusts for the number of explanatory terms in a model. The R^2 adjusted value will only improve if the terms added or subtracted from the model improve the model more than can be expected by chance (Mason et al, 1989). No matter how many insignificant effects were removed from the model, no other effect became significant.

The graphical diagnostics do not corroborate the quantitative results. The plot of the actual versus predicted values indicate a mediocre fit. The most telling graphical diagnostics are the plot of the residual by predicted values and the scatterplot matrix. The residual by predicted plot in Figure 4.26 shows a definite quadratic trend. This means that there is un-modeled trend and that it is quadratic. The bottom row of the scatterplot matrix in Figure 4.27 depicts the residuals versus the factors in the model. Trend is seen in the residuals for all three factors. Hydroxamate in particular demonstrates quadratic trend. It is clear from the graphical diagnostics that a linear model does not provide an adequate fit for the data.

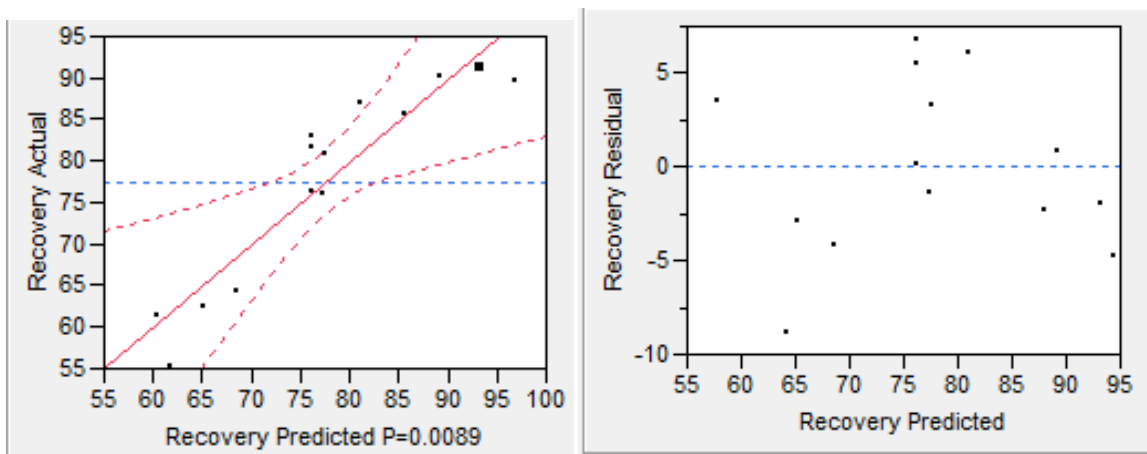


Figure 4.26: Actual by predicted (R) and residual by predicted plot (L) for a linear model.

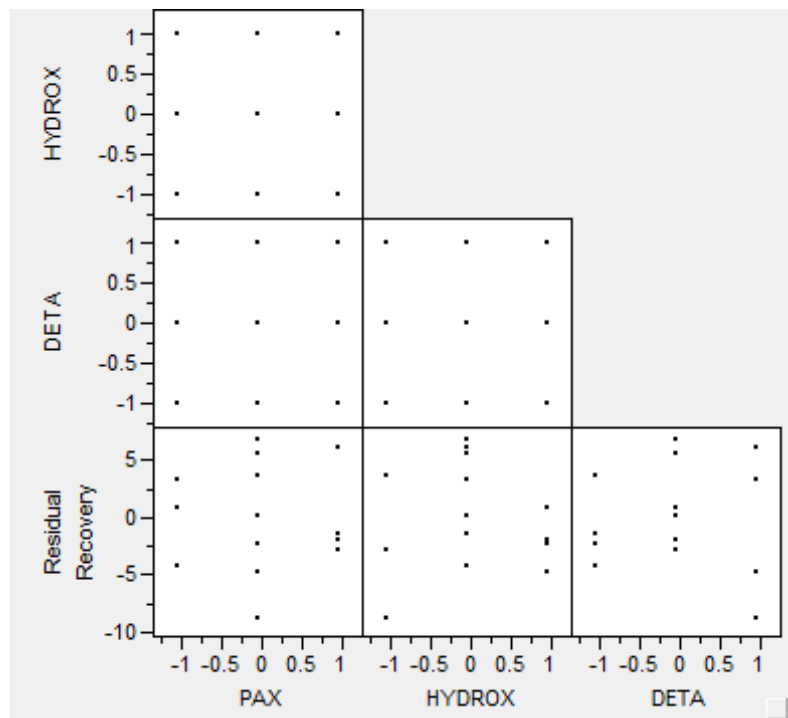


Figure 4.27: Scatterplot matrix for a linear model for copper recovery.

Since a linear model was inadequate, a quadratic response surface model was created. Initially, a full second order quadratic model was created. The theoretical equation for that model is seen below:

$$Y = \beta_0 + \beta_{11}x_1^2 + \beta_{22}x_2^2 + \beta_{33}x_3^2 + \beta_1x_1 + \beta_2x_2 + \beta_3x_3 + \beta_{12}x_1x_2 + \beta_{13}x_1x_3 + \beta_{23}x_2x_3$$

The full model had similar problems to the linear model. Only the hydroxamate main effect was significant at the 95 % confidence interval. The model was assessed with the same qualitative and quantitative diagnostics. The R^2 and R^2 adjusted were 0.91 and 0.73 respectively. This indicates that a significant amount of trend was picked up, but there was a penalty for the large number of estimated parameters. The MSR/MSE ratio was significant meaning that trend was picked up and the trend was not due to noise. The model passed the lack of fit test. In the plot of the actual versus predicted values, all the points are clustered relatively close to the $y = \hat{y}$ line. The residual versus predicted plot shows no discernable trend remaining. The residual by row number plot shows some cyclical trend which indicates that there was a systematic shift that changed from test to test. A scatterplot matrix of the explanatory variables and the residuals is shown in Figure 4.28. It confirms that there is trend remaining in the residuals, regardless that every possible parameter is included. The JMP output for this model can be seen in Figure D.2 of Appendix D.

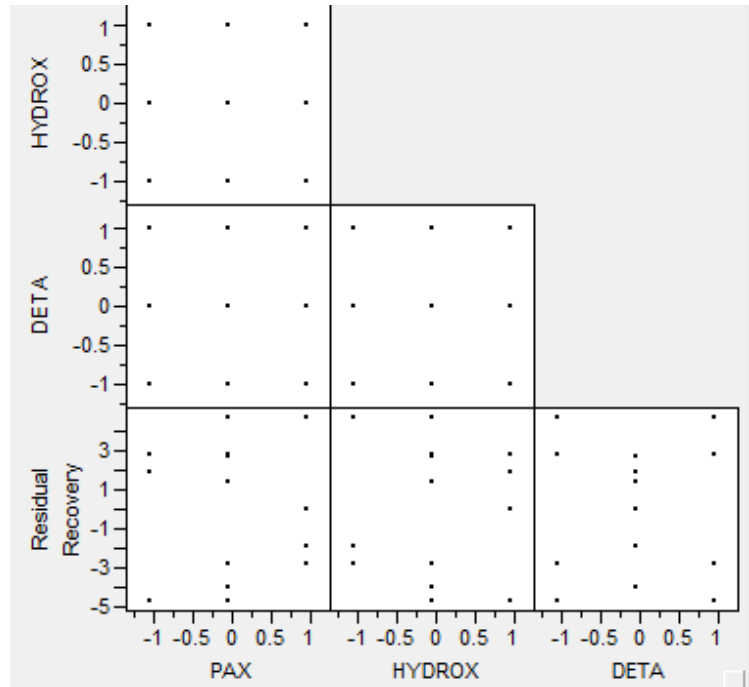


Figure 4.28: Scatterplot matrix for the full quadratic response surface model for copper recovery.

In order to simplify this model, there are many possible combinations of parameter omissions. To narrow down the possibilities, criteria were imposed. The PCA indicated that PAX was the most significant effect. This is not mirrored in the parameter estimates. The t-test that is performed to assess parameter significance was created to be used on large data sets. Since there are only 14 observations in this data set, it is quite possible for the t-test to misrepresent the significance of a parameter. Due to this, the PAX main effect was never omitted. The purpose of this thesis was to propose collector dosages that provided an optimum flotation response. In order to propose such collector dosages, the model needed to be able to calculate a response surface. If too many parameters are removed from the model, regardless of their level of significance, the program loses the ability to calculate a response surface. This occurs when there are too many degrees of freedom in the system.

With the criteria set out above, there was still a large amount of models that could be created. Surprisingly, with each model iteration, very little changed in the quantitative and graphical diagnostics. Hydroxamate remained the only significant parameter estimate. The MSR/MSE ratio always indicated significant trend and that no lack of fit was found. The R^2 and R^2 adjusted values varied, but were good in every case. The graphical diagnostics were comparable, except in cases where too many parameters were omitted. At this point, a slight quadratic trend became visible in the residual by predicted plot.

Once the qualitative diagnostics become too similar to provide a good method of model comparison, graphical diagnostics are the next criteria. The analysis of graphical diagnostics is subjective. It depends upon the user's judgment, which breaks down when comparing many seemingly similar plots. To narrow down the potential number of models to compare, the Akaike information criterion (AIC) was employed. The AIC was developed as a measure of the goodness of fit of an estimated statistical model. It is used to describe the tradeoff between bias and variance in a model used to represent experimental data. Essentially, it is a criterion that penalizes for having too many parameters in a model. It is not analogous to hypothesis testing, but is used as a tool of model selection. Models can be ranked in terms of their AIC with the lowest AIC being the better model. The AIC is calculated as shown in the equation below where n is the number of observations, k is number of parameters and RSS is the residual sum of squares (Akaike, 1974).

$$AIC = 2k + n[\ln(RSS/n)].$$

Table 4.3 gives the AIC for each of the potential models tested. From the AIC values, it can be seen that the main effect of DETA should not be omitted. The models that only used the PAX and hydroxamate main effects gave AIC values higher than that achieved by the full response surface model. This is important to note because the models without the DETA main

effect have less parameters than that of the full model, meaning that they give a poorer overall fit. Also, from the scatterplot matrix of the full response surface model in Figure 4.28, it can be seen that there is a quadratic trend in the residuals versus the explanatory variable DETA. This indicates that although the parameter is insignificant, it contributes to the model. The model that resulted in the lowest AIC, 46.62, was the model that omitted all interaction effects. This AIC value was much lower than the majority of the other values; so, it is potentially the best model for the data. This corroborates with the correlation table in Table 4.2 which indicated that there was negligible systematic relationships between the explanatory variables. It would make sense that their interaction effects would not contribute well to a model.

Table 4.3: Akaike Information Criterion (AIC) for potential models. The models are classified by parameters omitted. P=PAX, H=Hydroxamate and D=DETA.

Model	AIC
FULL	51.23
D*D	50.50
P*D	49.72
D*D &P*D	49.11
P*H,P*D,D*H	46.62
H*D	51.33
P*H	50.00
D*D,P*D	49.11
D*D,H*D	50.44
D*D P*H,H*D	48.52
D*D,P*H,H*D	49.73
D*D,P*D,H*D	48.97
D*D,P*H,P*D,D*H	48.21
D	51.74
D,P*H	50.64

The model with no interaction effects was examined more closely to determine its adequacy. The full JMP output for this model can be seen in Figure D.3 of Appendix D. Although it presents the lowest AIC, the model's quantitative and graphical diagnostics must still

be analysed. The R^2 and R^2 adjusted values are both high. The R^2 adjusted value is higher than in the full model, indicating that the omission of the interaction effects improved the fit. The MSR/MSE ratio is highly significant. This indicates that a large amount of trend was picked up and little was due to noise. The model passes the lack of fit test with no significant lack of fit detected. The plot of the actual versus predicted values has all the points within the confidence interval and is closely clustered around the $y=\hat{y}$ line. The residual versus predicted plot shows no discernable trend. These plots can be seen in Figure 4.29. The residual versus row and the scatter plot matrix, seen in Figure 4.30, still indicate remaining un-modeled trend. Since this was also seen in the full model, it should not be considered to make this model inadequate. From quantitative and graphical diagnostics, this model is determined to be adequate and will now be referred to as the final model. It must be noted that this model is only adequate within the scope of this thesis. The number of insignificant parameters, the un-modeled trend and the large AIC values are all indicators of a poor model fit. However, the model is predicting a response that makes physical sense for the flotation circuit.

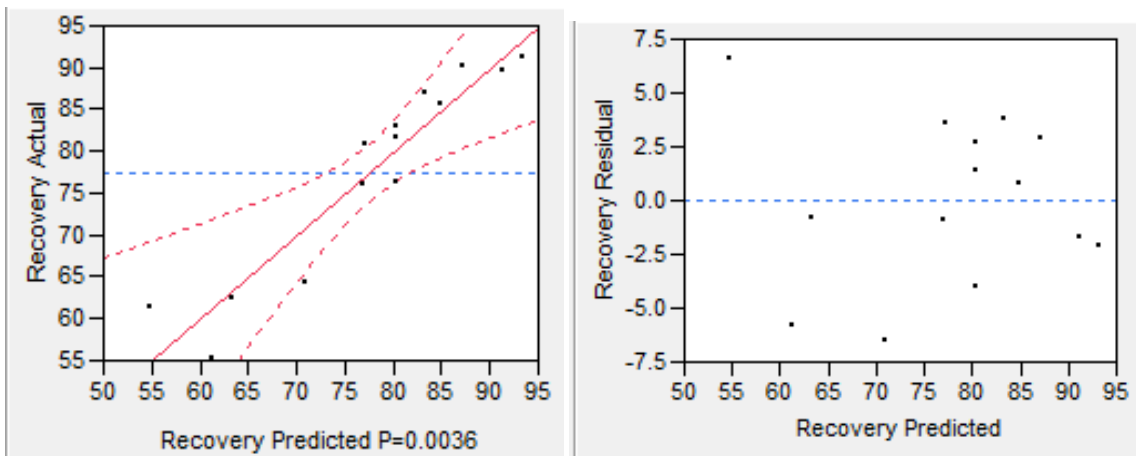


Figure 4.29: Actual by predicted (R) and residual by predicted plot (L) for the response surface model with no interaction effects.

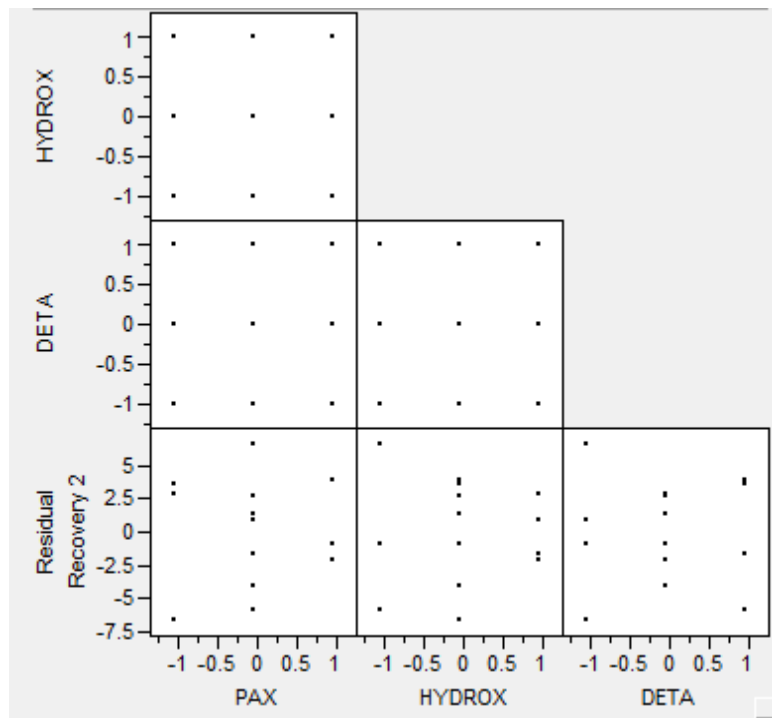


Figure 4.30: Scatterplot matrix for the response surface model with no interaction effects.

The response surface profiles calculated by JMP are shown in Figure 4.31. These surfaces model the interaction effects between each of the explanatory variables. These interaction effects were not statistically significant and were not included in the final model. These interaction effects should be understood as they are present in the flotation cell. It can be seen from Figure 4.31 that hydroxamate has a strong influence on copper recovery. As the collector dosage increases from 0g/t to 408 g/t the recovery rises 40%. PAX has a lesser effect on copper recovery, with a stronger effect at low hydroxamate dosage. This is likely due to the fact that the effect of hydroxamate will begin to mask the PAX effect as it is stronger. The interaction between the two collectors can theoretically enhance the recovery from below 90 % to nearly 100%. The interaction effect between PAX and DETA is negligible. From the axes on the graph, it appears that the effect of DETA is almost quadratic. However, the graph is only shown on a

limited recovery axis, meaning that the effects are essentially flat. This means that even if no DETA, or a very high dosage of DETA was added to the cell, there would be a small effect on flotation response. This can be seen clearly in the interaction surface between hydroxamate and DETA. The hydroxamate has a significant effect on copper recovery and the small effect of DETA is accurately seen.

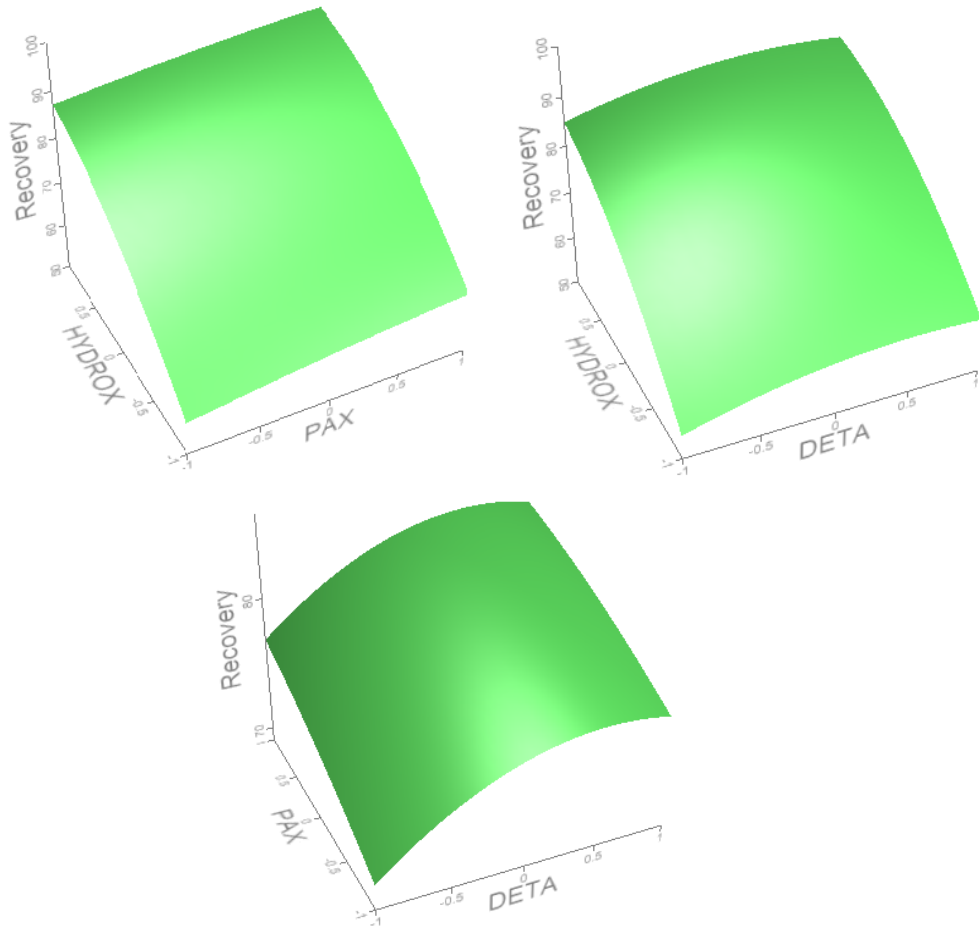


Figure 4.31 : JMP surface profile for the interaction effects between the explanatory variables for the copper recovery model.

The response surface for the final model was solved in JMP. It was found to have a critical value outside the process space. The critical value corresponded to a predicted maximum of 98.05% copper recovery. The collector dosages that correspond to this maximum recovery are

202.7g/t PAX, 674.99 g/t hydroxamate and 61.9 g/t DETA. The equation for the final model can be seen below. PAX, hydroxamate and DETA are represented by x_1 , x_2 and x_3 respectively.

$$y = 80.28 + 3.04x_1 + 15.05x_2 + 3.15x_3 - 0.525x_1^2 - 4.55x_2^2 - 2.70x_3^2$$

4.3.3.2 Malachite Recovery

Malachite is a non-sulphide copper mineral that has proved resistant to conventional collectors. The malachite recovery was modeled using response surface methodology and the data obtained during the Box-Behnken experimentation. The malachite recovery data was analysed with the same methods as the overall copper recovery model. The standard least squares model was used. The malachite recovery was plotted by test number to check for outliers. Unlike the overall copper recovery, there are no clear outliers present in Figure 4.32. No values were excluded in the creation of the malachite recovery model.

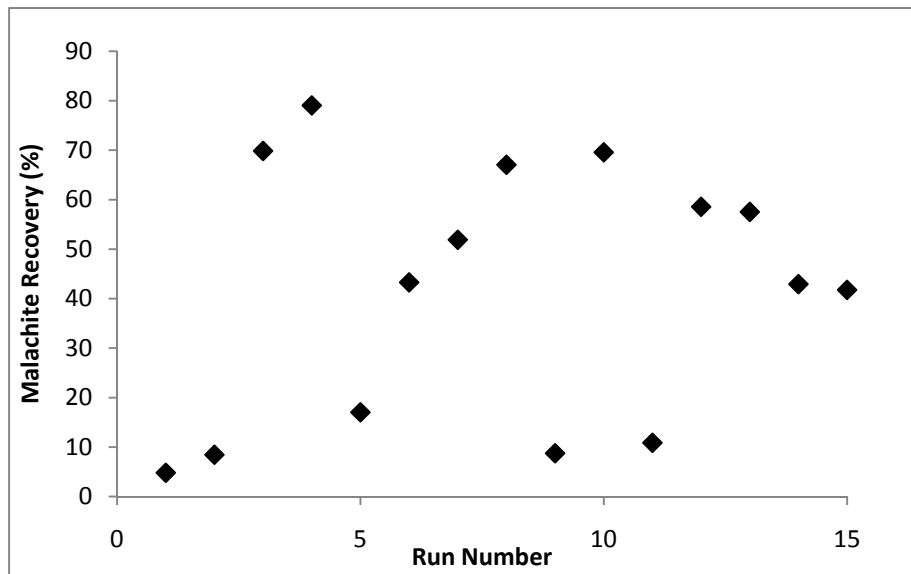


Figure 4.32: Malachite recovery versus run number for the Box-Behnken experiments.

A principal component analysis was performed to determine which explanatory variables contribute the most to the model. The PCA performed in JMP can be seen in Figure 4.33. It was

found that the principal components were the same as with the overall copper recovery. PAX was the first principal component followed closely by hydroxamate. DETA accounted for the least amount of variance in the data at 28 %. Although the three explanatory variables account for different amounts of trend, they are all in a similar range. PAX is the first principal component, but it accounts for less than 10 % more than DETA. This is taken to mean that all three effects are important for the modeling of the data, and none should be omitted from the final model.

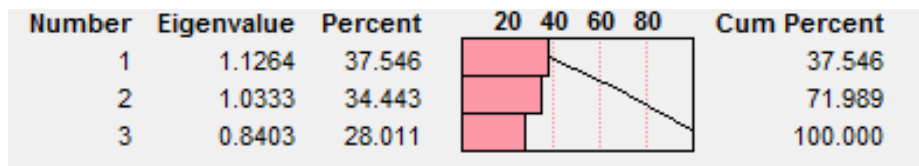


Figure 4.33: Principal component analysis output from JMP. The effects are PAX (1), hydroxamate (2) and DETA (3).

The correlation matrix can be seen below in Table 4.4. Correlation is present between all of the explanatory variables. The largest correlation occurs between hydroxamate and DETA. The correlations are negligible, even that of hydroxamate and DETA. No significant systematic linear relationship is present between any of the explanatory variables.

Table 4.4: Correlation table for the explanatory variables in the malachite recovery model.

	PAX	HYDROX	DETA
PAX	1.0000	-0.0608	-0.0442
HYDROX	-0.0608	1.0000	-0.1251
DETA	-0.0442	-0.1251	1.0000

A linear full factorial model was fit to the malachite recovery data. Hydroxamate was the only significant parameter and the three factor interaction zeroed. Once the three factor interaction term was removed, the qualitative and graphical diagnostics were assessed. The full JMP output for this model can be seen in Figure D.4 in Appendix D. The quantitative diagnostics indicate an adequate model fit. The R^2 and R^2 adjusted indicate that modest trend was picked up.

The values were 0.85 and 0.72 respectively. The MSR/MSE ratio was significant and the lack of fit test indicated a good model fit. The graphical diagnostics did not support the quantitative findings. The actual versus predicted plot and residual versus predicted plot are shown in Figure 4.34. The actual versus predicted plot shows most of the values clustered around the $y=\hat{y}$ line but some points lie outside of the 95 % confidence interval. The residual versus predicted plot contains a sinusoidal trend. This is indicative of an inadequate model. The residual by observation numbers shows no particular trend. No systematic shifts occurred during the course of the experiments.

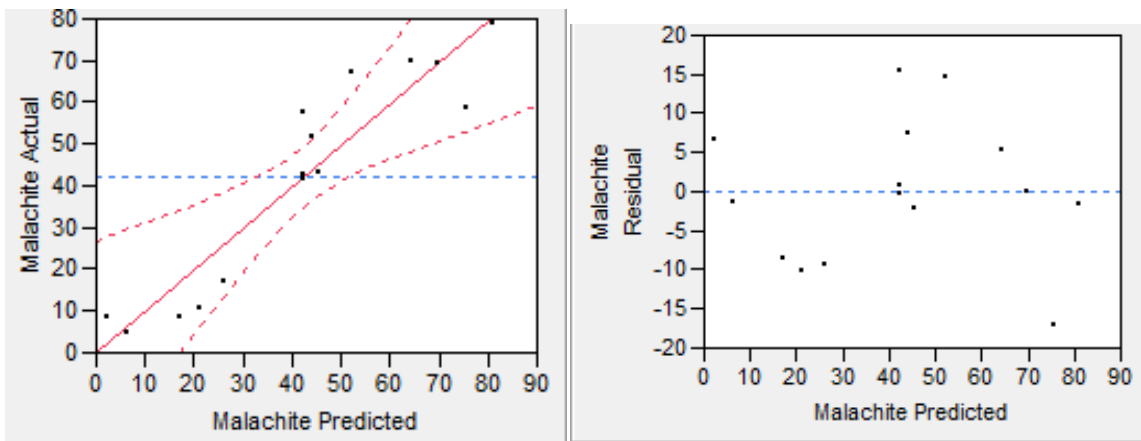


Figure 4.34: Actual by predicted (R) and residual by predicted plot (L) for the linear model of malachite recovery.

A scatterplot matrix (Figure 4.35) was constructed to evaluate the residuals versus the explanatory variables. The scatterplot indicates significant un-modeled trend with each explanatory variable. In particular, hydroxamate residuals show a distinct quadratic trend. PAX and DETA show similar un-modeled trends that are slightly curved towards the high level. On the basis of the graphical diagnostics, it is concluded that a linear model for malachite recovery is inadequate. Since the process space is clearly not in the hillside region and quadratic trends remain un-modeled, a quadratic response surface model was fit to the data.

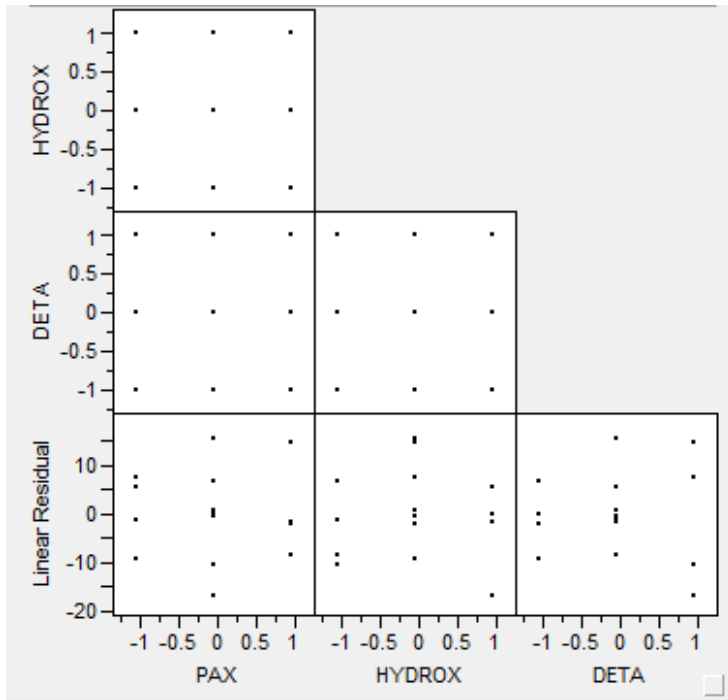


Figure 4.35: Scatterplot matrix for the linear model of malachite recovery.

Since the process space is clearly not in the hillside region and quadratic trends remain un-modeled, a quadratic response surface model was fit to the data. PAX and hydroxamate main effects were never removed from the model as they are the two most significant principal components. Another caveat applied to the model was that it remained able to calculate a solution to the response surface. This meant that the degrees of freedom had to be kept reasonable thus all insignificant parameters could not be removed from the model.

The full response surface model had the hydroxamate main effect as the only significant parameter. Again, the t-test performed to asses parameter significance is performed with only 15 data points and the number required to get a trustworthy t-test is much higher. The quantitative diagnostics were indicative of an adequate model. The R^2 and R^2 adjusted value indicated that trend was picked up. The MSR/MSE ratio was significant; the trend modeled was not due only to noise. No significant lack of fit was present. The graphical diagnostics mostly confirmed the

conclusion from the quantitative diagnostics. The points on the actual versus predicted plot were within the 95 % confidence interval and were clustered along the length of the $y=\hat{y}$ line. The residual versus predicted value plot showed remnants of the sinusoidal trend present in the linear model. Similar to the copper recovery model, trend was still visible in the scatterplot matrix of the residuals versus the explanatory variables seen in Figure 4.36. The remaining trend is less than in the linear model. Once again, there was an uncontrolled effect on the system that was unaccounted for in the model. The JMP output for this model can be seen in Figure D.5 in Appendix D.

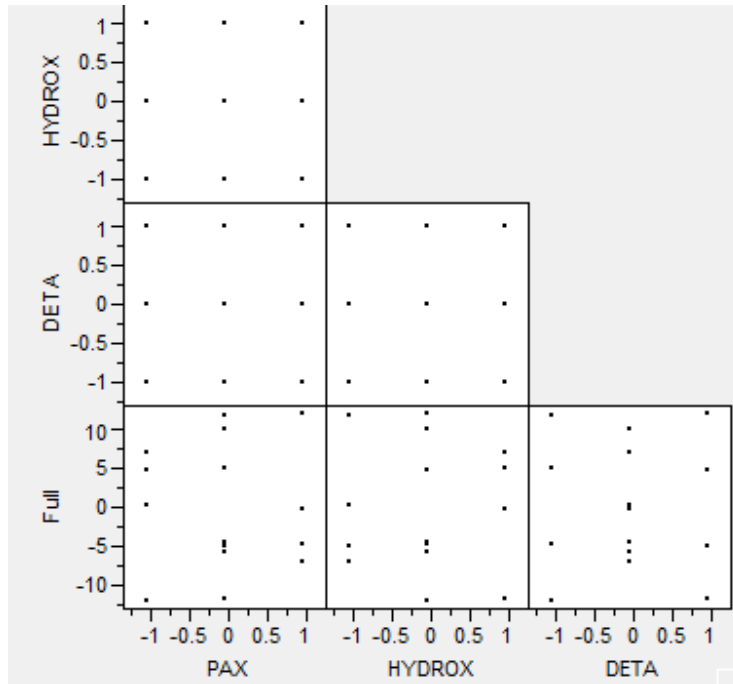


Figure 4.36 : Scatterplot matrix for the full response surface model for malachite recovery.

Similar results were obtained as parameters were removed from the full response surface models. The models created all presented good R^2 values, significant MSR/MSE ratios and no lack of fit. Another commonality between the models created was the slight sinusoidal behaviour in the residual versus predicted plot. To compare the models most

effectively, the Aikaike Information Criterion was calculated in each case. The AIC values are shown in

Table 4.5. It can be seen that the DETA main effect should not be excluded from the final model. When only PAX and hydroxamate were used to model the malachite recovery data, the AIC value was almost as high as for the full model despite having four fewer parameters. The model with the lowest AIC value was found to be the model with no quadratic DETA term or interaction effects.

Table 4.5: AIC values calculated for the malachite recovery models. Parameters are PAX(P), hydroxamate (H) and DETA (D).

Model	AIC
FULL	79.72
-D	77.35
-D, P*H	75.44
-P	77.23
-P, H*D	75.71
-P,D	75.08
-P*H,P*D,H*D	75.00
-D*D	78.29
-D*D,P*H	76.41
-D*D,P*D	76.77
-D*D,D*H	76.95
-D*D, P*D,P*H	74.88
-D*D, P*D,D*H	75.07
-D*D, P*D, P*H	75.41
-D*D, P*D, P*H, H*P	73.52

The AIC is a tool of model selection. In terms of model adequacy, it must be used alongside other diagnostic tools to make a prognosis. The model with the lowest AIC was unable to provide a solution for the quadratic response surface. The slight sinusoidal trend was also still present in the residual vs predicted plot. As it is a goal of this thesis to provide collector dosages

that give an optimum recovery, the model with the second lowest AIC was analysed. This model omitted the DETA quadratic term along with the PAX interaction terms. This agrees with the correlation table in Table 4.3. Although the hydroxamate and DETA interaction effect was negligible, it had the stronger systematic interaction.

The quantitative diagnostics indicated an adequate model. The R^2 and R^2 adjusted were high at 0.89 and 0.81 respectively. The MSR/MSE ratio was significant meaning that the trend that was picked up was not due to noise. No lack of fit was detected. The actual versus predicted plot and the residual vs predicted plot can be seen in Figure 4.37. The points in the actual versus predicted plot follow the $y=\hat{y}$ line with few values outside of the 95 % confidence interval. The residual versus predicted plot shows no systematic trend. Most notably, it shows no evidence of the sinusoidal pattern visible in the other models. Due to this lack of visible trend, this model leaves less trend un-modeled than the model with the lowest AIC. No systematic patterns were visible in the residual by row plot. A scatterplot matrix was created and can be seen in Figure 4.38. Trend remains between the residuals and the explanatory variables. From the quantitative and graphical diagnostics, this model was found to be adequate for the purposes of this thesis. Similar to the copper recovery model, there are indicators of poor model fit. Since the model is still predicting collector dosage levels that make physical sense to the system, it is still adequate. From this point on, this model is referred to as the final malachite recovery model. The full JMP output can be seen in Figure D.6 in Appendix D.

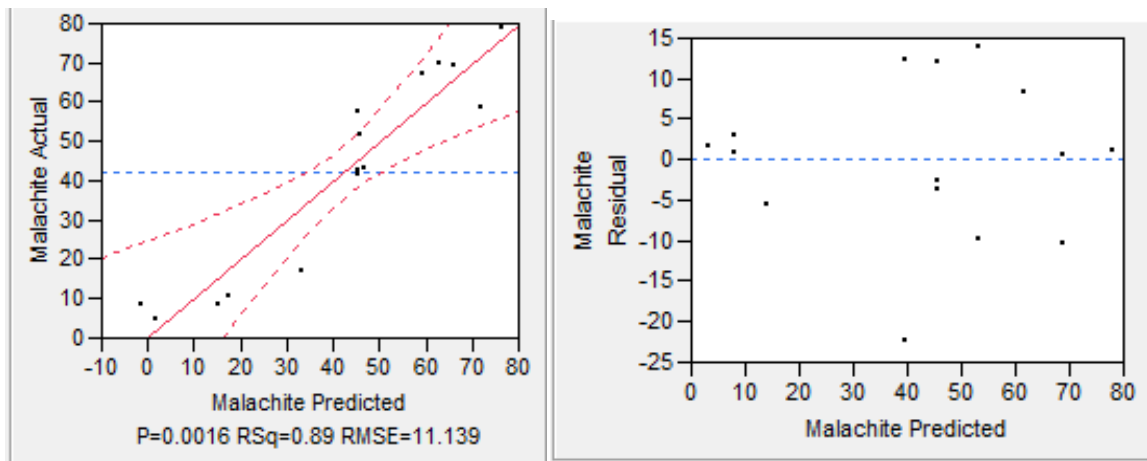


Figure 4.37: Actual by predicted (R) and residual by predicted plot (L) for the final model of malachite recovery.

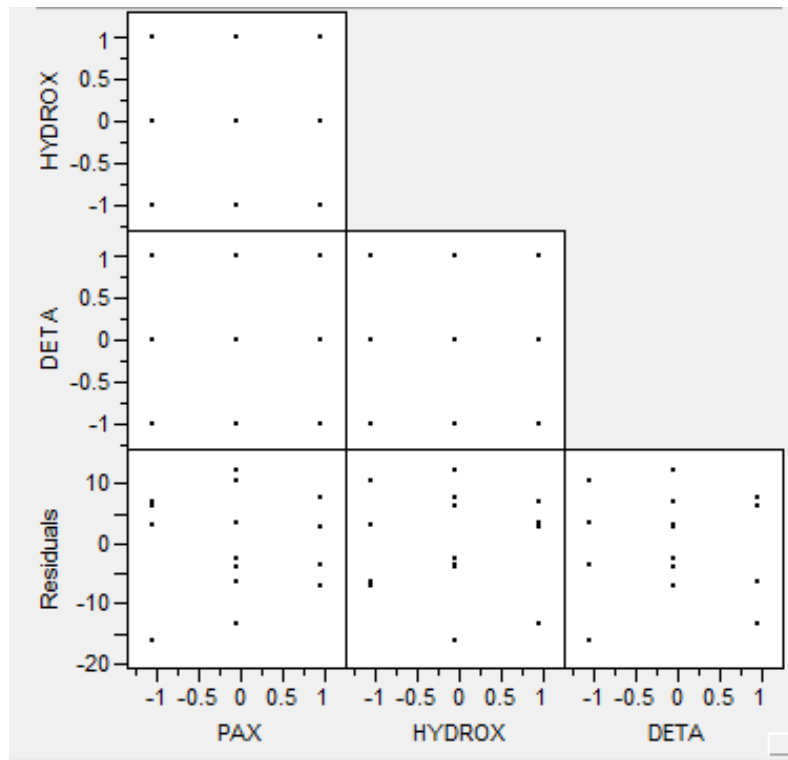


Figure 4.38: Scatterplot matrix for the final model for malachite recovery.

The interaction surface profiles in Figure 4.39 were created in JMP. It can be seen that hydroxamate has the most significant effect. The quadratic character of the hydroxamate effect can also be clearly seen. When either PAX or DETA are at their lowest level, hydroxamate alone is able to raise the malachite recovery from less than 10 % to almost 80 %. Neither PAX nor DETA are able to increase malachite recovery to this extent. The interaction effect between PAX and DETA appears to linearly increase malachite recovery by 10 %. The interaction effects with hydroxamate are similar between PAX and DETA. With the aid of PAX and DETA, the malachite recovery is increased 15 % on average. These interaction effects were not statistically significant, but they exist within the flotation cell. The hydroxamate effect dominates, but it is clear from the interaction profiles that PAX and DETA also play roles in malachite recovery.

The final malachite recovery model was solved in JMP. According to the canonical analysis, the solution was a saddle point located at 62 % recovery. Higher malachite recoveries were obtained during the course of the Box-Behnken experiments, confirming the saddle point solution. The highest malachite recoveries were obtained with hydroxamate and PAX dosages. In fact, the runs with the highest malachite recovery were the ones with the highest copper recovery. Given the correlation between high malachite recovery and high overall copper recovery, higher malachite recovery lies with similar collector dosages as the overall copper model. This means higher hydroxamate and PAX dosages. This is also confirmed by the significance of the hydroxamate parameter in the statistical models. The interaction term between hydroxamate and DETA was kept in the model, and this could indicate that there is a synergistic effect. From the preliminary investigations, it was noted that concentrates with hydroxamate and DETA appeared to collect more malachite. The equation for the final malachite recovery model as stated by JMP is :

$$y = 45.50 + 6.78x_1 + 30.52x_2 + 6.22x_3 + 0.74x_1^2 - 7.13x_2^2 - 3.28x_2x_3$$

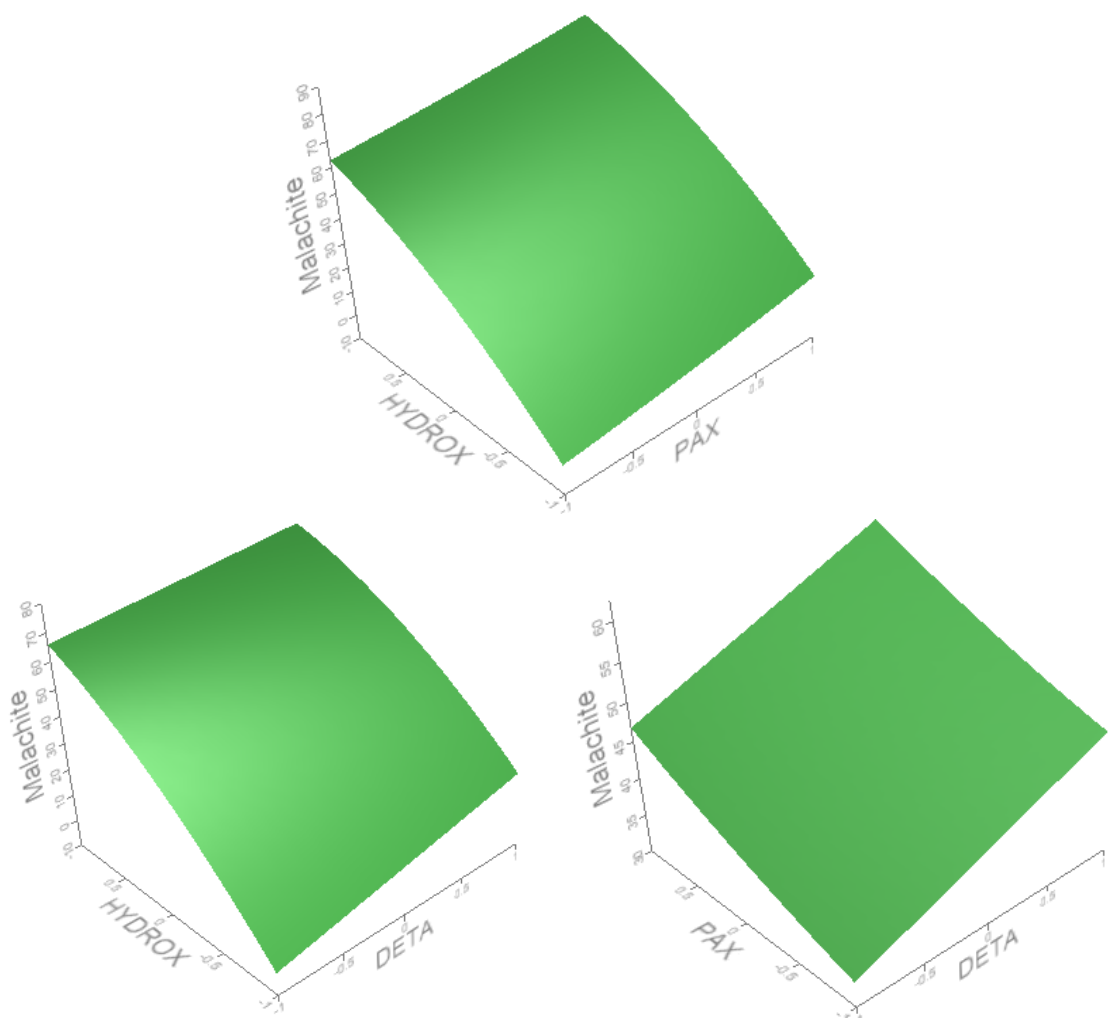


Figure 4.39: JMP surface profile for the interaction effects between the explanatory variables in the final malachite recovery model.

4.3.3.3 Minor Copper

The mineralogical equations used to determine malachite and bornite recovery indicated that there were another copper minerals present. Bornite and malachite recoveries were calculated based on sulphur and carbon data. Once these were calculated, there was still copper that was unaccounted for. This copper was determined to be due minor inclusions of other copper sulphide and oxide minerals. The recovery of the minor copper based on PAX, hydroxamate and DETA was modeled.

The recovery of the minor copper was plotted with respect to run number to identify potential outliers. From the plot in Figure 4.40, the first run was determined to be an outlier. This run was conducted with only DETA addition. A collectorless flotation circuit would not happen in practice. The omission of this data point makes both statistical and practical sense.

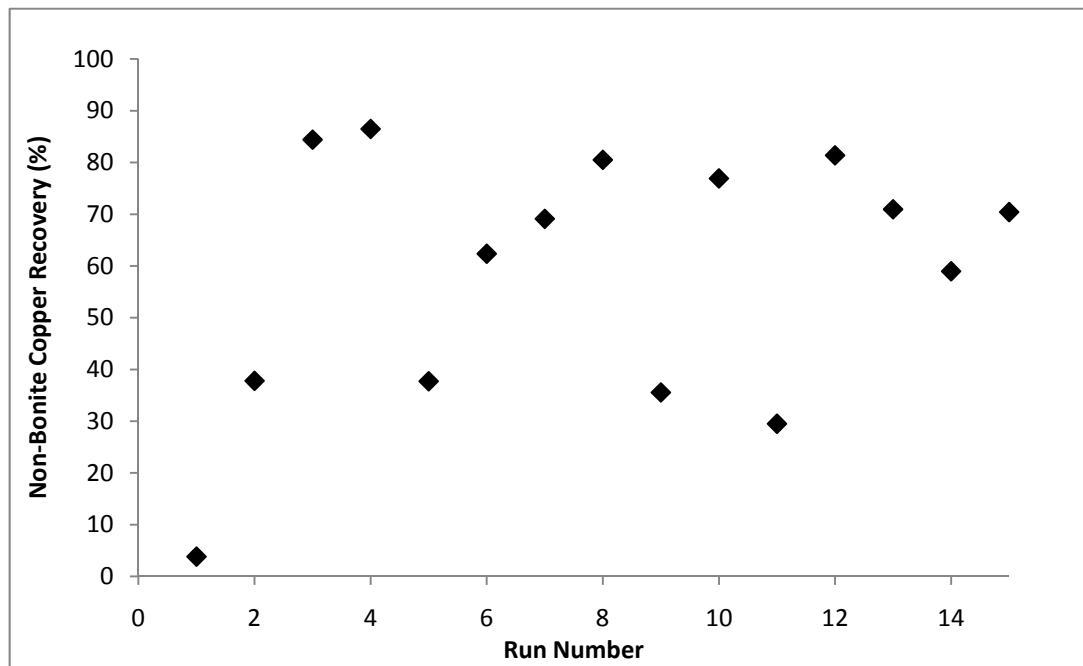


Figure 4.40 : Minor copper recovery versus run number.

The results of the principal component analysis can be seen in Figure 4.41. Similar to both the copper and malachite recovery models, PAX is the first principal component followed by hydroxamate and DETA. The variance modeled by each main effect is in a similar range. Each main effect should be included in the final model.

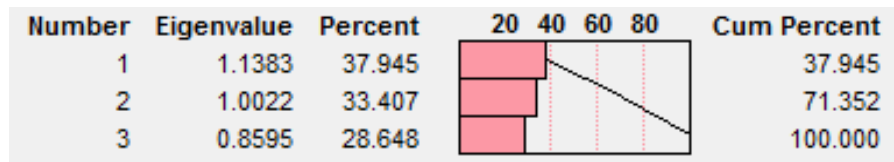


Figure 4.41 : Principal component analysis for the minor copper recovery model.

The correlation matrix is shown in Table 4.6. It indicates negligible linear systematic relationship between each of the explanatory variables. The correlation between PAX and hydroxamate is the largest, but it is still insignificant. All three explanatory variables are independent.

Table 4.6 : Correlation table for the explanatory variables used in the minor copper recovery model.

	PAX	HYDROX	DETA
PAX	1.0000	-0.1336	-0.0398
HYDROX	-0.1336	1.0000	-0.0040
DETA	-0.0398	-0.0040	1.0000

Up to this point, the behaviour of the models has been remarkably similar. An attempt was made to fit a linear model to the recovery data. A full factorial model was fit to the data. The full JMP output for this model can be seen in Figure D.7 in Appendix D. Hydroxamate was the only significant parameter and the three factor interaction zeroed. When the three factor interaction was removed, the model adequacy was assessed. The R^2 and R^2 adjusted are both good at 0.85 and 0.73 respectively. The MSR/MSE ratio is significant and there is no evidence of

lack of fit. The actual by predicted plot and the residual by predicted plot are shown in Figure 4.42. The points are clustered about the length of the $y = \hat{y}$ line. No distinct outliers are present although some values lie outside of the 95% confidence interval. The residual versus predicted plot shows leftover trend. The trend appears to be quadratic in nature, similar to the results achieved in the copper recovery model.

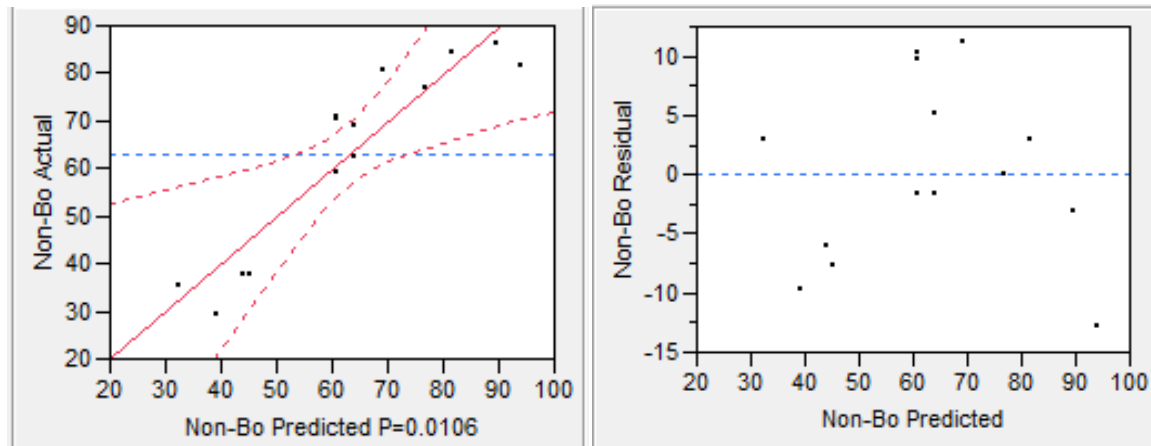


Figure 4.42: Actual versus predicted and residual versus predicted plots for the linear model for minor copper recovery.

A scatterplot matrix, seen in Figure 4.43, was created to ascertain if there was trend remaining in the residuals with respect to the explanatory variables. Un-modeled trend remains for all three explanatory variables. Hydroxamate again presents quadratic trend. PAX and DETA show a slightly curved trend that rises towards higher dosages.

From the graphical diagnostics, a linear model is not adequate to represent the minor copper recovery. From the un-modeled trend remaining in the residuals of the residual by predicted plot, a quadratic model will be fit to the data. The scatterplot matrix shows trend remaining in the residuals for all the explanatory variables, so none of the main effects of PAX, hydroxamate or DETA will be omitted from the final model.

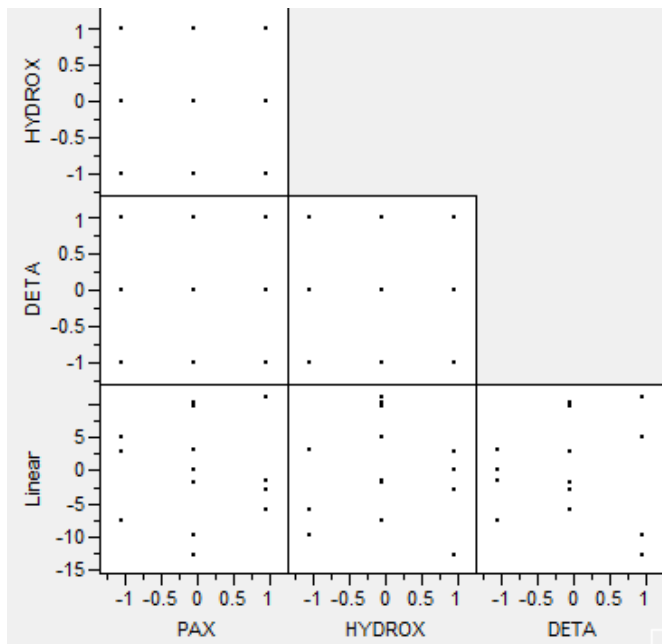


Figure 4.43 : Scatterplot matrix of the residuals versus the explanatory variables in for the linear minor copper recovery model.

The full quadratic response surface model was created in JMP. The quantitative diagnostics indicate a decent model fit. The R^2 value is artificially high, 0.90, due to the amount of parameters fitted to the model. The R^2 adjusted is poor at only 0.68. Hydroxamate was the only significant parameter. The MSR/MSE ratio showed that trend was picked up and no significant lack of fit was found. The graphical diagnostics were indicative of an adequate model. The actual versus predicted and the residual versus predicted plots can be seen in Figure 4.44. The actual versus predicted plot shows good fit. The points are clustered along the length of the $y = \hat{y}$ line with no points lying outside of the 95 % confidence interval. The residual versus predicted graph shows no discernable pattern. The center point runs are tightly clustered in the middle of the residual versus predicted graph, indicating that some systematic error may have occurred. The full JMP output can be found in Figure D.8 in Appendix D.

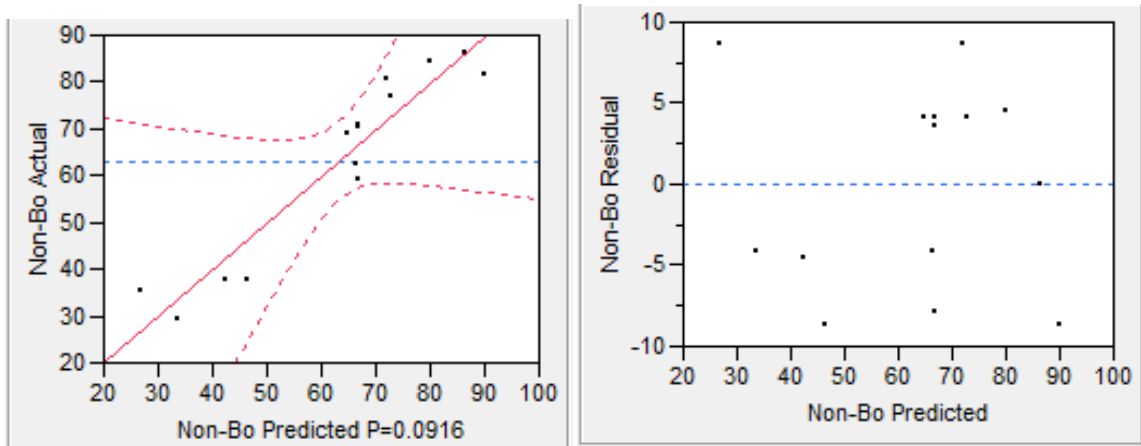


Figure 4.44: Actual versus predicted and residual versus predicted plots for the full quadratic response surface model for minor copper recovery.

A scatterplot matrix was constructed to determine leftover trend in the residuals with respect to the explanatory variables. The scatterplot can be seen in Figure 4.45. Un-modeled trend remains in the residuals. In the case of hydroxamate, the quadratic curve seen in the linear model is partially accounted for in the quadratic model. A pronounced quadratic appears in the residuals of DETA.

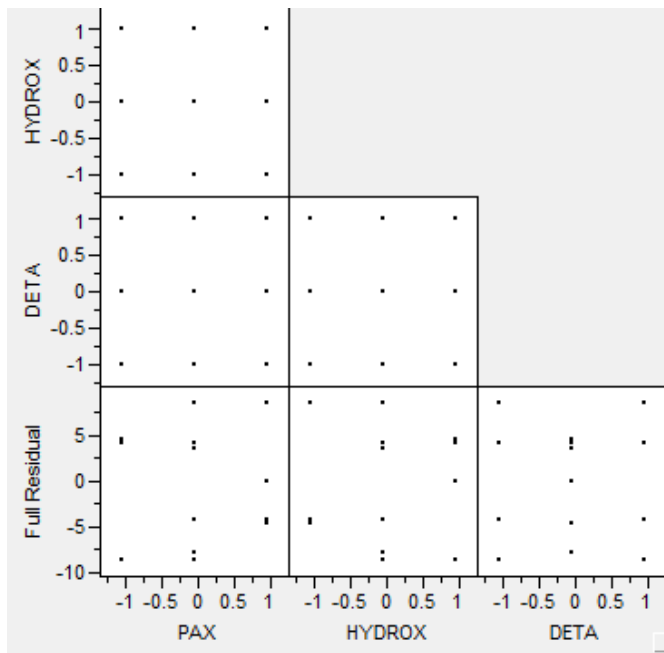


Figure 4.45 : Scatterplot matrix of the residuals versus the explanatory variables for the full quadratic response surface model of minor copper recovery.

The Akaike information criterion was used to select the best model to fit the minor copper recovery. During the selection process, all the attempted models presented similar characteristics. The AIC values calculated for each iterative model are seen in Table 4.7. Models are classified by omitted parameters. Hydroxamate was the only significant parameter, so it was never omitted from a model. Being the first principal component, PAX was also never omitted. DETA was omitted to test a model with only PAX and hydroxamate but the AIC values were very close to that of the full model. This indicated that the removal of DETA and its associated effects did not improve the model greatly. The model with the lowest AIC was the model that omitted the DETA; however, the residuals versus DETA from the full model indicated a strong quadratic trend. For this reason, this model was not chosen. The model with the next lowest AIC was a model with only main effects and their quadratic terms. The AIC for this model was only slightly higher.

Table 4.7 : AIC values calculated for the minor recovery models. Parameters are PAX (P), hydroxamate (H) and DETA (D).

Model	AIC
FULL	70.04
-D	70.09
-D, P*H	68.81
-D*D	68.82
-H*D,P*H	67.42
-H*D,P*D	67.92
-P*H,P*D	67.83
-P*H,H*D,P*D	66.50
D*D,P*H,H*D,P*D	65.66
-D*D,P*H	68.01
-D*D,H*D	67.53
-D*D,P*D	67.94
-D*D,P*D, P*H	67.05
-D*D,P*D, H*D	66.60
-D*D,P*H, H*D	66.67

The quantitative diagnostics for the final minor recovery model were assessed. The R^2 value remained high at 0.88. The R^2 adjusted improved to 0.76 after the interaction parameters were deleted. The MSR/MSE ratio was significant and no lack of fit was detected. Hydroxamate was once again the only significant parameter. The graphical diagnostics confirm the quantitative findings. In the actual versus predicted plot in Figure 4.46, the values are mostly within the 95 % confidence interval and lie along the length of the $y=\hat{y}$ line. There is no discernable pattern visible in the residual versus predicted plot, also in Figure 4.46. The residuals are also equally spaced above and below 0. No systematic trend was visible in the residual by row plot. The full JMP output for the minor copper recovery model can be seen in Figure D.9 in Appendix D.

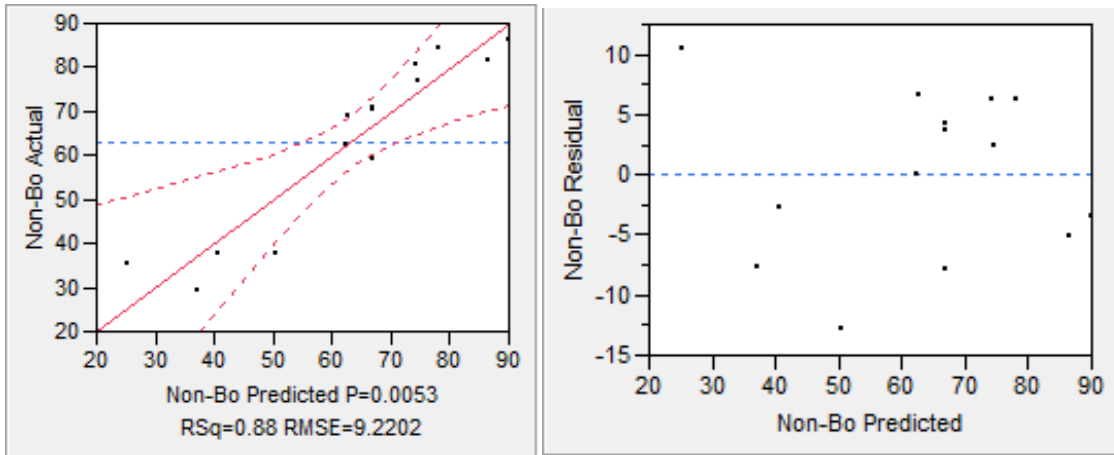


Figure 4.46 : Actual versus predicted and residual by predicted plots for the final minor copper recovery model.

A scatterplot matrix was constructed with the residuals from the final minor copper model. The scatterplot in Figure 4.47 looks similar to the one constructed for the full quadratic model of minor copper recovery. There is significant leftover trend in the residuals versus the explanatory variables. Since a full model with every possible parameter included was not able to model the entire trend, it cannot be expected that a model with less parameters can. The trend remaining in the residuals according to the explanatory variables does not fully discount the findings of this model. For the purposes of this thesis, the model is found to be adequate.

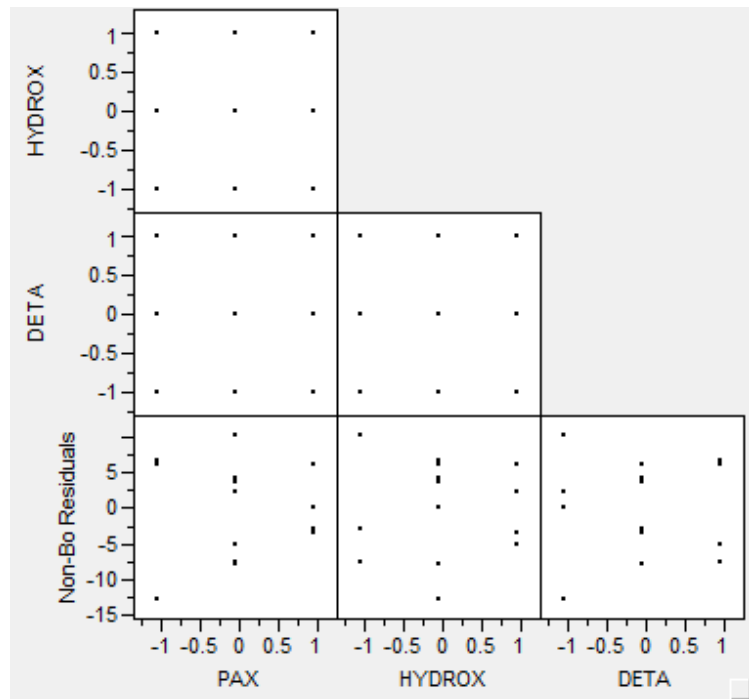


Figure 4.47 : Scatterplot matrix of the residuals versus the explanatory variables for the full quadratic response surface model of minor copper recovery.

The interaction surfaces between the explanatory variables were plotted in JMP and are shown in Figure 4.48. These effects were removed from the final model, but can still affect the flotation response. The significant effect of hydroxamate is plain from the interaction surfaces. The ability for the Cytec 6494 Promoter to collect the minor copper masks the effects of PAX and DETA. The interaction between PAX and hydroxamate is able to increase recovery from below 80 % with just hydroxamate to almost 100 %. The interaction with DETA increases the recovery to the low 90 % range. DETA's quadratic profile from the scatterplot in Figure 4.47 is mirrored in its interaction surfaces. It is more visible in the PAX-DETA interaction surface as it is not masked by the hydroxamate.

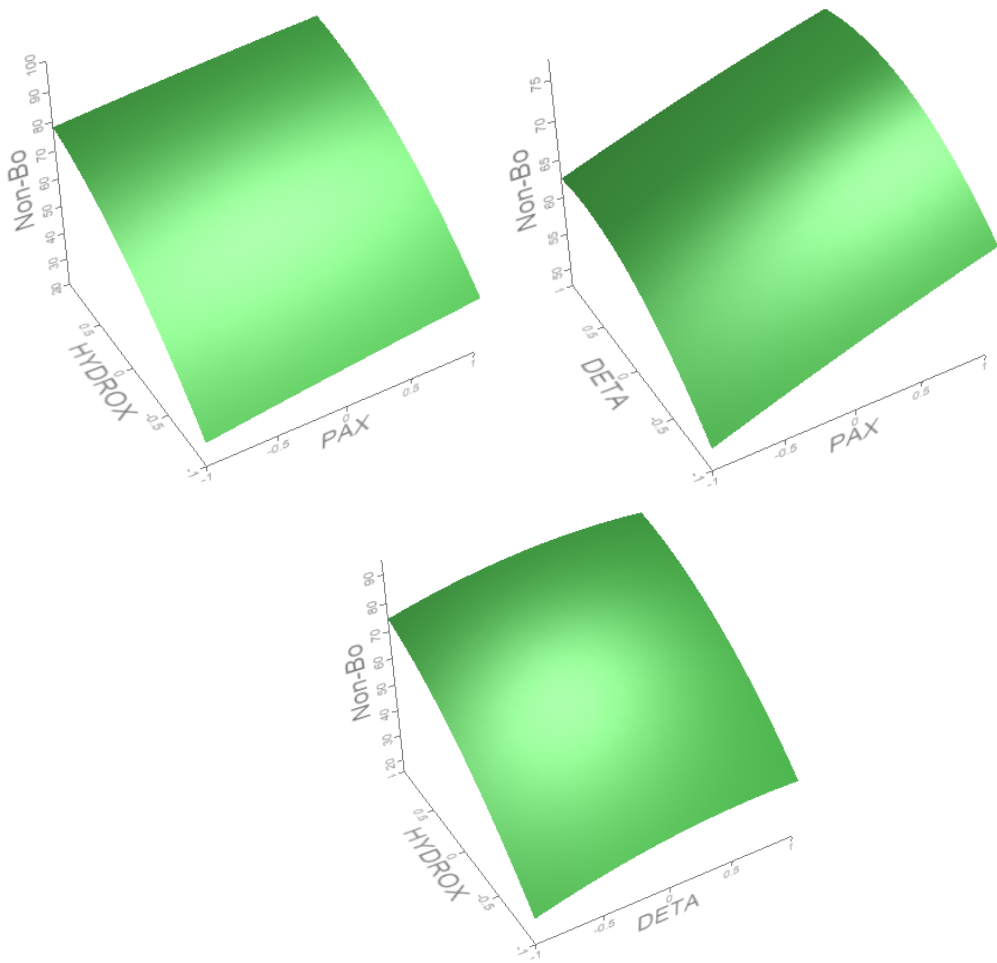


Figure 4.48 : JMP surface profile for the interaction effects between the explanatory variables in the final minor copper recovery model.

The response surface was solved in JMP. It was found to have a critical value outside of the process space. When JMP solved for the critical value, it was found that it corresponded to a maximum with a recovery of 90.8 %. The collector dosages calculated for this maximum recovery were 44.5 g/t PAX, 606.6 g/t hydroxamate and 103 g/t DETA. The equation formulated by JMP to model minor copper recovery can be seen below:

$$y = 66.78 + 5.89x_1 + 24.70x_2 + 5.89x_3 - 0.41x_1^2 - 7.00x_2^2 - 3.94x_3^2$$

4.3.3.4 Copper Grade

The cumulative copper grade of the Box-Behnken experiments was modeled using JMP. Fluctuations in copper grade ranged between 4.18 % and 5.31 %. To model the data statistically, the copper grades were normalized to the mean value of 4.78 %. The normalized results were comparable to the raw copper results. Although numerical values differed slightly, the overall appearance of the data remained the same, as shown in Figure 4.49. For the use of the least squares method, outliers must be removed from the dataset. No outliers were found in Figure 4.49, so all 15 data points were used in model.

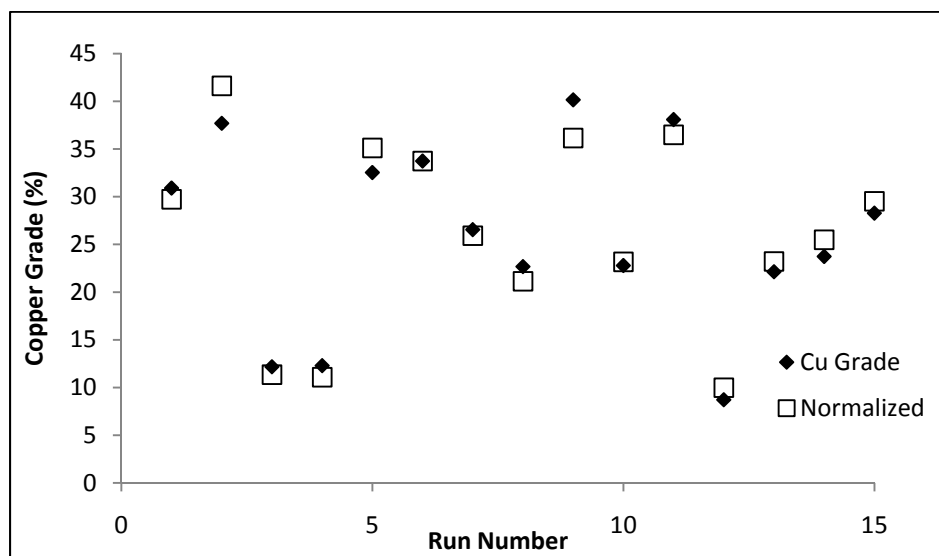


Figure 4.49 : Copper grade versus run number for the Box-Behnken experiments.

A principal component analysis was performed on the normalized copper grades to determine which explanatory variable explains the majority of the variance in the data. From Figure 4.50, it can be seen that PAX is the first principal component and accounts for 37 % of the variability in the data. Hydroxamate is the second principal component followed by DETA. In this model, the percent variance accounted for by the explanatory variables is the closest. In comparison to the recovery models, the difference between PAX and DETA is the smallest. This indicates that all three reagents are important parameter in the determination of copper grade.

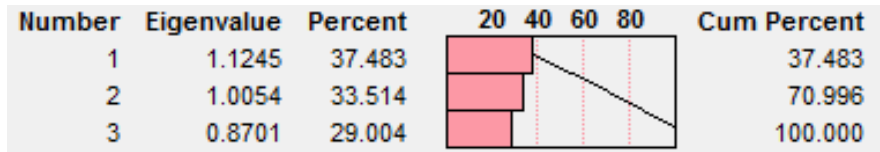


Figure 4.50 : Principal component analysis for the copper grade model. The explanatory variables are PAX (1), hydroxamate (2) and DETA (3).

The correlation table between PAX, hydroxamate and DETA can be seen in Table 4.8. It can be seen that all three variables are independent of one another. There are small correlations between the variables, but they indicate negligible systematic trend.

Table 4.8 : Correlation table between the explanatory variables.

	PAX	HYDROX	DETA
PAX	1.0000	-0.0559	-0.0069
HYDROX	-0.0559	1.0000	-0.1141
DETA	-0.0069	-0.1141	1.0000

The copper grade was fit to a full factorial linear model. It is unlikely that the linear model will fit; it is to eliminate the possibility of being in the hillside region. The three factor interaction term zeroed in the model, and it was removed before the quantitative and graphical diagnostics were assessed. The complete JMP output for this model can be seen in Figure D.10 in Appendix D. The R^2 and R^2 adjusted values were high at 0.89 and 0.81 respectively, indicating that moderate trend was picked up. The MSR/MSE ratio was significant and the lack of fit test did not indicate any lack of fit. As a result, the trend that was modeled was not due to noise, and the model fits the data. The hydroxamate and DETA main effects were significant. From the previous models, only hydroxamate was significant. Despite being the smallest principal component, DETA has a significant effect on the final copper grade.

The graphical diagnostics were assessed. In Figure 4.51, the actual versus predicted plot and the residual versus predicted plot can be found. The data points in the actual versus predicted plot lie along the length of the $y = \hat{y}$ line. Some values lie outside of the 95 % confidence interval, but they are generally clustered about the line. No discernable quadratic trend is visible in the residual by predicted plot. However, there is a distinct line of three points to the left of the graph, indicating an effect not accounted for in the model. The residual versus row number plot (Figure D.10) shows evidence of slight oscillation due to an effect that changed from run to run.

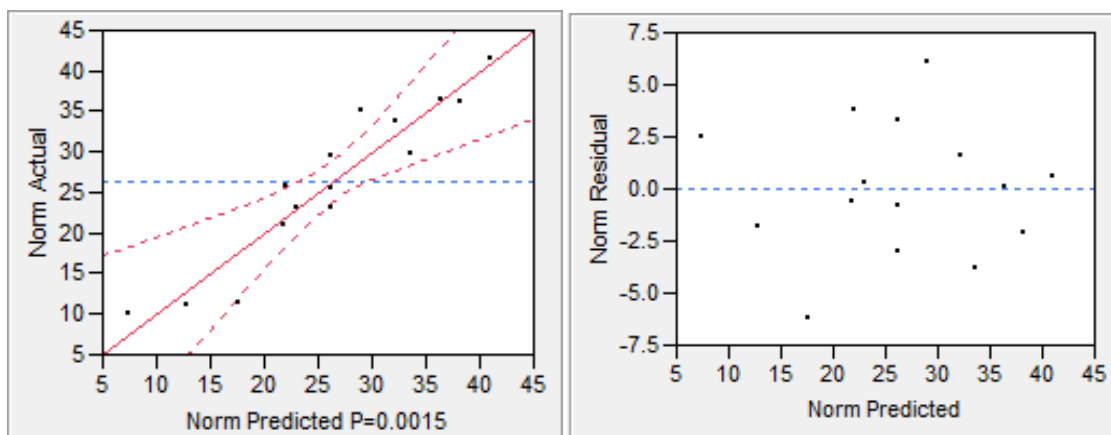


Figure 4.51: Actual versus predicted and residual versus predicted plots for the linear copper grade model.

A scatterplot matrix was created to examine the residuals versus the three explanatory variables. This is done for two reasons: to detect un-modeled trend and to determine if an explanatory variable can be removed from the model. If the explanatory variable has trend remaining in the residuals, it should not be omitted from the model. The scatter plot matrix can be seen in Figure 4.52. Prominent trend is visible in the residuals of the three explanatory variables. With PAX, the trend appears to behave linearly with a distinct change in variance across the plot. Hydroxamate and DETA present pronounced quadratic behaviour. All three main effects will

need to be included in a final response surface model due to the trend associated with each. From the assessment of the graphical diagnostics, a linear model does not provide an adequate fit.

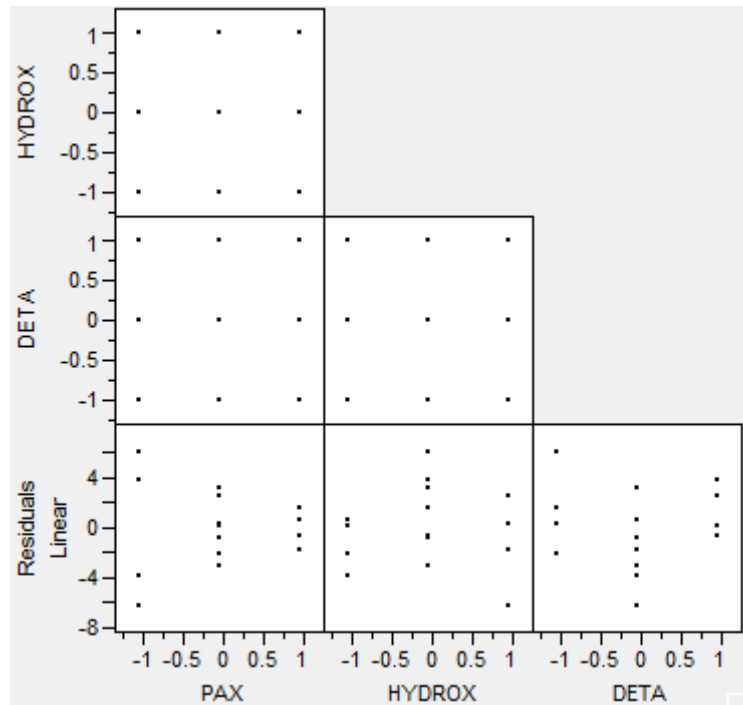


Figure 4.52 : Scatterplot matrix for the linear copper recovery model.

A full quadratic response surface model was fit to the data. The JMP output for this model can be seen in Figure D.11 in Appendix D. The quantitative diagnostics indicate a good model fit. The R^2 and R^2 adjusted values were 0.94 and 0.83 respectively. The MSR/MSE ratio confirms that the trend modeled is not due solely to noise. The lack of fit test indicated no significant lack of fit. DETA and hydroxamate were the significant model parameters. Hydroxamate is the more significant parameter due to its lower t-ratio. The graphical diagnostics were also assessed. The actual versus predicted and the residual by predicted plots are shown in Figure 4.53. The actual by predicted graph corresponds to the high R^2 value. The data points are tightly clustered around the $y=\hat{y}$ line. The residual by predicted plot shows no discernable trend.

The residual by row plot, seen in Figure D.11 in Appendix D, has a random placement of data points indicating no systematic error.

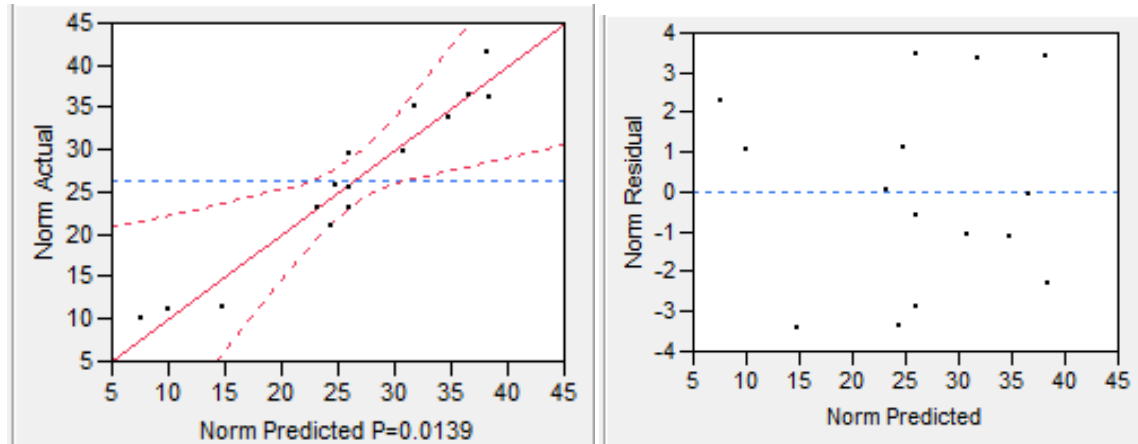


Figure 4.53 : Actual by predicted and residual by predicted plots for the full quadratic response surface model of copper grade.

A scatterplot matrix (Figure 4.54) was constructed to examine the residuals as they pertain to the explanatory variables. It can be seen that there is still remaining trend, but it is much less pronounced than for the previously constructed linear model. Curvature remains in the residuals of hydroxamate and DETA. The trend that was visible in the linear model with PAX and the residuals is less significant, indicating that the PAX effect has been almost fully modeled. From the quantitative and graphical diagnostics, the model appears to be adequate.

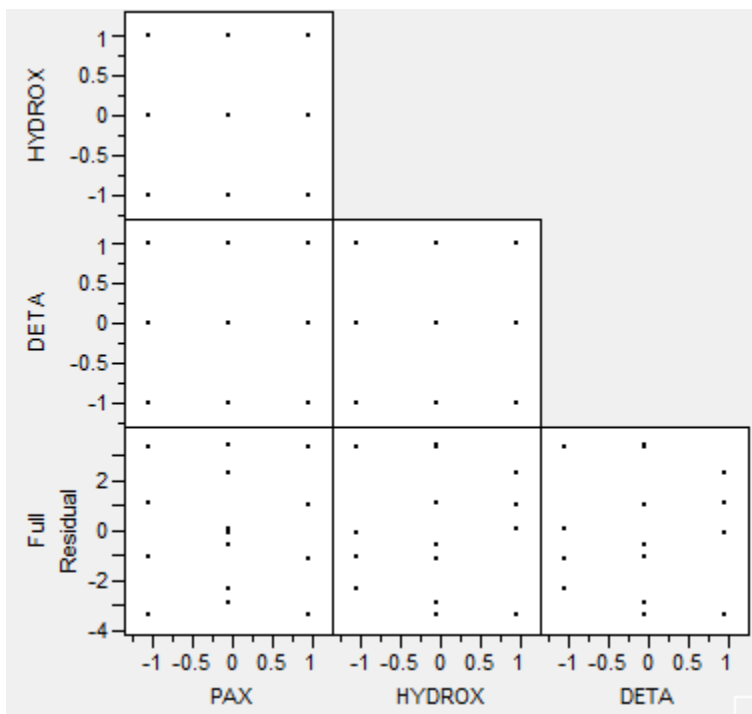


Figure 4.54 : Scatterplot matrix for the full quadratic response model for copper grade.

As with so many insignificant parameters, it is likely that the fit can be improved by eliminating certain parameters. The Akaike Information Criterion was used for a tool of model selection. The main effects were never omitted from the model as the quantitative and graphical diagnostics point to their significance; PAX was the first principal component and the hydroxamate and DETA parameters were statistically significant. Table 4.9 shows the AIC values calculated for the potential models. It should be noted that less combinations of parameter omissions were attempted due to the significance of the DETA main effect. It can be seen that the model with the eliminated PAX-DETA interaction effect has the lowest AIC. The model with no interaction effects had the smallest number of parameters fit to the data, yet, it had one of the highest AIC values. This speaks to the importance of the interaction effects to model the copper grade.

Table 4.9: AIC values calculated for the copper grade models. Parameters are PAX (P), hydroxamate (H) and DETA (D).

Model	AIC
FULL	43.30
Linear	45.76
-D*D	46.32
-P*H	46.94
-H*D	48.02
-P*D	41.83
-P*D, H*D, P*H	48.12
-P*D, D*H	46.36
-P*H, D*H	49.86
-P*H, P*D	45.31

The model without the PAX-DETA interaction term was assessed with quantitative and graphical diagnostics to determine its adequacy. The quantitative diagnostics indicated a good model fit. The R^2 and R^2 adjusted were high at 0.93 and 0.85. These values are also closer together than the values obtained in the full response surface model. The MSR/MSE ratio determined that the trend modeled was significant and not due to noise in the data. The lack of fit test determined that no significant lack of fit was present. The full JMP output can be seen in Figure D.12 in Appendix D.

The actual versus predicted plot and residual versus predicted plot can be seen in Figure 4.55. The actual versus predicted plot shows the points clustered tightly along the length of the $y=\hat{y}$ line. There are values on the of the 95 % confidence interval. The residual by predicted plot shows no discernable trend. In comparison to the residual versus predicted plot for the full model (Figure 4.53), the residuals appear more evenly spaced across the plot. Random and evenly distributed residuals are indicators of a good model. The residual by row plot (Figure D.12)

indicates that there was no significant systematic error during the experiments. For the purposes outlined in this thesis, the model is deemed to be adequate.

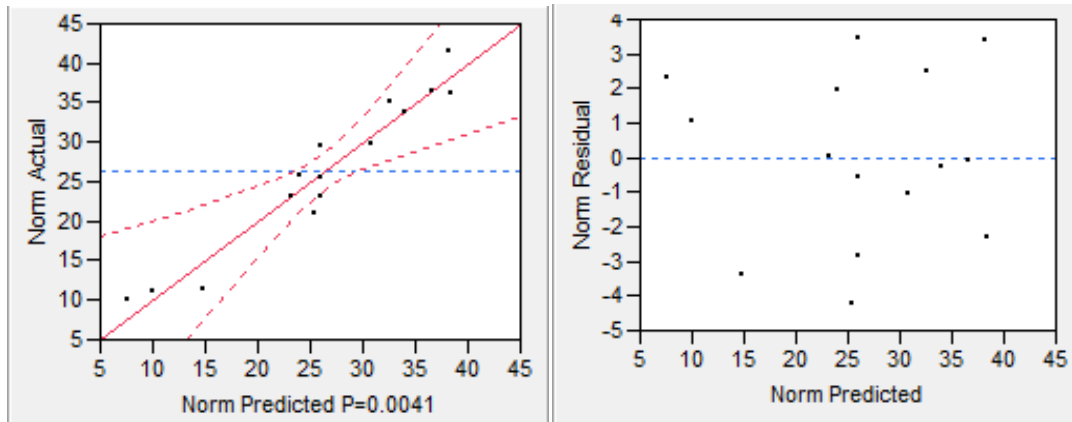


Figure 4.55 : Actual versus predicted and residual versus predicted plot for the final copper grade model.

To examine the residuals versus the explanatory variables, a scatterplot matrix was constructed. From Figure 4.56, it can be seen that trend still remains in the residuals versus the explanatory variables. There is slight curvature seen with PAX and hydroxamate. DETA exhibits a slight quadratic behaviour. The presence of trend remaining in the residuals indicates that there is trend in the data that is not accounted for in the model. The copper grades were normalized before analysis to remove bias from the grade fluctuations. It can be concluded that copper grade fluctuations are not the sole source of un-modeled trend in the data.

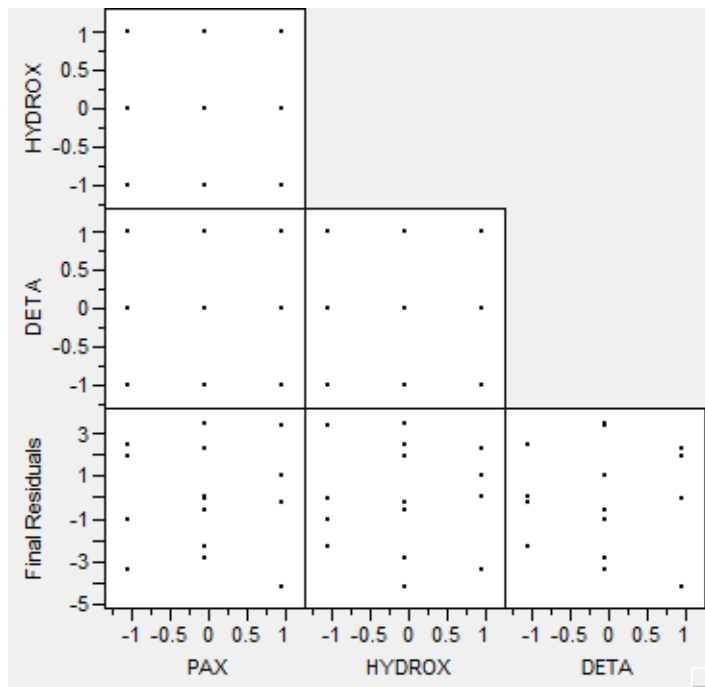


Figure 4.56 : Scatterplot matrix for the final response model for copper grade.

The interaction surface profiles in Figure 4.57 were created by JMP. Hydroxamate dosage has a dominant effect on copper grade. This is expected as hydroxamate was the significant parameter in the copper recovery models. There is a tradeoff to be made between copper grade and copper recovery. Lower recoveries have higher grades. As the collector dosages are lowered, the grade rises. This can be seen in the interaction effects between hydroxamate and PAX. When both collectors are at their maximum, the grade is minimized. It should be noted that when the hydroxamate dosage is at zero, an increase in PAX improves copper grade. This could be due to its collection power towards bornite, which has a higher copper content than malachite. The DETA interaction with PAX appears exponential. As the DETA dosage approaches zero, the grade rises significantly. There is only a small change in copper grade when DETA is at its maximum. Thus, the PAX-DETA interaction is not significant. This corresponds to the parameter that was omitted from the final model. The negative effect of hydroxamate on the copper grade

overshadows the DETA effect. It can be seen that grade drops sharply as DETA and hydroxamate are increased.

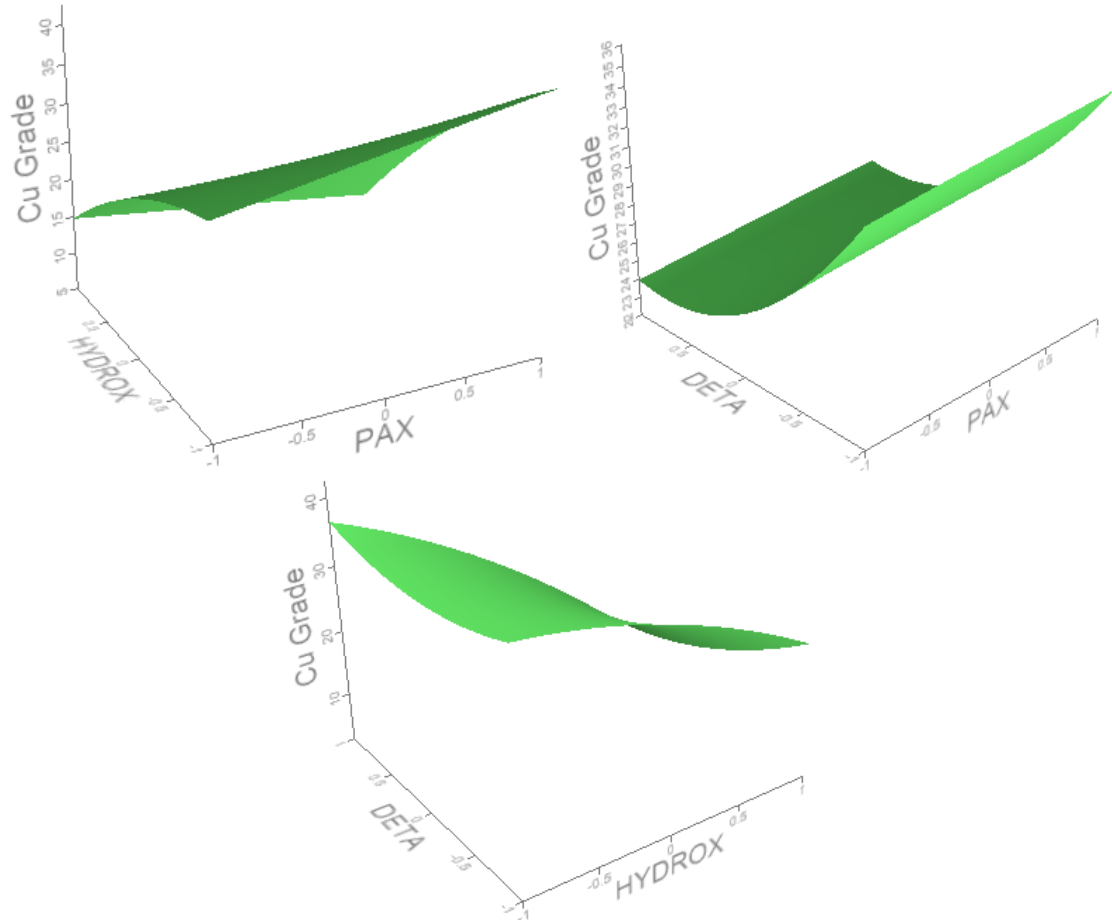


Figure 4.57 : JMP surface profile for the interaction effects between the explanatory variables in the final copper grade model.

The response surface of the model was solved using JMP. The solution was found to have a saddle point at 19.8 % Cu. The optimum copper grade would require the lowest collector dosages as increases in recovery come with sacrifices in grade. From the final copper grade model it is clear that high hydroxamate dosages are detrimental to copper grade due to its

collecting power. DETA, which was thought to improve copper recovery and grade, has a negative effect on copper grade. The equation for the final copper grade model as stated by JMP is :

$$y = 26.07 + 0.685x_1 - 11.05x_2 - 4.33x_3 - 0.05x_1^2 - 2.57x_2^2 + 2.95x_3^2 - 3.04x_1x_2 - 3.38x_2x_3$$

4.3.4 N-Benzoyl

The N-benzoyl collector was promising during the initial micro-flotation tests. It was active towards malachite and it caused rapid agglomeration within the micro-flotation cell. The N-benzoyl collector was tried on a bench-scale in lieu of the Cytec 6494 hydroxamate. Two run conditions from the Box-Behnken experiment were repeated. The runs that were repeated had PAX and N-benzoyl, but no DETA. The N-benzoyl dosage was calculated to be the same molarity as the hydroxamate so that the collector effect could be seen without interference from dosage levels.

BZ1 was performed with the mid-level dosage, 204 g/t, of N-Benzoyl. The collector was added as-is in powder form to the flotation cell. This test was also performed with 70 g/t PAX. The first three concentrates collected mainly bornite. It did not collect well and the froth quickly turned from black to grey. This phenomenon occurred even in the first concentrate. Bornite normally collects well over the entire 2 minute collection time. This test is similar to the collector-less test performed in the Box-Behnken experiment. The N-Benzoyl has solubility problems and did not dissolve enough during the one minute conditioning time. In this sense, it was almost like a collector-less run. This could be indicative of slime activation, or the collection of bornite or malachite middlings. The third concentrate was not black but a muddy brown

colour. Concentrates three through six were found to have slimy water, which is un-characteristic of the de-slimed charges, making it unlikely that it was simply middlings.

The recovery versus grade curve for BZ1 can be seen below in Figure 4.58. N-benzoyl seems to be triggering a response from another mineral besides malachite and bornite. The final copper recovery obtained in BZ1 was 54.5 % with a grade of 48 %, as seen in Figure 4.59 and Figure 4.60 respectively. Due to equipment failure, no mineral recoveries could be calculated. From a visual inspection of the concentrates, only bornite can be seen in the initial concentrates. No malachite appears to have been recovered, and the concentrates are made up of very fine, brown particles.

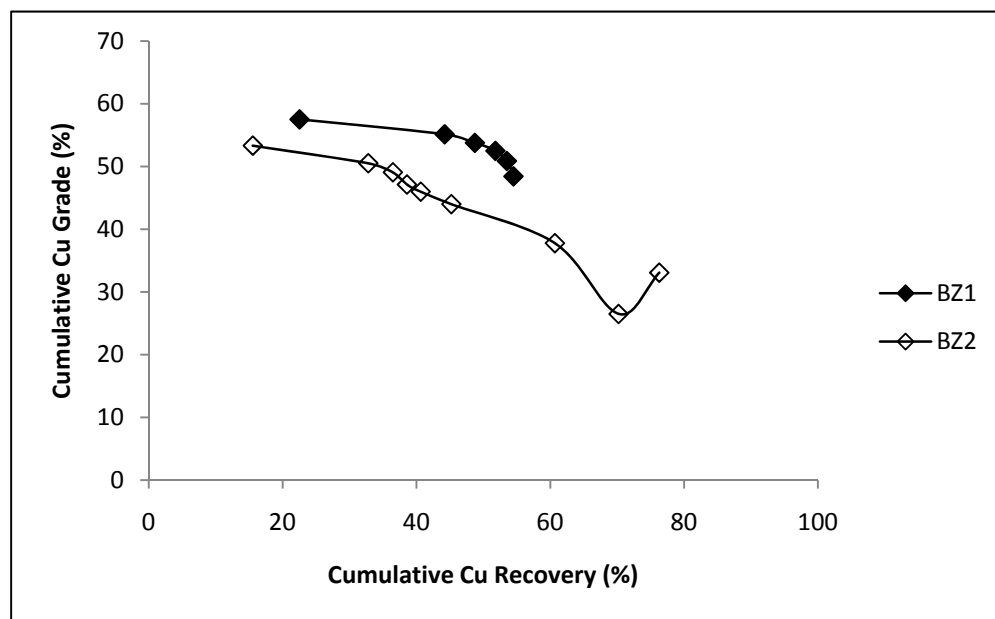


Figure 4.58: Copper recovery versus grade for tests BZ1 and BZ2.

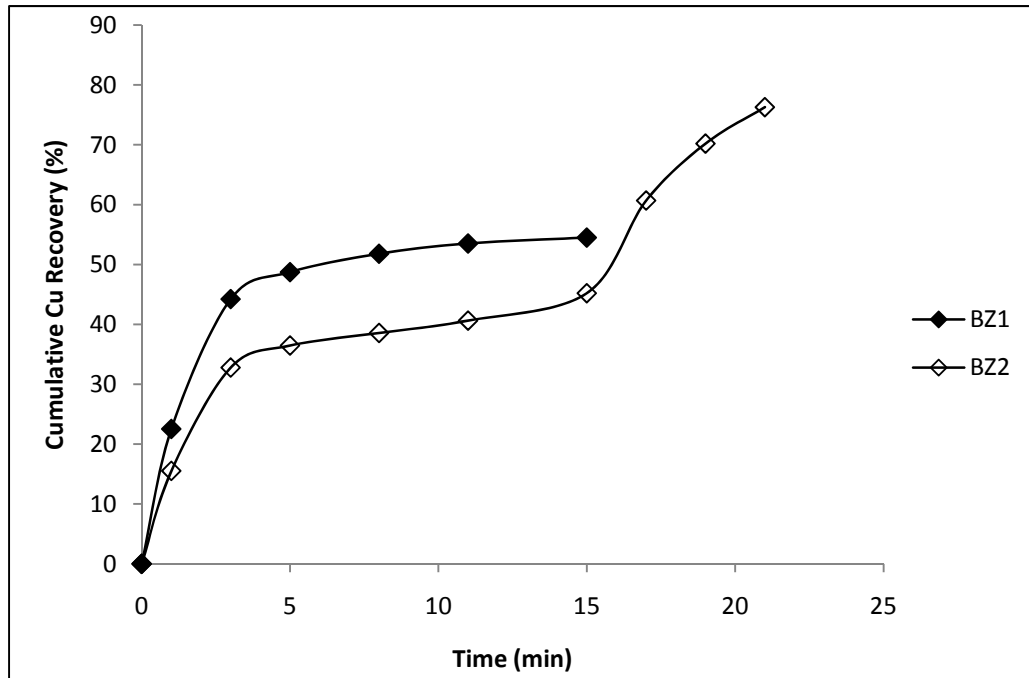


Figure 4.59: Copper recovery for tests BZ1 and BZ2.

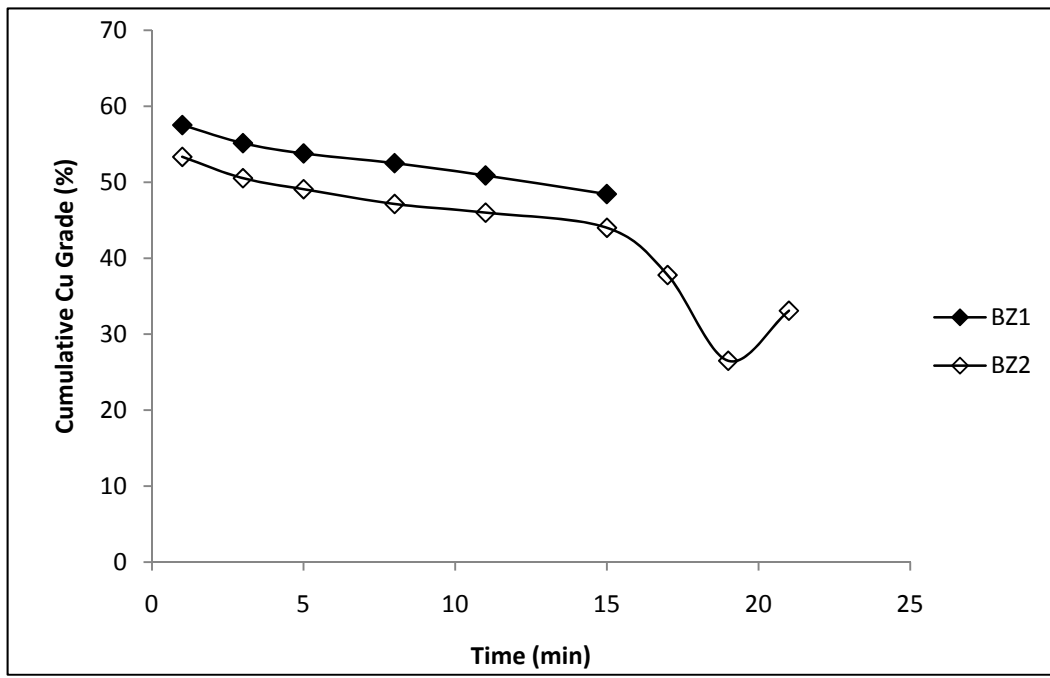


Figure 4.60: Cumulative grade for tests BZ1 and BZ2.

BZ2 used a higher N-benzoyl dosage of 408 g/t along with 35 g/t PAX. Due to the solubility problems noted in the micro-flotation testing and BZ1, the collector was dissolved in hot water. To dissolve the collector, it was placed on a hot plate and stirred often. Once dissolved, the N-benzoyl was a peach-coloured liquid. N-benzoyl was kept on the hot plate until it was added to the flotation cell. The first concentrate had visible green particles along with the black particles. Concentrate 2 recovered slimes at the beginning of the flotation time. These slimes could be carrying finely ground malachite or bornite. The froth grew barren, and then a small amount of black particles was recovered at the end of the collection time. Flocs of fine particles were clearly visible in the concentrate. It appears that the dosage in BZ1 was not sufficient to display the agglomerating properties of N-benzoyl. Concentrates 3-5 exhibited similar behaviour. These concentrates collected only fine, brownish particles with some recovery of bornite. The collection of fines is due to their agglomeration to a flutable size by N-benzoyl. Prior to agglomeration, the fines can only be recovered via hydraulic entrainment on other particles. After concentrate 6 was barren, the Cytec hydroxamate was added for three more concentrates. The three concentrates using the hydroxamate were bright green. The malachite responded rapidly and efficiently to the hydroxamate. The effect of the hydroxamate addition in the final concentrates can be clearly seen as the rapid rise in both copper recovery and grade in Figure 4.59 and Figure 4.60. The final copper recovery was 76 % with a copper grade of 33 %.

It was assumed that the N-benzoyl would be an effective collector of malachite from the results of the micro-flotation tests. The flotation behaviour achieved with N-Benzoyl indicates that N-benzoyl may be more active towards other components in the test ore as well as a depressant for bornite and malachite. The grade and recovery suffered when the N-benzoyl dosage was increased. It is intuitive that when a collector dosage is raised, that the recovery should increase while the grade decreases. This would be the case unless the collector acts as a depressant for the economic minerals. It is also possible that the lower recovery and grade is due

to a change in the PAX dosage as it was higher in BZ1. The recoveries achieved in the micro-flotation cell could have been because the malachite and bornite were the only minerals in the cell. When exposed to the mineral make up in the ore, the N-benzoyl did not collect an appreciable amount of economic minerals.

Chapter 5

Discussion

This chapter presents a discussion of the results outlined in Chapter 4. The adsorption, micro-flotation and Eh-pH results are compared with the literature presented in Chapter 2 and discussed as they pertain to bench-scale flotation. The characteristics and the limitations of the models developed from the Box-Behnken experiments are outlined; then, these models were evaluated from a practical and economic standpoint.

5.1 Adsorption, Micro-flotation and Eh-pH Results

The results obtained from the fundamental adsorption and micro-flotation experiments in this thesis are comparable to work done by previous researchers. As stated in Chapter 2, the potential of using chelating agents as flotation collectors has long been known. Various collectors have been studied, but hydroxamic acids have been of particular interest. Previous studies of octyl hydroxamate, an active component in Cytec Promoter 6494, have yielded several characteristics: an adsorption and micro-flotation peak around pH 9.5; and, multi-layer collector formation.

Lenormand et al (1979) and Fuerstenau and Pradip (1984) both found that malachite has a maximum flotation response at pH 9.5. Lenormand and coworkers worked specifically with malachite as a single mineral with octyl hydroxamate. They investigated the adsorption behaviour of the system as well as the micro-flotation behaviour. It should be noted that although the collector dosages and gas flow rates in this thesis are dissimilar from the work performed by Lenormand and his colleagues, the results obtained were still comparable. The malachite flotation curve developed by Lenormand et al (1979) showed a sharp drop in malachite recovery after pH 9.5, except at high collector dosages. The highest collector dosages used by Lenormand was 60.2

mg/L, which is similar to the 67.6 mg/L dosages used in this thesis. The 60.2 mg/L curve by Lenormand and the 67.6 mg/L curve were almost identical. Additionally, the dip in flotation recovery noted in the adsorption and micro-flotation results at pH 7.5 corresponds closely to the dissolution of copper oxides noted by Poling (1973).

The theories that octyl hydroxamate proceeds through surface reaction-type adsorption mechanisms is reflected in the results of this thesis. Researchers such as D.W Fuerstenau have proposed this mechanism on several occasions. Minerals such as hematite, barite, calcite and bastnaesite have all shown the tendency to form multiple collector layers (Raghavan and Fuerstenau (1974); Fuerstenau and Pradip (1983); Pradip and Fuerstenau (1984)). In this thesis, multiple collector layers were confirmed on the mineral surfaces. At their adsorption peaks, 8 and 9 collector mono-layers were formed on the surface of bornite and malachite respectively.

The specific behaviours of adsorption and micro-flotation of bornite have not been studied. Bornite is a sulphide mineral; therefore, results obtained with other copper sulphide minerals were used as a comparison. Fuerstenau, Herrera-Urbina and McGlashan (2000) conducted contact angle measurements between mineral surfaces and potassium octyl hydroxamate. They found that no contact angles were formed between hydroxamate and copper sulphide surfaces. However, Hanson and Fuerstenau (1987) found that octyl hydroxamate could adsorb onto the surface of chalcocite, a copper sulphide mineral, under certain electrochemical conditions. They found that xanthates adsorbed onto sulphide surfaces in the least oxidizing conditions whereas octyl hydroxamate required high potentials. The potential readings taken during the micro-flotation tests are consistent with Hanson and Fuerstenau's findings. Bornite collected well with octyl hydroxamate in regions of high potential. As pH rose, bornite recovery dropped with the potential. This is a result of hydroxide formation on the bornite surface. The bornite adsorption results followed a similar pattern. The discrepancy between the bornite

adsorption results with PAX and its flotation can be explained by elemental sulphur formation as suggest by Tukel (2002). This would also help to explain the collectorless flotation of bornite.

The Eh-pH readings taken during the micro-flotation tests confirmed the reactivity of PAX and hydroxamate in the system. The species distribution diagram for cupric and malachite confirms the results seen in the adsorption test. The adsorption and flotation response of malachite is poor in the acidic range. This is due to malachite dissolution and the subsequent release of copper ions. Collector molecules interact with the copper in solution and precipitate. It is recommended by Barbaro et al (1997) that flotation occurs well above the pH at which mineral solubility is constant. Malachite dissolution does not begin until pH 4.2; it is likely that dissolution can still occur at higher pH levels because the Eh level of the system was not controlled.

The flotation conditions for the bench-scale flotation were gauged based on the adsorption and micro-flotation results. These results gave insight into the behaviour of the mineral-collector systems. It is desirable to operate a flotation circuit with the least amount of reagents required. pH adjustment and control is a major concern in ore processing. Ideally, an ore could be processed at its natural pH. This is not possible for all ores. Sulphide minerals in the ores influence the pH of the flotation environment. This can drive the pH of an ore down, causing corrosion and equipment wear problems. If an ore is naturally in the neutral to alkaline pH range, it can be processed without pH management. Lee et al 2008, performed bench-scale flotation tests on a similar sulphide-oxide ore. They floated at pH 7.5, the natural pH of the ore, establishing a precedent. The natural pH of the ground sulphide-oxide ore was approximately pH 7.8. This is an acceptable flotation pH as long as it makes sense for collection purposes. Based on the adsorption and micro-flotation results, pH 7.8 was suitable as the collectors' adsorption on malachite and bornite was near their peaks. As bornite was removed from the flotation cell, the pH rose to a final value of approximately pH 8.30. Bornite collection occurred within the first two

concentrates. When only malachite remains in the flotation cell, the higher pH value is beneficial to hydroxamate adsorption. This is important as xanthate will adsorb onto the malachite surface, but will not aid in collection as it is easily removed by attrition.

The suitability of this pH range is further confirmed by the Eh-pH data. The main hydroxamate-copper chelate is $\text{Cu}(\text{HXM})_2$. It reaches a maximum between pH 7.5 and pH 11.5. In this range, it has a species distribution of almost 50 %. The hydrophobic xanthate entity, CuEX, has a 50 % distribution in this range. This confirms that both collector species are highly reactive in the natural pH range of the ore. Additionally, malachite reactivity peaks from pH 7.5-9 based on the data in the species distribution diagram shown in Figure 4.15. The natural pH of the ore lies in a region of maximum malachite and collector reactivity, making it quite an appropriate pH for effective flotation.

The minimum conditioning time for the bench-scale flotation was 1 minute. The adsorption results confirmed that this was sufficient time for a collector coating to form. The bornite-PAX system took the longest to form a mono-layer at 40s. After a minute, each mineral-collector system had reached equilibrium with multiple collector layers. If a layer was removed due to attrition in the cell, collection was still possible.

Bornite and malachite behaved similarly in the presence of the hydroxamate Cytec Promoter 6494. The adsorption density, kinetics and collector uptake were comparable for both minerals. The minerals performed different at the ends of the pH spectrum. At low pH, bornite had recoveries over 90 % with hydroxamate where only 60 % of malachite was recovered. This situation was reversed at high pH. In the pH range of the bench-scale flotation, recoveries of over 90 % were achieved for both minerals. This indicates that a mixed xanthate-hydroxamate collector system is not the only method to process a mixed sulphide-oxide ore. As the hydroxamate tested effectively collects both the sulphide and the oxide, it is possible that no xanthate is needed.

5.2 Bench Scale Flotation

The results of the bench scale flotation testing presented in this thesis, while preliminary, may be used to make inroads into the development of a successful process flow sheet. The exploratory work and preliminary testing offered insight into the flotation behaviour of the ore. The Box-Behnken experiments provided indications of optimal collector dosages despite mediocre models.

The flotation of the test ore proved problematic. Despite the easy collection of bornite, without malachite, the overall copper recovery was poor. Slime problems were the main barrier to malachite recovery. Even after a short 10 minute grind time, there was significant slime production. The gangue minerals are the cause of the sliming. Components that slime easily are carbonates and silicates, namely: calcite, clays, micas, quartz, feldspars and chlorites (Aliferova, et al, 2005). The XRD scan of the slime fractions confirmed the presence of calcite, quartz, muscovite, albite and clinochlore. Albite is the sodium rich plagioclase feldspar and clinochlore is a soft chlorite mineral that is often considered a part of the clay group. From the composition of the gangue, it is not surprising that slime generation is prevalent.

Cytec Industries, the makers of the hydroxamate collector, warn against ores with sliming problems. They note that excessive slime production will interfere with copper oxide recovery along with causing excess frothing (Lee et al, 1998). Excess frothing will lead to slime collection by hydraulic entrainment. Slime production will result in low copper recovery and poor copper grades. Once a de-sliming step was implemented, malachite recovery improved.

The results obtained from the bench scale flotation regime were comparable with the results presented in literature. Researchers Lee et al (2008) worked with a similar ore and added between 420 g/t of hydroxamate, but only 15 g/t PAX. They achieved a final copper recovery, malachite recovery and copper grade of 95%, 89.4 % and 20% respectively. It should be noted

that although the ore tested by Lee and coworkers contained bornite and malachite. It also contained chalcopyrite and possessed no sliming problems. Dekun, Jingqing and Weizhi (1984) performed bench, commercial and plant scale tests on a skarn-type oxide ore. At the bench scale, they found that 300 g/t xanthate and 300 g/t hydroxamate resulted in copper recoveries of 92.84 % with a grade of 17.85 %. These results are comparable to the flotation circuit results obtained in this thesis despite the different collector dosages.

5.2.1 Statistical Models

The construction of statistical models to predict collector dosages for a maximum flotation response was the main goal of this thesis. Models were constructed, but they were not ideal. The models were composed of mainly insignificant parameters and left trend un-modeled. Despite these facts, a response surface was generated and the collector dosages for a maximum flotation recovery were proposed.

Four models were constructed: copper recovery; malachite recovery; minor copper recovery and copper grade. The recovery models were strikingly similar. The models all represent one part of a whole. Overall copper recovery hinges on the malachite and minor copper recovery. It would make sense that all three responses could be modeled using the same parameters. For example, the highest copper recovery in the Box-Behnken experiments was 91.24 %. It is logical that this run also had the highest malachite and minor copper recovery. Bornite recovery was not a deciding factor in improving overall copper recovery. Bornite recoveries were consistently above 99 %, save for the run performed with no collector. It is known that the collector dosages proposed by JMP from the recovery response surface solutions are skewed. The presence of un-modeled trend and insignificant model parameters still allows for the interpretation of the recovery model results.

The collector dosages calculated by JMP for optimum copper recovery are 202.7g/t PAX, 674.99 g/t hydroxamate and 61.9 g/t DETA. The dosages for the saddle point malachite recovery were 0g/t PAX, 771g/t hydroxamate and 112.4 g/t DETA. The dosages for maximum minor copper recovery were 44 g/t PAX, 603.85 g/t hydroxamate and 102.8 g/t DETA. The hydroxamate value seems large, but hydroxamate dosage is strongly dependent on the oxide mineral content. This is demonstrated by the higher dosage required for malachite recovery. In comparison to other researchers who have investigated the use of hydroxamate, the dosages lie in the middle. Cytec Industries recommended between 25-100 g/t as a preliminary dosage and Lee et al (2008) used over 1300 g/t to process a particularly oxide rich ore. The viability of the proposed collector dosages cannot be determined through literature comparison alone. They must be evaluated with the knowledge obtained about the test ore behaviour. The ore studied by Lee et al (2008) was not a problematic ore. It did not possess the sliming gangue fraction. It also did not possess gangue minerals that were inadvertently activated by the high collector dosages. Neither of the hydroxamate dosages proposed in literature would be effective with the test ore. When hydroxamate dosage was only 204 g/t, copper recovery was only 64 %. At the high hydroxamate dosage of 408 g/t, flooding behaviour was observed.

The highest recovery within the process space was 91.24 % with a collector dosage of 71 g/t PAX, 408 g/t hydroxamate and 53 g/t DETA. To achieve 98 % copper recovery, JMP calculated that the PAX dosage needs to be more than doubled and the hydroxamate dosage increased by over 40 %. This is a large increase in reagent requirements for only a 7 % increase above an already good recovery level. Recovery level is not the only criteria by which a flotation circuit is evaluated. The copper grade of the concentrates is important. There is a tradeoff between grade and recovery. A recovery level of 100 % may seem ideal, but it results in no separation between economic minerals and gangue. With the majority of the ore reporting to the cleaner stage, the cleaner cells would need to be almost as large as the rougher cells. This is a

waste of capital and operational costs. The copper grade at 91 % recovery was 12 %. The predicted maximum recovery of 98 % means that the copper grade will be even lower. This critical value was outside of the process space. The recovery is higher, but the collector dosages are much higher than the dosages used in the experimental space.

The test ore exhibited flooding behaviour with high collector dosages. JMP's proposed dosages for optimum copper recovery would produce uncontrollable flooding. Even the lowest collector dosages proposed for minor copper recovery, 44.5 g/t PAX, 606.6 g/t hydroxamate and 103 g/t DETA, would result in flooding. The dosages proposed by JMP made sense based on precedent, but are unacceptably high for the test ore.

The critical value of the copper grade model response surface is a saddle point at 19 % Cu. As expected, higher cumulative copper grades required low collector dosages. To achieve the grade at the saddle point, the dosages required were 0 g/t PAX, 167 g/t hydroxamate and 101 g/t DETA. From the interaction profiles, it is clear that hydroxamate and DETA have a negative effect on copper grade. To achieve higher grades than the saddle point value, hydroxamate and DETA dosages need to be minimized. DETA was assumed to have appreciable activity towards malachite as concentrates pulled with high DETA dosages were very green. From the copper grade model, it is clear that DETA is more active towards the gangue than the economic minerals. The green of the DETA concentrates is possibly due to the presence of clinochlore, the green chlorite mineral. Although the PAX dosage was solved to be 0 g/t, its parameter indicated that it had a positive effect on copper grade, unlike hydroxamate and DETA. This could be due to the effective bornite recovery with PAX. Also, PAX has shown that it is not very active towards gangue components as tests performed with only PAX did not collect appreciable slimes or gangue.

Another explanation for the aforementioned similarity of the recovery models could be due to effects that were not controlled in the experiments. Evidence of systematic changes during

the experiments was evident in the residual by row plots developed in JMP. Un-modeled trend was also found in the scatterplots of the residual vs. explanatory variables for each final recovery model. The scatterplots can be seen in Figure 4.30, Figure 4.38 and Figure 4.47. The residual by row plots can be seen in Appendix D. Slight oscillations were observed in the residual by row plots. This is generally an indication that time was not included as a parameter when it should have been. Timing is carefully controlled during a flotation experiment. Any changes with respect to time would be due to experimental error as opposed to an uncontrolled factor. Head grade is another example of such an effect. Despite efforts to achieve a constant head grade for the charges, variations occurred. The head grades of the charges varied from 4.1-5.3 % with an average grade of 4.78 %. Head grade can skew experimental results, particularly from a statistical point of view. As head grade changes, so does the amount of copper present in the flotation cell. It is difficult to effectively account for the changes in head grade as it is only precisely known post analysis. This situation was unavoidable for the Box-Behnken experiments because of the limited sample size. There was only enough sample ore for 15 experimental runs after the exploratory and preliminary tests. If this experimental design were repeated on a larger scale, runs of identical head grade would be used to construct the statistical models.

Timing and head grade fluctuations could account for the phenomena seen in the statistical models for recovery. Head grade, in particular, could have affected the flotation system more than the collector levels. This would explain why the majority of the parameters in the statistical models were insignificant. This is not to mean that they did not influence the system, but their effects were overshadowed by the grade fluctuation. Time could also have this type of overshadowing effect. Collector conditioning time has been widely studied. Generally speaking, the longer a collector has to condition, the more effectively it collects. If some concentrates were allowed to condition longer than others, it would affect the recovery. It is more likely that the copper grade had a more significant effect.

The copper grade model used normalized copper grades. The grades were normalized to the mean value of 4.78 % copper. This model had the same problems with insignificant parameters and leftover trend in the residuals. It is important to note that the copper grades were normalized, so the uncontrolled effect of copper grade fluctuations should have been eliminated. This indicates that there is an additional un-modeled effect.

Aeration rate was not controlled during the course of the Box-Behnken experiments. The aeration rate is a variable that is carefully controlled in industry as it has a large effect on flotation. It is likely that slight changes in the aeration rate were the source of the un-modeled trend. The high collector dosages proposed by Lee et al (2008) could be possible if the aeration rate was kept very low. This would counteract the flooding behaviour of the natural ore.

Each of the statistical models had indicators of inadequacy. Despite the apparent inadequacy, they are capable of providing usable results for this thesis. The dosages predicted by the JMP models make physical sense to the system. High collector dosages result in high recovery whereas low dosages give high copper grades. This indicates that the model inadequacies have not prevented the models from giving important insight into the system behaviour. Additionally, the fundamental data supports the findings of the principal component analysis. The Eh-pH data showed significant PAX activity in the experimental region. The PCA supported this by identifying that PAX was able to account for approximately 40 % of the variance in the data in each model.

It is possible that some of the model inadequacy could be due to a low sample size. Only 15 data points were used to calculate the test statistic. It is recommended that at least 30 data points be used for an accurate t-test (Montgomery et al, 2004). The lack of data points is likely the source of the insignificant parameters due to an inaccurate t-test. The t-test statistic is likely the reason why the PAX parameter was insignificant in the models when it clearly had a strong effect on the system. The t-test requirements do not explain the presence of the un-modeled trend.

Since the un-modeled trend did not prevent the model from giving sensible results, it can be assumed that the un-modeled effects would not affect the results greatly. However, it would be advantageous to identify and model the effects to have a complete picture of the process space.

From the results of the JMP models, several insights and new possibilities for the system were gained. In flotation, it is advantageous to add smaller doses of fewer reagents. This limits the reagent costs and keeps the chemistry within the flotation cell simple. The test ore was collector dependent. It was observed in the preliminary testing that smaller, frequent collector dosages produced the best flotation behaviour. From the results of the Box-Behnken experiments, the highest recovery was achieved with the use of all three collectors. The second highest recovery was 90.12 % using only hydroxamate and DETA. It would be possible to simplify the reagent make up and use primarily the Cytec 6494 hydroxamate collector. This would be possible for several reasons. DETA was found to be the least significant principal component and its effects were statistically insignificant. DETA did appear to improve malachite recoveries, and the Cytec hydroxamate proved to be just as effective on its own. The copper grade model proved that the DETA was more active towards gangue components because it was detrimental to copper grades. The adsorption and micro-flotation tests indicated that bornite responded as well to hydroxamate as malachite; it could be possible to collect them both using only hydroxamate.

Based on the flotation behaviour of the test ore, recommended hydroxamate dosages would lay between 300-400 g/t. This could be augmented with PAX as synergistic effects between hydroxamate and xanthate were observed. During the Box-Behnken experiments there were two runs that did not include DETA. One run was performed with 204 g/t hydroxamate. The other was performed at the same hydroxamate dosage, but with 71 g/t PAX. The copper recoveries were 64.33% and 76.01 % respectively. Malachite recovery rose from 17.03% to 43.28% with the addition of PAX. The xanthate is known not to collect malachite as it attacks the mineral surface causing dissolution. This behaviour uncovers copper ions buried in the malachite

crystal lattice. Since the hydroxamate selectively complexes with copper ions only, the increased availability of copper ions uncovered by the xanthate attack is beneficial.

The hydroxamate and PAX do not need to be added simultaneously. They were added in this manner to preserve the symmetry of the Box-Behnken experimental design. Dekun, Jingqing and Weizhi (1984) performed their mixed-collector flotation circuit with staggered collector addition. This would work well for the test ore. If PAX were added up front, it would collect the bornite quickly in the initial concentrates. PAX has proven that it is not able to collect malachite on a bench scale. Once PAX removed the bornite from the cell, the Cytec hydroxamate would be added to collect the malachite. This would be an effective use of the hydroxamate as its collection power would be directed towards the mineral that only it could collect.

In light of prior work and the data collected in this thesis, a PAX-hydroxamate collector system would be suitable for the bornite-malachite test ore.

Chapter 6

Conclusions and Future Work

PAX-hydroxamate flotation systems show promise for the processing of mixed copper ores through the simultaneous collection of sulphides and oxides. As discussed in Chapter 1, this thesis addressed two objectives: first, to gain insight into the behaviour of bornite and malachite with PAX and hydroxamate through fundamental work and second, to propose a collector regime to optimize copper recovery from a natural ore with problematic clays.

6.1 Adsorption, Micro-flotation and Eh-pH

The results from the fundamental tests presented in Chapter 4 and discussed in Chapter 5, indicated that bornite and malachite respond positively to PAX and hydroxamate collectors in their own characteristic ways.

The adsorption testing with the pure minerals confirmed appreciable collector adsorption. PAX adsorption on malachite was pH dependent. It adsorbed well in the neutral pH range, but dropped off in the acidic and alkaline regions. After 90s, the maximum adsorption density of PAX on malachite occurred at pH 9.5 with a value of $36.56 \mu\text{mol}/\text{m}^2$. Hydroxamate adsorbed more rapidly onto the surface of malachite. The characteristic hydroxamate adsorption peak at pH 9.5 coincided with an adsorption density of $72.44 \mu\text{mol}/\text{m}^2$. Hydroxamate uptake dropped off sharply at pH 10.5, effectively delineating the region of collector effectiveness.

The adsorption behaviour of PAX on bornite was unexpected. The formation of a monolayer took approximately 40 s. This was the longest time observed for monolayer formation, but monolayer formation is not an absolute requirement for successful flotation. After 2 minutes,

the system reached an equilibrium adsorption density of $17.5 \mu\text{mol}/\text{m}^2$. PAX uptake was under 50% when the system reached equilibrium. The adsorption of hydroxamate on bornite was comparable to its adsorption on malachite. A hydroxamate monolayer was formed within 10s, with a maximum adsorption density of $70.91 \mu\text{mol}/\text{m}^2$ at pH 6.5. The hydroxamate monolayer formed more rapidly on malachite than on bornite. This uncharacteristic hydroxamate adsorption peak at pH 6.5 was due to hydroxide formation on the bornite surface.

The results suggest that the adsorption mechanism involves chemisorption of a first layer followed by multilayer formation through surface reactions. The numbers of hypothetical collector layers formed were: 6, 9, 3 and 8 for the malachite-PAX, malachite-hydroxamate, bornite-PAX and bornite-hydroxamate systems respectively. The highest adsorption density occurred with the malachite-hydroxamate system. This confirms that hydroxamate is an effective collector for non-sulphide copper minerals. Bornite responded to hydroxamate similarly to malachite. The adsorption data suggests that it may be possible to use only hydroxamate to effectively collect both bornite and malachite. The use of only a chelating agent to collect both sulphide and oxides has not yet been proposed, and it merits further investigation.

The micro-flotation technique was used as an initial indicator of flotation behaviour. The collecting ability of three collectors was tested on pure malachite and bornite samples. PAX was determined to be an effective malachite collector in the narrow pH range of 8.5 to 9.5. Recovery dropped sharply on either side of this peak. In the acidic range, xanthates will attack the copper oxide surfaces and cause precipitation. This increases reagent consumption and reduces flotation response. The Cytec 6494 hydroxamate achieved malachite recoveries of 90 % between pH 8.5 and 11.5. It did not perform well under acidic conditions at pH 5.5 due to excessive collector consumption by the copper ions in solution.

Xanthates are known as effective sulphide collectors. Bornite responded predictably to PAX. Bornite recoveries were above 90 % over the pH range. Involvement of elemental sulphur has been hypothesized to explain high recoveries as they did not collaborate with the adsorption behaviour. However, a monolayer was formed on the bornite surface within 40s, which is still faster than the 1 minute conditioning time. Thus, the speed at which PAX adsorbs onto the surface is not an issue because the mineral surface is at least partially covered once collection begins. With hydroxamate, bornite recoveries were over 90 % until pH 9.5, where recovery dropped off.

N-benzoyl, an aromatic chelating collector, was used in the micro-flotation tests. It was very active towards malachite and bornite. With malachite, it caused instant particle agglomeration. With N-benzoyl, malachite recoveries were almost 100 % in the range of pH 6.5-9.5. These observations indicate that interaction of this reagent with malachite is very strong. This was not apparently the case for the bench scale tests because of more complicated mineral interactions. Recoveries were low outside of this range. Bornite recovery was above 90 % with N-benzoyl in the range of pH 5.5-9.5.

The Eh-pH measurements taken during the micro-flotation experiments confirmed the reactivity of hydroxamate and PAX in the bench-scale flotation region. Malachite dissolution was observed to be high around pH 4, but processes are almost never operated in the acidic range. Even slight dissolution could interfere with the collector action. According to equilibrium calculations, the most active hydroxamate chelate was Cu(HXM)₂. Its species distribution was 50% at the pH of the natural ore. The most active xanthate species in the flotation system was CuEX. It displayed excellent stability across the whole pH spectrum.

The major findings from fundamental investigations may be summarized in point form:

1. PAX and Cytec 6494 Promoter hydroxamate adsorb onto the surfaces of bornite and malachite and form multilayers.
2. The highest adsorption density of hydroxamate on malachite is $72.44 \mu\text{mol}/\text{m}^2$.
The adsorption density of PAX on bornite was unexpectedly low at $17.5 \mu\text{mol}/\text{m}^2$. This did not affect flotation response due to suspected elemental sulphur formation.
3. The effective pH ranges of the collectors with the minerals lies between pH 8-10. Malachite responds better in the alkaline region whereas bornite responds better in the acidic range. Malachite had an adsorption and flotation maximum at pH 9.5. Bornite collected well under pH 10.5 and had an adsorption maximum with hydroxamate at pH 6.5.
4. The mechanism through which collector adsorption takes place is via the chemisorption of a first layer monolayer. Surface reactions then form hypothetical multilayers.
5. Bornite and malachite responded similarly to hydroxamate. It could be possible to effectively float both minerals with only hydroxamate as a collector
6. N-benzoyl has an effective agglomeration and collection action on malachite in a single mineral flotation system.
7. PAX and hydroxamate are reactive in the pH range of the bench-scale flotation. This is predicted by thermodynamic analysis. Cu(HXM)₂ and CuEX, are the most active hydroxamate chelate and xanthate species. They are responsible for the development of hydrophobicity.

6.2 Bench Scale Flotation

The second objective of this thesis was to propose an effective collector regime to improve copper recovery from a mixed sulphide-oxide ore. To do this, a Box-Behnken experimental program was used to create a second order response surface model. Due to a limited number of samples for bench tests, a path of steepest ascent could not be determined. Exploratory and preliminary testing experiments were performed to gain insight into the flotation behaviour of the ore and to determine an appropriate process space.

The exploratory work exposed a major issue with the test ore. There was found to be a sliming problem. The gangue minerals produced large amount of slimes, even with a short grinding time. The slimes consumed reagents, coated mineral surfaces and adversely affected their collection. Even overdoses in collectors did not result in acceptable recovery levels. A de-sliming step was implemented with the hopes of improving recovery. Bornite, the copper sulphide, collected rapidly and completely in the initial concentrates. Malachite was not collected with PAX. Cytec 6494 was able to collect malachite effectively.

The process space was defined in the preliminary testing. The exploratory variables were PAX, hydroxamate and DETA dosages. The charges were ground and de-slimed prior to flotation. The de-slimed ores had higher recoveries and higher grade concentrates. Malachite was collector dependent, benefiting from frequent small collector doses. If hydroxamate doses were too high, flooding occurred. PAX overdosing did not produce flooding. Hydroxamate enhanced frothing behaviour, allowing frother to be minimized. Additionally, DETA and hydroxamate appeared to have a synergistic effect on malachite recovery.

N-benzoyl was used to replace hydroxamate for two investigatory tests with PAX. Initially 204 g/t N-benzoyl was added equally in powdered form over 6 concentrates. N-benzoyl flotation was unsuccessful on a bench-scale. No malachite was recovered, and the bornite recovered was due to PAX addition. Due to the solubility issues associated with N-benzoyl, it

was dissolved in hot water and kept on a hot plate. The second run used 408 g/t N-benzoyl. The recovery was poor and the concentrates were slimy; a characteristic not noted for the other de-slimed charges. N-benzoyl did not collect any malachite, appearing to be more active towards the gangue components of the ore.

These findings can be summarized in point form as follows:

1. The test sulphide-oxide ore possesses a sliming problem that is detrimental to copper recovery. When a de-sliming step was implemented after grinding, recovery improved.
2. Bornite collects rapidly regardless of collector conditions.
3. The Cytec 6494 hydroxamate is an effective malachite collector in measured doses. At high hydroxamate levels, flooding occurs and produces low concentrate grades. It also enhances frothing activity.
4. DETA appears to enhance malachite recovery and acts synergistically with hydroxamate.
5. N-benzoyl is a poor collector for the natural ore. When added in dry form, it had very low solubility as well as an observed affinity for the slimy gangue components.

6.3 Box-Behnken

The data obtained from the Box-Behnken experimental program was processed in JMP to produce four models: copper recovery; malachite recovery; minor copper recovery and copper grade. Linear models were fit to the data, but they were proved to be inadequate due to unmodeled quadratic trend leftover in the residuals. It was determined that the process space did not contain the optimum recovery of grade values, but was very close.

The three recovery models were similar. A principal component analysis determined that PAX was always the first principal component followed by hydroxamate then DETA. This collaborated with the xanthate reactivity determined by the Eh-pH measurements. In each recovery model, hydroxamate was the only significant parameter. Numerous models were fit to the data, but no other effects became significant. Quantitative and graphical criteria were assessed to determine model adequacy. The model variations made to improve the fit created a number of potential models, each with different pros and cons. The creation of a model is a subjective process. To narrow down the model options, the Akaike Information Criterion (AIC) was used. The AIC is a tool of model selection that indicates how well a model fits the data. The model with the lowest AIC was selected and then assessed further to determine its adequacy.

The final copper recovery model had all three main effects along with their quadratic terms. No interaction terms were added. From the quantitative and graphical assessment of the model, it was found to be adequate. Un-modeled trend was found in the residuals, but since this phenomenon was present in the full model, it was accepted. JMP solved the response surface and determined that the maximum copper recovery achievable was 98 % using 202.7 g/t PAX, 674.9 g/t hydroxamate and 61.9 g/t DETA .

The final malachite recovery model had the three main effects, the PAX and hydroxamate quadratic terms and the hydroxamate-DETA interaction. Similar to the copper recovery model, the quantitative and graphical assessments indicated an adequate model despite the remaining trend. JMP solved the malachite recovery response surface and found a saddle point at 62 %. The dosages for the saddle point malachite recovery were 0g/t PAX, 771g/t hydroxamate and 112.4 g/t DETA. Since malachite recovery is essential to good copper recovery, it was concluded that the maximum lay with higher collector dosages. A higher hydroxamate dosage would be effective as indicated by its parameter significance and the fundamental work.

The minor copper model had the same form as the copper recovery model. All three main effects and their quadratic terms were present. The model was determined to be adequate. The solution to the response surface was a maximum recovery of 90.8 %. This corresponded with 44.5 g/t PAX, 606.6 g/t hydroxamate and 103 g/t DETA.

The copper grade model was performed with the copper head grades normalized to 4.78% Cu to eliminate the effect of head grade fluctuation. The final copper grade model omitted only the PAX-DETA interaction term. JMP solved the response surface to find a saddle point at 19 % Cu. The collector dosages at this location were 0 g/t PAX, 167 g/t hydroxamate and 101 g/t DETA. As expected, to achieve higher grades, low recovery is achieved. This is why low collector dosages are required. It was found that DETA had a negative effect on copper grade. This suggests that it has an affinity for gangue components. It is likely that the green colour associated with high DETA dosages was not always malachite, but clinochlore.

The trend present in the residuals of the models indicates an effect due to an uncontrolled factor which was not included in the model. This effect is likely to be the copper head grade fluctuation for the recovery models. Despite the best efforts to obtain the same head grade in every charge, fluctuations occurred. The copper head grade determines how much copper is present in the flotation cell. As the head grade differs, so will the concentrate grade and recovery. When the copper feed grade was normalized, it eliminated the effects of head grade fluctuations. Trend remained in the residuals, so it can be concluded that the fluctuations in copper head grade was not the only un-modeled effect on the system.

The four statistical models had indicators of inadequacy. Only 15 data points were used to determine the statistical models. Parameter effects are deemed significant by a t-test. It is recommended that 30 or more values be used to perform an accurate t-test. It is possible that significant effects were deemed insignificant due to a poor t-test value. This is corroborated by

the principal component analysis performed for every model. The PCA indicated that PAX was the first principal component, yet it was insignificant in every model.

The un-modeled trend left in the residuals is indicative that an effect was left out of the model. The collector dosages provided by the JMP models make physical sense to the system. This is a caveat of an adequate model. Despite the apparent problems with the statistical models, their results were interpreted and applied as a guideline for future work.

The collector dosages proposed by JMP are high. Although they lie in the middle of previously proposed dosages, they are not applicable to the test ore. At 408 g/t hydroxamate, flooding behaviour was observed. If the hydroxamate collector dosage was raised over 600 g/t with simultaneous PAX and DETA addition, there is no doubt that flooding would occur. The recovery would be high, but with un-acceptable copper grades. At a recovery level of 90 %, the copper grade was 12 %. Thus, the collector dosages proposed by the models are not to be taken as exact, but as guidelines for future work.

The conclusions specific to Box-Benken analysis are summarized as follows:

1. The process space determined by the preliminary testing does not hold the critical value, but is nearby. The models exhibited curvature and were unable to be fit using a linear model.
2. The copper recovery response surface has a maximum value at 98 %. This corresponds to collector dosages of 202.7g/t PAX, 674.99 g/t hydroxamate and 61.9 g/t DETA.
3. The malachite recovery model was solved to have a saddle point at 62% recovery. This corresponds to 0g/t PAX, 771g/t hydroxamate and 112.4 g/t DETA. Higher collector dosages, particularly hydroxamate, would aid recovery.

4. The minor copper model predicted a maximum recovery of 90.8 % using 44.5 g/t PAX, 606.6 g/t hydroxamate and 103 g/t DETA.
5. The copper grade model was found to have a saddle point at 19 % Cu. The collector dosages at this location were 0 g/t PAX, 167 g/t hydroxamate and 101 g/t DETA.
6. The collector dosages for high recovery calculated by JMP are too high for the test ore. Flooding would occur. While providing high recoveries, the concentrates would have low copper grades. The dosages collected for high copper grade are too low for the test ore. High grades would be achieved, but with low recoveries.
7. Small fluctuations in the copper head grade are likely the cause of the un-modeled trend found in the residuals of the recovery models. Aeration rate is likely another source of un-modeled trend.
8. Parameter effects could have been falsely declared inadequate due to a faulty t-test statistic.
9. The models provide results that make physical sense to the flotation system. Thus, they are able to provide indicators for future work despite their shortcomings.

6.4 Future Work

As discussed in Chapters 1 and 2, the use of chelating agents in mineral processing is limited to laboratory investigations. It has not been largely implemented on a commercial scale. The study of mixed collector systems is even less prevalent. The tests conducted in this thesis provide insight into the adsorption and flotation behaviours of bornite and malachite as well as a first attempt at collector dosages for a rougher flotation stage for the test ore. The work performed in this thesis uncovered potential areas for further study. This section discusses the author's recommendations for future research.

The synergistic effects between PAX and hydroxamate have been noted in literature and observed in this thesis. With the same hydroxamate dosage and the addition of PAX, the recovery rose over 11 %. The preliminary testing focused on determining an appropriate hydroxamate dosage level for the Box-Behnken experiments. Optimizing the synergistic effects between PAX and hydroxamate was not considered. In theory, there should be a ratio between PAX and hydroxamate that produces optimum synergy. This could be investigated using adsorption testing by using different collector ratios and measuring their respective adsorptions. Once this theoretical ratio was found, further testing could be done via micro-flotation before it was implemented on a bench scale.

The models constructed in JMP used only 15 data points. In some cases, only 14 points were used due to outliers. This is enough data to get a general indication of the process space, but it should be used as guidelines for future work. An exploration of a smaller process space within the confines of the results from this thesis' experiments is recommended. This could be done using further response surface designs, but it would be recommended to use the conventional approach of varying one factor at a time. This is more plausible as the experimental region would be considerably smaller. The advantage of the conventional testing is that the number and position of the runs is unconstrained. The Box-Behnken design required the explicit placement of runs to maintain its rotatability. If the process space were covered with runs and then modeled statistically, this would increase the reliability of the test statistics to produce a more accurate assessment of collector dosages.

Due to the aforementioned rotatability of the Box-Behnken designs, the collectors were added in equal doses over 6 concentrates. This was done solely for the statistical modeling. It is possible that staggered collector addition is advantageous. For example, PAX would be added in the initial concentrates to collect bornite followed by hydroxamate addition to collect malachite. Each mineral fraction would be collected using the most effective reagent. It was observed that

malachite does not seem to be recovered using PAX. It is a waste of reagent to continue adding PAX when only hydroxamate is responsible for non-sulphide collection. Additionally, the Cytec 6494 hydroxamate was found to be equally effective with bornite and malachite. If the cost differences were not taken into account, it could be possible for a suitable hydroxamate to efficiently recover both bornite and malachite. It is recommended that a staggered collection system as well as a hydroxamate only collection system be explored on a bench scale.

The formation of elemental sulphur on bornite was used to explain the lack of xanthate adsorption on bornite. This aspect should be further investigated for confirmation experimentally using sulphur extraction tests. The processing of the slime fraction of the test ore was not in the scope of this thesis. The slimes were found to contain copper bearing species. In the current processing of the ore, these slimes are discarded, but it should be possible to recover the copper within them. It is recommended that acid leaching tests be performed on the slimes in order to determine an effective means of copper recovery.

Further mineralogical studies are recommended to obtain a more complete picture of the test ore. This would include professional polished thin section analysis along with QEMSCAN analysis to determine mineral abundances. This would allow the collector system to be more tailored to the ore at hand.

6.5 Concluding Remarks

The objectives of this thesis were met. Insight was gained into the behaviour of malachite and bornite with PAX and hydroxamate. Adsorption studies characterized collector adsorption and delineated effective pH ranges. The micro-flotation tests confirmed the adsorption findings and allowed the flotation behaviour of bornite and malachite to be previewed.

The statistical models were assessed through quantitative and graphical diagnostics and deemed adequate to provide an initial estimate for collector dosages. The work done in this thesis

met the stated objectives, but it also provided insight into potential areas for future research. It was recommended that fundamental adsorption tests be used to uncover a PAX- hydroxamate ratio where their synergy is optimized. Now that the JMP models have found the region where the optimums lie, a conventional approach to studying the area was recommended to provide more precise model fits. Different flotation circuits were proposed: a PAX- hydroxamate system with staggered collector addition, and a hydroxamate only system. The slimes removed from the charges are copper bearing. Although the copper contained in the slimes is minor, research into a potential leaching circuit to recover this copper could be beneficial.

References

- Ackerman, P.K. Harris, G.H., Klimpel, R.R and Aplan, F.F “ Use of Chelating Agents As Collectors in the Flotation of Copper Sulphides and Pyrite”, Minerals and Metallurgical Processing 16(1); 27-35 (1999)
- Agrawal, Y.K., Tandon, S.G., “Metal-Ligand Stability Constants of Hydroxamic Acids”, J. Inorg. Nucl. Chem. 36 : 869-873 (1974)
- Aikaike, H., “A New Look at the Statistical Model Identification”, IEE Transactions on Automatic Control (AC9:6), 1974.
- Aliferova, S., Titkov, S., Sabirov, R., Novoselov, V., Panteleeva N., “Application of Non-Ionic Surface Active Substances in Combination with Acrylamide Flocculants for Silicate and Carbonate Mineral Flotation”, Minerals Engineering (18:10): pp.1020-1023 (2005)
- Aplan, F.F and Fuerstenau, D.W., “The Flotation of Crysocolla by Mercaptan,” Int. J. Miner. Process. 13: 105-115, (1984)
- N. Aslan, Cebeci, Y., “ Application of Box–Behnken Design and Response Surface Methodology For Modeling of some Turkish Coals”, Fuel 86: pp 90-97 (2007).
- Aslan, N., Cifci, F., and Yan. D., “Optimzation of Process Parameters for Producing Graphite Concentrate Using Response Surface Methodology,” Separation and Purification Technology 59 : 9-16 (2008)
- Aslan, N., Fidan, R., “ Optimization of Pb Flotation Using Statistical Technique and Quadratic Programming”, Separation and Purification Technology 62 : 160-165 (2008)
- Assis, S.M., Montenegro, L.C.M., and Peres, A.E.C., “ Utilisation of Hydroxamates In Minerals Froth Flotation”, Minerals Engineering 9(1); 103-114 (1996)

Barbaro, M., Herra-Urbina R., Cozza, C. and Fuerstenau, D., " Flotation of Oxidized Minerals of Copper Using a New Synthetic Chelating Reagent as Collector," Int. J. Miner. Process. 50: 275-287 (1997)

Barnes, H.L., "Geochemistry of Hydrothermal Ore Deposits, 3rd Ed", J.Wiley and Sons, 1997.

Bartlett, R.W., "Solution Mining : Leaching and Fluid Recovery of Materials, 2nd Ed." Gordon and Breach Science Publishers. 1998

Bessiere, J. and Khayar, M., "Analysis of Collector Adsorption onto Malachite by Means of Dielectric Measurement," Int. J. Miner. Process. 39: 107-118 (1993)

Bessiere, J., El Housni, A., Predali, J.J., " Dielectric Study of Activation and Deactivation of Malachite by Sulphide Ions," Int. J. of Miner. Process 33: 165-183 (1991)

Buckley, A.N., I. C. Hamilton, I.C., Woods, R., "Flotation of sulfide minerals", K. S. E. Förssberg, Ed, : Elsevier, Amsterdam, pp.41 (1985)

Callen, T. (2007). "Emerging Markets Main Engine of Growth". *IMF Survey Magazine*. Available online:
<http://www.imf.org/external/pubs/ft/survey/so/2007/NUM1017A.htm>. Last accessed:July 14, 2009.

Castro, S., Goldfarb, J., and Laskowski, J., "Sulphidizing Reactions in the Flotation of Oxidized Copper Minerals, I. Chemical Factors in the Sulphidization of Copper Oxide," Int. J. Miner. Process. 1: 141-149, (1974)

Castro, S., Soto, H., Goldfarb, J., and Laskowski, J., "Sulphidizing Reactions in the Flotation of Oxidized Copper Minerals, II. Role of the Adsorption and Oxidization of Sodium Sulphide in the Floatation of Chrysocolla and Malachite," Int. J. Miner. Process. 1: 151-161, (1974)

Castro, S., Gaytan, H., and Goldfarb J., " The Stabilizing Effect of Na₂S on the Collector Coating of Crysocolla," Int. J. Miner. Process. 3: 71-82, (1976)

Chander, S., "Electrochemistry of Sulfide Flotation: Growth Characteristics of Surface Coatings and their Properties, with Special Reference to Chalcopyrite and Pyrite", Int. Journal of Mineral Processing, 33: pp. 121-134 (1991)

Clark, D.W., Newell, J.H., Chilman, G.F., and Capps, P.G., "Improving Flotation Recovery of Copper Sulphides by Nitrogen Gas and Sulphidization Conditioning," Minerals Engineering. 13:1197-1206, (2006)

Dekun, K., Jingqing, C., and Weizhi, Z., "Application of Hydroxamic Acid and Hydroxamic -Xanthate Collector System in Metal Ore Flotation" Reagents Miner. Ind., Pap., M.J Jones and R.Oblatt, eds., Inst. Min. Met., 169 London, UK: 169-173 (1984)

Eriksson, G.A., "An algorithm for the Computation of Aqueous Multicomponent, Multiphase Equilibria", Analyt. Chim. Acta, (112), pp. 375-383, (1979).

Everard, L., De Cuyper, J., "Flotation of Copper-Cobalt Oxide Ores with Alkylhydroxamates." Proc. 11th Inter. Min. Proc. Congr., Instituto di Arte Mineraria, Cagliari, pp. 655–669 (1975)

Forssberg K.S.E., Antti B.-M. and Palsson, B.I., "Computer Assisted Calculations of Thermodynamic Equilibria in the Chalcopyrite-Ethyl Xanthate System", Reagents Miner. Ind., Pap., M.J Jones and R.Oblatt, eds., Inst. Min. Met., London, UK:, pp. 251-264 (1984).

Fuerstenau, D.W., and Abouzeid, A-Z. M., "The energy efficiency of ball milling in communiton" Int. J. Miner. Process. 67: 161-185 (2002)

Fuerstenau, D.W., Herrera-Urbina, R., and McGlashan, D.W., "Studies on the Applicability of Chelating Agents as Universal Collectors for Copper Minerals," Int. J. Miner. Process. 58: 15-33 (2000)

Fuerstenau, D.W., Pradip, "Mineral Flotation with Hydroxamate Collectors" Reagents Miner. Ind., Pap., M.J Jones and R.Oblatt, eds., Inst. Min. Met., London, UK: 161-168 (1984).

Fuerstenau, M.C, Harper, R.W and Miller, J.D., " Hydroxamate vs. Fatty Acid Flotation Of Iron Oxide" Trans. AIME 247: 69-73 (1970)

Fullston, D., Fornasiero, D., Ralston, J., "Zeta Potential Study of the Oxidation of Copper Sulphide Minerals", Colloids and Surfaces A: Physicochemical and Engineering Aspects (146:1-3) : 131-121 (199)

Gutzeit, G., "Chelate Forming Organic Compounds as Flotation Reagents" Trans. Am. Inst. Min. Engrs 169: pp. 272-286 (1946).

Hanson, J.S., Fuerstenau, D.W., " An Electrochemical Investigation of the Adsorption Of Octyl Hydroxamate on Chalcocite." Colloids and Surfaces 26 : 133-140 (1987)

Hart, B., Dimov S., Martin, C. and Lang J. (2009.) "The Chemical Reactivity of an Ore: A Predictive and Diagnostic Tool for Flotation Behaviour using ToF-SIMS Analyses." COM2009, August 22-26, Sudbury, ON.

Hinz, C., "Description of Sorption Data with Isotherm Equations", Geoderma 99: 225-243 (2001).

Infomine (2008). "Commodity Mine"

Available online :

<http://www.infomine.com/commodities/>

Last accessed : May 30, 2009.

Jones, M.H., Woodcock, J.T., " Optimization and Control of Laboratory Sulphidization of Oxidized Copper Ores with an Ion Selective Electrode." Proc. Australas Inst. Min. Metall. No. 266 (1978)

Kelebek, S, Nanthkumar, B, "Characterization of Stockpile Oxidation of Pentlandite and Pyrrhotite Through Kinetic Analysis of their Flotation", Int. J. Miner. Process. 84: pp 69–80 (2007).

Kirkham, R. V. and Sinclair, W. D " Porphyry Copper, Gold, Molybdenum, Tungsten, Tin and Silver; in Geology of Canadian Mineral Deposits Types: O. R. Eckstrand, W. D. Sinclair and R. I. Thorpe (eds.), Geological Survey of Canada, Geology of Canada, n. 8 (1996)

Kordosky, G.A., "Copper Recovery Using Leach/Solvent Extraction/Electrowinning Technology: Forty Years of Innovation, 2.2 Million Tonnes of Copper Annually." J. South African Institute of Mining and Metallurgy. (2002)

Lee, J.S., Nagaraj, D.R., and Coe, J.E., " Practical Aspects of Oxide Copper Recovery With Alkyl Hydroxamates," Minerals Engineering, 11(10): 929-939 (1998)

Lee, K., Archiblad, D., McLean J., and Reuter, M.A., " Flotation of Mixed Copper Oxide And Sulphide Minerals with Xanthate and Hydroxamate Collectors" Minerals Engineering 2008 : 1-7 (2008)

Lenormand, J., Salman, T., and Yoon, R.H. "Hydroxamate Flotation of Malachite" Can. Met. Quart 18: 125-129 (1979)

Mason, R.L., Gunst, R.F., Hess, J.L., "Statistical Design and Analysis of Experiments With Application to Engineering and Science", John Wiley and Sons, Canada, 1989.

Marabini, A.M., Barbaro, M., and Alesse, V., " New Reagents in Sulphide Mineral Flotation," Int. J. Miner. Process. 33: 291-306 (1991)

Martinez, E., Hollander, M.L., "Reactions of Metal Oxides and Sulfur Studied by Thermoanalysis: Copper Oxides" Trans. AIME: 300-306 (1964)

Martinez-L, A., Uribe-S, A., Carillo-P, F.R., Coreno-A, J., Ortiz, J.C., "Study of Celestite Flotation Efficiency Using Sodium Dodecyl Sulfonate Collector : Factorial Experiment and Statistical Analysis of Data", Int. J. Miner. Process 70 (1-4) : pp 83-97 (2003).

Mielczarski, J., Suoninen, E., Johansson, L-S., Laajalehto, K., "An XPS Study of Adsorption of Methyl and Amyl Xanthates on Copper" Int. J. Miner. Process. 26 : 181-191 (1989).

Montgomery, D.C., Runger, G.C., Hubele, N.F., "Engineering Statistics, 3rd Ed" John Wiley and Sons, USA (2004)

Moon, C.J., Whateley, M.K.G., Evans, A.M., Barrett, W.L., Introduction to mineral exploration: Second Ed. Blackwell Publishing, Oxford (2006).

Nagaraj, D.R., Somasundaran, P., "Chelating Agents as Collectors in Flotation: Oximes-Copper Minerals System.AIME Annual Meeting, New Orleans (1979)

Nanthakumar, B., Kelebek, S., " Stagewise Analysis of Flotation by Factorial Design Approach with an Application fo the Flotation of Oxidized Pentlandite and Pyrrhotite," Int. J. Miner. Process. 84: 192-206 (2007)

Oprea, G., Michnea, A., and Mihali, C., " Adsorption Kinetic of 8-Hydrozyquiline on Malachite," Amer. J. of App. Sci, 4(8): 592-596, (2007)

Palmer, B.R., Gutierrez, B., and Fuerstenau, M.C., "Mechanisms Invovled in the Flotation of Oxides and Silicates with Anionic Collectors: Parts 1 and 2", Trans. AIME, 258 : 257-260 (1975)

Pavez, O., Brandao, P.R.G., and Peres A.E.C., " Techical Note : Adsorption of Oleate And Octyl-Hydroxamate on to Rare-Earth Minerals," Minerals Engineering, 9(3) : 357-366 (1996)

Partridge, A.C., Smith, G.W., " Technical notes, Small-sample flotation testing: a new cell," Trans. IMM 80 :pp. C199–C200 (1971)

Peterson H.D., Fuerstenau, M.C., Rickard R.S and Miller, J.D., "Chrysocolla Flotation by The Formation of Insoluble Surface Chelates" AIME Transactions 232 : 388-392 (1965)

Poling, G.W., "Flotation of Oxidized Copper". First South American Congress of Mineral Processing, Santiago (1973).

Pradip, Fuerstenau, D.W., " Adsorption of Hydroxamate Collectors on Semi-Soluble Minerals I. Adsorption on Barite, Calcite and Bastnaesite" Colloids and Surfaces 8: 103-119 (1983)

Pradip, Fuerstenau, D.W., " Adsorption of Hydroxamate Collectors on Semi-Soluble Minerals II. Effect of Temperatuer on Adsoprtion" Colloids and Surfaces 15: 137-146 (1985)

Price Waterhouse Cooper (2008). "Engineering & Construction Industry Sector".

Available online:

<http://www.pwc.com/gx/en/engineering-construction/index.jhtml>

Last accessed: July 14, 2009.

Raghavan. S., Fuerstenau, D.W., " The Adsorption of Aqueous Octylhydroxamate On Ferric Oxide," Journal of Colloid and Interface Science 50(2): 319-330 (1975)

Rao, S.R., Finch, J.A., "Processing of Metallurgical Residues by Flotation with Hydroxamate-Bench Scale Studies on Industrial Products": Jia, C.Q., Pickles, C.A., Brienne S., Rao,S.R (eds.), 47th Annual Conference of Metallurgists of CIM, Winnipeg: pp. 37-44 (2008)

Rascoe, A., Trevethan, N., (2008). "U.S Metal Demand Battered by Housing, Construction "

Available online :

<http://www.reuters.com/article/reutersEdge/idUSN1435102120080414>

Last accessed July 14, 2009.

Roodman, D.M., Lenssen, N., "Our Buildings, Ourselves". *World Watch* 7(6) : pp. 21-29 (1994)

Rubio, J., Phil, M., "Conditioning Effects of Flotation of Finely Divided Non-Sulphide Copper Ore" Trans. Inst. Min. Metall. C. Vol. 87 (1978)

Sall, J., Creighton. L., Lehman, A., "JMP Start Statistics : A Guide to Statistics and Data Analysis Using JMP and JMP IN Software", Thompson Brooks/Cole, Belmont CA, 2005.

Santana, R.C., Farnese, A.C.C., Fortes, M.C.B, Ataide, C.H and Barrozo, M.A.S.,
"Influence of Particle Size and Reagent Dosage on the Performance of
Apatite Flotation," Separation and Purification Technology 64: 8-15 (2008)

Schoenert, K., "On the limitation of energy saving in milling. 1". World Congress Particle Technology, Part II, Comminution, Nurnberg, April 16– 19, p. 1. (1986)

Ser, F., MacDonald, J.D., Whyte, R.M and J.E Hillary, " Sulphydric Flotation of Previously Sulphidized Oxide Copper Minerals of Nchanga Consolidated Copper Mines Limited" RUDY, IX International Mineral Processing Congress, Prague (1970)

Sinclair, W.D., "Porphyry Deposits in Mineral Deposits of Canada" GAC-MDD Special Publication n.5 (2007).

Sreenivas, T., Padmanabhan, N.P.H., "Surface Chemistry and Flotation of Cassiterite With Alkyl Hydroxamates" Colloids and Surfaces, 205 : 47-59 (2002)

Takahashi, K., Wakamatsu, T., " The Role of Amio Acid on the Xanthate Adsorption at The Water-Mineral Interface," Int. J. Miner. Process. 12:127-143 (1984)

Tukel, C., "Interactions of Chelating Agents in the Processing of Complex Nickel-Copper Sulphide Ores with Emphasis on Pyrrhotite Rejection", Ph.D. Thesis, Queen's Univ., 2002.

Werneke, M.F., Jones, J.A., "Monoalkyldithiocarbamates as Promoters for Copper Carbonate Minerals", Mining Engineering : 72-76 (1978)

Workman, L., Eloranta, J., "The Effects of Crushing and Grinding Efficiency and Energy Consumption" Proceedings of Twenty-Ninth Conference on Explosives and Blasting Technique, Volume I, Feb. 2-5 2003, Nashville, Tennessee, International Society of Explosives Engineers, pp. 131-140.

Uwadiale, G.G.O.O., " Flotation of Iron Oxides and Quartz- A Review", Miner. Process. And Extract. Met. Rev. 11 : 129-161 (1992)

Zhang, L., "Technical Note Electrochemical Equilibrium Diagrams for Sulphidization of Oxide Copper Minerals," Minerals Engineering, 7(7): 927-932 (1994)

Zhou, R., and Chander, S., " Kinetics of Sulphidization of Malachite in Hydrosulphide and Tetrasulphide Solutions," Int. J. Miner. Process. 37: 257-272, (1993)

Appendix A

XRD Reports

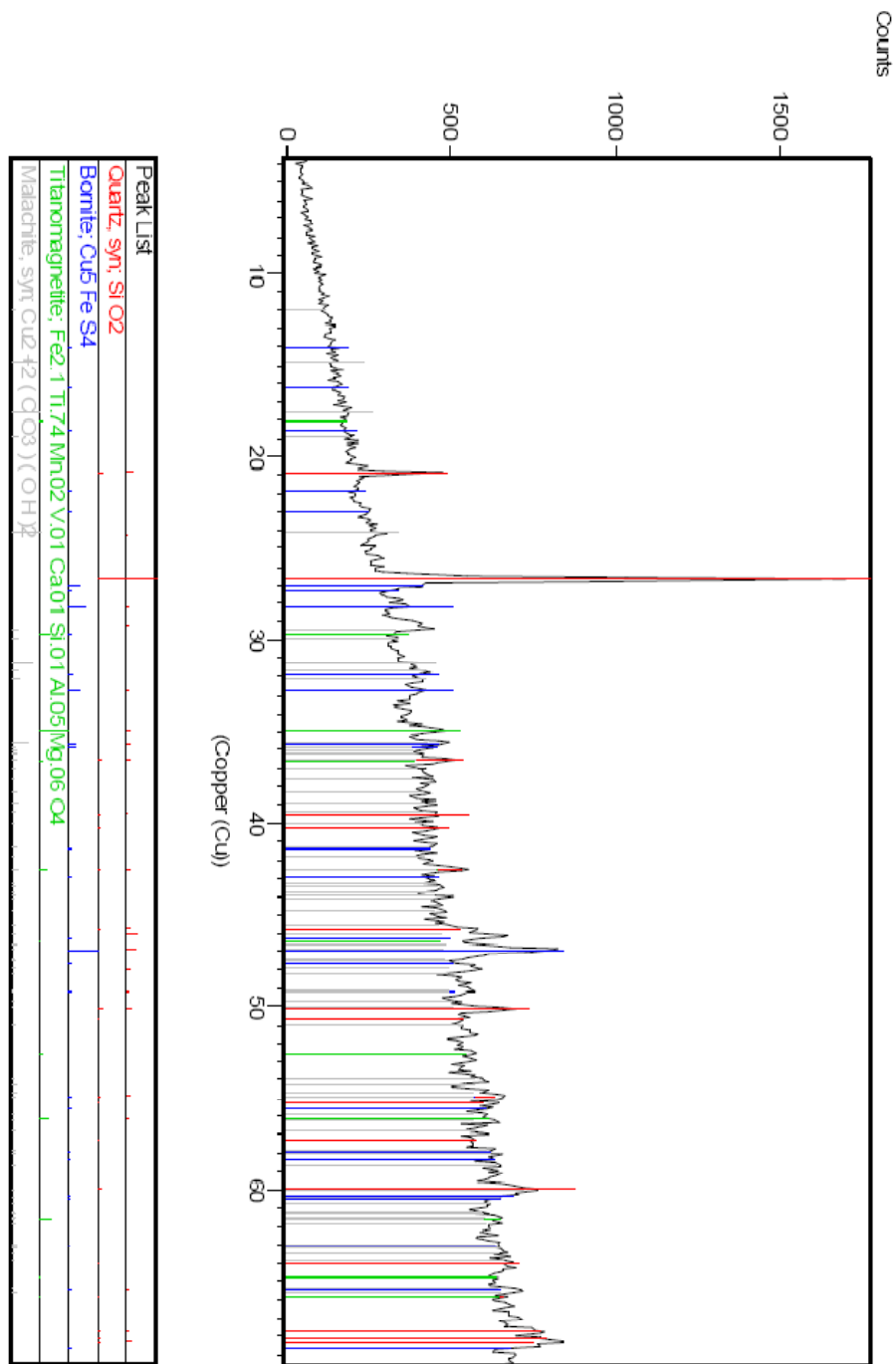


Figure A.1 : XRD report for a combined sulphide concentrate.

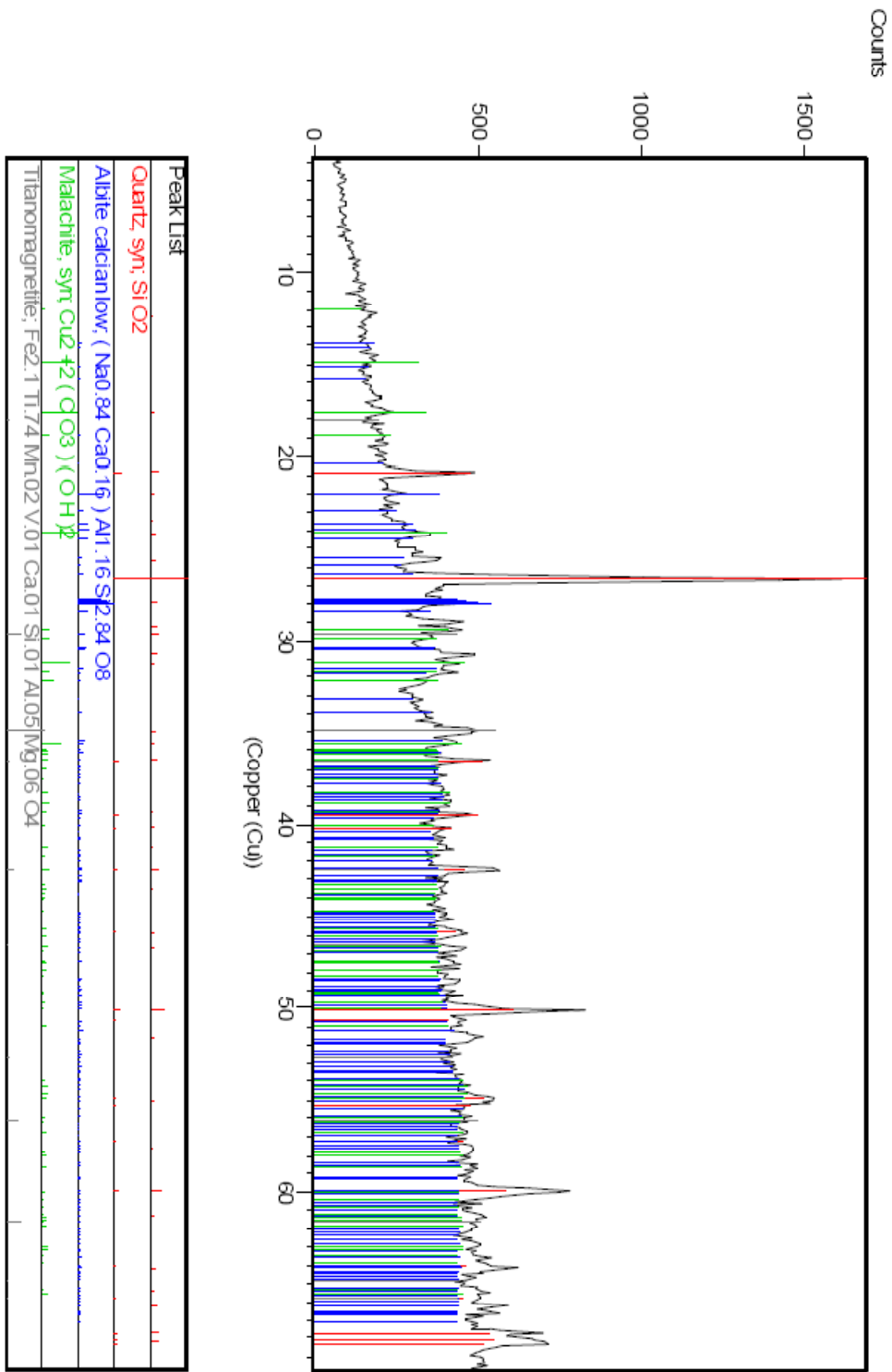


Figure A.2 : XRD report for a combined oxide concentrate.

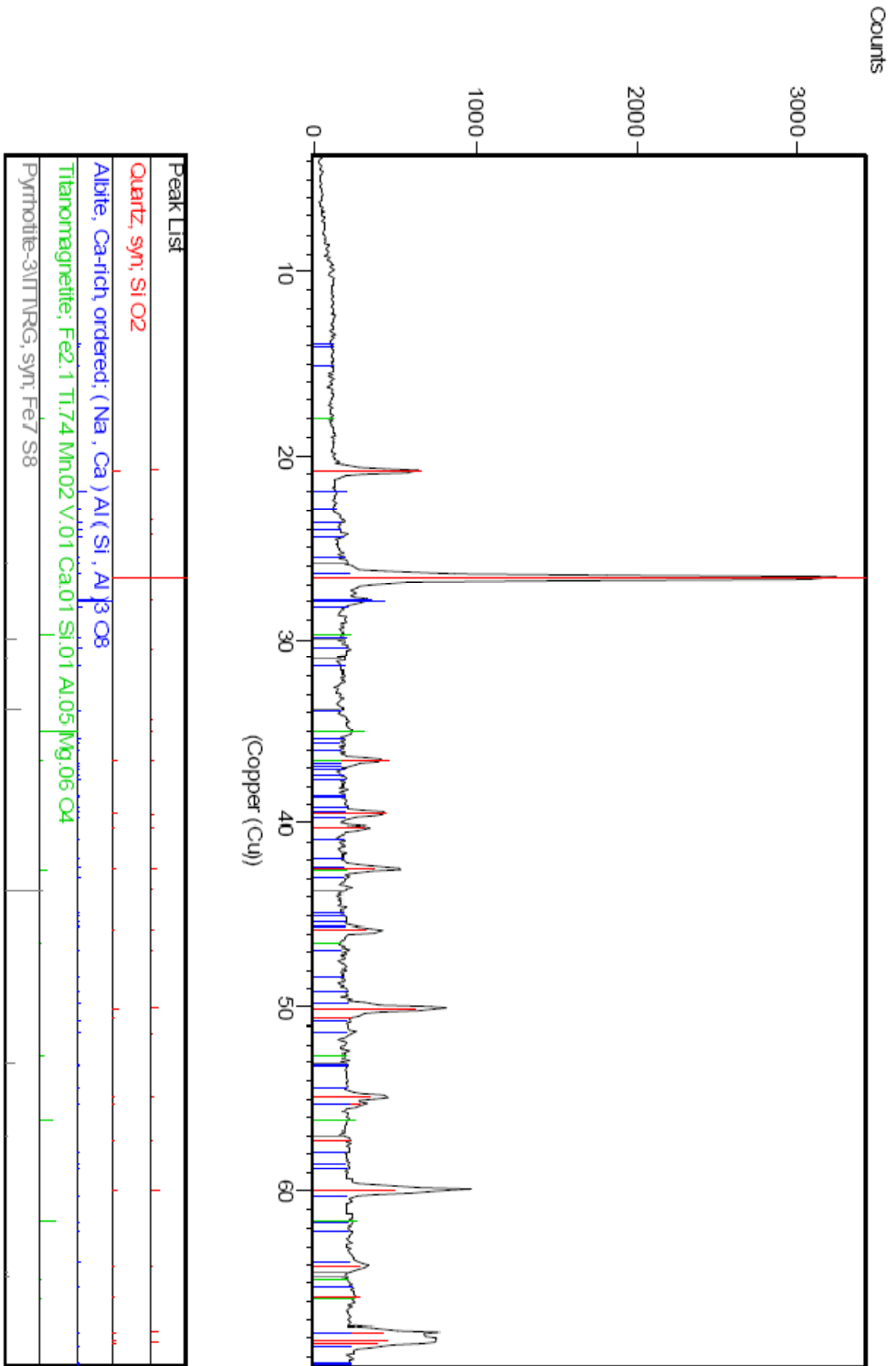


Figure A.3 : Tailings XRD report.

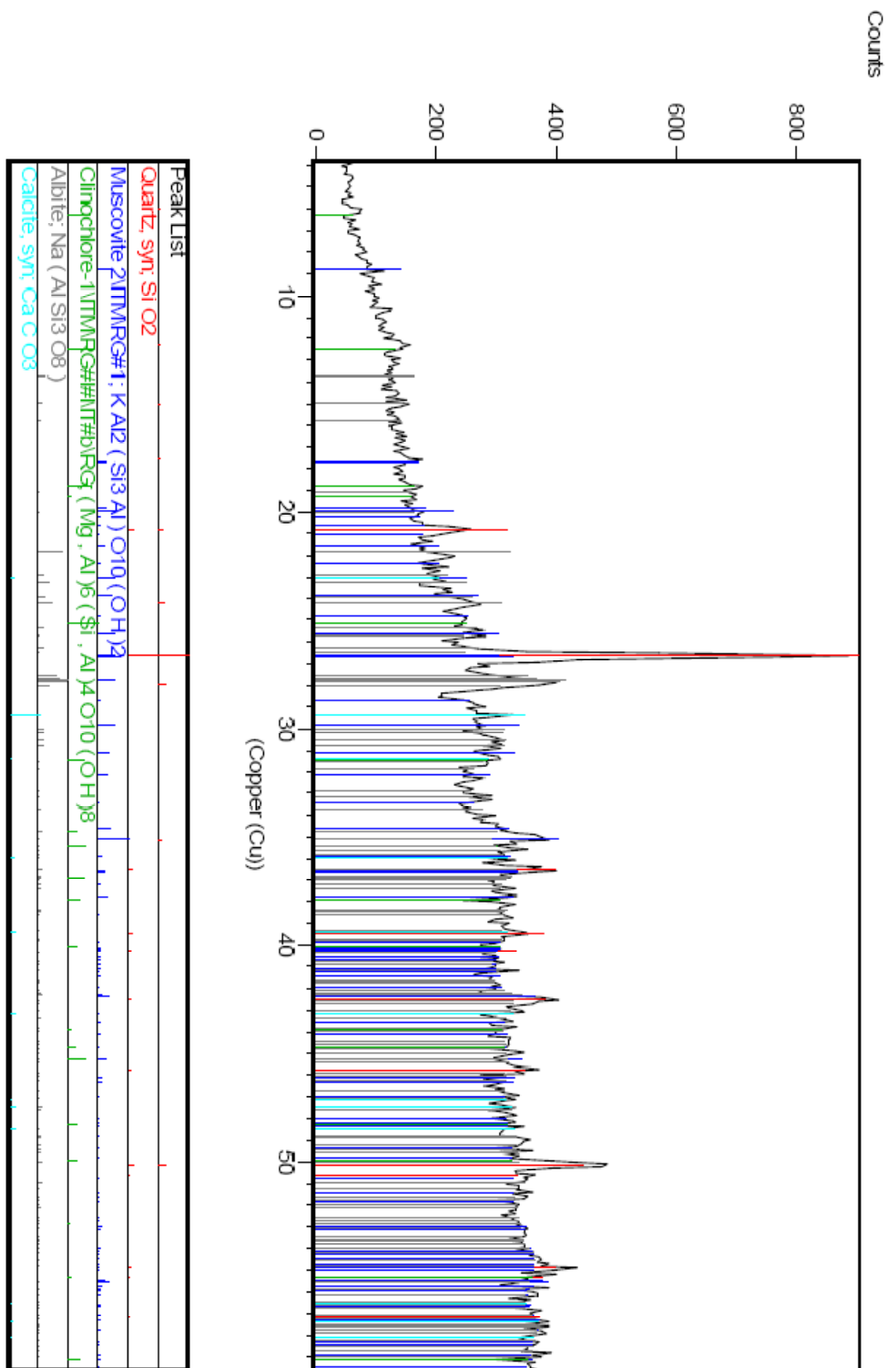


Figure A.4 : XRD report for the slime fraction.

Appendix B

Adsorption and Eh-pH Data

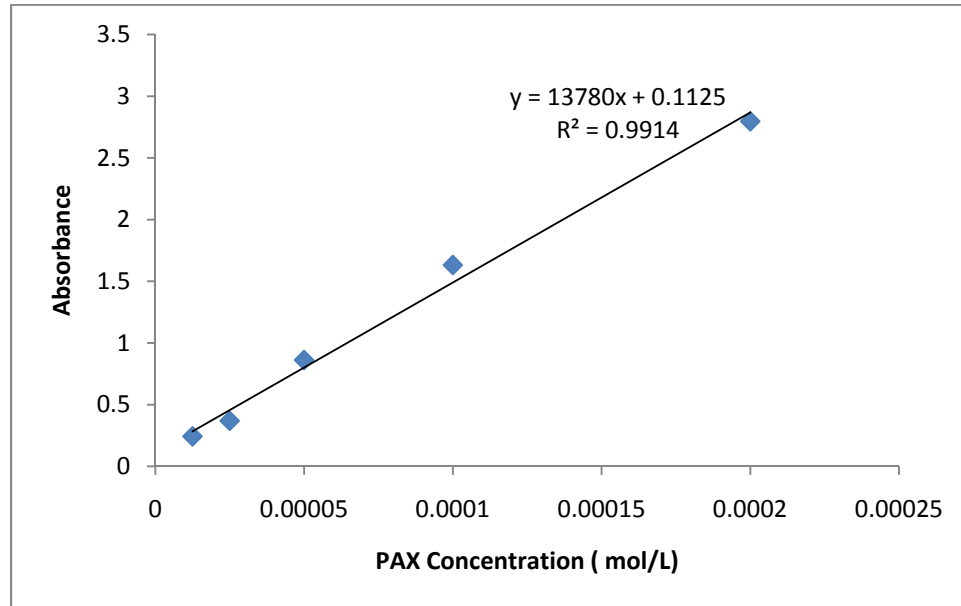


Figure B.1 : PAX calibration curve.

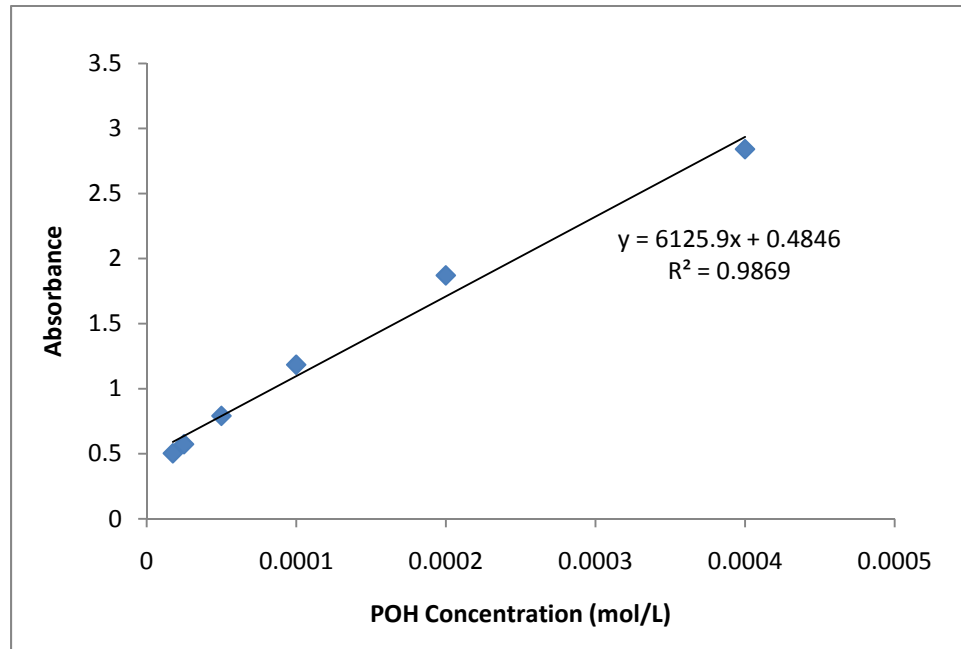


Figure B.2 : Hydroxamate calibration curve.

Sample Calculations for Adsorption Density :

This sample calculation is performed for the Hydroxamate-malachite system at pH 8.5 and 30 s. The calculations for the other pH levels and the other mineral-collector systems are performed in the same fashion.

Convert absorbance to concentration:

$$\begin{aligned}\text{Concentration} &= 6125.9(\text{Absorbance}) + 0.4846 \\ &= 6125.9(2.0261) + 0.4846 \\ &= 2.52 \times 10^{-4} \text{ mol/L}\end{aligned}$$

Calculate moles in solution:

$$\text{Mol (sol'n)} = 0.05\text{L} \times 2.52 \times 10^{-4} \text{ mol/L} = 1.25 \times 10^{-5} \text{ mol}$$

Calculate initial moles in system:

$$\text{Mol (initial)} = 1 \times 10^{-3} \text{ mol/L} \times 0.05 \text{ L} = 5 \times 10^{-5} \text{ mol}$$

Calculate mol adsorbed:

$$\text{Mol (ads)} = 5 \times 10^{-5} - 1.25 \times 10^{-5} = 3.74 \times 10^{-5} \text{ mol}$$

Calculate mineral surface area:

$$\text{SA (mal)} = 0.431 \text{ g} \times 1.2201 \text{ m}^2/\text{g} = 0.5259 \text{ m}^2$$

Calculate adsorption density:

$$\text{Ads. Density} = 3.74 \times 10^{-5} \text{ mol} / 0.5259 \text{ m}^2 = 7.115 \times 10^{-5} \text{ mol/m}^2 = 71.15 \text{ mmol/m}^2$$

Table B.1 : Absorbance values for the PAX-Malachite system.

Time (s)	pH						
	5.5	6.5	7.5	8.5	9.5	10.5	11.5
0	3.0678	3.061	3.0576	3.0484	3.0742	3.0586	3.0641
15	2.5329	2.7626	1.9244	2.058	2.4472	2.5167	2.8547
30	2.4139	1.8479	1.1631	1.2245	1.5549	1.6207	2.5959
60	1.5155	0.82828	0.39175	0.36731	0.37549	0.61638	1.5928
90	0.59784	0.36438	0.2791	0.29959	0.23294	0.41004	0.89976

Table B.2 : Absorbance data for the Hydroxamate-Malachite system.

Time (s)	pH						
	5.5	6.5	7.5	8.5	9.5	10.5	11.5
0	3.2377	3.1979	3.1662	3.2087	3.0338	3.324	3.2745
15	2.2912	2.2025	2.25525	2.0605	2.0744	2.47785	2.5508
30	2.27745	2.0803	2.1082	2.0261	2.0319	2.46995	2.5323
60	2.224	2.0776	2.04055	2.0011	2.02255	2.4298	2.5098
90	2.22095	2.0356	2.0597	1.9665	1.9454	2.4281	2.4606

Table B.3 : Absorbance data for the PAX-Bornite system.

Time (s)	pH						
	5.5	6.5	7.5	8.5	9.5	10.5	11.5
0	3.0678	3.071	3.0638	3.0774	3.0794	3.0897	3.0641
120	3.0447	3.0599	3.0439	3.0576	3.0506	3.0545	3.0431
360	3.0434	3.0588	3.0424	3.0567	3.0458	3.0535	3.0427

Table B.4 : Absorbance data for the Hydroxamate-Bornite system.

Time (s)	pH						
	5.5	6.5	7.5	8.5	9.5	10.5	11.5
0	3.13415	3.1466	3.1939	3.2748	3.4488	3.3554	3.28245
15	2.06665	2.0901	2.11185	2.09535	2.29415	2.54025	2.57305
30	2.05275	2.08265	2.0872	2.0933	2.2813	2.5379	2.56225
60	2.0436	2.0761	2.01545	2.08355	2.2368	2.5232	2.5467
90	2.0114	1.9796	1.9972	2.0474	2.2344	2.5122	2.5464

Table B.5 : Micro-flotation and Eh-pH data for the PAX-malachite system.

	Initial	Flotation	Final	Recovery (%)
pH	5.26	5.29	5.96	16.5
Eh	310	327	317	
pH	6.15	5.54	6.85	50.02
Eh	352	341	308	
pH	7.51	7.37	7.62	84.05
Eh	286	240	258	
pH	8.55	8.3	8.19	94.87
Eh	223	196	237	
pH	9.15	9.12	8.87	98
Eh	206	170	186	
pH	10.08	10.08	10.05	80.02
Eh	142	143	140	
pH	11.24	11.2	11.08	57.67
Eh	111	89	100	

Table B.6 : Micro-flotation and Eh-pH data for the Hydroxamate-malachite system.

	Initial	Collector	Final	Recovery (%)
pH	5.8	5.58	5.8	59.58
Eh	315	306	350	
pH	6.16	5.95	5.22	89.22
Eh	352	371	388	
pH	7.4	7.62	5.88	84.9
Eh	355	321	386	
pH	8.34	8.23	6.18	96.67
Eh	316	231	362	
pH	9.2	9.2	9.05	97.64
Eh	255	212	230	
pH	10.08	10.1	10	95.7
Eh	199	166	199	
pH	11.08	11.05	10.91	
Eh	142	146	155	92.79

Table B.7 : Micro-flotation and Eh-pH data for the N-Benzoyl-malachite system. The pH values in bold indicate the pH of flotation.

	Initial	Flotation	Final	Recovery (%)
pH	5.3	5.35	6.12	18.87
Eh	258	283	303	
pH	6.12	5.97	6.34	99.5
Eh	340	334	330	
pH	7.54	7.18	7.04	99.5
Eh	225	212	227	
pH	8.66	8.23	8.05	99
Eh	156	155	173	
pH	9.18	9.08	9.16	91.36
Eh	156	137	156	
pH	10.48	10.19	10.24	59.87
Eh	138	120	139	
pH	11.07	11.06	10.98	20.73
Eh	98	87	100	

Table B.8 : Micro-flotation and Eh-pH data for the PAX-bornite system.

	Initial	Flotation	Final	Recovery (%)
pH	5.89	5.77	6.85	97.97
Eh	281	76	68	
pH	6.65	6.88	7.27	97.44
Eh	232	66	56	
pH	7.69	7.59	7	96.63
Eh	190	76	2	
pH	8.55	8.22	7.64	94.04
Eh	170	58	-29	
pH	9.15	9.23	8.74	99.04
Eh	91	30	-13	
pH	10.22	10.1	10.01	94.47
Eh	51	-12	-5	
pH	11.06	11.03	11.02	89.04
Eh	38	-23	-8	

Table B.9 : Micro-flotation and Eh-pH data for the Hydroxamate-bornite system.

	Initial	Flotation	Final	Recovery (%)
pH	5.73	5.55	6.11	93.49
Eh	248	226	205	
pH	7.03	6.51	6.85	94.04
Eh	200	201	185	
pH	7.43	7.44	7.2	96.63
Eh	161	142	146	
pH	8.4	8.48	8.19	96.08
Eh	139	115	129	
pH	9.66	9.43	9.18	93.18
Eh	110	99	109	
pH	10.43	10.38	10.41	70
Eh	88	52	52	
pH	11.11	11.09	10.97	69.49
Eh	44	49	33	

Table B.10 : Micro-flotation and Eh-pH data for the N-Benzoyl-bornite system.

	Initial	Flotation	Final	Recovery
pH	4.74	4.63	4.73	84.43
Eh	222	234	220	
pH	5.88	5.65	6.31	94.66
Eh	206	216	168	
pH	6.16	5.95	5.22	95.5
Eh	352	371	388	
pH	7.69	7.86	7.79	95.21
Eh	151	129	133	
pH	8.4	8.32	9.31	92.74
Eh	155	122	69	
pH	9.3	9.41	9.06	84.45
Eh	116	95	103	
pH	10.2	10.34	10.21	45.26
Eh	76	62	27	
pH	11.24	11.23	11.1	19.79
Eh	6	-4	-15	

Table B.11 : Micro-flotation and Eh-pH data for the collectorless bornite system.

	Initial	Final	Recovery (%)
pH	5.67	6.7	21.19
Eh	208	177	
pH	9.15	8.65	82.18
Eh	130	137	
pH	10.99	10.65	65.22
Eh	64	38	

Table B.12: Thermodynamic data used for construction of species distribution diagrams from WinSGW Version 2.5.

Components	Log K _f	Stoichiometry Matrices								Soluble	Use
		C	1	0	0	0	0	0	0		
H+	0	C	1	0	0	0	0	0	0	Soluble	Use
e-	0	C	0	1	0	0	0	0	0	Soluble	Use
BHMA	0	C	0	0	1	0	0	0	0	Soluble	Use
H ₂ CO ₃	0	C	0	0	0	1	0	0	0	Soluble	Use
Cu(II)	0	C	0	0	0	0	0	1	0	Soluble	Use
EX ⁻	0	C	0	0	0	0	0	0	1	Soluble	Use
HEX	1.52		1	0	0	0	0	0	1	Soluble	Use
(EX) ₂ (aq)	-2.54		0	-2	0	0	0	0	2	Soluble	Use
Cu ⁺	2.68		0	1	0	0	1	0	0	Soluble	Use
Cu(OH) ⁺	-7.7		-1	0	0	0	1	0	0	Soluble	Use
Cu(OH) ³⁻	-27.1		-3	0	0	0	1	0	0	Soluble	Use
Cu(OH) ₄ ²⁻	-39.6		-4	0	0	0	1	0	0	Soluble	Use
Cu(OH) ₂ aq	-14.7		-2	0	0	0	1	0	0	Soluble	Use
Cu ₂ (OH) ₂ ²⁺	-10.3		-2	0	0	0	2	0	0	Soluble	Use
CuCO ₃ aq	-9.93		-2	0	0	1	1	0	0	Soluble	Use
Cu[CO ₃] ₂ aq	-23.44		-4	0	0	2	1	0	0	Soluble	Use
CuBHMA aq	10.29		0	0	1	0	1	0	0	Soluble	Use
Cu[BHMA] ₂ aq	19.02		0	0	2	0	1	0	0	Soluble	Use
Cu(OH) ₂ s	-8.27		-2	0	0	0	1	0	0	Solid	Use
Cu ₂ O s	6.76		-2	2	0	0	2	0	0	Solid	Use
CuCO ₃ s	-7.05		-2	0	0	1	1	0	0	Solid	Use
Cu ₂ (OH) ₂ CO ₃ s	-10.9		-4	0	0	1	2	0	0	Solid	Use
CuEX s	21.87		0	1	0	0	1	1	0	Solid	Use
Cu(EX) ₂ s	23		0	0	0	0	1	2	0	Solid	Use
(EX) ₂ L	2.37		0	-2	0	0	0	2	0	Solid	Use
Cu(OH)EX s	8.5		-1	0	0	0	1	1	0	Solid	Use

Appendix C

Graphical Box-Behnken Results

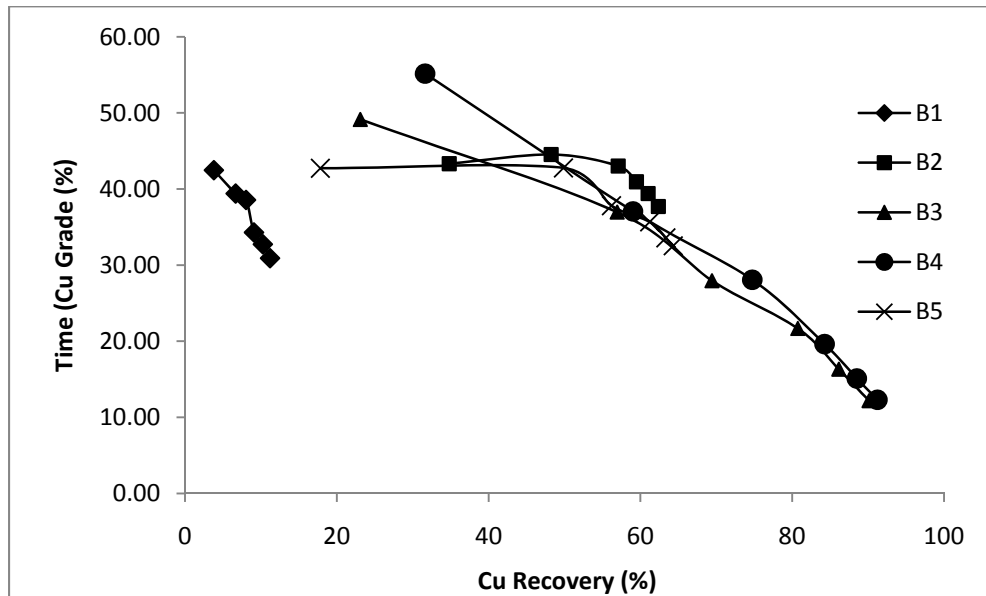


Figure C.1 : Cu grade vs. Cu recovery for B1-B5 of the Box-Behnken experiments.

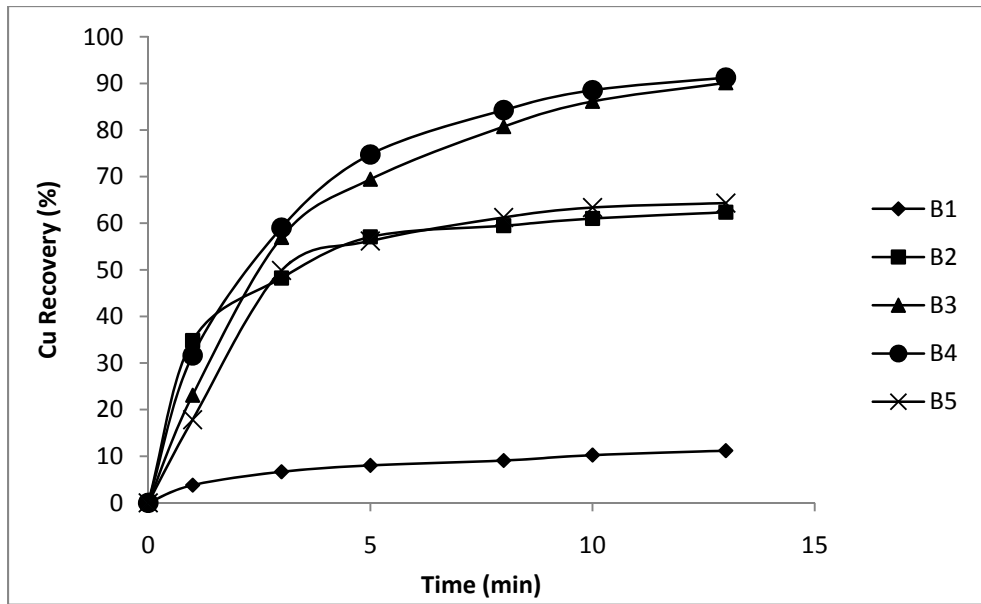


Figure C.2 : Cu recovery vs. time for B1-B5 of the Box-Behnken experiments.

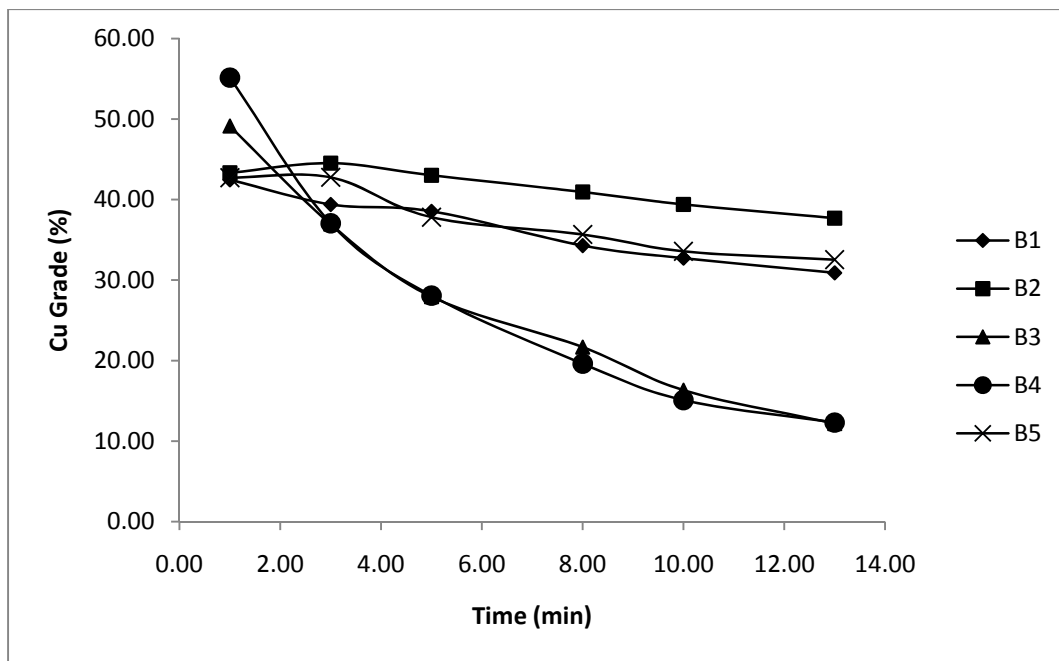


Figure C.3 : Cu grade vs. time for B1-B5 of the Box-Behnken experiments.

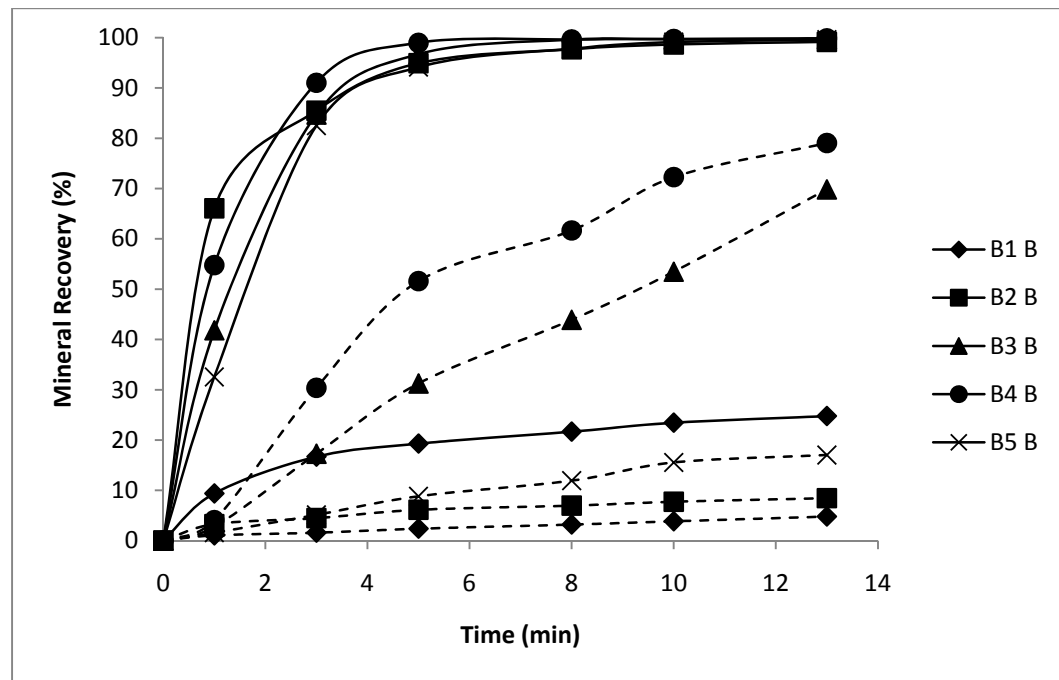


Figure C.4 : Mineral recovery vs. time for B1-B5 of the Box-Behnken experiments. Bornite recovery and malachite recovery are shown with a solid line and dashed line respectively.

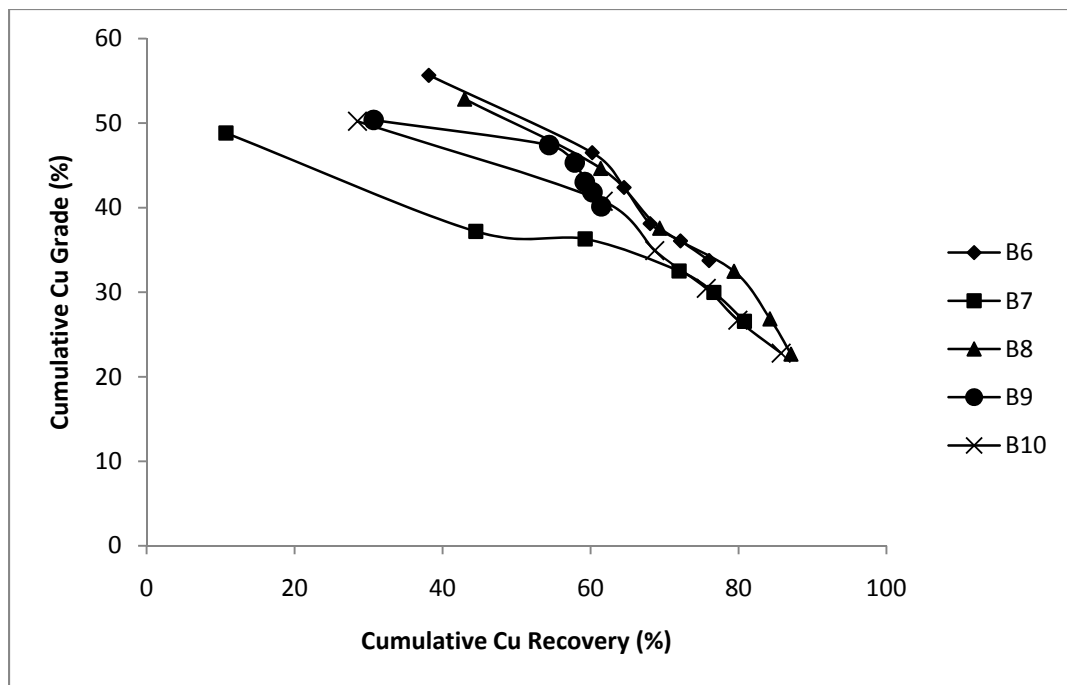


Figure C.5 : Cu grade vs. Cu recovery for B6-B10 of the Box-Behnken experiments.

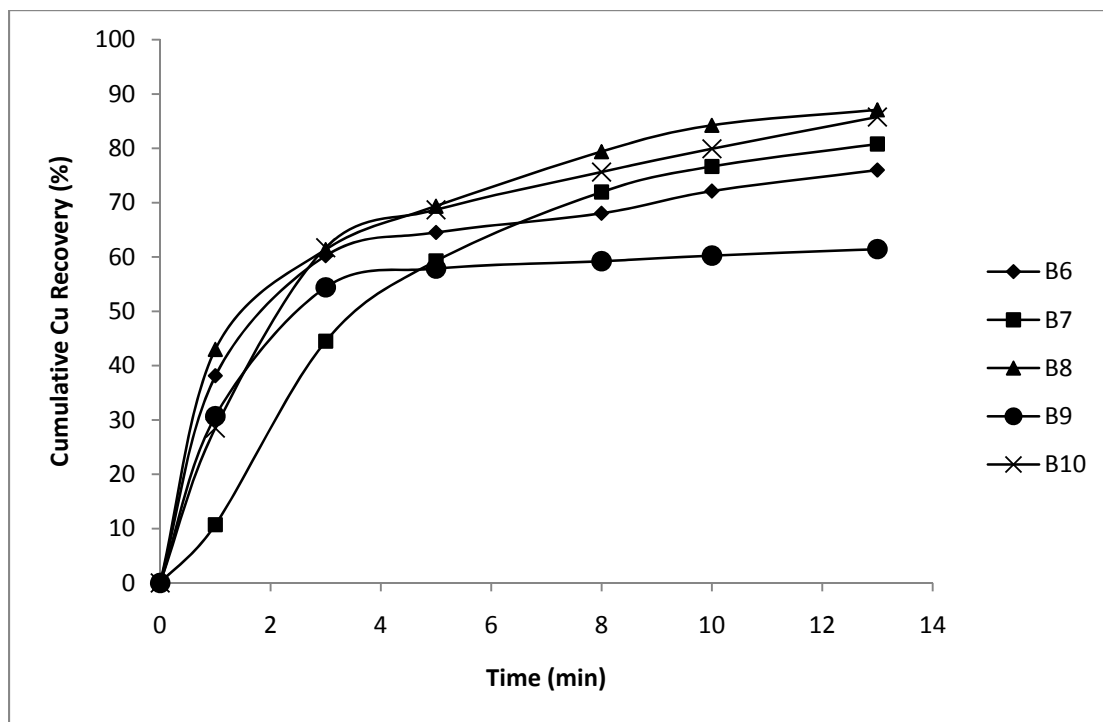


Figure C.6 : Cu recovery vs. time for B6-B10 of the Box-Behnken experiments.

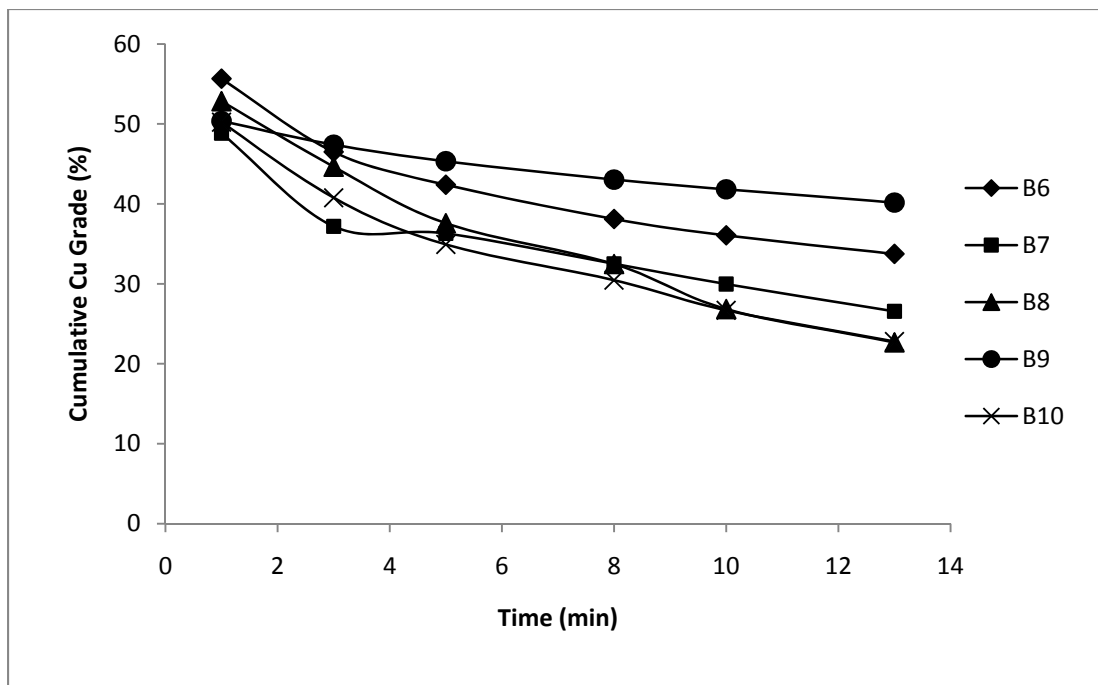


Figure C.7: Cu grade vs. time for B6-B10 of the Box-Behnken experiments.

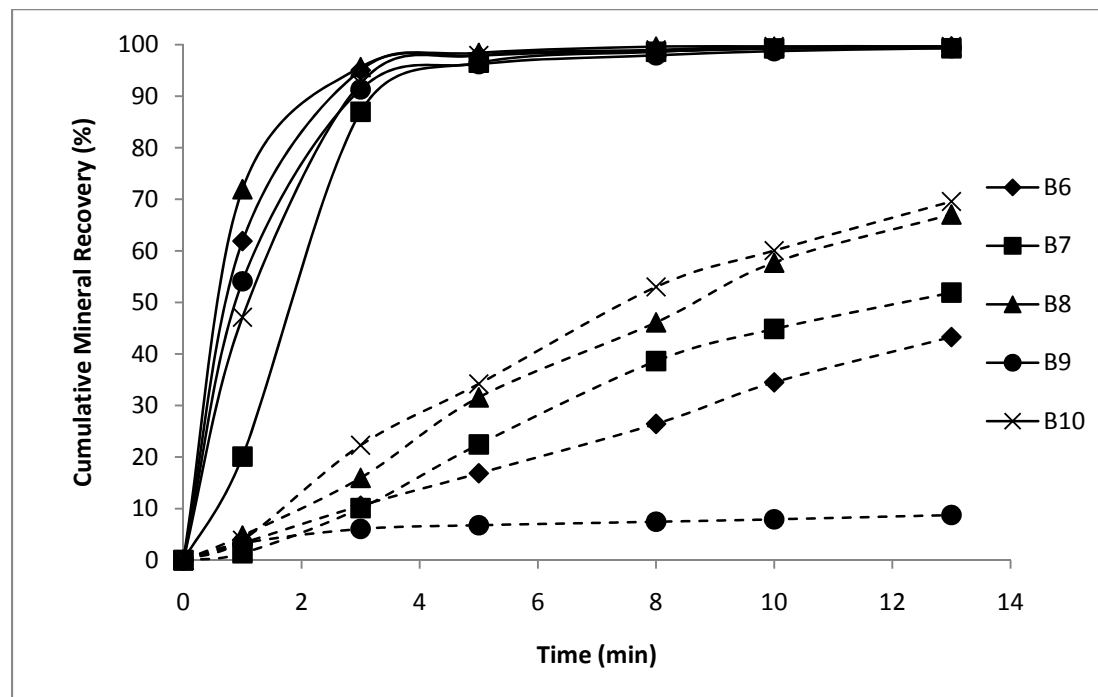


Figure C.8 : Mineral recovery vs. time for B6-B10 of the Box-Behnken experiments. Bornite recovery and malachite recovery are shown with a solid line and dashed line respectively.

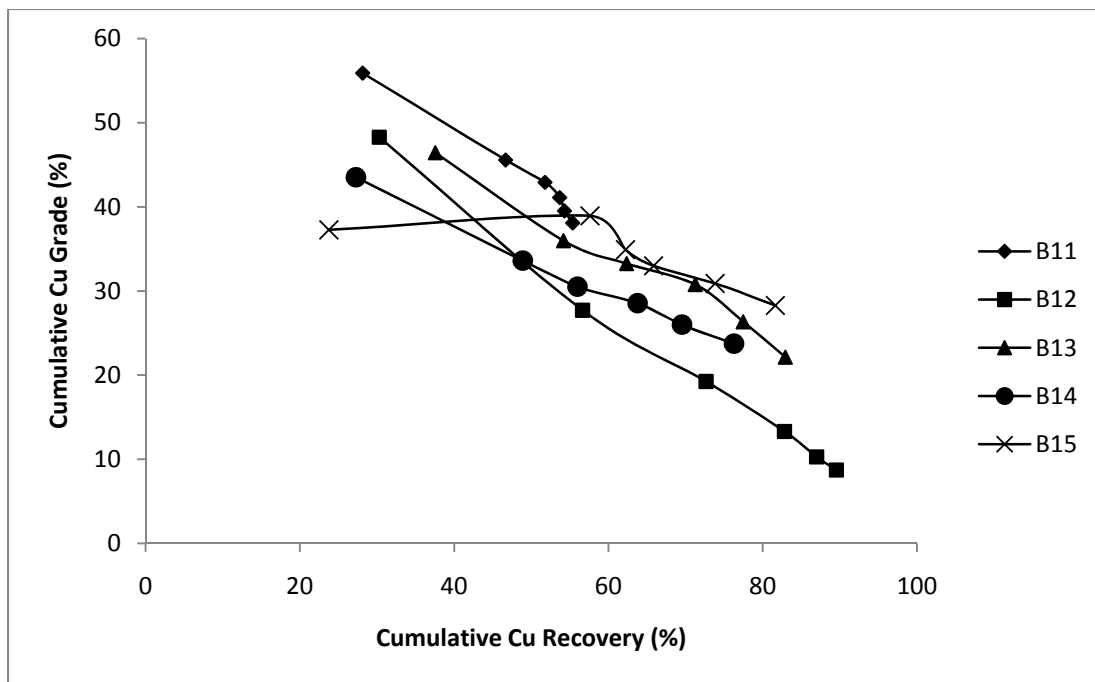


Figure C.9: Cu grade vs. Cu recovery for B11-B15 of the Box-Behnken experiments.

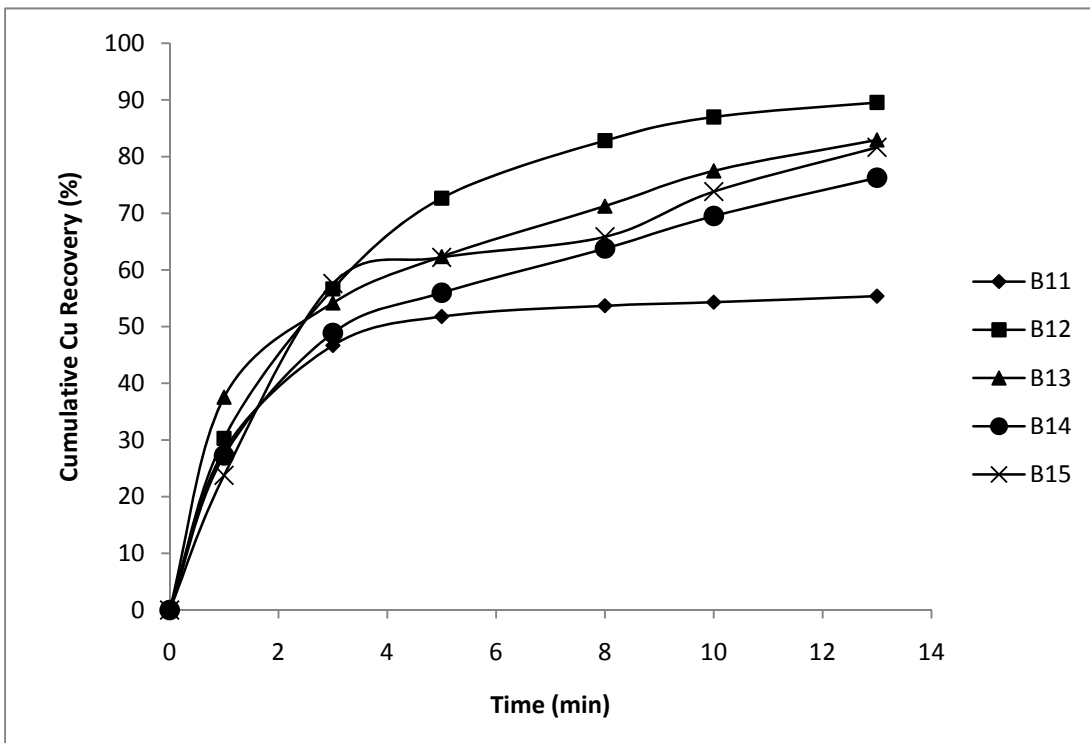


Figure C.10 : Cu recovery vs. time for B11-B15 of the Box-Behnken experiments.

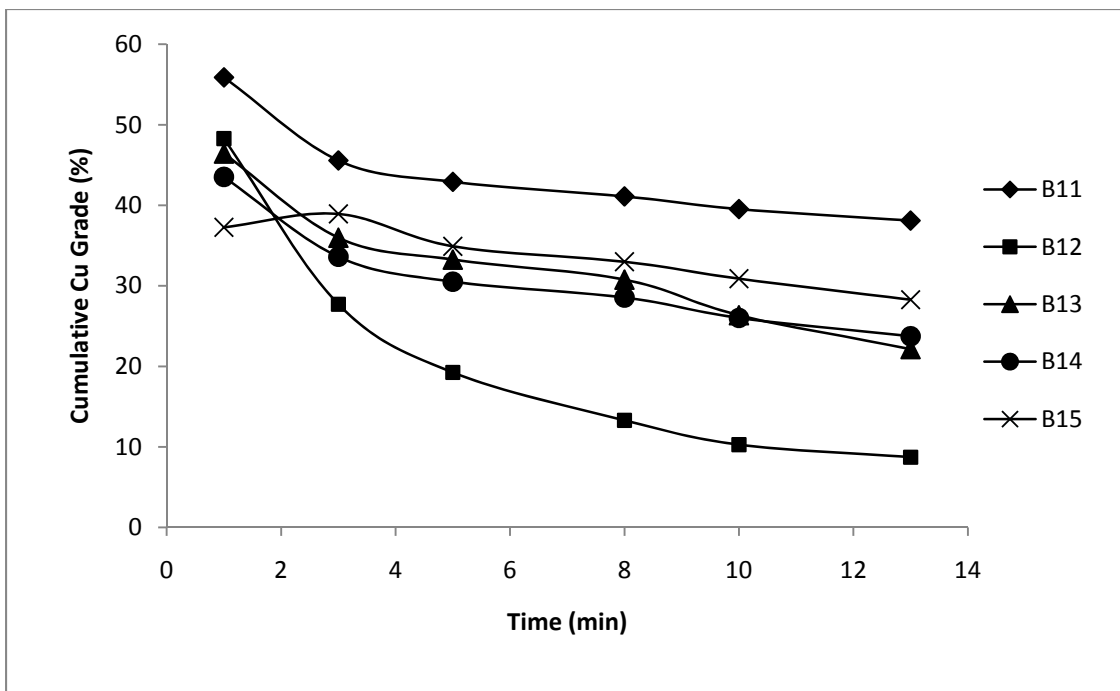


Figure C.11 : Cu grade vs. time for B11-B15 of the Box-Behnken experiments.

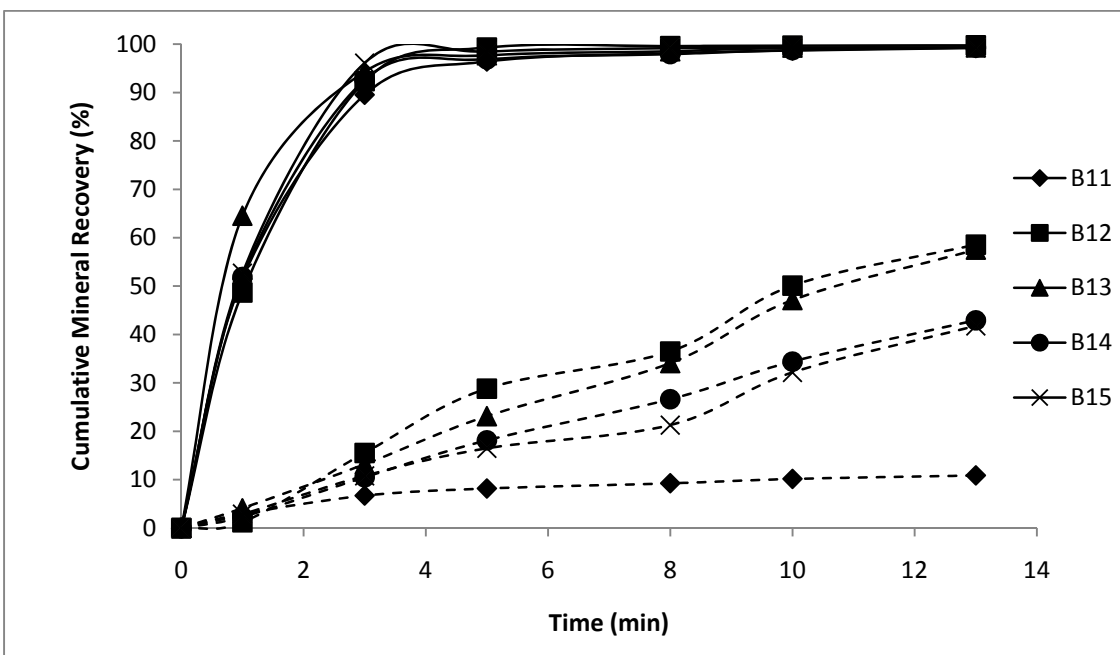


Figure C.12 : Mineral recovery vs. time for B11-B15 of the Box-Behnken experiments.

Bornite recovery and malachite recovery are shown with a solid line and dashed line respectively.

Appendix D

JMP Output

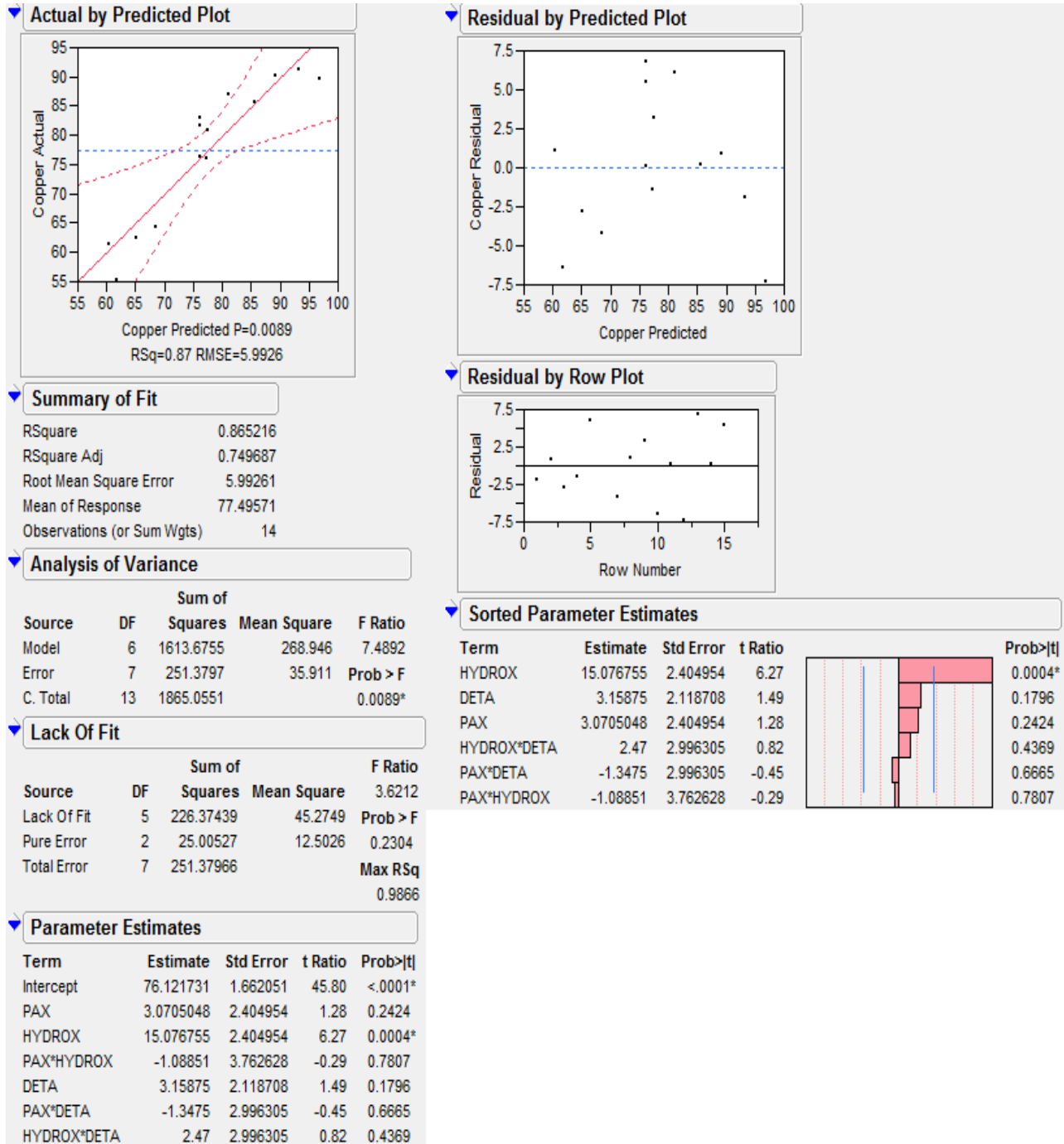


Figure D.1: JMP output for the linear copper recovery model.

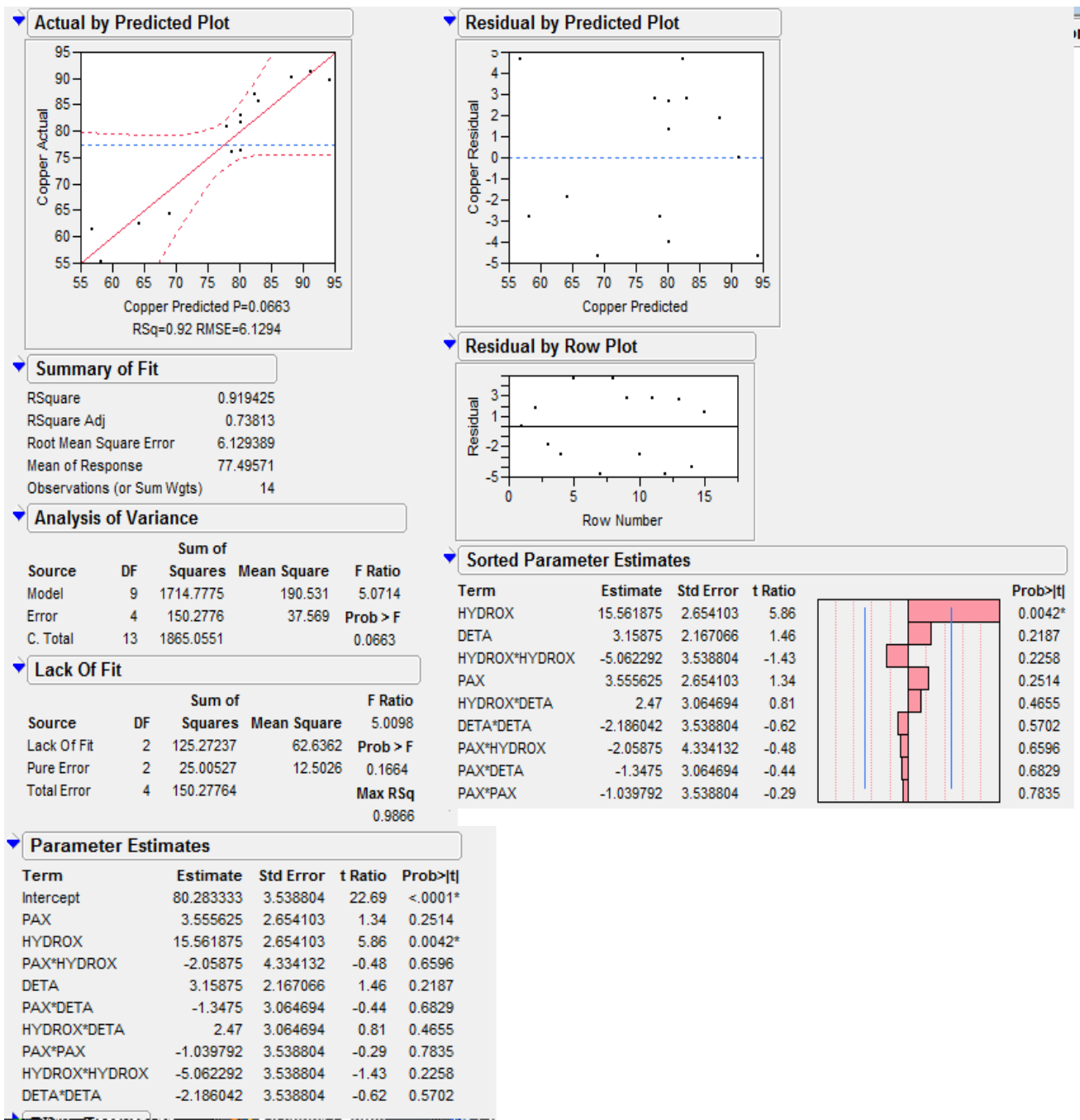


Figure D.2: JMP output for the full quadratic response surface model of copper recovery.

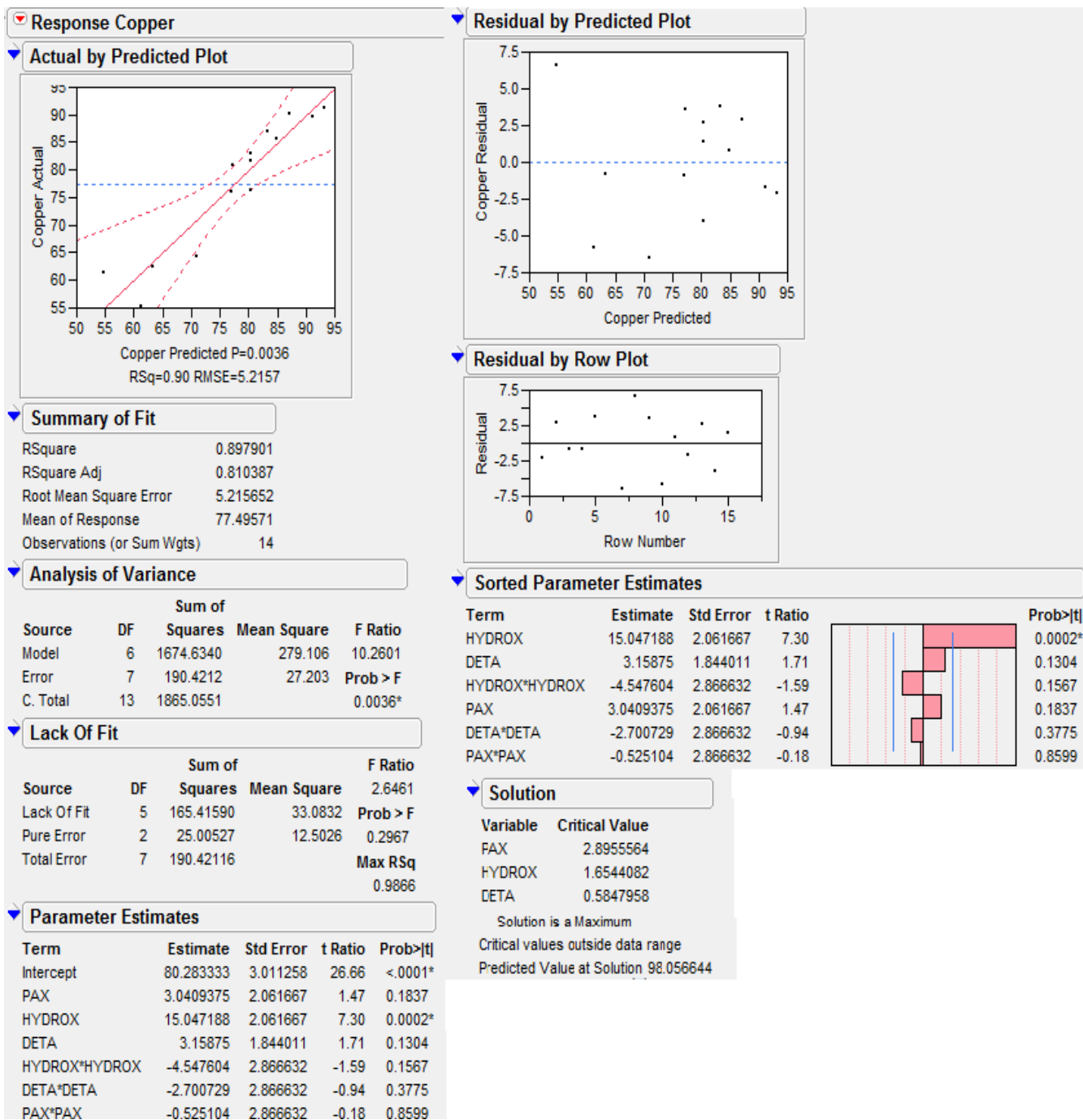


Figure D.3: JMP output for final copper recovery model.

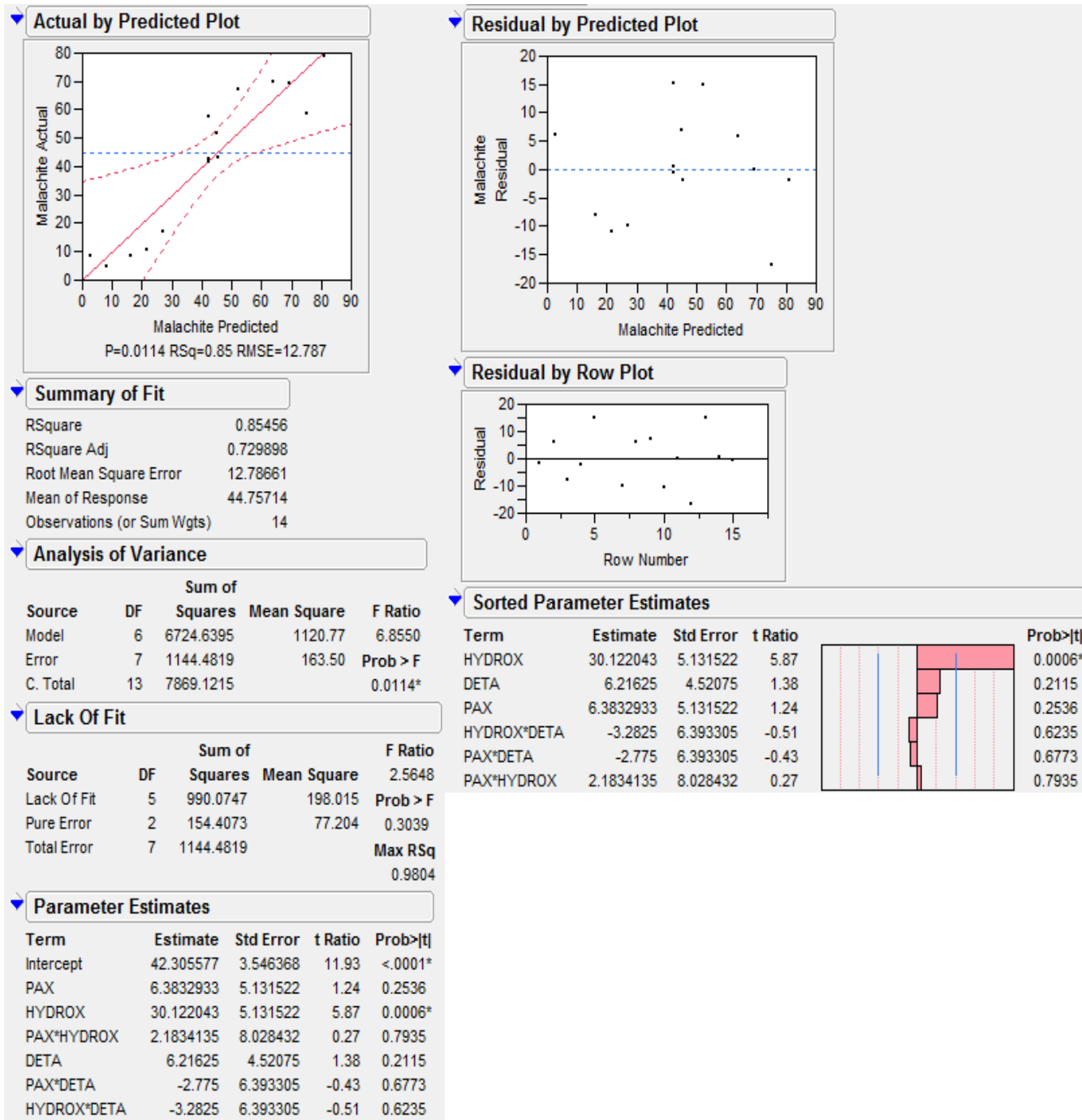


Figure D.4: JMP output for the linear model of malachite recovery.

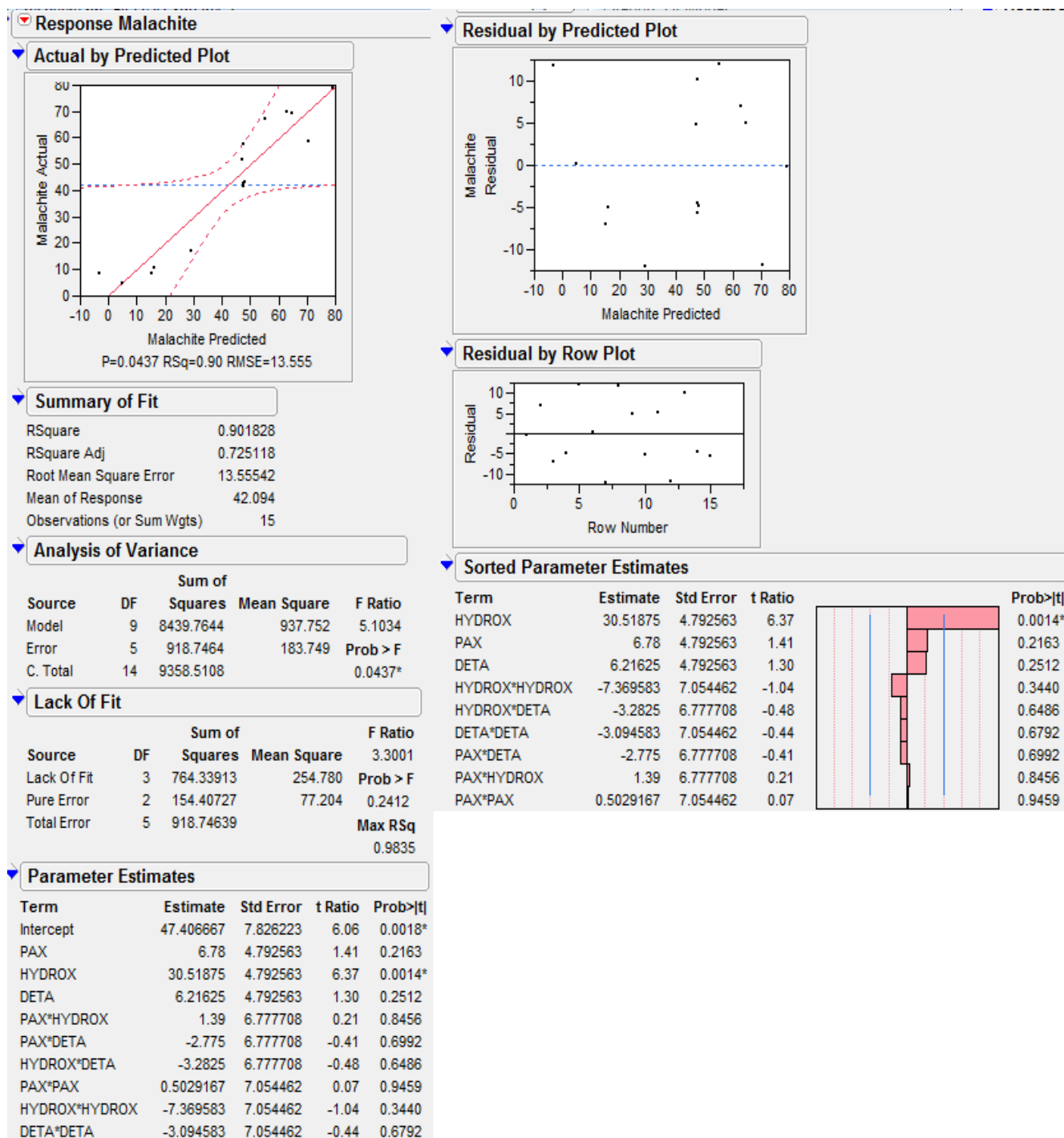


Figure D.5 : JMP output for the full quadratic response surface for malachite recovery.

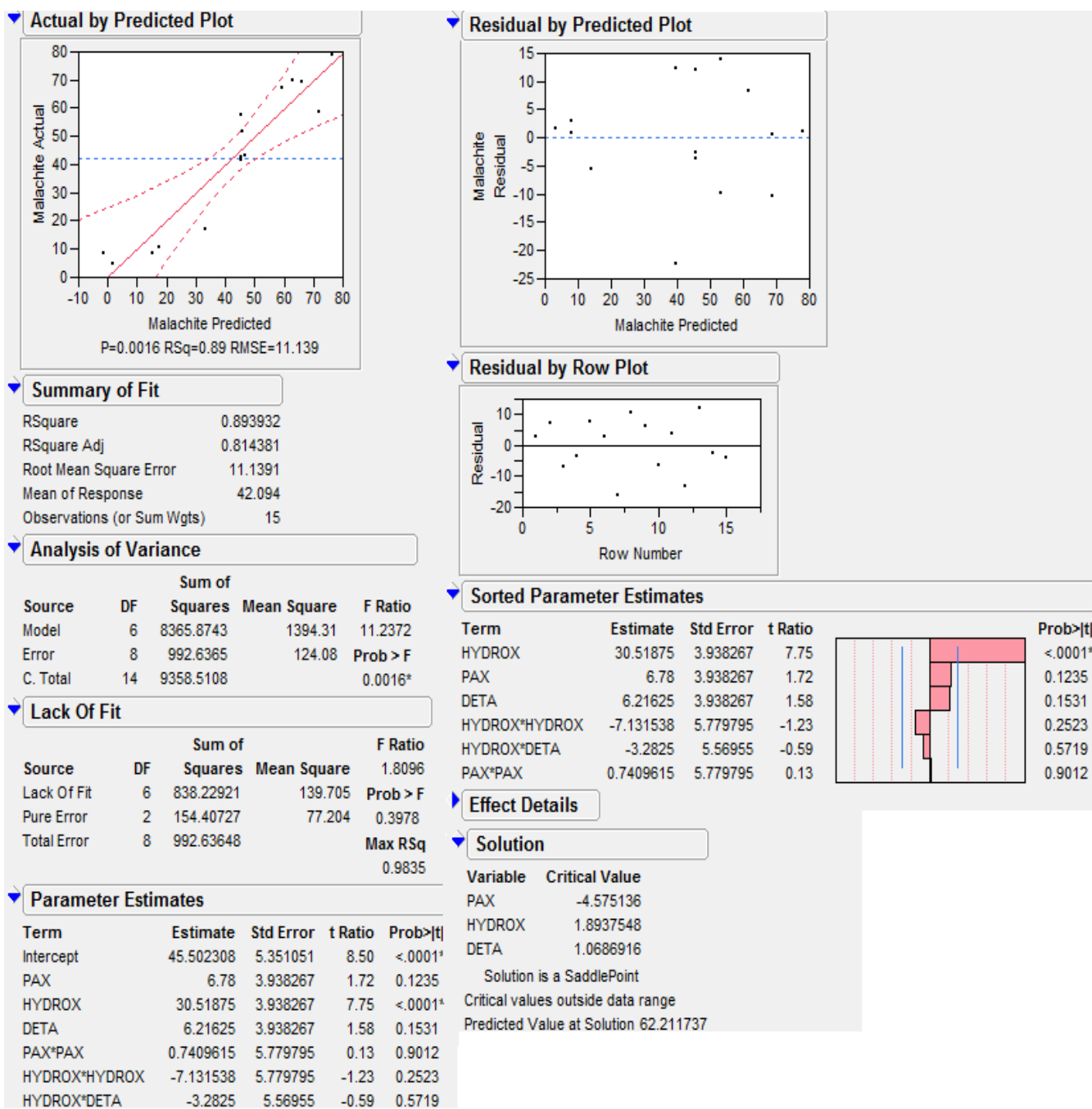


Figure D.6: JMP output for the final malachite recovery model.

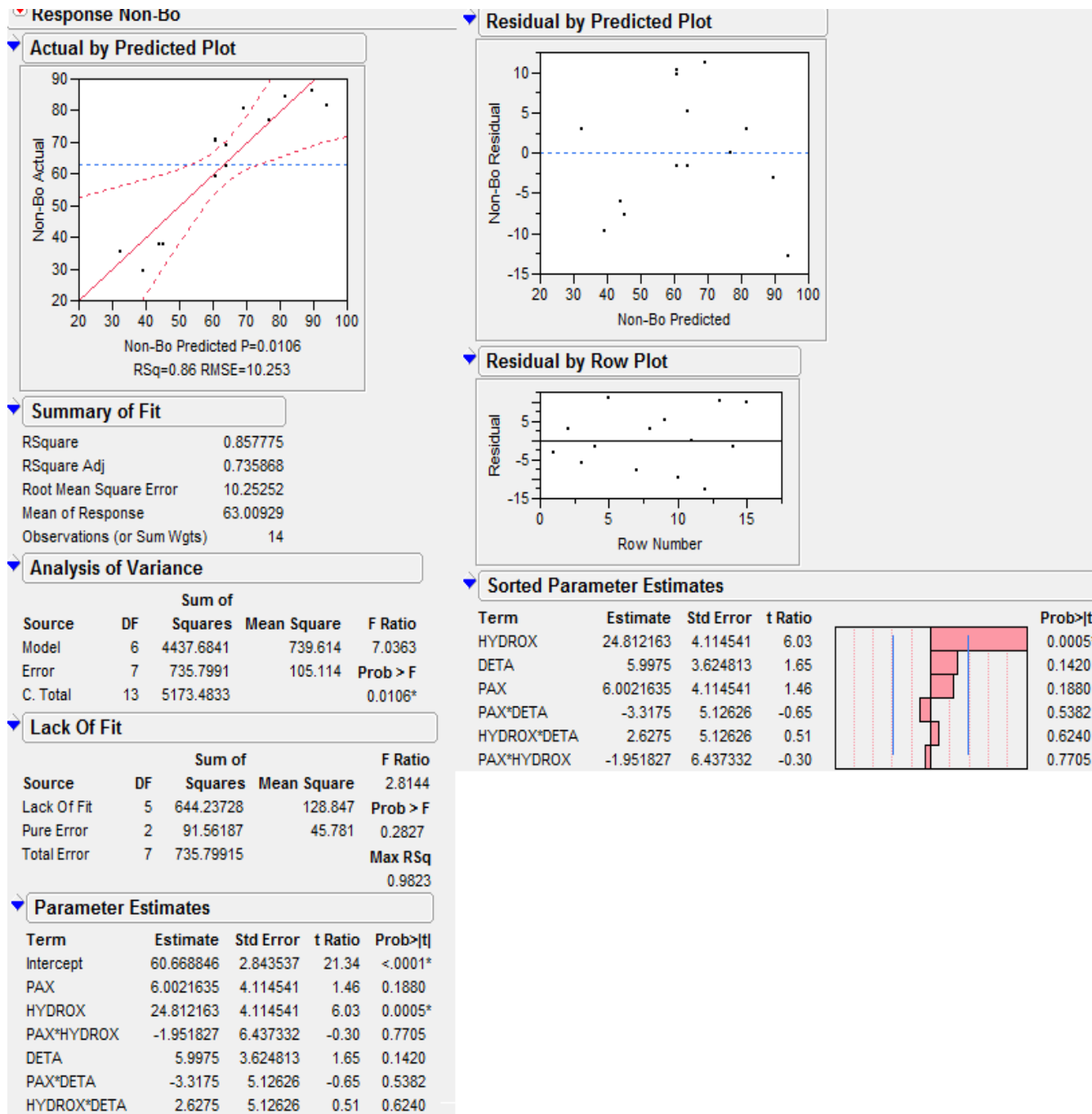


Figure D.7 : JMP output for the linear minor copper recovery model.

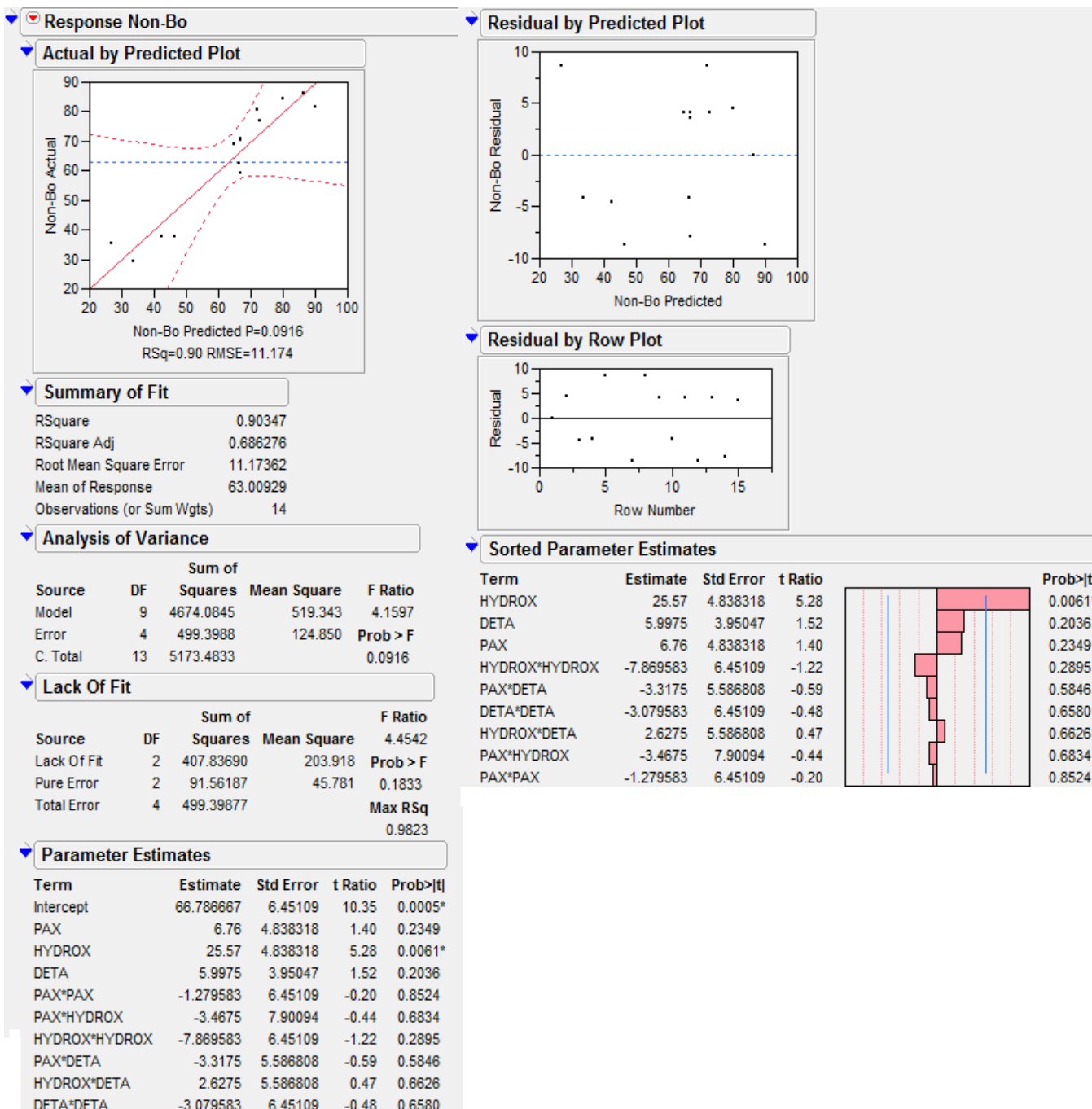


Figure D.8: JMP output for the full quadratic model for minor copper recovery.

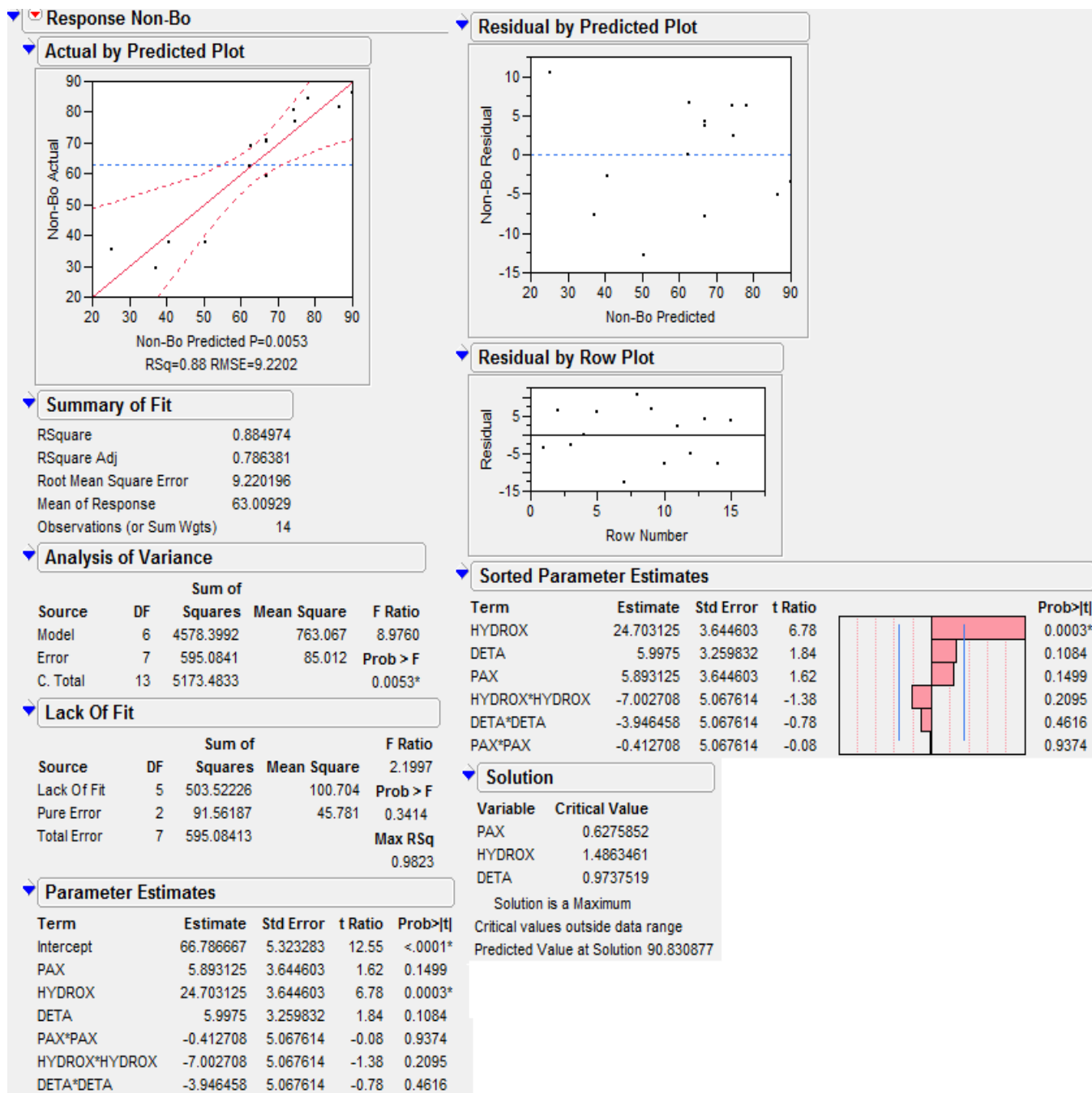


Figure D.9: JMP output for the final minor copper recovery model.

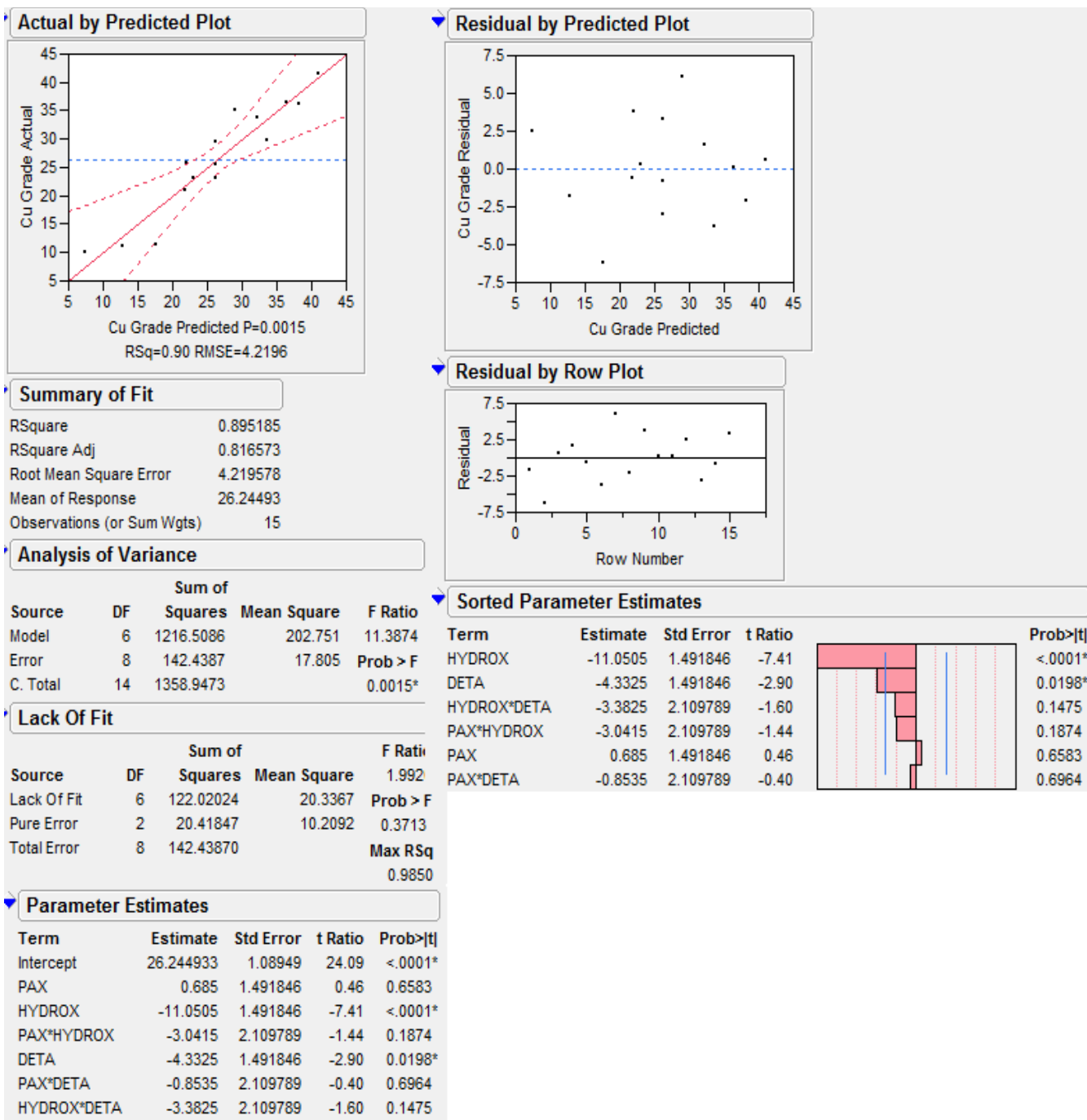


Figure D.10 : JMP output for the linear model of copper recovery.

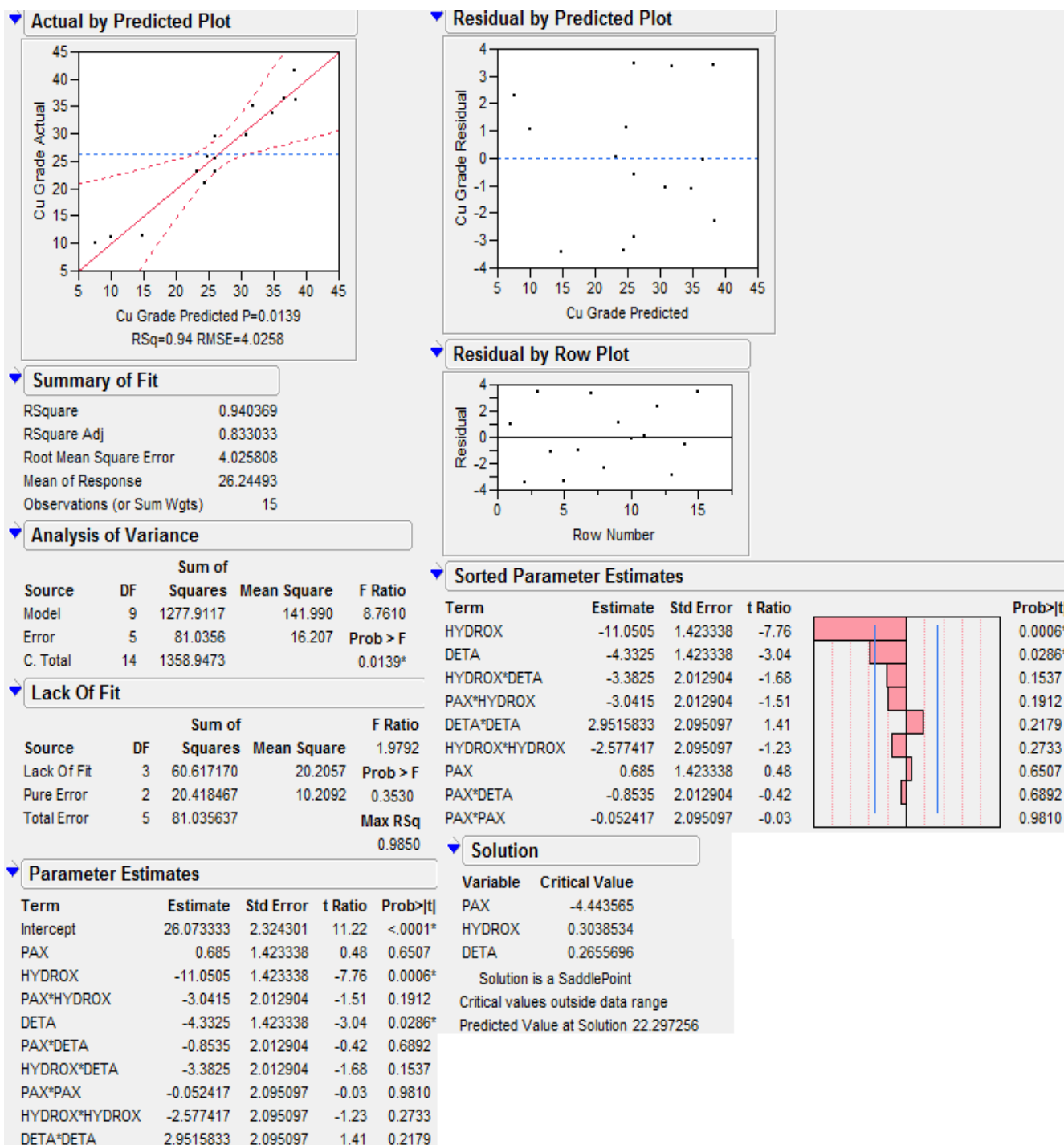


Figure D.11 : JMP output for the full quadratic response surface model for copper recovery.

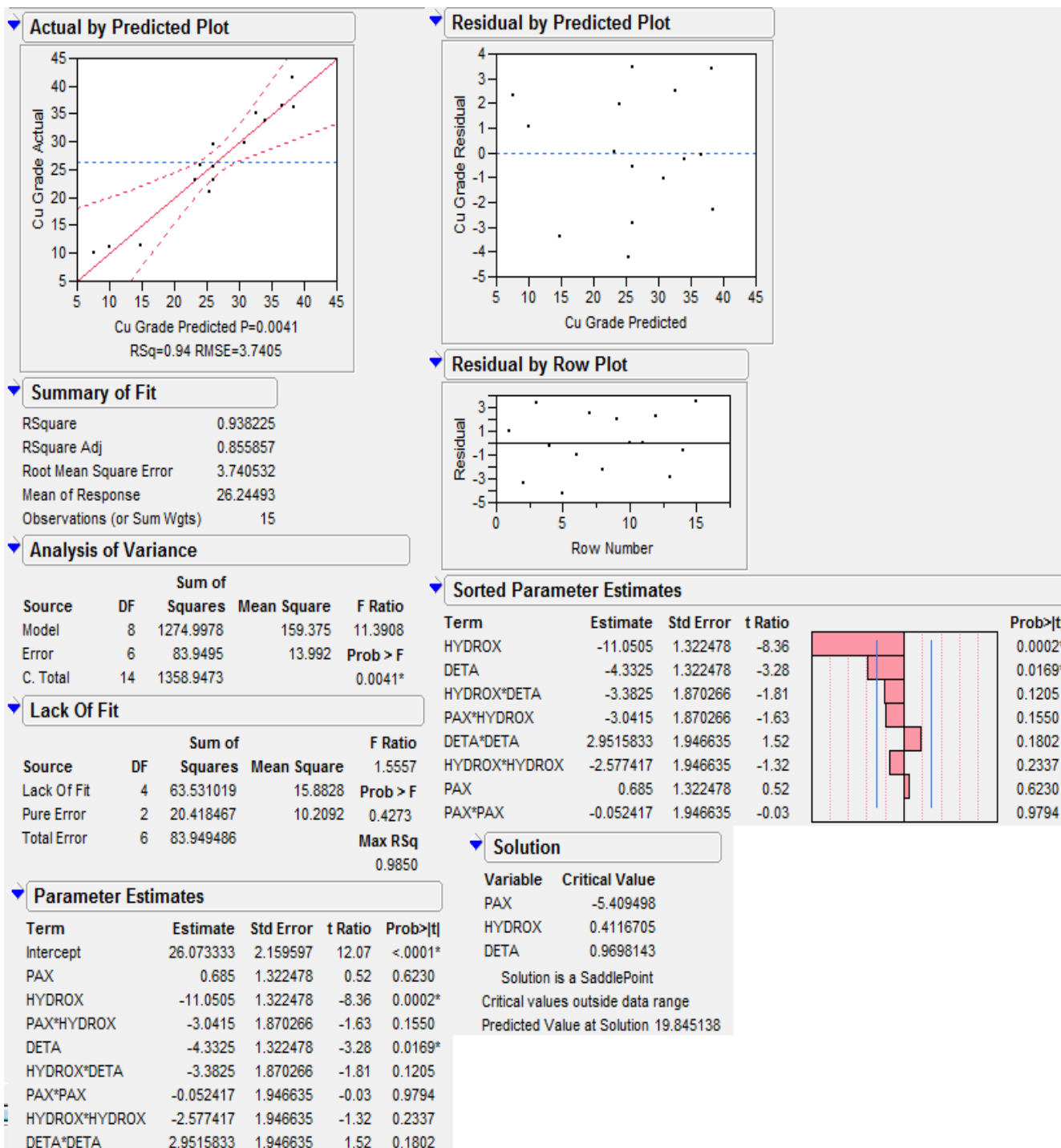


Figure D.12 : JMP output for the final model of copper grade.

Appendix E

Flotation Reports and Results

Table E.1 : Flotation report for T1 of the exploratory work.

TEST	T1							Feed:	Bornite - Malachite ore		
OBJECTIVE:	Exploratory Wor							FLOAT CONDITIONS:	FLOATED BY: SK & MD		
GRINDING CONDITIONS (Denver Mill):								CELL TYPE & VOLUME:	2 L	GAS:	Air
MILL TYPE:	Rod Mill	ROD TYPE/Charge :	As is							IMPELLER RPM:	1200
CHARGE (g):	885g	65 % solids								REPULP WATER:	tap
WATER:	to level (2L)							by air valve			
GRIND:	10 min								# of STROKES: Ro:	30/min	
REAGENTS	ml/g	g/Ton	STAGE	COND	FLOAT	pH	Eh	OBSERVATIONS			
Redox				TIME	TIME			8.05	234		
KAXanthe (0.1 %)	22	24.9	Cond.	2						Rich Froth	
DowFroth250 (0.1%)	22	24.9		0.5							
			Conc. 1		0.5						
KAXanthe (0.1 %)	22	24.9	Cond.	1							
DowFroth250 (0.1%)	22	24.9		0.5							
			Conc. 2		1						
KAXanthe (0.1 %)	22	24.9	Cond.	1							
DowFroth250 (0.1%)	22	24.9		0.5							
			Conc. 3		1.5					Bornite still floating	
KAXanthe (0.1 %)	22	24.9	Cond.	1							
Sodium Silicate	44	50.0									
DowFroth250 (0.1%)	10	14.7		0.5							
			Conc. 4		2						
KAXanthe (0.1 %)	22	24.9	Cond.	1							
Sodium Silicate	44	50.0									
DowFroth250 (0.1%)	0	0.0		0.5							
			Conc. 5		2						
KAXanthe (0.1 %)	22	24.9	Cond.							Mostly slimes coming.	
Sodium Silicate	44	50.0									
DowFroth250 (0.1%)	10	14.7		0.5							
			Conc. 6		3						
KAXanthe (0.1 %)	66	7.4	Cond.	1							
DowFroth250 (0.1%)	0	10.0	14.7	0.5							
			Conc. 7		3						
KAXanthe (0.1 %)	66	7.4	Cond.							Oily yellow colour. Too much xanthate.	
Cytec Hydroxamate	15 drps	170.0									
DowFroth250 (0.1%)	10	14.7		0.5							
			Conc. 8		3						
KAXanthe (0.1 %)	0	0.0	Cond.							Collected mostly slimes	
Cytec Hydroxamate	3	34.0								Froth structure changed	
DowFroth250 (0.1%)	0	0.0		0.5							
			Conc. 9		2						
KAXanthe (0.1 %)	22	24.9	Cond.	1						Malachite starting to respond.	
Cytec Hydroxamate	6	68.0									
DowFroth250 (0.1%)	0	0.0		0.5							
			Conc. 10		3.75						

Table E.2 : Flotation results spreadsheet for T1 of the exploratory work.

AA					UNITS					CUMULATIVE UNITS			
	Cu	Fe	S	C		Cu	Fe	S	C	Cu	Fe	S	C
Conc.1	44.59	10.34				65.49	15.19	31.88	0.69	65.49	15.19	31.88	0.69
Conc.2	35.83	9.18				119.64	30.64	54.76	1.85	185.13	45.83	86.64	2.34
Conc.3	28.86	8.22				55.30	15.74	22.61	1.17	240.43	61.57	109.24	3.50
Conc.4	15.42	7.44				13.87	6.69	3.82	0.84	254.30	68.26	113.07	4.34
Conc.5	10.92	7.02				5.38	3.45	1.04	0.58	259.68	71.71	114.11	4.92
Conc.6	9.57	6.70				5.20	3.64	0.73	0.69	264.88	75.36	114.83	5.61
Conc.7	9.62	5.99				4.52	2.81	0.53	0.63	269.40	78.17	115.36	6.25
Conc.8	8.72	5.92				3.89	2.64	0.35	0.63	273.28	80.81	115.71	6.87
Conc.9	6.44	5.01				4.66	3.63	0.19	0.85	277.95	84.44	115.90	7.72
Conc.10	16.92	4.14				37.74	9.24	1.23	5.04	315.68	93.68	117.13	12.76
Tails	2.27	1.77				198.61	155.14	0.00	42.77	514.30	248.81	117.13	55.54
						514.30	248.81	117.13	55.54				
GRADE	Time (Min)	Wt.(g)	Wt.%	Cu	S	Fe	C		RECOVERIES (%)				
Conc.1	0.50	12.92	1.47	44.59	21.7	10.34	0.468		Cu	S	Fe	C	
Conc.2	1.00	29.37	3.34	35.83	16.4	9.18	0.494		Conc.1	12.73464	27.21322	6.104718	1.237877
Conc.3	1.50	16.85	1.92	28.86	11.8	8.22	0.609		Conc.2	23.26	46.75	12.31	2.37
Conc.4	2.00	7.91	0.90	15.42	4.25	7.44	0.93		Conc.3	10.75	19.30	6.33	2.10
Conc.5	2.00	4.33	0.49	10.92	2.11	7.02	1.18		Conc.4	2.70	3.26	2.69	1.51
Conc.6	3.00	4.78	0.54	9.57	1.34	6.70	1.27		Conc.5	1.05	0.89	1.39	1.05
Conc.7	3.00	4.13	0.47	9.62	1.13	5.99	1.35		Conc.6	1.01	0.62	1.46	1.24
Conc.8	3.00	3.92	0.45	8.72	0.786	5.92	1.41		Conc.7	0.88	0.45	1.13	1.14
Conc.9	2.00	6.37	0.72	6.44	0.259	5.01	1.17		Conc.8	0.76	0.30	1.06	1.13
Conc.10	3.75	19.62	2.23	16.92	0.552	4.14	2.26		Conc.9	0.91	0.16	1.46	1.53
Tails		769.35	87.47	2.27	0	1.77	0.489		Conc.10	7.34	1.05	3.71	9.08
Calc. Head	21.75	879.55	100	5.14	1.17	2.49	0.56		Tails	38.62	0.00	62.35	77.02
									TOTAL	100.00	100.00	100.00	100.00
CUMULATIVE GRADES (%)													
	Cu	S	Fe	C					CUMULATIVE RECOVERIES (%)				
	Wt. (%)	0	0	0					Cu	S	Fe	C	
Conc.1	1.47	44.586	21.700	10.340	0.468				0	0	0	0	
Conc.2	4.81	38.504	18.019	9.532	0.486				Conc.1	12.73	27.21	6.10	1.24
Conc.3	6.72	35.757	16.247	9.157	0.521				Conc.2	36.00	73.97	18.42	4.21
Conc.4	7.62	33.358	14.832	8.954	0.569				Conc.3	46.75	93.27	24.75	6.31
Conc.5	8.12	31.998	14.060	8.837	0.606				Conc.4	49.45	96.53	27.43	7.81
Conc.6	8.66	30.590	13.262	8.703	0.648				Conc.5	50.49	97.41	28.82	8.86
Conc.7	9.13	29.512	12.638	8.563	0.684				Conc.6	51.50	98.04	30.29	10.10
Conc.8	9.57	28.544	12.086	8.440	0.718				Conc.7	52.38	98.49	31.42	11.25
Conc.9	10.30	26.989	11.254	8.199	0.750				Conc.8	53.14	98.79	32.48	12.38
Conc.10	12.53	25.196	9.349	7.477	1.019				Conc.9	54.04	98.95	33.94	13.90
Tails	100.00	5.143	1.171	2.488	0.555				Conc.10	61.38	100.00	37.65	22.98
									Tails	100.00	100.00	100.00	100.00

Table E.3 : Flotation Report for T2 of the exploratory work.

TEST	T2					Feed:	Bornite -Malachite ore		
OBJECTIVE:	Exploratory Wor								
GRINDING CONDITIONS (Denver Mill):				FLOAT CONDITIONS:					
MILL TYPE:	Rod Mill	ROD TYPE/Charge :	As is		CELL TYPE & VOLUME:	2 L	GAS: Air		
CHARGE (g):	885g	65 % solids			IMPELLER RPM:	1200	REPULP WATER: tap by air valve		
WATER:	to level (2L)					# of STROKES: Ro:	30/min		
GRIND:	10 min								
		ml/g	g/Ton	STAGE	COND	FLOAT	pH		
REAGENTS				TIME		TIME	Eh		
Redox						8.05	234		
KAXanthe (0.1 %)	22	24.9	Cond.	2					
DowFroth250 (0.1%)	22	24.9		0.5					
			Conc. 1		0.5				
KAXanthe (0.1 %)	22	24.9	Cond.	1					
DowFroth250 (0.1%)	22	24.9		0.5					
			Conc. 2		1				
KAXanthe (0.1 %)	22	24.9	Cond.	1					
DowFroth250 (0.1%)	22	24.9		0.5					
			Conc. 3		1.5				
KAXanthe (0.1 %)	22	24.9	Cond.	1			Very muddy.		
DowFroth250 (0.1%)	10	14.7		0.5					
			Conc. 4		2				
KAXanthe (0.1 %)	22	24.9	Cond.	1					
Cytec Hydroxamate	3	34.0							
DowFroth250 (0.1%)	0	0.0		0.5					
			Conc. 5		2				
KAXanthe (0.1 %)	0	0.0	Cond.	1					
Cytec Hydroxamate	3	34.0							
DowFroth250 (0.1%)	10	14.7		0.5					
			Conc. 6		2				
KAXanthe (0.1 %)	0	0.0	Cond.	1					
Cytec Hydroxamate	3	34.0							
DowFroth250 (0.1%)	10	14.7	14.7	0.5					
			Conc. 7		3				
KAXanthe (0.1 %)	0	0.0	Cond.	1					
Cytec Hydroxamate	3	34.0							
DowFroth250 (0.1%)	10	14.7		0.5					
			Conc. 8		3				
KAXanthe (0.1 %)	0	0.0	Cond.	1					
Cytec Hydroxamate	3	34.0							
DowFroth250 (0.1%)	0	0.0		0.5					
			Conc. 9		3				
KAXanthe (0.1 %)	0	0.0	Cond.	1					
Cytec Hydroxamate	3	34.0							
DowFroth250 (0.1%)	0	0.0		0.5					
			Conc. 10		3				

Table E.4 : Flotation results spreadsheet for T2 of the exploratory work.

AA		UNITS				CUMULATIVE UNITS				
	Cu	Fe		S	C		Cu	Fe	S	C
(%)	(%)									
Conc.1	44.67	10.69				57.47	13.75	28.30	0.62	
Conc.2	35.97	9.63				86.73	23.22	41.72	1.14	57.47
Conc.3	32.34	8.10				79.24	19.84	34.30	1.42	144.21
Conc.4	20.86	6.52				21.90	6.84	8.25	0.87	223.44
Conc.5	17.57	2.98				37.45	6.36	1.72	6.37	245.34
Conc.6	13.33	3.99				43.84	13.14	0.80	8.22	282.80
Conc.7	8.13	3.53				11.62	5.04	0.38	2.06	326.64
Conc.8	6.10	3.47				14.37	8.17	0.00	2.55	338.26
Conc.9	4.77	3.13				9.50	6.22	0.02	1.69	352.63
Conc.10	4.22	2.55				2.59	1.57	0.18	0.87	362.14
Slimes	5.75	3.79				104.60	69.05	0.00	0.00	364.73
Tails	0.92	1.29				57.57	80.91	0.00	14.94	469.33
						526.90	254.12	115.67	40.75	526.90
RECOVERIES (%)										
GRADE							Cu	S	Fe	C
	Time (Min)	Wt. (g)	Wt.%	Cu	S	Fe	C			
Conc.1	0.50	11.31	1.29	44.67	22	10.69	0.482	Conc.1	10.91	24.47
Conc.2	1.00	21.2	2.41	35.97	17.3	9.63	0.472	Conc.2	16.46	36.07
Conc.3	1.50	215.4	2.45	32.34	14	8.10	0.579	Conc.3	15.04	29.66
Conc.4	2.00	9.23	1.05	20.86	7.86	6.52	0.827	Conc.4	4.16	7.13
Conc.5	2.00	18.74	2.13	17.57	0.806	2.98	2.99	Conc.5	7.11	1.49
Conc.6	2.00	28.91	3.29	13.33	0.243	3.99	2.5	Conc.6	8.32	0.69
Conc.7	3.00	12.56	1.43	8.13	0.263	3.53	1.44	Conc.7	2.20	0.32
Conc.8	3.00	20.72	2.36	6.10	0	3.47	1.08	Conc.8	2.73	0.00
Conc.9	3.00	17.5	1.99	4.77	0.0077	3.13	0.85	Conc.9	1.80	0.01
Conc.10	3.00	5.4	0.61	4.22	0.298	2.55	1.42	Conc.10	0.49	0.16
Slimes		159.99	18.20	5.75	0	3.79	0	Slimes	19.85	0.00
Tails		552.04	62.79	0.92	0.00	1.29	0.238	Tails	10.93	0.00
Calc. Head.	20.50	879.14	100.00	5.27	1.16	2.54	0.41	TOTAL	100.00	100.00
CUMULATIVE RECOVERIES (%)										
CUMULATIVE GRADES (%)							Cu	S	Fe	C
		Cu	S	Fe	C					
	Wt. (%)	0	0	0	0					
Conc.1	1.29	44.675	22.000	10.690	0.482					
Conc.2	3.70	38.996	18.935	9.997	0.475					
Conc.3	6.15	36.344	16.968	9.241	0.517					
Conc.4	7.20	34.085	15.640	8.843	0.562					
Conc.5	9.33	30.312	12.251	7.505	1.117					
Conc.6	12.62	25.887	9.121	6.590	1.477					
Conc.7	14.05	24.081	8.220	6.278	1.473					
Conc.8	16.40	21.497	7.039	5.875	1.417					
Conc.9	18.39	19.688	6.278	5.577	1.356					
Conc.10	19.01	19.188	6.085	5.479	1.358					
Slimes	37.21	12.614	3.109	4.655	0.694					
Tails	100.00	5.269	1.157	2.541	0.408					

Table E.5 : Flotation report for T4 of the preliminary investigations.

TEST	T4										
OBJECTIVE:	Preliminary Investigations				Feed:	Bornite - Malachite ore					
GRINDING CONDITIONS (Denver Mill):				FLOAT CONDITIONS: FLOATED BY: SK & MD							
MILL TYPE:	Rod Mill	ROD TYPE/Charge :	As is		CELL TYPE & VOLUME:		2 L	GAS:	Air		
CHARGE (g):	~680	65 %	solids		IMPELLER RPM:		1200	REPULP WATER:	tap		
WATER:	to level (2L)				by air valve						
GRIND:	12 min					# of STROKES: Ro:	30/min				
		ml/g	g/Ton	STAGE	COND	FLOAT	pH	Eh	OBSERVATIONS		
REAGENTS				TIME	TIME						
Redox							7.85	243			
KAXanthe (0.1 %)	10	14.7	Cond.	2							
Cytec Hydroxamate	2 drps	22.6									
DowFroth250 (0.1%)	10	14.7		0.5							
			Conc. 1		1	7.95					
KAXanthe (0.1 %)	10	14.7	Cond.	1							
Cytec Hydroxamate	2 drps	22.6									
DowFroth250 (0.1%)	5	7.4		0.5							
			Conc. 2		2	8.01					
									Notable change in colour		
KAXanthe (0.1 %)	10	14.7	Cond.	1					Malachite is recovering.		
Cytec Hydroxamate	2 drps	22.6							Too much frother.		
DowFroth250 (0.1%)	5	7.4		0.5							
			Conc. 3		2	8.23					
									Slightly greener with some slimes		
KAXanthe (0.1 %)	5	7.4	Cond.	1					Need more collector		
Cytec Hydroxamate	3 drps	34.0									
DowFroth250 (0.1%)	5	7.4		0.5							
			Conc. 4		3	8.26					
									Green particles.		
KAXanthe (0.1 %)	5	7.4	Cond.	1							
Cytec Hydroxamate	4 drps	45.3									
DowFroth250 (0.1%)	0	0.0		0.5							
			Conc. 5		3						
									Appears to be a lot more to float in		
KAXanthe (0.1 %)	5	7.4	Cond.	1					cell. Higher collector dosages required		
Cytec Hydroxamate	5 drps	56.6									
DowFroth250 (0.1%)	0	0.0		0.5							
			Conc. 6		4				Extremely muddy		
KAXanthe (0.1 %)	5	7.4	Cond.	1					Far too much collector		
Cytec Hydroxamate	15 drps	170.0							Flooding occurs and collecting mainly		
DowFroth250 (0.1%)	0	0.0		0.5					gangue		
			Conc. 7		3						

Table E.6: Flotation results spreadsheet for T4 of the preliminary work.

AA	Cu		Fe		UNITS					CUMULATIVE UNITS						
	(%)	(%)			Cu	Fe	S	C	Bo	Ma	Cu	Fe	S	C	Bo	Ma
Conc.1	44.20	8.81			199.74	39.82	91.29	2.01	226.13	21.24	199.74	39.82	91.29	2.01	226.13	21.24
Conc.2	31.78	7.99			74.90	18.82	27.10	2.38	67.13	25.20	274.65	58.64	118.40	4.39	293.26	46.44
Conc.3	18.89	6.40			20.95	7.10	4.51	1.84	11.18	19.49	295.60	65.74	122.91	6.23	304.43	65.92
Conc.4	15.36	4.80			12.18	3.81	0.63	2.16	1.56	22.91	307.77	69.54	123.54	8.39	305.99	88.83
Conc.5	12.31	2.87			14.46	2.20	0.56	4.38	1.38	46.38	322.24	72.92	124.09	12.77	307.37	135.21
Conc.6	24.03	4.41			69.65	15	0.04	8.29	0.09	87.77	391.89	85.70	124.13	21.06	307.45	222.97
Conc.7	3.66	3.06			92.03	76.80	0.24	14.17	0.61	149.96	483.92	162.51	124.37	35.23	308.06	372.93
Tails	0.92	1.78			57.29	110.32	0.61	13.34	1.51	141.18	541.21	272.82	124.98	48.57	309.57	514.11
					541.21	272.82	124.98	48.57	309.57	514.11	541.21	272.82	124.98	48.57	309.57	514.11
GRADE																
	Time (Min)	Wt. (g)	Wt. (%)	Cu	S	Fe	C	Bo	Ma	RECOVERIES (%)						
Conc.1	1.00	29.59	4.52	44.20	20.2	8.81	0.444	50.03338	4.700006	Cu	S	Fe	C	Bo	Ma	
Conc.2	2.00	15.43	2.36	31.78	11.5	7.99	1.01	28.48435	10.69146	Conc.1	36.91	73.05	14.60	4.13	73.05	4.13
Conc.3	2.00	7.26	1.11	18.89	4.07	6.40	1.66	10.08098	17.5721	Conc.2	13.84	21.69	6.90	4.90	21.69	4.90
Conc.4	2.00	5.19	0.79	15.36	0.793	4.80	2.73	1.964182	28.89869	Conc.3	3.87	3.61	2.60	3.79	3.61	3.79
Conc.5	2.00	7.69	1.17	12.31	0.473	2.87	3.73	1.171574	39.48429	Conc.4	2.25	0.50	1.39	4.46	0.50	4.46
Conc.6	2.00	18.98	2.90	24.03	0.0122	4.41	2.86	0.030218	30.27482	Conc.5	2.67	0.44	1.24	9.02		
Conc.7	2.00	164.45	25.12	3.66	0.00973	3.06	0.564	0.0241	5.970278	Conc.6	12.87	0.03	4.69	17.07	0.03	17.07
Tails		406.13	62.03	0.92	0.00982	1.78	0.22	0.024323	2.275904	Conc.7	17.01	0.20	28.15	29.17	0.20	29.17
Calc. Head	13.00	654.72	100.00	5.41	1.25	2.73	0.49	3.095686	5.141091	Tails	10.59	0.49	40.44	27.46	0.49	27.46
CUMULATIVE GRADES (%)																
		Cu	S	Fe	C					CUMULATIVE RECOVERIES (%)						
	Wt. (%)	0	0	0	0	0	0	0	0	Cu	S	Fe	C	Bo	Ma	
Conc.1	4.52	44.196	20.200	8.811	0.444	50.033	4.700			Conc.1	36.91	73.05	14.60	4.13	73.05	4.13
Conc.2	6.88	39.942	17.218	8.528	0.638	42.648	6.753			Conc.2	50.75	94.73	21.49	9.03	94.73	9.03
Conc.3	7.99	37.019	15.392	8.233	0.780	38.125	8.256			Conc.3	54.62	98.34	24.10	12.82	98.34	12.82
Conc.4	8.78	35.063	14.074	7.923	0.956	34.860	10.120			Conc.4	56.87	98.84	25.49	17.28	98.84	17.28
Conc.5	9.95	32.378	12.469	7.327	1.283	30.884	13.586			Conc.5	59.54	99.29	26.73	26.30	99.29	26.30
Conc.6	12.85	30.434	9.659	6.669	1.639	23.924	17.350			Conc.6	72.41	99.32	31.41	43.37	99.32	43.37
Conc.7	37.97	12.745	3.276	4.280	0.928	8.113	9.822			Conc.7	89.41	99.51	59.56	72.54	99.51	72.54
Tails	100.00	5.412	1.250	2.728	0.486	3.096	5.141			Tails	100.00	100.00	100.00	100.00	100.00	100.00

Table E7 : Flotation report for T5 of the preliminary investigations.

TEST	T5							Feed:	Bornite -Malachite ore		
OBJECTIVE:	Preliminary Investigations							Feed:	Bornite -Malachite ore		
GRINDING CONDITIONS (Denver Mill):				FLOAT CONDITIONS: FLOATED BY: SK & MD							
MILL TYPE:	Rod Mill	ROD TYPE/Charge :	As is			CELL TYPE & VOLUME: 2 L			GAS: Air		
CHARGE (g):	~680	65 % solids				IMPELLER RPM: 1200	REPULP WATER: tap				
WATER:	to level (2L)						by air valve				
GRIND:	12 min				# of STROKES: Ro:	30/min					
	ml/g	g/Ton	STAGE	COND	FLOAT	pH	Eh	OBSERVATIONS			
REAGENTS				TIME	TIME						
Redox						7.84	243				
KAXanthe (0.1 %)	10	14.7	Cond.	2							
Cytec Hydroxamate	2 drps	22.6									
DowFroth250 (0.1%)	10	14.7		0.5							
			Conc. 1		1	7.85					
KAXanthe (0.1 %)	10	14.7	Cond.	1				Slightly greenish. Bornite is completely recovered			
Cytec Hydroxamate	3 drps	34.0									
DowFroth250 (0.1%)	5	7.4		0.5							
			Conc. 2		2	8.01		1 minute is sufficient conditioning			
KAXanthe (0.1 %)	10	14.7	Cond.	1							
Cytec Hydroxamate	4 drps	45.3									
DowFroth250 (0.1%)	0	0.0		0.5							
			Conc. 3		2	8.04					
KAXanthe (0.1 %)	5	7.4	Cond.	1							
Cytec Hydroxamate	5 drps	56.6									
DowFroth250 (0.1%)	0	0.0		0.5							
			Conc. 4		3	8.15		Rich froth. Appears to be too much frother in cell.			
KAXanthe (0.1 %)	5	7.4	Cond.	1							
Cytec Hydroxamate	6 drps	68.0									
DowFroth250 (0.1%)	5	7.4		0.5							
			Conc. 5		3			Flooding occurs at high collector doses...add more often and in smaller doses.			
KAXanthe (0.1 %)	5	7.4	Cond.	1							
Cytec Hydroxamate	8 drps	90.6									
DowFroth250 (0.1%)	0	0.0		0.5							
			Conc. 6		4			Brown froth with slight flooding			
KAXanthe (0.1 %)	5	7.4	Cond.	1							
Cytec Hydroxamate	5 drps	56.6									
DowFroth250 (0.1%)	0	0.0		0.5							
			Conc. 7		3			Similar to conc 7. Not much is left at the end.			
KAXanthe (0.1 %)	5	7.4	Cond.	1							
Cytec Hydroxamate	5 drps	56.6									
DowFroth250 (0.1%)	0	0.0		0.5				need balanced collector dosages			
			Conc. 8		4			c			

Table E.8 : Flotation results spreadsheet for T5 of the preliminary work.

AA	Cu (%)	Fe (%)	UNITS						CUMULATIVE UNITS							
			Cu	Fe	S	C	Bo	Ma	Cu	Fe	S	C	Bo	Ma		
Conc.1	52.24	10.34	258.25	51.11	95.90	2.46	237.53	26.06	258.25	51.11	95.90	2.46	237.53	26.06		
Conc.2	25.23	2.98	73.98	8.75	26.83	5.01	66.44	53.07	332.23	59.86	122.72	7.47	66.44	53.07		
Conc.3	14.07	8.23	23.26	13.61	1.89	5.24	4.67	55.49	355.49	73.47	124.61	12.72	4.67	55.49		
Conc.4	16.14	3.54	37.81	8.30	1.32	6.30	3.27	66.69	393.30	81.77	125.93	19.02	3.27	66.69		
Conc.5	6.55	3.20	36.00	17.57	0.12	7.81	0.30	82.63	429.30	99.34	126.05	26.82	0.30	82.63		
Conc.6	6.48	3.43	22.58	11.96	0.80	3.45	1.98	36.53	451.88	111.31	126.85	30.27	1.98	36.53		
Conc.7	4.69	3.28	19.82	13.88	0.31	2.32	0.77	24.57	471.70	125.19	127.16	32.60	0.77	24.57		
Conc.8	2.67	2.62	14.68	14.42	0.15	2.21	0.36	23.37	486.37	139.60	127.31	34.80	0.36	23.37		
Tails	0.80	1.59	55.25	110.49	1.34	9.72	3.32	102.89	541.62	250.10	128.65	44.52	318.65	471.31		
			541.62	250.10	128.65	44.52	318.65	471.31								
GRADE	Time (Min)	Wt. (g)	Wt.%	Cu	S	Fe	C	Bo	Ma	RECOVERIES (%)						
										Cu	S	Fe	C	Bo	Ma	
Conc.1	1.00	33.03	4.94	52.24	19.4	10.34	0.498	48.05186	5.271629	Conc.1	47.68	74.54	20.43	5.53	74.54	5.53
Conc.2	2.00	19.59	2.93	25.23	9.15	2.98	1.71	22.66364	18.10138	Conc.2	13.66	20.85	3.50	11.26	20.85	11.26
Conc.3	1.50	11.05	1.65	14.07	1.14	8.23	3.17	2.823666	33.55635	Conc.3	4.30	147	5.44	11.77	147	11.77
Conc.4	2.00	15.65	2.34	16.14	0.564	3.54	2.69	1.396972	28.47526	Conc.4	6.98	103	3.32	14.15	103	14.15
Conc.5	3.00	36.73	5.50	6.55	0.0222	3.20	1.42	0.054987	15.03155	Conc.5	6.65	0.09	7.03	17.53	0.09	17.53
Conc.6	4.00	23.27	3.48	6.48	0.23	3.43	0.991	0.569687	10.49033	Conc.6	4.17	0.62	4.78	7.75	0.62	7.75
Conc.7	3.00	28.25	4.23	4.69	0.0731	3.28	0.549	0.181061	5.811494	Conc.7	3.66	0.24	5.55	5.21	0.24	5.21
Conc.8	4.00	36.7	5.49	2.67	0.0267	2.62	0.402	0.066133	4.255411	Conc.8	2.71	0.11	5.76	4.36	0.11	4.36
Tails		463.93	69.43	0.80	0.0193	1.59	0.14	0.047804	1.481984	Tails	10.20	1.04	44.18	21.83	1.04	21.83
Calc. Head	20.50	668.20	100.00	5.42	1.29	2.50	0.445233	3.186462	4.713061	TOTAL	100.00	100.00	100.00	100.00	100.00	100.00
CUMULATIVE GRADES (%)																
	Cu	S	Fe	C						CUMULATIVE RECOVERIES (%)						
	Wt. (%)	0	0	0	0	0	0	0	0	Cu	S	Fe	C			
Conc.1	4.94	52.245	19.400	10.339	0.498	13.442	5.272			Conc.1	47.68	74.54	20.43	5.53	74.54	5.53
Conc.2	7.87	42.189	15.584	7.601	0.949	0.593	6.739			Conc.2	61.34	95.39	23.93	16.79	95.39	16.79
Conc.3	9.53	37.308	13.077	7.710	1.335	0.343	5.824			Conc.3	65.64	96.86	29.38	28.56	96.86	28.56
Conc.4	11.87	33.132	10.608	6.888	1.602	0.025	5.618			Conc.4	72.62	97.89	32.70	42.71	97.89	42.71
Conc.5	17.37	24.719	7.258	5.720	1.544	0.114	4.758			Conc.5	79.26	97.98	39.72	60.24	97.98	60.24
Conc.6	20.85	21.673	6.084	5.338	1.452	0.037	1.752			Conc.6	83.43	98.60	44.50	68.00	98.60	68.00
Conc.7	25.08	18.809	5.071	4.992	1.300	0.014	0.980			Conc.7	87.09	98.84	50.06	73.21	98.84	73.21
Conc.8	30.57	15.910	4.164	4.567	1.138	10.423	0.785			Conc.8	89.80	98.96	55.82	78.17	98.96	78.17
Tails	100.00	5.416	1.286	2.501	0.445	3.186	4.713			Tails	100.00	100.00	100.00	100.00	100.00	100.00

Table E.9: Flotation report for T6 of the preliminary investigations.

TEST	T6								Feed:	Bornite -Malachite ore		
OBJECTIVE:	Preliminary Investigations								Feed:	Bornite -Malachite ore		
GRINDING CONDITIONS (Denver Mill):					FLOAT CONDITIONS:	FLOATED BY: SK & MD						
MILL TYPE:	Rod Mill	ROD TYPE/Charge :	As is		CELL TYPE & VOLUME:	2 L	GAS:	Air				
CHARGE (g):	-680	65 % solids			IMPELLER RPM:	1200	REPULP WATER:	tap				
WATER:	to level (2L)					by air valve						
GRIND:	12 min					# of STROKES: Ro:	30/min					
		ml/g	g/Ton	STAGE	COND	FLOAT	pH	Eh	OBSERVATIONS			
REAGENTS					TIME	TIME						
Redox							7.77	254				
KAXanthe (0.1 %)	5	7.4	Cond.		2							
Cytec Hydroxamate	1 drps	11.3										
DowFroth250 (0.1%)	10	15.0			0.5							
					Conc. 1		1	7.8				
KAXanthe (0.1 %)	5	7.4	Cond.		1							
Cytec Hydroxamate	2 drps	22.6				1.5						
DowFroth250 (0.1%)	5	7.4			0.5							
					Conc. 2		2	8.13				
KAXanthe (0.1 %)	5	7.4	Cond.		1							
Cytec Hydroxamate	2 drps	22.6				1.5						
DowFroth250 (0.1%)	0	0.0			0.5							
					Conc. 3		2	8.25				
KAXanthe (0.1 %)	2.5	3.7	Cond.		1							
Cytec Hydroxamate	3 drps	34.0				2						
DowFroth250 (0.1%)	0	0.0			0.5							
					Conc. 4		3	8.12				
KAXanthe (0.1 %)	2.5	3.7	Cond.		1							
Cytec Hydroxamate	4 drps	45.3										
DowFroth250 (0.1%)	5	7.4			0.5							
					Conc. 5		3					
KAXanthe (0.1 %)	2.5	3.7	Cond.		1							
Cytec Hydroxamate	4 drps	45.3				3						
DowFroth250 (0.1%)	0	0.0			0.5							
					Conc. 6		4	8.29				
KAXanthe (0.1 %)	2.5	3.7	Cond.		1							
Cytec Hydroxamate	3 drps	34.0				4						
DowFroth250 (0.1%)	0	0.0			0.5							
					Conc. 7		3					
KAXanthe (0.1 %)	2.5	3.7	Cond.		1							
Cytec Hydroxamate	3 drps	34.0										
DowFroth250 (0.1%)	0	0.0			0.5							
					Conc. 8		4	8.26	233			

Table E.10 : Flotation results spreadsheet for T6 of the preliminary investigations.

AA	Cu (%)		Fe (%)		UNITS						CUMULATIVE UNITS							
	Cu (%)	Fe (%)	Cu	Fe	S	C	Bo	Ma	Cu	Fe	S	C	Bo	Ma				
Conc.1	49.17	23.49			162.33	79.16	74.47	0.48	184.46	5.10		162.33	79.16	74.47	0.48	184.46	5.10	
Conc.2	36.80	21.31			105.84	61.28	37.68	1.19	93.33	12.57		268.18	140.44	112.15	1.67	277.79	17.68	
Conc.3	20.37	15.24			17.70	13.24	5.88	0.77	14.57	8.13		285.88	153.68	118.04	2.44	292.36	25.81	
Conc.4	14.77	11.85			7.35	5.90	0.92	0.84	2.28	8.86		293.23	159.58	118.96	3.27	294.64	34.67	
Conc.5	13.05	3.86			13.70	4.05	1.15	2.19	2.86	23.23		306.93	163.63	120.11	5.47	297.50	57.89	
Conc.6	13.32	3.84			11.81	3.40	0.56	2.21	1.39	23.38		318.75	167.03	120.67	7.68	298.89	81.27	
Conc.7	9.66	4.33			6.26	2.80	0.38	1.77	0.94	18.72		325.00	169.84	121.05	9.45	299.83	99.99	
Conc.8	9.32	3.89			5.48	2.28	0.27	1.08	0.67	11.45		330.48	172.12	121.32	10.53	300.50	111.44	
Tails	1.89	1.77			168.77	157.49	0.77	18.65	1.90	197.38		499.25	329.62	122.09	29.17	302.40	308.82	
					499.25	329.62	122.09	29.17	302.40	308.82								
GRADE	Time (Min)	Wt. (g)	Wt.%	Cu	S	Fe	C	Bo	Ma	RECOVERIES (%)								
Conc.1	1.00	22.53	3.37	48.17	22.1	23.49	0.143	54.73949	1513741	Conc.1	32.52	24.02	24.02	0.24	61.00	0.24		
Conc.2	1.50	19.23	2.88	36.80	13.1	21.31	0.413	32.44739	4.371853	Conc.2	21.20	18.59	18.59	0.60	30.86	0.60		
Conc.3	1.50	5.81	0.87	20.37	6.77	15.24	0.884	16.76861	9.35767	Conc.3	3.55	4.02	4.02	0.39	4.82	0.39		
Conc.4	2.00	3.33	0.50	14.77	1.85	11.85	1.68	4.582265	17.78381	Conc.4	1.47	1.79	1.79	0.42	0.75	0.42		
Conc.5	3.00	7.02	1.05	13.05	1.1	3.86	2.09	2.72459	22.1239	Conc.5	2.74	1.23	1.23	1.11	0.95	1.11		
Conc.6	3.00	5.93	0.89	13.32	0.631	3.84	2.49	15.62924	26.35814	Conc.6	2.37	1.03	1.03	1.12	0.46	1.12		
Conc.7	4.00	4.33	0.65	9.66	0.585	4.33	2.73	14.48987	28.89869	Conc.7	1.25	0.85	0.85	0.90	0.31	0.90		
Conc.8	4.00	3.93	0.59	9.32	0.458	3.89	1.84	11.3442	19.4775	Conc.8	1.10	0.69	0.69	0.55	0.22	0.55		
Tails		596.47	89.21	1.89	0.00861	1.77	0.209	0.021326	2.21239	Tails	33.80	47.78	47.78	94.66	0.63	94.66		
Calc. Head	20.00	668.58	100.00	4.99	1.22	3.30	0.29	3.023985	3.088156	TOTAL	100.00	100.00	100.00	100.00	100.00	100.00		
CUMULATIVE GRADES (%)		Cu	S	Fe	C	CUMULATIVE RECOVERIES (%)						Cu	S	Fe	C			
Wt. (%)	0	0	0	0	0	0	0	0	0	0	0	0	0	0	0			
Conc.1	3.37	48.172	22.100	23.490	0.143	82.434	1.514					Conc.1	32.52	24.02	24.02	0.24	61.00	0.24
Conc.2	6.25	42.935	17.956	22.484	0.267	46.807	2.830					Conc.2	53.72	42.61	42.61	0.85	91.86	0.85
Conc.3	7.12	40.179	16.589	21.599	0.343	41.411	3.627					Conc.3	57.26	46.62	46.62	1.24	96.68	1.24
Conc.4	7.61	38.517	15.625	20.961	0.430	39.078	4.553					Conc.4	58.73	48.41	48.41	1.66	97.44	1.66
Conc.5	8.66	35.430	13.885	18.888	0.631	34.501	6.683					Conc.5	61.48	49.64	49.64	2.78	98.38	2.78
Conc.6	9.55	33.376	12.636	17.490	0.804	31.395	8.510					Conc.6	63.85	50.68	50.68	3.90	98.84	3.90
Conc.7	10.20	31.870	11.870	16.654	0.926	29.467	9.805					Conc.7	65.10	51.53	51.53	4.80	99.15	4.80
Conc.8	10.79	30.641	11.248	15.958	0.976	28.037	10.332					Conc.8	66.20	52.22	52.22	5.34	99.37	5.34
Tails	100.00	4.992	1.221	3.296	0.292	3.024	3.088					Tails	100.00	100.00	100.00	100.00	100.00	100.00

Table E.11: Flotation report for T7 of the preliminary investigations.

TEST	T7								
OBJECTIVE:	Preliminary Investigations				Feed:		Bornite -Malachite ore		
GRINDING CONDITIONS (Denver Mill):				FLOAT CONDITIONS: FLOATED BY: SK & MD					
MILL TYPE:	Rod Mill	ROD TYPE/Charge :		As is	CELL TYPE & VOLUME:		2 L	GAS: Air	
CHARGE (g):	~680	65 % solids			IMPELLER RPM:		1200	REPULP WATER: tap	
WATER:	to level (2L)				by air valve				
GRIND:	12 min					# of STROKES: Ro:	30/min		
		ml/g	g/Ton	STAGE	COND	FLOAT	pH	Eh	OBSERVATIONS
REAGENTS					TIME	TIME			
Redox							7.84	226	
									Good frothing behaviour
KAXanthe (0.1 %)		18	26.5	Cond.	2				Not pure black because of high malachite activation
Cytec Hydroxamate		16 drps	181.2						
Pine oil		2 drps	2.9		0.5				
				Conc. 1		1	8.23		
									No flooding
KAXanthe (0.1 %)		8	12.0	Cond.	1				
Cytec Hydroxamate		8 drps	90.6						
Pine oil		1 drp	1.5		0.5				
				Conc. 2		2	7.94		
KAXanthe (0.1 %)		6	6.0	Cond.	1				
Cytec Hydroxamate		6 drps	68.0						
Pine oil		1 drp	1.5		0.5				
				Conc. 3		2	8		
									1 inch froth depth
KAXanthe (0.1 %)		4	6.0	Cond.	1				
Cytec Hydroxamate		4 drps	45.3						
Pine oil		1 drp	1.5		0.5				
				Conc. 4		3	8.22		
KAXanthe (0.1 %)		4	6.0	Cond.	1				
Cytec Hydroxamate		3 drps	34.0						
Pine oil		0	0.0		0.5				
				Conc. 5		3			
KAXanthe (0.1 %)		4	6.0	Cond.	1				
Cytec Hydroxamate		3 drps	34.0						
Pine oil		1 drp	1.5		0.5				
				Conc. 6		4	8.46	172	

Table E.12 : Flotation results spreadsheet for T7 of the preliminary testing.

AA	Cu	Fe	UNITS						CUMULATIVE UNITS							
	(%)	(%)	Cu	Fe	S	C	Bo	Ma	Cu	Fe	S	C	Bo	Ma		
Conc.1	28.23	7.37	345.02	90.07	100.33	16.38	248.51	173.34	345.02	90.07	100.33	16.38	248.51	173.34		
Conc.2	7.77	3.52	122.09	55.23	22.46	13.46	55.62	142.46	467.11	145.31	122.79	29.83	304.13	315.80		
Conc.3	4.03	2.42	43.70	26.26	4.32	5.63	10.69	59.57	510.81	171.57	127.10	35.46	314.82	375.37		
Conc.4	2.97	2.22	21.87	16.32	0.88	2.72	2.19	28.81	532.68	187.89	127.98	38.18	317.00	404.18		
Conc.5	2.39	2.04	9.93	8.46	0.16	1.37	0.41	14.51	542.61	196.35	128.15	39.55	317.41	418.69		
Conc.6	1.29	1.47	5.79	6.62	0.26	1.46	0.64	15.43	548.40	202.97	128.41	41.01	318.05	434.11		
Tails	0.90	1.79	40.51	81.08	0.06	11.13	0.15	117.77	588.91	284.05	128.47	52.14	318.20	551.89		
			588.91	284.05	128.47	52.14	318.20	551.89								
<hr/>																
GRADE																
Time (Min)	Wt. (g)	Wt.%	Cu	S	Fe	C	Bo	Ma	RECOVERIES (%)							
Conc.1	1.00	81.05	12.22	28.23	8.21	7.37	1.34	20.3353	14.1847	Conc.1	58.59	78.10	31.71	31.41	78.10	31.41
Conc.2	1.50	104.15	15.70	7.77	1.43	3.52	0.857	3.54197	9.07186	Conc.2	20.73	17.48	19.45	25.81	17.48	25.81
Conc.3	1.50	71.91	10.84	4.03	0.398	2.42	0.519	0.98581	5.49393	Conc.3	7.42	3.36	9.25	10.79	3.36	10.79
Conc.4	2.00	48.78	7.35	2.97	0.12	2.22	0.37	0.29723	3.91667	Conc.4	3.71	0.69	5.75	5.22	0.69	5.22
Conc.5	3.00	27.55	4.15	2.39	0.0395	2.04	0.33	0.09784	3.49325	Conc.5	1.69	0.13	2.98	2.63	0.13	2.63
Conc.6	3.00	29.83	4.50	1.29	0.0577	1.47	0.324	0.14292	3.42973	Conc.6	0.98	0.20	2.33	2.80	0.20	2.80
Tails	4.00	299.96	45.23	0.90	0.00132	1.79	0.25	0.00327	2.60406	Tails	6.88	0.05	28.54	21.34	0.05	21.34
Calc. Head	16.00	663.23	100.00	5.89	1.28	2.84	0.52136	3.18201	5.51888	TOTAL	100.00	100.00	100.00	100.00	100.00	100.00
<hr/>																
CUMULATIVE GRADES (%)																
	Cu	S	Fe	C							CUMULATIVE RECOVERIES (%)					
Wt. (%)	0	0	0	0	0	0	0	0	0	0	0	0	0	0	0	0
Conc.1	12.22	28.233	8.210	7.371	1.340	20.335	14.185	Conc.1	58.59	78.10	31.71	31.41	78.10	31.41		
Conc.2	27.92	16.728	4.397	5.204	1.068	10.891	11.309	Conc.2	79.32	95.58	51.15	57.22	95.58	57.22		
Conc.3	38.77	13.177	3.279	4.426	0.915	8.121	9.683	Conc.3	86.74	98.94	60.40	68.02	98.94	68.02		
Conc.4	46.12	11.550	2.775	4.074	0.828	6.873	8.763	Conc.4	90.45	99.62	66.15	73.24	99.62	73.24		
Conc.5	50.28	10.793	2.549	3.905	0.787	6.313	8.328	Conc.5	92.14	99.75	69.12	75.86	99.75	75.86		
Conc.6	54.77	10.012	2.344	3.706	0.749	5.807	7.926	Conc.6	93.12	99.95	71.46	78.66	99.95	78.66		
Tails	100.00	5.889	1.285	2.841	0.521	3.182	5.519	Tails	100.00	100.00	100.00	100.00	100.00	100.00		

Table E.13: Flotation report for T8 of the preliminary investigations.

TEST	T8								Feed:	Bornite -Malachite ore
OBJECTIVE:	Preliminary Investigations									
GRINDING CONDITIONS (Denver Mill):						FLOAT CONDITIONS:		FLOATED BY: SK & MD		
MILL TYPE:	Rod Mill	ROD TYPE/Charge :	As is		CELL TYPE & VOLUME:		2 L	GAS:	Air	
CHARGE (g):	~680	65 %	solids		IMPELLER RPM:		1200	REPULP WATER:	tap by air valve	
WATER:	to level (2L)					# of STROKES: Ro:		30/min		
GRIND:	12 min					OBSERVATIONS				
REAGENTS		ml/g	g/Ton	STAGE	COND	FLOAT	pH	Eh		
Redox					TIME	TIME			7.82	177
KAXanthe (0.1 %)	12	18.0	Cond.	2					Thick,black froth that grows barren towards the end of the float time.	
Cytec Hydroxamate	8 drps	90.6								
Pine oil	1 drp	1.5		0.5						
			Conc. 1			1			Greener froth, but bornite particles still visible	
KAXanthe (0.1 %)	10	14.7	Cond.	1						
Cytec Hydroxamate	6 drps	68.0								
Pine oil	1 drp	1.5		0.5						
			Conc. 2			2				
DETA (0.5%)	5	36.8							Dark froth. DETA cause a decrease in bubble size	
KAXanthe (0.1 %)	8	12.0	Cond.	1						
Cytec Hydroxamate	6 drps	68.0							Green.	
Pine oil	1 drp	1.5		0.5						
			Conc. 3			2				
DETA (0.5%)	6	37							Smaller bubbles with lots of coalition	
KAXanthe (0.1 %)	6	9.0	Cond.	1						
Cytec Hydroxamate	6 drps	68.0							Low air flow due to initial flooding behaviour	
Pine oil	1 drp	1.5		0.5						
			Conc. 4			3				
DETA (0.5%)	0	0							Not much recovered.	
KAXanthe (0.1 %)	4	6.0	Cond.	1						
Cytec Hydroxamate	3 drps	34.0								
Pine oil	0	0.0		0.5						
			Conc. 5			3	9.7			
DETA (0.5%)	2.5	18.4							White froth. Not much material left to recover.	
KAXanthe (0.1 %)	4	6.0	Cond.	1						
Cytec Hydroxamate	6 drps	68.0								
Pine oil	1 drp	1.5		0.5						
			Conc. 6			4	9.37			

Table E.14: Flotation results spreadsheet for T8 of the preliminary testing.

AA		UNITS						CUMULATIVE UNITS							
	Cu (%)	Fe (%)	Cu	Fe	S	C	Bo	Ma	Cu	Fe	S	C	Bo	Ma	
Conc.1	37.11	8.44	144.97	32.97	70.71	3.59	175.14	38.00	144.97	32.97	70.71	3.59	175.14	38.00	
Conc.2	17.63	4.70	101.39	27.06	39.69	11.33	98.31	119.96	246.36	60.03	110.40	14.92	273.45	157.96	
Conc.3	11.60	4.33	89.14	33.28	8.76	9.46	21.71	100.10	335.50	93.31	119.16	24.38	295.16	258.06	
Conc.4	6.04	3.08	50.06	25.50	3.28	6.83	8.13	72.30	385.56	118.81	122.45	31.21	303.29	330.36	
Conc.5	2.69	2.82	12.42	13.02	0.28	2.31	0.70	24.47	397.98	131.83	122.73	33.52	303.99	354.83	
Conc.6	1.60	2.05	6.85	8.78	0.04	2.46	0.10	26.00	404.83	140.61	122.77	35.98	304.08	380.84	
Tails	0.75	1.60	48.85	104.59	0.03	11.98	0.08	126.81	453.68	245.20	122.80	47.96	304.16	507.65	
			453.68	245.20	122.80	47.96	304.16	507.65							
GRADE		RECOVERIES (%)						CUMULATIVE RECOVERIES (%)							
Time (Min)	Wt. (g)	Wt.%	Cu	S	Fe	C	Bo	Ma	Cu	S	Fe	C	Bo	Ma	
Conc.1	1.00	25.86	3.91	37.11	18.1	8.44	0.919	44.8319	9.72817	31.95	57.58	13.45	7.49	57.58	7.49
Conc.2	2.00	38.08	5.75	17.63	6.9	4.70	1.97	17.0906	20.8536	22.35	32.32	11.04	23.63	32.32	23.63
Conc.3	2.00	50.89	7.69	11.60	1.14	4.33	1.23	2.82367	13.0203	19.65	7.14	13.57	19.72	7.14	19.72
Conc.4	3.00	54.87	8.29	6.04	0.396	3.08	0.824	0.98085	8.72253	11.03	2.67	10.40	14.24	2.67	14.24
Conc.5	2.00	30.61	4.62	2.69	0.0609	2.82	0.5	0.15084	5.2928	2.74	0.23	5.31	4.82	0.23	4.82
Conc.6	3.00	28.33	4.28	1.60	0.00919	2.05	0.574	0.02276	6.07613	1.51	0.03	3.58	5.12	0.03	5.12
Tails	0.00	433.33	65.46	0.75	0.0005	1.60	0.18	0.00124	1.93716	10.77	0.03	42.66	24.98	0.03	24.98
Calc. Head	13.00	661.97	100.00	4.54	1.23	2.45	0.47956	3.04164	5.07646	TOTAL	100.00	100.00	100.00	100.00	100.00
CUMULATIVE GRADES (%)		CUMULATIVE RECOVERIES (%)						CUMULATIVE RECOVERIES (%)							
	Wt. (%)	Cu	S	Fe	C			Cu	S	Fe	C				
Conc.1	3.91	37.109	18.100	8.439	0.919	44.832	9.728	0	0	0	0	0	0		
Conc.2	9.66	25.506	11.430	6.215	1.545	28.310	16.354	Conc.1	31.95	57.58	13.45	7.49	57.58	7.49	
Conc.3	17.35	19.341	6.870	5.379	1.405	17.015	14.877	Conc.2	54.30	89.90	24.48	31.12	89.90	31.12	
Conc.4	25.64	15.040	4.776	4.635	1.217	11.831	12.887	Conc.3	73.95	97.04	38.05	50.83	97.04	50.83	
Conc.5	30.26	13.152	4.056	4.357	1.108	10.046	11.726	Conc.4	84.98	99.71	48.45	65.08	99.71	65.08	
Conc.6	34.54	11.721	3.554	4.071	1.042	8.804	11.026	Conc.5	87.72	99.94	53.76	69.90	99.94	69.90	
Tails	100.00	4.537	1.228	2.452	0.480	3.042	5.076	Conc.6	89.23	99.97	57.34	75.02	99.97	75.02	
								Tails	100.00	100.00	100.00	100.00	100.00	100.00	

Table E.15: Flotation report for B1 of the Box-Behnken.

TEST	B1									
OBJECTIVE:	Box-Behnken Experiments				Feed:		Bornite -Malachite ore			
GRINDING CONDITIONS (Denver Mill):				FLOAT CONDITIONS: FLOATED BY: SK & MD						
MILL TYPE:	Rod Mill	ROD TYPE/Charge :		As is	CELL TYPE & VOLUME:		2 L	GAS:	Air	
CHARGE (g):	~680	65 % solids			IMPELLER RPM:	1200	REPULP WATER:	tap		
WATER:	to level (2L)						by air valve			
GRIND:	12 min	# of STROKES: Ro:				30/min				
		ml/g	g/Ton	STAGE	COND	FLOAT	pH	Eh	OBSERVATIONS	
REAGENTS				TIME	TIME					
Redox						7.84	270			
DETA (0.1%)	6	9							Very few particles coming	
KAXanthe (0.1 %)	0	0.0	Cond.		2				Black particles, appears to be bornite	
Cytec Hydroxamate	0	0.0								
Pine oil				0.5						
			Conc. 1			1	7.92			
DETA (0.1%)	6	9							Not even slime is collecting	
KAXanthe (0.1 %)	0	0.0	Cond.		1				Likely that collection is only due to	
Cytec Hydroxamate	0	0.0							bornite's self induced flotability	
Pine oil	1			0.5						
			Conc. 2			2	8.03			
DETA (0.1%)	6	9.0							Black particles	
KAXanthe (0.1 %)	0	0.0	Cond.		1					
Cytec Hydroxamate	0	0.0								
Pine oil	1			0.5						
			Conc. 3			2	8.07			
DETA (0.5%)	6	9.0							Few black particles	
KAXanthe (0.1 %)	0	0.0	Cond.		1				Some slimes coming	
Cytec Hydroxamate	0	0.0								
Pine oil	1			0.5						
			Conc. 4			3	8.13			
DETA (0.5%)	6	9.0							Some slimes- brownish	
KAXanthe (0.1 %)	0	0.0	Cond.		1					
Cytec Hydroxamate	0	0.0								
Pine oil	1			0.5						
			Conc. 5			3	8.19			
DETA (0.5%)	6	9.0							Slimes-brownish	
KAXanthe (0.1 %)	0	0.0	Cond.		1				Very little collected	
Cytec Hydroxamate	0	0.0								
Pine oil	0			0.5						
			Conc. 6			4	8.19	249		

Table E.16: Flotation results spreadsheet for B1 of the Box-Behnken experiments.

GRADE		Time (Min)	Wt. (g)	Wt.%	Cu	S	Fe	C	Bo	Ma(C)	(Non Bo) Cu
Conc.1		1.00	2.98	0.45	42.47	23.60	10.45	0.42	58.45	4.44	5.46
Conc.2		2.00	2.66	0.40	35.96	20.60	8.62	0.24	51.02	2.50	3.66
Conc.3		2.00	1.3	0.19	34.90	14.90	9.46	0.72	36.91	7.64	11.53
Conc.4		3.00	1.88	0.28	18.55	9.49	6.19	0.52	23.51	5.46	3.67
Conc.5		2.00	1.61	0.24	24.18	8.28	6.43	0.48	20.509	5.07	11.19
Conc.6		3.00	1.64	0.24	19.29	6.05	6.73	0.68	14.985	7.23	9.81
Tails		0.00	657.37	98.20	4.50	0.86	2.65	0.17	2.122	1.81	3.15
Calc. Head		13.00	669.44	100.00	4.97	1.12	2.75	0.18	2.77	1.87	3.22

UNITS		Cu	S	Fe	C	Bo	Ma(C)	(Non Bo) Cu
18.90		10.51	4.65	0.19	26.0	2.0	2.4	
14.29		8.19	3.43	0.09	20.3	1.0	1.5	
6.78		2.89	1.84	0.14	7.2	1.5	2.2	
5.21		2.67	1.74	0.14	6.6	1.5	1.0	
5.81		1.99	1.55	0.12	4.9	1.2	2.7	
4.73		1.48	1.65	0.17	3.7	1.8	2.4	
441.72		84.15	259.86	16.79	208.4	177.8	309.8	
497.44		111.87	274.71	17.64	277.09	186.73	322.02	

CUMULATIVE GRADES (%)											
	Time (Min)	Wt. (g)	Wt.%	Cu	S	Fe	C	Bo	Ma(C)	(Non Bo) Cu	
Conc.1	1.00	2.98	0.45	42.47	23.60	10.45	0.42	58.45	4.44	5.46	
Conc.2	3.00	5.64	0.84	39.40	22.19	9.59	0.33	54.95	3.52	4.61	
Conc.3	5.00	6.94	1.04	38.56	20.82	9.56	0.41	51.57	4.29	5.91	
Conc.4	8.00	8.82	1.32	34.29	18.41	8.84	0.43	45.59	4.54	5.43	
Conc.5	10.00	10.43	1.56	32.73	16.84	8.47	0.44	41.72	4.62	6.32	
Conc.6	13.00	12.07	1.80	30.91	15.38	8.24	0.47	38.08	4.98	6.79	
Tails	13.00	669.44	100.00	4.97	1.12	2.75	0.18	2.77	1.87	3.22	

CUMULATIVE UNITS											
	Cu	S	Fe	C	Bo	Ma(C)	(Non Bo) Cu				
18.90		10.51	4.65	0.19	26.0	1.97	2.43				
33.19		18.69	8.08	0.28	46.30	2.97	3.88				
39.97		21.58	9.91	0.42	53.46	4.45	6.12				
45.18		24.25	11.65	0.57	60.06	5.99	7.15				
51.00		26.24	13.20	0.68	65.00	7.20	9.85				
55.72		27.72	14.85	0.85	68.67	8.98	12.25				
497.44		111.87	274.71	17.64	277.09	186.73	322.02				

RECOVERIES (%)											
	Time (Min)	Wt. (g)	Wt.%	Cu	S	Fe	C	Bo	Ma(C)	(Non Bo) Cu	
Conc.1	1.00	2.98	0.45	3.80	9.39	1.69	1.06	9.39	1.06	0.75	
Conc.2	2.00	2.66	0.40	2.87	7.32	1.25	0.53	7.32	0.53	0.45	
Conc.3	2.00	1.30	0.19	1.36	2.59	0.67	0.79	2.59	0.79	0.70	
Conc.4	3.00	1.88	0.28	1.05	2.38	0.63	0.82	2.38	0.82	0.32	
Conc.5	2.00	1.61	0.24	1.17	1.78	0.56	0.65	1.78	0.65	0.84	
Conc.6	3.00	1.64	0.24	0.95	1.32	0.60	0.95	1.32	0.95	0.75	
Tails	0.00	657.37	98.20	88.80	75.22	94.59	95.19	75.22	95.19	96.20	
TOTAL	13.00	669.44	100.00	100.00	100.00	100.00	100.00	100.00	100.00	100.00	

CUMULATIVE RECOVERIES (%)											
	Time (Min)	Wt. (g)	Wt.%	Cu	S	Fe	C	Bo	Ma(C)	(Non Bo) Cu	
Conc.1	1.00	2.98	0.45	3.80	9.39	1.69	1.06	9.39	1.06	0.75	
Conc.2	3.00	5.64	0.84	6.67	16.71	2.94	1.59	16.71	1.59	1.21	
Conc.3	5.00	6.94	1.04	8.04	19.29	3.61	2.38	19.29	2.38	1.90	
Conc.4	8.00	8.82	1.32	9.08	21.68	4.24	3.21	21.68	3.21	2.22	
Conc.5	10.00	10.43	1.56	10.25	23.46	4.81	3.86	23.46	3.86	3.06	
Conc.6	13.00	12.07	1.80	11.20	24.78	5.41	4.81	24.78	4.81	3.80	
Tails	13.00	669.44	100.00	100.00	100.00	100.00	100.00	100.00	100.00	100.00	

Table E.17: Flotation report for B2 of the Box-Behnken.

TEST	B2	Box-Behnken Experiments				Feed:	Bornite -Malachite ore		
OBJECTIVE:	Box-Behnken Experiments				FLOAT CONDITIONS:	FLOATED BY: SK & MD			
GRINDING CONDITIONS (Denver Mill):					CELL TYPE & VOLUME:	2 L		GAS:	Air
MILL TYPE:	Rod Mill	ROD TYPE/Charge :	As is		IMPELLER RPM:	1200		REPULP WATER:	tap
CHARGE (g):	~680	65 % solids						by air valve	
WATER:	to level (2L)				# of STROKES: Ro:	30/min			
GRIND:	12 min	ml/g	g/Ton	STAGE	COND	FLOAT	pH	Eh	OBSERVATIONS
REAGENTS				TIME	TIME				
Redox						7.83	190		
DETA (0.1%)	6	9							Very black particles
KAXanthe (0.1 %)	8	12.0	Cond.		2				
Cytec Hydroxamate	0	0.0							
Pine oil	1 drp	1.5			0.5				
			Conc. 1			1	7.97		
DETA (0.1%)	6	9							Froth appears barren after 1 min
KAXanthe (0.1 %)	8	12.0	Cond.		1				Could possible only need 1 min at this stage.
Cytec Hydroxamate	0	0.0							
Pine oil	0				0.5				
			Conc. 2			2	8.17		
DETA (0.1%)	6	9							Still blackish particles coming
KAXanthe (0.1 %)	8	12.0	Cond.		1				Slight greenish hue
Cytec Hydroxamate	0	0.0							Very low recoveries
Pine oil	1 drp	1.5			0.5				As float time is increasing, slimes are coming.
			Conc. 3			2	8.18		
DETA (0.5%)	6	9							Very small mass coming
KAXanthe (0.1 %)	8	12.0	Cond.		1				Froth appears white
Cytec Hydroxamate	0	0.0							
Pine oil	1 drp	1.5			0.5				
			Conc. 4			3			
DETA (0.5%)	6	9							Very pale froth. Slow floating bornite is still coming - likely the middlings.
KAXanthe (0.1 %)	8	12.0	Cond.		1				DETA might not aid with mass rec.
Cytec Hydroxamate	0	0.0							
Pine oil	1 drp	1.5			0.5				
			Conc. 5			3			
DETA (0.5%)	6	9							Very little collected
KAXanthe (0.1 %)	8	12.0	Cond.		1				
Cytec Hydroxamate	0	0.0							
Pine oil	1 drp	1.5			0.5				
			Conc. 6			4	8.2	158	

Table E.18: Flotation results spreadsheet for B2 of the Box-Behnken experiments.

GRADE										UNITS											
	Time (Min)	Wt. (g)	Wt.%	Cu	S	Fe	C	Bo	Ma(C)	(Non Bo) Cu	Cu	S	Fe	C	Bo	Ma(C)	(Non Bo) Cu				
Conc.1	1.00	23.22	3.48	43.32	21.00	9.40	0.47	52.01	4.96	10.39	150.76	73.07	32.70	1.63	181.0	17.3	36.2				
Conc.2	2.00	8.09	1.21	47.99	17.70	10.93	0.49	43.84	5.20	20.23	58.18	21.46	13.25	0.60	53.2	6.3	24.5				
Conc.3	2.00	7.03	1.05	36.31	9.90	9.61	0.78	24.52	8.24	20.78	38.25	10.43	10.13	0.82	25.8	8.7	21.9				
Conc.4	3.00	3.64	0.55	19.07	5.62	6.77	0.76	13.92	7.99	10.25	10.40	3.07	3.69	0.41	7.6	4.4	5.6				
Conc.5	2.00	2.78	0.42	16.09	2.51	6.55	0.92	6.217	9.76	12.16	6.70	1.05	2.73	0.38	2.6	4.1	5.1				
Conc.6	3.00	3.05	0.46	12.68	1.26	5.51	0.78	3.121	8.26	10.70	5.80	0.58	2.52	0.36	1.4	3.8	4.9				
Tails	0.00	619.49	92.84	1.76	0.01	1.36	0.49	0.025	5.19	1.74	163.02	0.93	126.31	45.49	2.3	481.5	161.6				
Calc. Head	13.00	667.30	100.00	4.33	1.11	1.91	0.50	2.74	5.26	2.60	433.11	110.58	191.32	49.69	273.89	525.99	259.71				
CUMULATIVE GRADES (%)										CUMULATIVE UNITS											
	Time (Min)	Wt. (g)	Wt.%	Cu	S	Fe	C	Bo	Ma(C)	(Non Bo) Cu	Cu	S	Fe	C	Bo	Ma(C)	(Non Bo) Cu				
Conc.1	1.00	23.22	3.48	43.32	21.00	9.40	0.47	52.01	4.96	10.39	150.76	73.07	32.70	1.63	181.00	17.28	36.17				
Conc.2	3.00	31.31	4.69	44.53	20.15	9.79	0.47	49.90	5.03	12.94	208.94	94.53	45.95	2.23	234.15	23.58	60.70				
Conc.3	5.00	38.34	5.75	43.02	18.27	9.76	0.53	45.25	5.61	14.38	247.19	104.96	56.07	3.05	259.98	32.26	82.60				
Conc.4	8.00	41.98	6.29	40.95	17.17	9.50	0.55	42.53	5.82	14.02	257.59	108.03	59.76	3.46	267.57	36.62	88.19				
Conc.5	10.00	44.76	6.71	39.40	16.26	9.32	0.57	40.28	6.07	13.90	264.29	109.07	62.49	3.84	270.16	40.68	93.25				
Conc.6	13.00	47.81	7.16	37.70	15.30	9.07	0.59	37.91	6.20	13.70	270.09	109.65	65.01	4.20	271.59	44.46	98.15				
Tails	13.00	667.30	100.00	4.33	1.11	1.91	0.50	2.74	5.26	2.60	433.11	110.58	191.32	49.69	273.89	525.99	259.71				
RECOVERIES (%)										CUMULATIVE RECOVERIES (%)											
	Time (Min)	Wt. (g)	Wt.%	Cu	S	Fe	C	Bo	Ma(C)	(Non Bo) Cu	Time (Min)	Wt. (g)	Wt.%	Cu	S	Fe	C	Bo	Ma(C)	(Non Bo) Cu	
Conc.1	1.00	23.22	3.48	34.81	66.08	17.09	3.28	66.08	3.28	13.93	0	0	0	0	0	0	0	0	0		
Conc.2	2.00	8.09	1.21	13.43	19.41	6.93	1.20	19.41	1.20	9.45	Conc.1	1.00	23.22	3.48	34.81	66.08	17.09	3.28	66.08	3.28	13.93
Conc.3	2.00	7.03	1.05	8.83	9.43	5.29	1.65	9.43	1.65	8.43	Conc.2	3.00	31.31	4.69	48.24	85.49	24.02	4.48	85.49	4.48	23.37
Conc.4	3.00	3.64	0.55	2.40	2.77	1.93	0.83	2.77	0.83	2.15	Conc.3	5.00	38.34	5.75	57.07	94.92	29.31	6.13	94.92	6.13	31.80
Conc.5	2.00	2.78	0.42	1.55	0.95	1.43	0.77	0.95	0.77	1.95	Conc.4	8.00	41.98	6.29	59.47	97.69	31.24	6.96	97.69	6.96	33.96
Conc.6	3.00	3.05	0.46	1.34	0.52	1.32	0.72	0.52	0.72	1.88	Conc.5	10.00	44.76	6.71	61.02	98.64	32.66	7.73	98.64	7.73	35.91
Tails	0.00	619.49	92.84	37.64	0.84	66.02	91.55	0.84	91.55	62.21	Conc.6	13.00	47.81	7.16	62.36	99.16	33.98	8.45	99.16	8.45	37.79
TOTAL	13.00	667.30	100.00	100.00	100.00	100.00	100.00	100.00	100.00	100.00	Tails	13.00	667.30	100.00	100.00	100.00	100.00	100.00	100.00	100.00	

Table E.19: Flotation report for B3 of the Box-Behnken.

TEST	B3								
OBJECTIVE:	Box-Behnken Experiments				Feed:		Bornite -Malachite ore		
GRINDING CONDITIONS (Denver Mill):				FLOAT CONDITIONS: FLOATED BY: SK & MD					
MILL TYPE:	Rod Mill	ROD TYPE/Charge :	As is		CELL TYPE & VOLUME:	2 L	GAS:	Air	
CHARGE (g):	~680	65 % solids			IMPELLER RPM:	1200	REPULP WATER:	tap	
WATER:	to level (2L)						by air valve		
GRIND:	12 min				# of STROKES: Ro:	30/min			
	ml/g	g/Ton	STAGE	COND	FLOAT	pH	Eh	OBSERVATIONS	
REAGENTS				TIME	TIME				
Redox						7.72	286		
DETA (0.1%)	6	9						Very black	
KAXanthe (0.1 %)	0	0.0	Cond.		2				
Cytec Hydroxamate	6 drp	68.0							
Pine oil	1 drp	1.5		0.5					
			Conc. 1			1	7.85		
DETA (0.1%)	6	9							
KAXanthe (0.1 %)	0	0.0	Cond.		1				
Cytec Hydroxamate	6 drp	68.0							
Pine oil	1 drp	1.5		0.5					
			Conc. 2			2	8		
DETA (0.1%)	6	9						Slight flooding behaviour	
KAXanthe (0.1 %)	0	0.0	Cond.		1			Flooding starts in later concentrates	
Cytec Hydroxamate	6 drp	68.0						as gangue begins to be activated	
Pine oil	1 drp	1.5		0.5					
			Conc. 3			2	8.03		
DETA (0.5%)	6	9							
KAXanthe (0.1 %)	0	0.0	Cond.		1				
Cytec Hydroxamate	6 drp	68.0							
Pine oil	1 drp	1.5		0.5					
			Conc. 4			3	8.18		
DETA (0.5%)	6	9							
KAXanthe (0.1 %)	0	0.0	Cond.		1				
Cytec Hydroxamate	6 drp	68.0							
Pine oil	1 drp	1.5		0.5					
			Conc. 5			3	8.15		
DETA (0.5%)	6	9							
KAXanthe (0.1 %)	0	0.0	Cond.		1				
Cytec Hydroxamate	6 drp	68.0							
Pine oil	1 drp	1.5		0.5					
			Conc. 6			4	8.2	168	

Table E.20: Flotation results spreadsheet for B3 of the Box-Behnken experiments.

GRADE									
	Time (Min)	Wt. (g)	Wt.%	Cu	S	Fe	C	Bo	Ma(C) (Non Bo) Cu
Conc.1	1.00	16.27	2.41	49.14	21.1	9.98	0.706	52.26	7.47 16.05
Conc.2	2.00	37.06	5.49	31.61	9.50	8.47	1.62	23.53	17.15 16.71
Conc.3	2.00	32.67	4.84	13.23	3.01	5.35	1.77	7.46	18.74 8.51
Conc.4	3.00	42.92	6.36	9.11	0.55	4.21	1.22	1.37	12.91 8.25
Conc.5	2.00	53.72	7.96	3.48	0.01	2.80	0.74	0.025	7.80 3.46
Conc.6	3.00	73.49	10.89	1.88	0.01	2.55	0.92	0.025	9.76 1.86
Tails	0.00	418.75	62.05	0.82	0.005	1.60	0.30	0.012	3.15 0.81
Calc. Head	13.00	674.88	100.00	5.13	1.22	2.73	0.61	3.01	6.49 3.22

UNITS						
Cu	S	Fe	C	Bo	Ma(C)	(Non Bo-Ma) Cu
118.46	50.87	24.05	1.70	126.0	18.0	38.7
173.59	52.17	46.50	8.90	129.2	94.2	91.8
64.06	14.57	25.91	8.57	36.1	90.7	41.2
57.97	3.51	26.75	7.76	8.7	82.1	52.5
27.70	0.08	22.27	5.87	0.2	62.1	27.6
20.45	0.11	27.80	10.04	0.3	106.3	20.3
50.68	0.31	99.43	18.49	0.8	195.7	50.2
512.89	121.62	272.70	61.32	301.23	649.13	322.18

CUMULATIVE GRADES (%)									
	Time (Min)	Wt. (g)	Wt.%	Cu	S	Fe	C	Bo	Ma(C) (Non Bo) Cu
Conc.1	1.00	16.27	2.41	49.14	21.10	9.98	0.71	52.26	7.47 16.05
Conc.2	3.00	53.33	7.90	36.96	13.04	8.93	1.34	32.30	14.20 16.51
Conc.3	5.00	86.00	12.74	27.95	9.23	7.57	1.50	22.86	15.92 13.47
Conc.4	8.00	128.92	19.10	21.68	6.34	6.45	1.41	15.70	14.92 11.73
Conc.5	10.00	182.64	27.06	16.32	4.48	5.38	1.21	11.09	12.83 9.30
Conc.6	13.00	256.13	37.95	12.18	3.20	4.57	1.13	7.92	11.95 7.17
Tails	13.00	674.88	100.00	5.13	1.22	2.73	0.61	3.01	6.49 3.22

CUMULATIVE UNITS						
Cu	S	Fe	C	Bo	Ma(C)	(Non Bo-Ma) Cu
118.46	50.87	24.05	1.70	125.99	18.02	38.69
292.04	103.04	70.55	10.60	255.21	112.19	130.47
356.11	117.61	96.46	19.17	291.30	202.89	171.69
414.08	121.12	123.21	26.93	300.00	285.02	224.15
441.77	121.20	145.48	32.79	300.19	347.12	251.72
462.22	121.31	173.27	42.83	300.46	453.40	271.99
512.89	121.62	272.70	61.32	301.23	649.13	322.18

RECOVERIES (%)									
	Time (Min)	Wt. (g)	Wt.%	Cu	S	Fe	C	Bo	Ma(C) (Non Bo) Cu
Conc.1	1.00	16.27	2.41	23.10	41.83	8.82	2.78	41.83	2.78 12.01
Conc.2	2.00	37.06	5.49	33.85	42.90	17.05	14.51	42.90	14.51 28.49
Conc.3	2.00	32.67	4.84	12.49	11.98	9.50	13.97	11.98	13.97 12.79
Conc.4	3.00	42.92	6.36	11.30	2.89	9.81	12.65	2.89	12.65 16.28
Conc.5	2.00	53.72	7.96	5.40	0.07	8.17	9.57	0.07	9.57 8.56
Conc.6	3.00	73.49	10.89	3.99	0.09	10.19	16.37	0.09	16.37 6.29
Tails	0.00	418.75	62.05	9.88	0.26	36.46	30.15	0.26	30.15 15.58
TOTAL	13.00	674.88	100.00	100.00	100.00	100.00	100.00	100.00	100.00 100.00

CUMULATIVE RECOVERIES (%)									
	Time (Min)	Wt. (g)	Wt.%	Cu	S	Fe	C	Bo	Ma(C) (Non Bo) Cu
Conc.1	1.00	16.27	2.41	23.10	41.83	8.82	2.78	41.83	2.78 12.01
Conc.2	3.00	53.33	7.90	56.94	84.72	25.87	17.28	84.72	17.28 40.50
Conc.3	5.00	86.00	12.74	69.43	96.70	35.37	31.26	96.70	31.26 53.29
Conc.4	8.00	128.92	19.10	80.73	99.59	45.18	43.91	99.59	43.91 69.57
Conc.5	10.00	182.64	27.06	86.13	99.66	53.35	53.47	99.66	53.47 78.13
Conc.6	13.00	256.13	37.95	90.12	99.74	63.54	69.85	99.74	69.85 84.42
Tails	13.00	674.88	100.00	100.00	100.00	100.00	100.00	100.00	100.00 100.00

Table E.21: Flotation report for B4 of the Box-Behnken experiments.

TEST	B4								Feed:	Bornite -Malachite ore			
OBJECTIVE:	Box-Behnken Experiments							Feed:	Bornite -Malachite ore				
GRINDING CONDITIONS (Denver Mill):						FLOAT CONDITIONS: FLOATED BY: SK & MD							
MILL TYPE:	Rod Mill	ROD TYPE/Charge :	As is		CELL TYPE & VOLUME: 2 L GAS: Air								
CHARGE (g):	~680	65 % solids			IMPELLER RPM:	1200	REPULP WATER:	tap					
WATER:	to level (2L)				by air valve								
GRIND:	12 min					# of STROKES: Ro:	30/min						
	ml/g	g/Ton	STAGE	COND	FLOAT	pH	Eh	OBSERVATIONS					
REAGENTS				TIME	TIME								
Redox						7.8	187						
DETA (0.1%)	6	9						Very black with thick froth					
KAXanthe (0.1 %)	8	12.0	Cond.	2									
Cytec Hydroxamate	6 drp	68.0											
Pine oil	1 drp	1.5		0.5									
			Conc. 1			1	7.86						
DETA (0.1%)	6	9						Can see both malachite and bornite in the froth					
KAXanthe (0.1 %)	8	12.0	Cond.	1									
Cytec Hydroxamate	6 drp	68.0											
Pine oil	1 drp	1.5		0.5									
			Conc. 2			2	8.02						
DETA (0.1%)	6	9						Initial froth was very green.					
KAXanthe (0.1 %)	8	12.0	Cond.	1				Air flow was reduced for the first minute of collection time to limit flooding.					
Cytec Hydroxamate	6 drp	68.0											
Pine oil	1 drp	1.5		0.5									
			Conc. 3			2	8.1						
DETA (0.5%)	6	9						Careful air control required to avoid excessive flooding					
KAXanthe (0.1 %)	8	12.0	Cond.	1				Lots of gangue activation.					
Cytec Hydroxamate	6 drp	68.0											
Pine oil	1 drp	1.5		0.5									
			Conc. 4			3	8.17						
DETA (0.5%)	6	9						High mass recovery.					
KAXanthe (0.1 %)	8	12.0	Cond.	1				No bornite observed- only greenish particles.					
Cytec Hydroxamate	6 drp	68.0											
Pine oil	1 drp	1.5		0.5									
			Conc. 5			3	8.23						
DETA (0.5%)	6	9											
KAXanthe (0.1 %)	8	12.0	Cond.	1									
Cytec Hydroxamate	6 drp	68.0											
Pine oil	1 drp	1.5		0.5									
			Conc. 6			4	8.25						

Table E.22: Flotation results spreadsheet for B4 of the Box-Behnken experiments.

GRADE											UNITS											
	Time (Min)	Wt. (g)	Wt.%	Cu	S	Fe	C	Bo	Ma(C)	(Non Bo) Cu		Cu	S	Fe	C	Bo	Ma(C)	(Non Bo-Ma) Cu				
Conc.1	1.00	20.49	3.04	55.15	21.6	9.06	0.522	53.50	5.53	21.28		167.94	65.77	27.59	1.59	162.9	16.8	64.8				
Conc.2	2.00	36.42	5.41	26.88	8.04	7.03	1.9	19.91	20.11	14.27		145.46	43.51	38.04	10.28	107.8	108.9	77.2				
Conc.3	2.00	38.2	5.68	14.70	1.68	5.00	1.46	4.16	15.45	12.06		83.42	9.54	28.37	8.29	23.6	87.7	68.5				
Conc.4	3.00	58.34	8.67	5.84	0.0916	2.98	0.454	0.23	4.81	5.69		50.60	0.79	25.86	3.94	2.0	41.7	49.4				
Conc.5	2.00	56	8.32	2.71	0.0146	2.57	0.498	0.036	5.27	2.69		22.57	0.12	21.38	4.14	0.3	43.9	22.4				
Conc.6	3.00	55.49	8.25	1.75	0.0194	2.48	0.321	0.048	3.40	1.72		14.46	0.16	20.42	2.65	0.4	28.0	14.2				
Tails	0.00	407.98	60.63	0.77	0.0026	1.46	0.135	0.006	1.43	0.76		46.52	0.16	88.68	8.18	0.4	86.6	46.3				
Calc. Head	13.00	672.92	100.00	5.31	1.20	2.50	0.39	2.97	4.14	3.43		530.97	120.06	250.33	39.07	297.36	413.61	342.71				
CUMULATIVE GRADES (%)											CUMULATIVE UNITS											
	Time (Min)	Wt. (g)	Wt.%	Cu	S	Fe	C	Bo	Ma(C)	(Non Bo) Cu		Cu	S	Fe	C	Bo	Ma(C)	(Non Bo-Ma) Cu				
Conc.1	1.00	20.49	3.04	55.15	21.60	9.06	0.52	53.50	5.53	21.28		167.94	65.77	27.59	1.59	162.91	16.83	64.81				
Conc.2	3.00	56.91	8.46	37.06	12.92	7.76	1.40	32.01	14.86	16.79		313.40	109.29	65.62	11.87	270.69	125.68	142.03				
Conc.3	5.00	95.11	14.13	28.08	8.41	6.65	1.43	20.82	15.10	14.89		396.82	118.82	93.99	20.16	294.31	213.41	210.50				
Conc.4	8.00	153.45	22.80	19.62	5.25	5.26	1.06	12.99	11.19	11.40		447.42	119.62	119.85	24.10	296.28	255.08	259.85				
Conc.5	10.00	209.45	31.13	15.10	3.85	4.54	0.91	9.53	9.60	9.07		469.99	119.74	141.23	28.24	296.58	298.95	282.23				
Conc.6	13.00	264.94	39.37	12.30	3.05	4.11	0.78	7.54	8.30	7.53		484.45	119.90	161.65	30.89	296.97	326.97	296.44				
Tails	13.00	672.92	100.00	5.31	1.20	2.50	0.39	2.97	4.14	3.43		530.97	120.06	250.33	39.07	297.36	413.61	342.71				
RECOVERIES (%)											CUMULATIVE RECOVERIES (%)											
	Time (Min)	Wt. (g)	Wt.%	Cu	S	Fe	C	Bo	Ma(C)	(Non Bo) Cu		Time (Min)	Wt. (g)	Wt.%	Cu	S	Fe	C	Bo	Ma(C)	(Non Bo) Cu	
Conc.1	1.00	20.49	3.04	31.63	54.78	11.02	4.07	54.78	4.07	18.91		0	0	0	0	0	0	0	0	0		
Conc.2	2.00	36.42	5.41	27.40	36.25	15.19	26.32	36.25	26.32	22.53		Conc.1	1.00	20.49	3.04	31.63	54.78	11.02	4.07	54.78	4.07	18.91
Conc.3	2.00	38.2	5.68	15.71	7.94	11.33	21.21	7.94	21.21	19.98		Conc.2	3.00	56.91	8.46	59.02	91.03	26.22	30.39	91.03	30.39	41.44
Conc.4	3.00	58.34	8.67	9.53	0.66	10.33	10.07	0.66	10.07	14.40		Conc.3	5.00	95.11	14.13	74.74	98.97	37.55	51.60	98.97	51.60	61.42
Conc.5	2.00	56.00	8.32	4.25	0.10	8.54	10.61	0.10	10.61	6.53		Conc.4	8.00	153.45	22.80	84.27	99.63	47.88	61.67	99.63	61.67	75.82
Conc.6	3.00	55.49	8.25	2.72	0.13	8.16	6.77	0.13	6.77	4.14		Conc.5	10.00	209.45	31.13	88.52	99.74	56.42	72.28	99.74	72.28	82.35
Tails	0.00	407.98	60.63	8.76	0.13	35.42	20.95	0.13	20.95	13.50		Conc.6	13.00	264.94	39.37	91.24	99.87	64.58	79.05	99.87	79.05	86.50
TOTAL	13.00	672.92	100.00	100.00	100.00	100.00	100.00	100.00	100.00	100.00		Tails	13.00	672.92	100.00	100.00	100.00	100.00	100.00	100.00	100.00	

Table E.23: Flotation report for B5 of the Box-Behnken experiments.

TEST	B5								Feed:	Bornite -Malachite ore		
OBJECTIVE:	Box-Behnken Experiments											
GRINDING CONDITIONS (Denver Mill):					FLOAT CONDITIONS: FLOATED BY: SK & MD							
MILL TYPE:	Rod Mill	ROD TYPE/Charge :	As is		CELL TYPE & VOLUME:			2 L	GAS:	Air		
CHARGE (g):	~680	65 % solids			IMPELLER RPM:	1200		REPULP WATER:	tap			
WATER:	to level (2L)							by air valve				
GRIND:	12 min					# of STROKES: Ro:	30/min					
	ml/g	g/Ton	STAGE	COND	FLOAT	pH	Eh	OBSERVATIONS				
REAGENTS				TIME	TIME							
Redox						7.85	264					
DETA (0.1%)	0	0						Initially froth is very black				
KAXanthe (0.1 %)	0	0.0	Cond.		2			Quickly turns whitish green				
Cytec Hydroxamate	3 drp	34.0										
Pine oil	1 drp	1.5		0.5								
			Conc. 1			1	8.53					
DETA (0.1%)	0	0						More greenish particles coming				
KAXanthe (0.1 %)	0	0.0	Cond.		1			White towards finish				
Cytec Hydroxamate	3 drp	34.0										
Pine oil	1 drp	1.5		0.5								
			Conc. 2			2	8.69					
DETA (0.1%)	0	0						Very pale froth				
KAXanthe (0.1 %)	0	0.0	Cond.		1							
Cytec Hydroxamate	3 drp	34.0										
Pine oil	1 drp	1.5		0.5								
			Conc. 3			2	8.65					
DETA (0.5%)	0	0						Slimes beginning to respond.				
KAXanthe (0.1 %)	0	0.0	Cond.		1							
Cytec Hydroxamate	3 drp	34.0										
Pine oil	1 drp	1.5		0.5								
			Conc. 4			3	8.55					
DETA (0.5%)	0	0										
KAXanthe (0.1 %)	0	0.0	Cond.		1							
Cytec Hydroxamate	3 drp	34.0										
Pine oil	1 drp	1.5		0.5								
			Conc. 5			3	8.56					
DETA (0.5%)	0	0										
KAXanthe (0.1 %)	0	0.0	Cond.		1							
Cytec Hydroxamate	3 drp	34.0										
Pine oil	1 drp	1.5		0.5								
			Conc. 6			4	8.76	260				
									NOTE : pH meter is suspected to be reading high by about 0.5 pH after Conc. 1			

Table E.24: Flotation results spreadsheet for B5 of the Box-Behnken experiments.

GRADE											UNITS									
	Time (Min)	Wt. (g)	Wt.%	Cu	S	Fe	C	Bo	Ma(C)	(Non Bo) Cu	Cu	S	Fe	C	Bo	Ma(C)	(Non Bo-Ma) Cu			
Conc.1	1.00	12.39	1.85	42.72	21.4	8.94	0.352	53.01	3.73	9.17	79.00	39.57	16.53	0.65	98.0	6.9	16.9			
Conc.2	2.00	22.23	3.32	42.80	18.3	10.03	0.44	45.33	4.66	14.10	141.97	60.71	33.27	1.46	150.4	15.5	46.8			
Conc.3	2.00	9.51	1.42	19.75	9.97	7.45	1.07	24.69	11.33	4.12	28.03	14.15	10.57	1.52	35.0	16.1	5.8			
Conc.4	3.00	6.84	1.02	21.90	4.38	6.21	1.25	10.85	13.23	15.03	22.35	4.47	6.34	1.28	11.1	13.5	15.3			
Conc.5	2.00	5.06	0.76	12.48	2.12	4.89	1.97	5.251	20.85	9.15	9.42	1.60	3.70	1.49	4.0	15.7	6.9			
Conc.6	3.00	2.68	0.40	10.76	1.37	4.53	1.53	3.393	16.20	8.61	4.30	0.55	1.81	0.61	1.4	6.5	3.4			
Tails	0.00	611.39	91.24	1.73	0.00539	1.57	0.374	0.013	3.96	1.72	158.10	0.49	142.95	34.12	1.2	361.2	157.3			
Calc. Head	13.00	670.10	100.00	4.43	1.22	2.15	0.41	3.01	4.35	2.53	443.17	121.54	215.17	41.13	301.04	435.36	252.59			
<hr/>																				
CUMULATIVE GRADES (%)										CUMULATIVE UNITS										
Time (Min)	Wt. (g)	Wt.%	Cu	S	Fe	C	Bo	Ma(C)	(Non Bo) Cu	Cu	S	Fe	C	Bo	Ma(C)	(Non Bo-Ma) Cu				
Conc.1	1.00	12.39	1.85	42.72	21.40	8.94	0.35	53.01	3.73	9.17	79.00	39.57	16.53	0.65	98.01	6.89	16.95			
Conc.2	3.00	34.62	5.17	42.77	19.41	9.64	0.41	48.08	4.32	12.33	220.97	100.28	49.80	2.11	248.38	22.34	63.72			
Conc.3	5.00	44.13	6.59	37.81	17.38	9.17	0.55	43.04	5.83	10.56	249.00	114.43	60.37	3.63	283.42	38.42	69.57			
Conc.4	8.00	50.97	7.61	35.67	15.63	8.77	0.64	38.72	6.83	11.16	271.35	118.90	66.71	4.90	294.50	51.92	84.91			
Conc.5	10.00	56.03	8.36	33.58	14.41	8.42	0.76	35.69	8.09	10.98	280.77	120.50	70.41	6.39	298.46	67.67	91.82			
Conc.6	13.00	58.71	8.76	32.54	13.82	8.24	0.80	34.22	8.46	10.87	285.08	121.05	72.22	7.00	299.82	74.15	95.26			
Tails	13.00	670.10	100.00	4.43	1.22	2.15	0.41	3.01	4.35	2.53	443.17	121.54	215.17	41.13	301.04	435.36	252.59			
<hr/>																				
RECOVERIES (%)										CUMULATIVE RECOVERIES (%)										
Time (Min)	Wt. (g)	Wt.%	Cu	S	Fe	C	Bo	Ma(C)	(Non Bo) Cu	Time (Min)	Wt. (g)	Wt.%	Cu	S	Fe	C	Bo	Ma(C)	(Non Bo) Cu	
Conc.1	1.00	12.39	1.85	17.83	32.56	7.68	1.58	32.56	1.58	6.71	0	0	0	0	0	0	0	0	0	
Conc.2	2.00	22.23	3.32	32.03	49.95	15.46	3.55	49.95	3.55	18.52	Conc.1	1.00	12.39	1.85	17.83	32.56	7.68	1.58	32.56	1.58
Conc.3	2.00	9.51	1.42	6.33	11.64	4.91	3.69	11.64	3.69	2.31	Conc.2	3.00	34.62	5.17	49.86	82.51	23.14	5.13	82.51	5.13
Conc.4	3.00	6.84	1.02	5.04	3.68	2.95	3.10	3.68	3.10	6.07	Conc.3	5.00	44.13	6.59	56.19	94.15	28.06	8.82	94.15	8.82
Conc.5	2.00	5.06	0.76	2.13	1.32	1.72	3.62	1.32	3.62	2.74	Conc.4	8.00	50.97	7.61	61.23	97.83	31.00	11.93	97.83	11.93
Conc.6	3.00	2.68	0.40	0.97	0.45	0.84	1.49	0.45	1.49	1.36	Conc.5	10.00	56.03	8.36	63.35	99.14	32.72	15.54	99.14	15.54
Tails	0.00	611.39	91.24	35.67	0.40	66.44	82.97	0.40	82.97	62.29	Conc.6	13.00	58.71	8.76	64.33	99.60	33.56	17.03	99.60	17.03
TOTAL	13.00	670.10	100.00	100.00	100.00	100.00	100.00	100.00	100.00	100.00	Tails	13.00	670.10	100.00	100.00	100.00	100.00	100.00	100.00	

Table E.25: Flotation report for B6 of the Box-Behnken experiments.

TEST	B6															
OBJECTIVE:	Box-Behnken Experiments					Feed:	Bornite -Malachite ore									
GRINDING CONDITIONS (Denver Mill):					FLOAT CONDITIONS: FLOATED BY: SK & MD											
MILL TYPE:	Rod Mill	ROD TYPE/Charge :			As is	CELL TYPE & VOLUME: 2 L GAS: Air										
CHARGE (g):	-680	65 % solids				IMPELLER RPM:	1200	REPULP WATER: tap								
WATER:	to level (2L)					by air valve										
GRIND:	12 min						# of STROKES: Ro:	30/min								
		ml/g	g/Ton	STAGE	COND	FLOAT	pH	Eh	OBSERVATIONS							
REAGENTS					TIME	TIME										
Redox							7.78	350								
DETA (0.1%)	0	0							Black particles							
KAXanthe (0.1 %)	8	12.0	Cond.			2										
Cytec Hydroxamate	3 drp	34.0														
Pine oil	1 drp	1.5			0.5											
			Conc. 1				1	7.79								
DETA (0.1%)	0	0							No flooding observed							
KAXanthe (0.1 %)	8	12.0	Cond.			1										
Cytec Hydroxamate	3 drp	34.0														
Pine oil	1 drp	1.5			0.5											
			Conc. 2				2	7.96								
DETA (0.1%)	0	0														
KAXanthe (0.1 %)	8	12.0	Cond.			1										
Cytec Hydroxamate	3 drp	34.0														
Pine oil	1 drp	1.5			0.5											
			Conc. 3				2	8.04								
DETA (0.5%)	0	0														
KAXanthe (0.1 %)	8	12.0	Cond.			1										
Cytec Hydroxamate	3 drp	34.0														
Pine oil	1 drp	1.5			0.5											
			Conc. 4				3	8.07								
DETA (0.5%)	0	0														
KAXanthe (0.1 %)	8	12.0	Cond.			1										
Cytec Hydroxamate	3 drp	34.0														
Pine oil	1 drp	1.5			0.5											
			Conc. 5				3	8.05								
DETA (0.5%)	0	0														
KAXanthe (0.1 %)	8	12.0	Cond.			1										
Cytec Hydroxamate	3 drp	34.0														
Pine oil	1 drp	1.5			0.5											
			Conc. 6				4	8.12	254							

Table E.26: Flotation results spreadsheet for B6 of the Box-Behnken experiments.

GRADE	Time (Min)	Wt. (g)	Wt.%	Cu	S	Fe	C	Bo	Ma(C)	(Non Bo) Cu
Conc.1	1.00	21.79	3.28	55.66	21.1	10.99	0.355	52.26	3.76	22.57
Conc.2	2.00	19.39	2.92	36.22	12.7	9.40	0.873	31.46	9.24	16.30
Conc.3	2.00	7.22	1.09	18.92	2.94	6.03	2.03	7.28	21.49	14.31
Conc.4	3.00	8.38	1.26	13.39	0.713	4.33	2.67	1.77	28.26	12.27
Conc.5	2.00	6.83	1.03	19.07	0.610	4.93	2.75	1.511	29.11	18.11
Conc.6	3.00	8.02	1.21	15.31	0.326	4.18	2.56	0.807	27.10	14.80
Tails	0.00	593.54	89.23	1.29	0.005	1.50	0.223	0.012	2.36	1.28
Calc. Head	13.00	665.17	100.00	4.78	1.12	2.20	0.35	2.77	3.71	3.03

UNITS	Cu	S	Fe	C	Bo	Ma(C)	(Non Bo-Ma) Cu
	182.33	69.12	36.00	1.16	171.2	12.3	73.9
	105.57	37.02	27.42	2.54	91.7	26.9	47.5
	20.54	3.19	6.55	2.20	7.9	23.3	15.5
	16.87	0.90	5.45	3.36	2.2	35.6	15.5
	19.58	0.63	5.06	2.82	1.6	29.9	18.6
	18.46	0.39	5.04	3.09	1.0	32.7	17.8
	114.67	0.45	134.05	19.90	1.1	210.6	114.0
	478.03	111.70	219.58	35.08	276.66	371.38	302.87

CUMULATIVE GRADES (%)	Time (Min)	Wt. (g)	Wt.%	Cu	S	Fe	C	Bo	Ma(C)	(Non Bo) Cu
Conc.1	1.00	21.79	3.28	55.66	21.10	10.99	0.36	52.26	3.76	22.57
Conc.2	3.00	41.18	6.19	46.50	17.14	10.24	0.60	42.47	6.34	19.62
Conc.3	5.00	48.40	7.28	42.39	15.03	9.62	0.81	37.22	8.60	18.83
Conc.4	8.00	56.78	8.54	38.11	12.91	8.84	1.09	31.99	11.50	17.86
Conc.5	10.00	63.61	9.56	36.07	11.59	8.42	1.27	28.71	13.39	17.89
Conc.6	13.00	71.63	10.77	33.74	10.33	7.94	1.41	25.59	14.93	17.54
Tails	13.00	665.17	100.00	4.78	1.12	2.20	0.35	2.77	3.71	3.03

CUMULATIVE UNITS	Cu	S	Fe	C	Bo	Ma(C)	(Non Bo-Ma) Cu
	182.33	69.12	36.00	1.16	171.20	12.31	73.94
	287.90	106.14	63.42	3.71	262.90	39.25	121.46
	308.44	109.33	69.97	5.91	270.81	62.57	136.99
	325.31	110.23	75.42	9.27	273.03	98.18	152.46
	344.89	110.86	80.48	12.10	274.58	128.07	171.06
	363.35	111.25	85.53	15.19	275.56	160.75	188.90
	478.03	111.70	219.58	35.08	276.66	371.38	302.87

RECOVERIES (%)	Time (Min)	Wt. (g)	Wt.%	Cu	S	Fe	C	Bo	Ma(C)	(Non Bo) Cu
Conc.1	1.00	21.79	3.28	38.14	61.88	16.40	3.31	61.88	3.31	24.41
Conc.2	2.00	19.39	2.92	22.09	33.14	12.49	7.25	33.14	7.25	15.69
Conc.3	2.00	7.22	1.09	4.30	2.86	2.98	6.28	2.86	6.28	5.13
Conc.4	3.00	8.38	1.26	3.53	0.80	2.48	9.59	0.80	9.59	5.11
Conc.5	2.00	6.83	1.03	4.10	0.56	2.31	8.05	0.56	8.05	6.14
Conc.6	3.00	8.02	1.21	3.86	0.35	2.30	8.80	0.35	8.80	5.89
Tails	0.00	593.54	89.23	23.99	0.40	61.05	56.72	0.40	56.72	37.63
TOTAL	13.00	665.17	100.00	100.00	100.00	100.00	100.00	100.00	100.00	

CUMULATIVE RECOVERIES (%)	Time (Min)	Wt. (g)	Wt.%	Cu	S	Fe	C	Bo	Ma(C)	(Non Bo) Cu
	0	0	0	0	0	0	0	0	0	0
Conc.1	1.00	21.79	3.28	38.14	61.88	16.40	3.31	61.88	3.31	24.41
Conc.2	3.00	41.18	6.19	60.23	95.03	28.88	10.57	95.03	10.57	40.10
Conc.3	5.00	48.40	7.28	64.52	97.88	31.86	16.85	97.88	16.85	45.23
Conc.4	8.00	56.78	8.54	68.05	98.69	34.35	26.44	98.69	26.44	50.34
Conc.5	10.00	63.61	9.56	72.15	99.25	36.65	34.48	99.25	34.48	56.48
Conc.6	13.00	71.63	10.77	76.01	99.60	38.95	43.28	99.60	43.28	62.37
Tails	13.00	665.17	100.00	100.00	100.00	100.00	100.00	100.00	100.00	100.00

Table E.27: Flotation report for B7 of the Box-Behnken experiments.

TEST	B7																							
OBJECTIVE:	Box-Behnken Experiments								Feed:				Bornite -Malachite ore											
GRINDING CONDITIONS (Denver Mill):					FLOAT CONDITIONS:					FLOATED BY: SK & MD														
MILL TYPE:	Rod Mill	ROD TYPE/Charge :	As is		CELL TYPE & VOLUME:					2 L	GAS: Air													
CHARGE (g):	~680	65 % solids			IMPELLER RPM:					1200	REPULP WATER: tap													
WATER:	to level (2L)									by air valve														
GRIND:	12 min					# of STROKES: Ro:					30/min													
	ml/g	g/Ton	STAGE	COND	FLOAT	pH	Eh	OBSERVATIONS																
REAGENTS				TIME	TIME																			
Redox								7.78	230															
DETA (0.1%)	12	18								Froth very shallow with some white spots among the black														
KAXanthe (0.1 %)	0	0.0	Cond.																					
Cytec Hydroxamate	3 drp	34.0																						
Pine oil	1 drp	1.5			0.5																			
			Conc. 1			1	7.97																	
DETA (0.1%)	12	18								Blacker froth with slight greenish tinge.														
KAXanthe (0.1 %)	0	0.0	Cond.							Air was reduced due to high water level for 20s														
Cytec Hydroxamate	3 drp	34.0			0.5																			
Pine oil	1 drp	1.5																						
			Conc. 2			2	8.05																	
DETA (0.1%)	12	18								Froth still black/green														
KAXanthe (0.1 %)	0	0.0	Cond.							Barren froth at the end of flotation time														
Cytec Hydroxamate	3 drp	34.0			0.5					Concentrate appears very selective towards green particles														
Pine oil	1 drp	1.5																						
			Conc. 3			2																		
DETA (0.5%)	12	18								Very green !														
KAXanthe (0.1 %)	0	0.0	Cond.																					
Cytec Hydroxamate	3 drp	34.0			0.5																			
Pine oil	1 drp	1.5																						
			Conc. 4			3																		
DETA (0.5%)	12	18								Not much gangue coming														
KAXanthe (0.1 %)	0	0.0	Cond.							Still green														
Cytec Hydroxamate	3 drp	34.0			0.5																			
Pine oil	1 drp	1.5																						
			Conc. 5			3																		
DETA (0.5%)	12	18								Froth initially green														
KAXanthe (0.1 %)	0	0.0	Cond.							Increasingly white towards end of time														
Cytec Hydroxamate	3 drp	34.0			0.5																			
Pine oil	1 drp	1.5																						
			Conc. 6			4	8.29	300																

Table E.28: Flotation results spreadsheet for B7 of the Box-Behnken experiments.

GRADE										UNITS											
	Time (Min)	Wt. (g)	Wt.%	Cu	S	Fe	C	Bo	Ma(C)	(Non Bo) Cu	Cu	S	Fe	C	Bo	Ma(C)	(Non Bo-Ma) Cu				
Conc.1	1.00	7.24	1.08	48.84	22.6	9.34	0.486	55.98	5.14	13.40	52.51	24.30	10.04	0.52	60.2	5.5	14.4				
Conc.2	2.00	32.23	4.79	34.58	16.9	9.53	0.723	41.86	7.65	8.08	165.51	80.89	45.60	3.46	200.4	36.6	38.7				
Conc.3	2.00	14.39	2.14	33.88	5.39	6.26	2.28	13.35	24.14	25.43	72.41	11.52	13.38	4.87	28.5	51.6	54.3				
Conc.4	3.00	19.17	2.85	21.85	0.894	4.13	2.24	2.21	23.71	20.45	62.20	2.55	11.75	6.38	6.3	67.5	58.2				
Conc.5	2.00	11.35	1.69	13.67	0.464	4.00	1.46	1.149	15.45	12.94	23.04	0.78	6.74	2.46	1.9	26.1	21.8				
Conc.6	3.00	16	2.38	8.52	0.0177	3.61	1.17	0.044	12.39	8.50	20.26	0.04	8.59	2.78	0.1	29.4	20.2				
Tails	0.00	572.95	85.09	1.11	0.01	1.81	0.223	0.025	2.36	1.09	94.09	0.85	154.07	18.98	2.1	200.9	92.8				
Calc. Head	13.00	673.33	100.00	4.90	1.21	2.50	0.39	3.00	4.18	3.00	490.03	120.93	250.16	39.45	299.54	417.60	300.39				
CUMULATIVE GRADES (%)										CUMULATIVE UNITS											
	Time (Min)	Wt. (g)	Wt.%	Cu	S	Fe	C	Bo	Ma(C)	(Non Bo) Cu	Cu	S	Fe	C	Bo	Ma(C)	(Non Bo-Ma) Cu				
Conc.1	1.00	7.24	1.08	48.84	22.60	9.34	0.49	55.98	5.14	13.40	52.51	24.30	10.04	0.52	60.19	5.53	14.41				
Conc.2	3.00	39.47	5.86	37.19	17.95	9.49	0.68	44.45	7.19	9.05	218.02	105.20	55.64	3.98	260.56	42.17	53.06				
Conc.3	5.00	53.86	8.00	36.31	14.59	8.63	1.11	36.14	11.72	13.43	290.43	116.71	69.02	8.86	289.09	93.75	107.41				
Conc.4	8.00	73.03	10.85	32.51	11.00	7.45	1.40	27.24	14.87	15.27	352.63	119.26	80.77	15.23	295.39	161.25	165.62				
Conc.5	10.00	84.38	12.53	29.98	9.58	6.98	1.41	23.73	14.95	14.96	375.68	120.04	87.51	17.69	297.33	187.31	187.44				
Conc.6	13.00	100.38	14.91	26.56	8.05	6.45	1.37	19.95	14.54	13.93	395.93	120.08	96.09	20.47	297.44	216.74	207.63				
Tails	13.00	673.33	100.00	4.90	1.21	2.50	0.39	3.00	4.18	3.00	490.03	120.93	250.16	39.45	299.54	417.60	300.39				
RECOVERIES (%)										CUMULATIVE RECOVERIES (%)											
	Time (Min)	Wt. (g)	Wt.%	Cu	S	Fe	C	Bo	Ma(C)	(Non Bo) Cu	Time (Min)	Wt. (g)	Wt.%	Cu	S	Fe	C	Bo	Ma(C)	(Non Bo) Cu	
Conc.1	1.00	7.24	1.08	10.72	20.09	4.01	1.32	20.09	1.32	4.80	0	0	0	0	0	0	0	0	0		
Conc.2	2.00	32.23	4.79	33.78	66.89	18.23	8.77	66.89	8.77	12.87	Conc.1	1.00	7.24	1.08	10.72	20.09	4.01	1.32	20.09	1.32	4.80
Conc.3	2.00	14.39	2.14	14.78	9.53	5.35	12.35	9.53	12.35	18.09	Conc.2	3.00	39.47	5.86	44.49	86.99	22.24	10.10	86.99	10.10	17.66
Conc.4	3.00	19.17	2.85	12.69	2.10	4.70	16.17	2.10	16.17	19.38	Conc.3	5.00	53.86	8.00	59.27	96.51	27.59	22.45	96.51	22.45	35.76
Conc.5	2.00	11.35	1.69	4.70	0.65	2.69	6.24	0.65	6.24	7.26	Conc.4	8.00	73.03	10.85	71.96	98.61	32.29	38.61	98.61	38.61	55.14
Conc.6	3.00	16.00	2.38	4.13	0.03	3.43	7.05	0.03	7.05	6.72	Conc.5	10.00	84.38	12.53	76.66	99.26	34.98	44.85	99.26	44.85	62.40
Tails	0.00	572.95	85.09	19.20	0.70	61.59	48.10	0.70	48.10	30.88	Conc.6	13.00	100.38	14.91	80.80	99.30	38.41	51.90	99.30	51.90	69.12
TOTAL	13.00	673.33	100.00	100.00	100.00	100.00	100.00	100.00	100.00	100.00	Tails	13.00	673.33	100.00	100.00	100.00	100.00	100.00	100.00	100.00	

Table E.29: Flotation report for B8 of the Box-Behnken experiments.

TEST	B8									
OBJECTIVE:	Box-Behnken Experiments					Feed:	Bornite - Malachite ore			
GRINDING CONDITIONS (Denver Mill):					FLOAT CONDITIONS: FLOATED BY: SK & MD					
MILL TYPE:	Rod Mill	ROD TYPE/Charge :	As is		CELL TYPE & VOLUME: 2 L GAS: Air					
CHARGE (g):	~680	65 % solids			IMPELLER RPM:	1200	REPULP WATER:	tap		
WATER:	to level (2L)				by air valve					
GRIND:	12 min				# of STROKES: Ro:	30/min				
	ml/g	g/Ton	STAGE	COND	FLOAT	pH	Eh	OBSERVATIONS		
REAGENTS				TIME	TIME					
Redox						8.35	325			
DETA (0.1%)	12	18						Black particles		
KAXanthe (0.1 %)	8	12.0	Cond.	2						
Cytec Hydroxamate	3 drp	34.0								
Pine oil	1 drp	1.5			0.5					
			Conc. 1			1	8.69			
DETA (0.1%)	12	18								
KAXanthe (0.1 %)	8	12.0	Cond.	1						
Cytec Hydroxamate	3 drp	34.0								
Pine oil	1 drp	1.5			0.5					
			Conc. 2			2	8.36			
DETA (0.1%)	12	18								
KAXanthe (0.1 %)	8	12.0	Cond.	1						
Cytec Hydroxamate	3 drp	34.0								
Pine oil	1 drp	1.5			0.5					
			Conc. 3			2	8.54			
DETA (0.5%)	12	18								
KAXanthe (0.1 %)	8	12.0	Cond.	1						
Cytec Hydroxamate	3 drp	34.0								
Pine oil	1 drp	1.5			0.5					
			Conc. 4			3	8.62			
DETA (0.5%)	12	18								
KAXanthe (0.1 %)	8	12.0	Cond.	1						
Cytec Hydroxamate	3 drp	34.0								
Pine oil	1 drp	1.5			0.5					
			Conc. 5			3				
DETA (0.5%)	12	18						Flooding occured		
KAXanthe (0.1 %)	8	12.0	Cond.	1				Initially, collection was very selective		
Cytec Hydroxamate	3 drp	34.0						Only gangue collected.		
Pine oil	1 drp	1.5			0.5			NOTE : Suspected pH meter error		
			Conc. 6			4	8.65	280		

Table E.30: Flotation results spreadsheet for B8 of the Box-Behnken experiments.

GRADE										UNITS											
	Time (Min)	Wt. (g)	Wt.%	Cu	S	Fe	C	Bo	Ma(C)	(Non Bo) Cu	Cu	S	Fe	C	Bo	Ma(C)	(Non Bo-Ma) Cu				
Conc.1	1.00	28.07	4.17	52.84	19.4	10.96	0.4341	48.05	4.60	22.42	220.36	80.90	45.72	1.81	200.4	19.2	93.5				
Conc.2	2.00	19.36	2.88	32.77	9.26	7.72	1.48	22.94	15.67	18.25	94.26	26.63	22.21	4.26	66.0	45.1	52.5				
Conc.3	2.00	16.25	2.41	16.95	1.29	4.97	2.46	3.20	26.04	14.92	40.91	3.11	12.01	5.94	7.7	62.9	36.0				
Conc.4	3.00	20.68	3.07	16.76	0.439	4.27	1.8	1.09	19.05	16.07	51.48	1.35	13.11	5.53	3.3	58.5	49.4				
Conc.5	2.00	23.92	3.55	7.00	0.00174	3.81	1.24	0.004	13.13	6.99	24.87	0.01	13.53	4.41	0.0	46.6	24.9				
Conc.6	3.00	24.23	3.60	4.05	0.00692	4.16	0.987	0.017	10.45	4.04	14.59	0.02	14.96	3.55	0.1	37.6	14.5				
Tails	0.00	540.59	80.31	0.82	0.005	1.67	0.156	0.012	1.65	0.82	66.16	0.40	133.82	12.53	1.0	132.6	65.5				
Calc. Head	13.00	673.10	100.00	5.13	1.12	2.55	0.38	2.78	4.03	3.36	512.62	112.43	255.36	38.02	278.48	402.52	336.31				
CUMULATIVE GRADES (%)										CUMULATIVE UNITS											
Conc.1	1.00	28.07	4.17	52.84	19.40	10.96	0.43	48.05	4.60	22.42	220.36	80.90	45.72	1.81	200.39	19.16	93.49				
Conc.2	3.00	47.43	7.05	44.65	15.26	9.64	0.86	37.80	9.11	20.72	314.61	107.54	67.93	6.07	266.36	64.22	145.98				
Conc.3	5.00	63.68	9.46	37.58	11.70	8.45	1.27	28.97	13.43	19.24	355.52	110.65	79.94	12.01	274.07	127.09	182.01				
Conc.4	8.00	84.36	12.53	32.47	8.94	7.42	1.40	22.13	14.81	18.46	407.00	112.00	93.05	17.54	277.41	185.63	231.37				
Conc.5	10.00	108.28	16.09	26.85	6.96	6.63	1.36	17.25	14.44	15.93	431.87	112.01	106.59	21.94	277.43	232.28	256.23				
Conc.6	13.00	132.51	19.69	22.68	5.69	6.17	1.30	14.10	13.71	13.75	446.46	112.03	121.55	25.50	277.49	269.89	270.78				
Tails	13.00	673.10	100.00	5.13	1.12	2.55	0.38	2.78	4.03	3.36	512.62	112.43	255.36	38.02	278.48	402.52	336.31				
RECOVERIES (%)										CUMULATIVE RECOVERIES (%)											
Conc.1	1.00	28.07	4.17	42.99	71.96	17.90	4.76	71.96	4.76	27.80	Conc.1	1.00	28.07	4.17	42.99	71.96	17.90	4.76	71.96	4.76	27.80
Conc.2	2.00	19.36	2.88	18.39	23.69	8.70	11.19	23.69	11.19	15.61	Conc.2	3.00	47.43	7.05	61.37	95.65	26.60	15.96	95.65	15.96	43.41
Conc.3	2.00	16.25	2.41	7.98	2.77	4.70	15.62	2.77	15.62	10.71	Conc.3	5.00	63.68	9.46	69.35	98.42	31.30	31.57	98.42	31.57	54.12
Conc.4	3.00	20.68	3.07	10.04	1.20	5.13	14.54	1.20	14.54	14.68	Conc.4	8.00	84.36	12.53	79.40	99.62	36.44	46.12	99.62	46.12	68.80
Conc.5	2.00	23.92	3.55	4.85	0.01	5.30	11.59	0.01	11.59	7.39	Conc.5	10.00	108.28	16.09	84.25	99.62	41.74	57.71	99.62	57.71	76.19
Conc.6	3.00	24.23	3.60	2.85	0.02	5.86	9.34	0.02	9.34	4.33	Conc.6	13.00	132.51	19.69	87.09	99.64	47.60	67.05	99.64	67.05	80.51
Tails	0.00	540.59	80.31	12.91	0.36	52.40	32.95	0.36	32.95	19.49	Tails	13.00	673.10	100.00	100.00	100.00	100.00	100.00	100.00	100.00	100.00
TOTAL	13.00	673.10	100.00	100.00	100.00	100.00	100.00	100.00	100.00	100.00											

Table E.31: Flotation report for B9 of the Box-Behnken experiments.

TEST	B9											
OBJECTIVE:	Box-Behnken Experiments					Feed:	Bornite -Malachite ore					
GRINDING CONDITIONS (Denver Mill):					FLOAT CONDITIONS: FLOATED BY: SK & MD							
MILL TYPE:	Rod Mill	ROD TYPE/Charge :	As is			CELL TYPE & VOLUME:	2 L	GAS:	Air			
CHARGE (g):	~680	65 % solids				IMPELLER RPM:	1200	REPULP WATER:	tap			
WATER:	to level (2L)					by air valve						
GRIND:	12 min						# of STROKES: Ro:	30/min				
		ml/g	g/Ton	STAGE	COND	FLOAT	pH	Eh	OBSERVATIONS			
REAGENTS					TIME	TIME						
Redox							8.41	340				
DETA (0.1%)	0	0							Black particles			
KAXanthe (0.1 %)	4	6.0	Cond.		2							
Cytec Hydroxamate	0	0.0										
Pine oil	1 drp	1.5			0.5							
					Conc. 1		1	8.35				
DETA (0.1%)	0	0							Little frothing activity			
KAXanthe (0.1 %)	4	6.0	Cond.		1							
Cytec Hydroxamate	0	0.0										
Pine oil	1 drp	1.5			0.5							
					Conc. 2		2	8.43				
DETA (0.1%)	0	0							Black particles			
KAXanthe (0.1 %)	4	6.0	Cond.		1							
Cytec Hydroxamate	0	0.0										
Pine oil	1 drp	1.5			0.5							
					Conc. 3		2	8.39				
DETA (0.5%)	0	0							Black particles			
KAXanthe (0.1 %)	4	6.0	Cond.		1							
Cytec Hydroxamate	0	0.0										
Pine oil	1 drp	1.5			0.5							
					Conc. 4		3	8.42				
DETA (0.5%)	0	0							Black particles			
KAXanthe (0.1 %)	4	6.0	Cond.		1							
Cytec Hydroxamate	0	0.0										
Pine oil	1 drp	1.5			0.5							
					Conc. 5		3	8.37				
DETA (0.5%)	0	0							Black particles			
KAXanthe (0.1 %)	4	6.0	Cond.		1							
Cytec Hydroxamate	0	0.0										
Pine oil	1 drp	1.5			0.5				NOTE : Suspected pH meter error			
					Conc. 6		4	8.57	281			

Table E.32: Flotation results spreadsheet for B9 of the Box-Behnken experiments.

GRADE										UNITS											
	Time (Min)	Wt. (g)	Wt.%	Cu	S	Fe	C	Bo	Ma(C)	(Non Bo) Cu	Cu	S	Fe	C	Bo	Ma(C)	(Non Bo-Ma) Cu				
Conc.1	1.00	19.00	3.24	50.37	23	10.25	0.524	56.97	5.55	14.30	162.99	74.42	33.17	1.70	184.3	17.9	46.3				
Conc.2	2.00	16.8	2.86	44.05	17.9	10.09	0.499	44.34	5.28	15.98	126.03	51.21	28.87	1.43	126.9	15.1	45.7				
Conc.3	2.00	4.02	0.68	26.86	9.86	8.38	0.545	24.42	5.77	11.40	18.39	6.75	5.73	0.37	16.7	3.9	7.8				
Conc.4	3.00	3.1	0.53	13.62	4.41	5.71	0.656	10.92	6.94	6.71	7.19	2.33	3.01	0.35	5.8	3.7	3.5				
Conc.5	2.00	2.02	0.34	16.01	3.26	6.58	0.71	8.075	7.52	10.90	5.51	1.12	2.26	0.24	2.8	2.6	3.7				
Conc.6	3.00	2.79	0.48	13.35	1.75	5.85	0.898	4.335	9.51	10.60	6.34	0.83	2.78	0.43	2.1	4.5	5.0				
Tails	0.00	539.46	91.87	2.23	0.01	2.16	0.512	0.025	5.42	2.21	204.80	0.92	198.01	47.04	2.3	497.9	203.4				
Calc. Head	13.00	587.19	100.00	5.31	1.38	2.74	0.52	3.41	5.46	3.15	531.24	137.59	273.83	51.55	340.79	545.71	315.49				
CUMULATIVE GRADES (%)										CUMULATIVE UNITS											
	Time (Min)	Wt. (g)	Wt.%	Cu	S	Fe	C	Bo	Ma(C)	(Non Bo) Cu	Cu	S	Fe	C	Bo	Ma(C)	(Non Bo-Ma) Cu				
Conc.1	1.00	19.00	3.24	50.37	23.00	10.25	0.52	56.97	5.55	14.30	162.99	74.42	33.17	1.70	184.34	17.95	46.28				
Conc.2	3.00	35.80	6.10	47.40	20.61	10.18	0.51	51.04	5.42	15.09	289.01	125.64	62.04	3.12	311.19	33.06	92.00				
Conc.3	5.00	39.82	6.78	45.33	19.52	9.99	0.52	48.35	5.46	14.72	307.40	132.39	67.77	3.50	327.91	37.01	99.80				
Conc.4	8.00	42.92	7.31	43.04	18.43	9.68	0.53	45.65	5.57	14.14	314.59	134.71	70.78	3.84	333.67	40.68	103.34				
Conc.5	10.00	44.94	7.65	41.82	17.75	9.54	0.53	43.96	5.65	13.99	320.10	135.84	73.05	4.09	336.45	43.26	107.09				
Conc.6	13.00	47.73	8.13	40.16	16.81	9.33	0.56	41.64	5.88	13.79	326.44	136.67	75.83	4.51	338.51	47.78	112.13				
Tails	13.00	587.19	100.00	5.31	1.38	2.74	0.52	3.41	5.46	3.15	531.24	137.59	273.83	51.55	340.79	545.71	315.49				
RECOVERIES (%)										CUMULATIVE RECOVERIES (%)											
	Time (Min)	Wt. (g)	Wt.%	Cu	S	Fe	C	Bo	Ma(C)	(Non Bo) Cu	Time (Min)	Wt. (g)	Wt.%	Cu	S	Fe	C	Bo	Ma(C)	(Non Bo) Cu	
Conc.1	1.00	19.00	3.24	30.68	54.09	12.11	3.29	54.09	3.29	14.67	0	0	0	0	0	0	0	0	0		
Conc.2	2.00	16.80	2.86	23.72	37.22	10.54	2.77	37.22	2.77	14.49	Conc.1	1.00	19.00	3.24	30.68	54.09	12.11	3.29	54.09	3.29	14.67
Conc.3	2.00	4.02	0.68	3.46	4.91	2.09	0.72	4.91	0.72	2.47	Conc.2	3.00	35.80	6.10	54.40	91.31	22.65	6.06	91.31	6.06	29.16
Conc.4	3.00	3.10	0.53	1.35	1.69	1.10	0.67	1.69	0.67	1.12	Conc.3	5.00	39.82	6.78	57.87	96.22	24.75	6.78	96.22	6.78	31.63
Conc.5	2.00	2.02	0.34	1.04	0.82	0.83	0.47	0.82	0.47	1.19	Conc.4	8.00	42.92	7.31	59.22	97.91	25.85	7.45	97.91	7.45	32.76
Conc.6	3.00	2.79	0.48	1.19	0.60	1.02	0.83	0.60	0.83	1.60	Conc.5	10.00	44.94	7.65	60.26	98.73	26.68	7.93	98.73	7.93	33.95
Tails	0.00	539.46	91.87	38.55	0.67	72.31	91.24	0.67	91.24	64.46	Conc.6	13.00	47.73	8.13	61.45	99.33	27.69	8.76	99.33	8.76	35.54
TOTAL	13.00	587.19	100.00	100.00	100.00	100.00	100.00	100.00	100.00	100.00	Tails	13.00	587.19	100.00	100.00	100.00	100.00	100.00	100.00	100.00	

Table E.33: Flotation report for B10 of the Box-Behnken experiments.

TEST	B10												
OBJECTIVE:	Box-Behnken Experiments							Feed:	Bornite -Malachite ore				
GRINDING CONDITIONS (Denver Mill):				FLOAT CONDITIONS: FLOATED BY: SK & MD									
MILL TYPE:	Rod Mill	ROD TYPE/Charge :	As is		CELL TYPE & VOLUME:	2 L	GAS:	Air					
CHARGE (g):	~680	65 % solids			IMPELLER RPM:	1200	REPULP WATER:	tap					
WATER:	to level (2L)							by air valve					
GRIND:	12 min				# of STROKES: Ro:	30/min							
	ml/g	g/Ton	STAGE	COND	FLOAT	pH	Eh		OBSERVATIONS				
REAGENTS				TIME	TIME								
Redox						7.89	365						
DETA (0.1%)	0	0							Very black froth				
KAXanthe (0.1 %)	4	6.0	Cond.		2								
Cytec Hydroxamate	6 drp	68.0											
Pine oil	1 drp	1.5		0.5									
			Conc. 1			1	7.93						
DETA (0.1%)	0	0							Black froth with greenish tinge				
KAXanthe (0.1 %)	4	6.0	Cond.		1				Flooding tendency observed				
Cytec Hydroxamate	6 drp	68.0							Air was halved until half time to limit flooding.				
Pine oil	1 drp	1.5		0.5									
			Conc. 2			2	8						
DETA (0.1%)	0	0							Flooding again				
KAXanthe (0.1 %)	4	6.0	Cond.		1				Greenish-brown colour				
Cytec Hydroxamate	6 drp	68.0							Gangue activation				
Pine oil	1 drp	1.5		0.5									
			Conc. 3			2	7.9						
DETA (0.5%)	0	0							Less flooding				
KAXanthe (0.1 %)	4	6.0	Cond.		1				Barren froth at end of flotation				
Cytec Hydroxamate	6 drp	68.0											
Pine oil	1 drp	1.5		0.5									
			Conc. 4			3	8						
DETA (0.5%)	0	0											
KAXanthe (0.1 %)	4	6.0	Cond.		1								
Cytec Hydroxamate	6 drp	68.0											
Pine oil	1 drp	1.5		0.5									
			Conc. 5			3	8.07						
DETA (0.5%)	0	0											
KAXanthe (0.1 %)	4	6.0	Cond.		1								
Cytec Hydroxamate	6 drp	68.0											
Pine oil	1 drp	1.5		0.5									
			Conc. 6			4	8.16	244					

Table E.34: Flotation results spreadsheet for B10 of the Box-Behnken experiments.

GRADE										UNITS											
	Time (Min)	Wt. (g)	Wt.%	Cu	S	Fe	C	Bo	Ma(C)	(Non Bo) Cu	Cu	S	Fe	C	Bo	Ma(C)	(Non Bo-Ma) Cu				
Conc.1	1.00	17.92	2.66	50.22	20.6	9.96	0.617	51.02	6.53	17.92	133.83	54.90	26.55	1.64	136.0	17.4	47.7				
Conc.2	2.00	29.89	4.45	35.10	11.9	9.06	1.76	29.48	18.63	16.44	156.00	52.90	40.29	7.82	131.0	82.8	73.1				
Conc.3	2.00	14.3	2.13	15.40	2.94	6.17	2.38	7.28	25.19	10.79	32.76	6.25	13.12	5.06	15.5	53.6	23.0				
Conc.4	3.00	16.33	2.43	13.46	0.519	3.33	3.29	1.29	34.83	12.64	32.68	1.26	8.09	7.99	3.1	84.6	30.7				
Conc.5	2.00	16.12	2.40	8.37	0.318	4.04	1.25	0.788	13.23	7.87	20.07	0.76	9.69	3.00	1.9	31.7	18.9				
Conc.6	3.00	24.29	3.61	7.61	0.00187	4.37	1.12	0.005	11.86	7.60	27.48	0.01	15.78	4.05	0.0	42.8	27.5				
Tails	0.00	553.59	82.33	0.81	0.005	1.64	0.157	0.012	1.66	0.80	66.88	0.41	134.82	12.93	1.0	136.8	66.2				
Calc. Head	13.00	672.44	100.00	4.70	1.16	2.48	0.42	2.89	4.50	2.87	469.70	116.49	248.34	42.49	288.52	449.74	287.04				
CUMULATIVE GRADES (%)										CUMULATIVE UNITS											
	Time (Min)	Wt. (g)	Wt.%	Cu	S	Fe	C	Bo	Ma(C)	(Non Bo) Cu	Cu	S	Fe	C	Bo	Ma(C)	(Non Bo-Ma) Cu				
Conc.1	1.00	17.92	2.66	50.22	20.6	9.96	0.62	51.02	6.53	17.92	133.83	54.90	26.55	1.64	135.98	17.41	47.75				
Conc.2	3.00	47.81	7.11	40.76	15.16	9.40	1.33	37.55	14.10	16.99	289.83	107.79	66.84	9.47	266.99	100.22	120.80				
Conc.3	5.00	62.11	9.24	34.93	12.35	8.66	1.57	30.58	16.65	15.56	322.59	114.05	79.96	14.53	282.48	153.80	143.75				
Conc.4	8.00	78.44	11.66	30.46	9.88	7.55	1.93	24.48	20.43	14.96	355.27	115.31	88.05	22.52	285.60	238.37	174.46				
Conc.5	10.00	94.56	14.06	26.69	8.25	6.95	1.81	20.44	19.21	13.75	375.35	116.07	97.74	25.51	287.49	270.09	193.34				
Conc.6	13.00	118.85	17.67	22.79	6.57	6.42	1.67	16.27	17.70	12.49	402.82	116.07	113.52	29.56	287.51	312.92	220.80				
Tails	13.00	672.44	100.00	4.70	1.16	2.48	0.42	2.89	4.50	2.87	469.70	116.49	248.34	42.49	288.52	449.74	287.04				
RECOVERIES (%)										CUMULATIVE RECOVERIES (%)											
	Time (Min)	Wt. (g)	Wt.%	Cu	S	Fe	C	Bo	Ma(C)	(Non Bo) Cu	Time (Min)	Wt. (g)	Wt.%	Cu	S	Fe	C	Bo	Ma(C)	(Non Bo) Cu	
Conc.1	1.00	17.92	2.66	28.49	47.13	10.69	3.87	47.13	3.87	16.63	0	0	0	0	0	0	0	0	0		
Conc.2	2.00	29.89	4.45	33.21	45.41	16.22	18.41	45.41	18.41	25.45	Conc.1	1.00	17.92	2.66	28.49	47.13	10.69	3.87	47.13	3.87	16.63
Conc.3	2.00	14.3	2.13	6.97	5.37	5.28	11.91	5.37	11.91	8.00	Conc.2	3.00	47.81	7.11	61.71	92.54	26.91	22.28	92.54	22.28	42.09
Conc.4	3.00	16.33	2.43	6.96	1.08	3.26	18.81	1.08	18.81	10.70	Conc.3	5.00	62.11	9.24	68.68	97.90	32.20	34.20	97.90	34.20	50.08
Conc.5	2.00	16.12	2.40	4.27	0.65	3.90	7.05	0.65	7.05	6.58	Conc.4	8.00	78.44	11.66	75.64	98.99	35.46	53.00	98.99	53.00	60.78
Conc.6	3.00	24.29	3.61	5.85	0.01	6.35	9.52	0.01	9.52	9.57	Conc.5	10.00	94.56	14.06	79.91	99.64	39.36	60.06	99.64	60.06	67.36
Tails	0.00	553.59	82.33	14.24	0.35	54.29	30.42	0.35	30.42	23.08	Conc.6	13.00	118.85	17.67	85.76	99.65	45.71	69.58	99.65	69.58	76.92
TOTAL	13.00	672.44	100.00	100.00	100.00	100.00	100.00	100.00	100.00	100.00	Tails	13.00	672.44	100.00	100.00	100.00	100.00	100.00	100.00	100.00	

Table E.35: Flotation report for B11 of the Box-Behnken experiments.

TEST	B11							Feed:	Bornite -Malachite ore			
OBJECTIVE:	Box-Behnken Experiments							Feed:	Bornite -Malachite ore			
GRINDING CONDITIONS (Denver Mill):				FLOAT CONDITIONS: FLOATED BY: SK & MD								
MILL TYPE:	Rod Mill	ROD TYPE/Charge :	As is		CELL TYPE & VOLUME:			2 L	GAS:	Air		
CHARGE (g):	~680	65 % solids			IMPELLER RPM:	1200		REPULP WATER:	tap			
WATER:	to level (2L)				by air valve							
GRIND:	12 min					# of STROKES: Ro:	30/min					
	ml/g	g/Ton	STAGE	COND	FLOAT	pH	Eh	OBSERVATIONS				
REAGENTS				TIME	TIME							
Redox						8.34	370					
DETA (0.1%)	12	18						Poor frothing. Very thin froth with large bubbles				
KAXanthe (0.1 %)	4	6.0	Cond.	2								
Cytec Hydroxamate	0	0.0										
Pine oil	1 drp	1.5			0.5							
			Conc. 1			1	8.6					
DETA (0.1%)	12	18										
KAXanthe (0.1 %)	4	6.0	Cond.	1								
Cytec Hydroxamate	0	0.0										
Pine oil	1 drp	1.5			0.5							
			Conc. 2			2	8.5					
DETA (0.1%)	12	18										
KAXanthe (0.1 %)	4	6.0	Cond.	1								
Cytec Hydroxamate	0	0.0										
Pine oil	1 drp	1.5			0.5							
			Conc. 3			2	8.51					
DETA (0.5%)	12	18										
KAXanthe (0.1 %)	4	6.0	Cond.	1								
Cytec Hydroxamate	0	0.0										
Pine oil	1 drp	1.5			0.5							
			Conc. 4			3	8.53					
DETA (0.5%)	12	18										
KAXanthe (0.1 %)	4	6.0	Cond.	1								
Cytec Hydroxamate	0	0.0										
Pine oil	1 drp	1.5			0.5							
			Conc. 5			3	8.52					
DETA (0.5%)	12	18										
KAXanthe (0.1 %)	4	6.0	Cond.	1								
Cytec Hydroxamate	0	0.0										
Pine oil	1 drp	1.5			0.5							
			Conc. 6			4	8.48	277				
									NOTE: suspected pH meter error			

Table E.36: Flotation results spreadsheet for B11 of the Box-Behnken experiments.

GRADE											UNITS										
	Time (Min)	Wt. (g)	Wt.%	Cu	S	Fe	C	Bo	Ma(C)	(Non Bo) Cu	Cu	S	Fe	C	Bo	Ma(C)	(Non Bo-Ma) Cu				
Conc.1	1.00	16.73	2.51	55.90	24.2	11.46	0.502	59.94	5.31	17.95	140.27	60.73	28.77	1.26	150.4	13.3	45.0				
Conc.2	2.00	17.32	2.60	35.59	17.3	9.96	0.631	42.85	6.68	8.46	92.46	44.95	25.88	1.64	111.3	17.4	22.0				
Conc.3	2.00	6.06	0.91	28.03	8.92	9.09	0.701	22.09	7.42	14.04	25.48	8.11	8.27	0.64	20.1	6.7	12.8				
Conc.4	3.00	3.3	0.50	19.12	3.96	7.30	0.94	9.81	9.95	12.91	9.47	1.96	3.61	0.47	4.9	4.9	6.4				
Conc.5	2.00	2.26	0.34	9.15	2.12	5.38	1.16	5.251	12.28	5.82	3.10	0.72	1.83	0.39	1.8	4.2	2.0				
Conc.6	3.00	2.65	0.40	13.40	1.56	5.91	0.784	3.864	8.30	10.95	5.33	0.62	2.35	0.31	1.5	3.3	4.4				
Tails	0.00	618.33	92.75	2.40	0.01	2.28	0.416	0.025	4.40	2.38	222.53	0.93	211.10	38.58	2.3	408.4	221.1				
Calc. Head	13.00	666.65	100.00	4.99	1.18	2.82	0.43	2.92	4.58	3.14	498.63	118.01	281.80	43.29	292.31	458.27	313.57				
CUMULATIVE GRADES (%)											CUMULATIVE UNITS										
Conc.1	1.00	16.73	2.51	55.90	24.20	11.46	0.50	59.94	5.31	17.95	140.27	60.73	28.77	1.26	150.43	13.34	45.04				
Conc.2	3.00	34.05	5.11	45.57	20.69	10.70	0.57	51.25	6.01	13.12	232.73	105.68	54.65	2.90	261.75	30.69	67.01				
Conc.3	5.00	40.11	6.02	42.92	18.91	10.46	0.59	46.84	6.22	13.26	258.21	113.79	62.91	3.54	281.84	37.43	79.78				
Conc.4	8.00	43.41	6.51	41.11	17.78	10.22	0.61	44.03	6.51	13.23	267.68	115.75	66.52	4.00	286.69	42.36	86.17				
Conc.5	10.00	45.67	6.85	39.53	17.00	9.98	0.64	42.11	6.79	12.87	270.78	116.47	68.35	4.39	288.47	46.52	88.14				
Conc.6	13.00	48.32	7.25	38.09	16.15	9.75	0.65	40.01	6.87	12.76	276.10	117.09	70.70	4.71	290.01	49.82	92.50				
Tails	13.00	666.65	100.00	4.99	1.18	2.82	0.43	2.92	4.58	3.14	498.63	118.01	281.80	43.29	292.31	458.27	313.57				
RECOVERIES (%)											CUMULATIVE RECOVERIES (%)										
Conc.1	1.00	16.73	2.51	28.13	51.46	10.21	2.91	51.46	2.91	14.36	0	0	0	0	0	0	0				
Conc.2	2.00	17.32	2.60	18.54	38.09	9.18	3.79	38.09	3.79	7.01	Conc.1	1.00	16.73	2.51	28.13	51.46	10.21	2.91	51.46	2.91	14.36
Conc.3	2.00	6.06	0.91	5.11	6.87	2.93	1.47	6.87	1.47	4.07	Conc.2	3.00	34.05	5.11	46.67	89.55	19.39	6.70	89.55	6.70	21.37
Conc.4	3.00	3.30	0.50	1.90	1.66	1.28	1.07	1.66	1.07	2.04	Conc.3	5.00	40.11	6.02	51.78	96.42	22.32	8.17	96.42	8.17	25.44
Conc.5	2.00	2.26	0.34	0.62	0.61	0.65	0.91	0.61	0.91	0.63	Conc.4	8.00	43.41	6.51	53.68	98.08	23.61	9.24	98.08	9.24	27.48
Conc.6	3.00	2.65	0.40	1.07	0.53	0.83	0.72	0.53	0.72	1.39	Conc.5	10.00	45.67	6.85	54.30	98.69	24.25	10.15	98.69	10.15	28.11
Tails	0.00	618.33	92.75	44.63	0.79	74.91	89.13	0.79	89.13	70.50	Conc.6	13.00	48.32	7.25	55.37	99.21	25.09	10.87	99.21	10.87	29.50
TOTAL	13.00	666.65	100.00	100.00	100.00	100.00	100.00	100.00	100.00	100.00	Tails	13.00	666.65	100.00	100.00	100.00	100.00	100.00	100.00	100.00	

Table E.37: Flotation report for B12 of the Box-Behnken experiments.

TEST	B12						Feed:	Bornite -Malachite ore	
OBJECTIVE:	Box-Behnken Experiments						Feed:	Bornite -Malachite ore	
GRINDING CONDITIONS (Denver Mill):						FLOAT CONDITIONS: FLOATED BY: SK & MD			
MILL TYPE:	Rod Mill	ROD TYPE/Charge :	As is				CELL TYPE & VOLUME:	2 L	GAS: Air
CHARGE (g):	~680	65 % solids					IMPELLER RPM:	1200	REPULP WATER: tap
WATER:	to level (2L)								by air valve
GRIND:	12 min						# of STROKES: Ro:	30/min	
	ml/g	g/Ton	STAGE	COND	FLOAT	pH	Eh	OBSERVATIONS	
REAGENTS				TIME	TIME				
Redox						7.81	360		
DETA (0.1%)	12	18						No flooding occurring even with high hydroxamate dosage	
KAXanthe (0.1 %)	4	6.0	Cond.		2				
Cytec Hydroxamate	6 drps	68.0							
Pine oil	1 drp	1.5		0.5					
			Conc. 1			1	7.94		
DETA (0.1%)	12	18						Malachite highly visible	
KAXanthe (0.1 %)	4	6.0	Cond.		1			Fast flotation rate	
Cytec Hydroxamate	6 drps	68.0							
Pine oil	1 drp	1.5		0.5					
			Conc. 2			2	8.02		
DETA (0.1%)	12	18						Flooding begins and air was cut until 1 min	
KAXanthe (0.1 %)	4	6.0	Cond.		1				
Cytec Hydroxamate	6 drps	68.0							
Pine oil	1 drp	1.5		0.5					
			Conc. 3			2	8.08		
DETA (0.5%)	12	18						Deep froth visible	
KAXanthe (0.1 %)	4	6.0	Cond.		1				
Cytec Hydroxamate	6 drps	68.0							
Pine oil	1 drp	1.5		0.5					
			Conc. 4			3	8.17		
DETA (0.5%)	12	18						large mass recovery	
KAXanthe (0.1 %)	4	6.0	Cond.		1				
Cytec Hydroxamate	6 drps	68.0							
Pine oil	1 drp	1.5		0.5					
			Conc. 5			3	8.21		
DETA (0.5%)	12	18							
KAXanthe (0.1 %)	4	6.0	Cond.		1				
Cytec Hydroxamate	6 drps	68.0							
Pine oil	1 drp	1.5		0.5					
			Conc. 6			4	8.31	158	

Table E.38: Flotation results spreadsheet for B12 of the Box-Behnken experiments.

GRADE										UNITS											
	Time (Min)	Wt. (g)	Wt.%	Cu	S	Fe	C	Bo	Ma(C)	(Non Bo) Cu	Cu	S	Fe	C	Bo	Ma(C)	(Non Bo-Ma) Cu				
Conc.1	1.00	17.59	2.62	48.28	22	11.79	0.286	54.49	3.03	13.78	126.61	57.69	30.91	0.75	142.9	7.9	36.1				
Conc.2	2.00	39.72	5.92	18.60	8.74	7.56	1.54	21.65	16.30	4.90	110.15	51.75	44.76	9.12	128.2	96.5	29.0				
Conc.3	2.00	48.54	7.24	9.25	1.14	4.69	1.17	2.82	12.39	7.46	66.93	8.25	33.97	8.47	20.4	89.6	54.0				
Conc.4	3.00	68.74	10.25	4.14	0.03	3.40	0.477	0.09	5.05	4.09	42.48	0.36	34.84	4.89	0.9	51.7	41.9				
Conc.5	2.00	62.7	9.35	1.86	0.012	3.03	0.926	0.030	9.80	1.84	17.41	0.11	28.35	8.66	0.3	91.6	17.2				
Conc.6	3.00	50.55	7.54	1.43	0.01	2.49	0.716	0.025	7.58	1.41	10.74	0.08	18.76	5.40	0.2	57.1	10.6				
Tails	0.00	382.93	57.09	0.76	0.005	1.66	0.462	0.012	4.89	0.76	43.63	0.29	94.54	26.37	0.7	279.2	43.2				
Calc. Head	13.00	670.77	100.00	4.18	1.19	2.86	0.64	2.94	6.74	2.32	417.96	118.53	286.13	63.65	293.58	673.78	232.09				
CUMULATIVE GRADES (%)										CUMULATIVE UNITS											
	Time (Min)	Wt. (g)	Wt.%	Cu	S	Fe	C	Bo	Ma(C)	(Non Bo) Cu	Cu	S	Fe	C	Bo	Ma(C)	(Non Bo-Ma) Cu				
Conc.1	1.00	17.59	2.62	48.28	22.00	11.79	0.29	54.49	3.03	13.78	126.61	57.69	30.91	0.75	142.9	7.94	36.14				
Conc.2	3.00	57.31	8.54	27.71	12.81	8.86	1.16	31.73	12.23	7.62	236.76	109.45	75.67	9.87	271.09	104.47	65.13				
Conc.3	5.00	105.85	15.78	19.24	7.46	6.95	1.16	18.47	12.30	7.55	303.69	117.70	109.63	18.34	291.52	194.10	119.13				
Conc.4	8.00	174.59	26.03	13.30	4.54	5.55	0.89	11.23	9.45	6.19	346.17	118.05	144.47	23.22	292.40	245.84	161.05				
Conc.5	10.00	237.29	35.38	10.28	3.34	4.89	0.90	8.27	9.54	5.04	363.58	118.17	172.83	31.88	292.69	337.47	178.28				
Conc.6	13.00	287.84	42.91	8.72	2.76	4.46	0.87	6.82	9.20	4.40	374.32	118.24	191.59	37.28	292.87	394.59	188.91				
Tails	13.00	670.77	100.00	4.18	1.19	2.86	0.64	2.94	6.74	2.32	417.96	118.53	286.13	63.65	293.58	673.78	232.09				
RECOVERIES (%)										CUMULATIVE RECOVERIES (%)											
	Time (Min)	Wt. (g)	Wt.%	Cu	S	Fe	C	Bo	Ma(C)	(Non Bo) Cu	Time (Min)	Wt. (g)	Wt.%	Cu	S	Fe	C	Bo	Ma(C)	(Non Bo) Cu	
Conc.1	1.00	17.59	2.62	30.29	48.67	10.80	1.18	48.67	1.18	15.57	0	0	0	0	0	0	0	0	0		
Conc.2	2.00	39.72	5.92	26.35	43.66	15.64	14.33	43.66	14.33	12.49	Conc.1	1.00	17.59	2.62	30.29	48.67	10.80	1.18	48.67	1.18	15.57
Conc.3	2.00	48.54	7.24	16.01	6.96	11.87	13.30	6.96	13.30	23.27	Conc.2	3.00	57.31	8.54	56.65	92.34	26.44	15.51	92.34	15.51	28.06
Conc.4	3.00	68.74	10.25	10.16	0.30	12.18	7.68	0.30	7.68	18.06	Conc.3	5.00	105.85	15.78	72.66	99.30	38.31	28.81	99.30	28.81	51.33
Conc.5	2.00	62.70	9.35	4.17	0.10	9.91	13.60	0.10	13.60	7.43	Conc.4	8.00	174.59	26.03	82.82	99.60	50.49	36.49	99.60	36.49	69.39
Conc.6	3.00	50.55	7.54	2.57	0.06	6.56	8.48	0.06	8.48	4.58	Conc.5	10.00	237.29	35.38	86.99	99.70	60.40	50.09	99.70	50.09	76.82
Tails	0.00	382.93	57.09	10.44	0.24	33.04	41.44	0.24	41.44	18.61	Conc.6	13.00	287.84	42.91	89.56	99.76	66.96	58.56	99.76	58.56	81.39
TOTAL	13.00	670.77	100.00	100.00	100.00	100.00	100.00	100.00	100.00	100.00	Tails	13.00	670.77	100.00	100.00	100.00	100.00	100.00	100.00	100.00	

Table E.39: Flotation report for B13 of the Box-Behnken experiments.

TEST	B13														
OBJECTIVE:	Box-Behnken Experiments							Feed:	Bornite -Malachite ore						
GRINDING CONDITIONS (Denver Mill):				FLOAT CONDITIONS: FLOATED BY: SK & MD											
MILL TYPE:	Rod Mill	ROD TYPE/Charge :	As is		CELL TYPE & VOLUME:			2 L	GAS:	Air					
CHARGE (g):	~680	65 %	solids		IMPELLER RPM:			1200	REPULP WATER:	tap					
WATER:	to level (2L)				by air valve										
GRIND:	12 min					# of STROKES: Ro:			30/min						
		ml/g	g/Ton	STAGE	COND	FLOAT	pH	Eh	OBSERVATIONS						
REAGENTS					TIME	TIME									
Redox							8.3	320							
DETA (0.1%)	6	9													
KAXanthe (0.1 %)	4	6.0	Cond.		2										
Cytec Hydroxamate	3 drps	34.0													
Pine oil	1 drp	1.5			0.5										
				Conc. 1			1	8.43							
DETA (0.1%)	6	9													
KAXanthe (0.1 %)	4	6.0	Cond.		1										
Cytec Hydroxamate	3 drps	34.0													
Pine oil	1 drp	1.5			0.5										
				Conc. 2			2	8.53							
DETA (0.1%)	6	9													
KAXanthe (0.1 %)	4	6.0	Cond.		1										
Cytec Hydroxamate	3 drps	34.0													
Pine oil	1 drp	1.5			0.5										
				Conc. 3			2	8.37							
DETA (0.5%)	6	9													
KAXanthe (0.1 %)	4	6.0	Cond.		1										
Cytec Hydroxamate	3 drps	34.0													
Pine oil	1 drp	1.5			0.5										
				Conc. 4			3	8.34							
DETA (0.5%)	6	9													
KAXanthe (0.1 %)	4	6.0	Cond.		1										
Cytec Hydroxamate	3 drps	34.0													
Pine oil	1 drp	1.5			0.5										
				Conc. 5			3	8.4							
DETA (0.5%)	6	9													
KAXanthe (0.1 %)	4	6.0	Cond.		1										
Cytec Hydroxamate	3 drps	34.0													
Pine oil	1 drp	1.5			0.5										
				Conc. 6			4	8.55	307						

NOTE : suspected pH meter error

Table E.40: Flotation results spreadsheet for B13 of the Box-Behnken experiments.

GRADE										UNITS											
	Time (Min)	Wt. (g)	Wt.%	Cu	S	Fe	C	Bo	Ma(C)	(Non Bo) Cu	Cu	S	Fe	C	Bo	Ma(C)	(Non Bo-Ma) Cu				
Conc.1	1.00	24.73	3.69	46.43	21.5	10.54	0.465	53.25	4.92	12.72	171.22	79.28	38.88	1.71	196.4	18.2	46.9				
Conc.2	2.00	21.32	3.18	23.84	11.5	5.33	1.2	28.48	12.70	5.81	75.79	36.56	16.93	3.81	90.6	40.4	18.5				
Conc.3	2.00	11.29	1.68	22.18	2.47	5.53	2.48	6.12	26.25	18.31	37.34	4.16	9.30	4.17	10.3	44.2	30.8				
Conc.4	3.00	13.47	2.01	20.20	0.519	4.45	2.29	1.29	24.24	19.39	40.57	1.04	8.94	4.60	2.6	48.7	38.9				
Conc.5	2.00	19.12	2.85	9.95	0.318	3.28	1.92	0.788	20.32	9.45	28.37	0.91	9.35	5.47	2.2	57.9	26.9				
Conc.6	3.00	24.64	3.67	6.78	0.02	3.80	1.19	0.050	12.60	6.75	24.91	0.07	13.98	4.37	0.2	46.3	24.8				
Tails	0.00	556.08	82.92	0.94	0.01	1.62	0.215	0.025	2.28	0.92	77.78	0.83	134.03	17.83	2.1	188.7	76.5				
Calc. Head	13.00	670.65	100.00	4.56	1.23	2.31	0.42	3.04	4.44	2.63	455.98	122.85	231.40	41.98	304.28	444.35	263.33				
CUMULATIVE GRADES (%)										CUMULATIVE UNITS											
	Time (Min)	Wt. (g)	Wt.%	Cu	S	Fe	C	Bo	Ma(C)	(Non Bo) Cu	Cu	S	Fe	C	Bo	Ma(C)	(Non Bo-Ma) Cu				
Conc.1	1.00	24.73	3.69	46.43	21.50	10.54	0.47	53.25	4.92	12.72	171.22	79.28	38.88	1.71	196.37	18.15	46.90				
Conc.2	3.00	46.05	6.87	35.97	16.87	8.13	0.81	41.79	8.52	9.52	247.01	115.84	55.81	5.53	286.92	58.53	65.36				
Conc.3	5.00	57.34	8.55	33.26	14.03	7.62	1.14	34.76	12.01	11.25	284.35	120.00	65.11	9.70	297.22	102.73	96.18				
Conc.4	8.00	70.81	10.56	30.77	11.46	7.01	1.35	28.39	14.34	12.80	324.92	121.04	74.05	14.30	299.80	151.42	135.12				
Conc.5	10.00	89.93	13.41	26.35	9.09	6.22	1.47	22.53	15.61	12.09	353.29	121.95	83.40	19.78	302.05	209.36	162.06				
Conc.6	13.00	114.57	17.08	22.14	7.14	5.70	1.41	17.69	14.96	10.94	378.20	122.02	97.38	24.15	302.23	255.64	186.86				
Tails	13.00	670.65	100.00	4.56	1.23	2.31	0.42	3.04	4.44	2.63	455.98	122.85	231.40	41.98	304.28	444.35	263.33				
RECOVERIES (%)										CUMULATIVE RECOVERIES (%)											
	Time (Min)	Wt. (g)	Wt.%	Cu	S	Fe	C	Bo	Ma(C)	(Non Bo) Cu	Time (Min)	Wt. (g)	Wt.%	Cu	S	Fe	C	Bo	Ma(C)	(Non Bo) Cu	
Conc.1	1.00	24.73	3.69	37.55	64.54	16.80	4.08	64.54	4.08	17.81	0	0	0	0	0	0	0	0	0		
Conc.2	2.00	21.32	3.18	16.62	29.76	7.32	9.09	29.76	9.09	7.01	Conc.1	1.00	24.73	3.69	37.55	64.54	16.80	4.08	64.54	4.08	17.81
Conc.3	2.00	11.29	1.68	8.19	3.38	4.02	9.95	3.38	9.95	11.70	Conc.2	3.00	46.05	6.87	54.17	94.29	24.12	13.17	94.29	13.17	24.82
Conc.4	3.00	13.47	2.01	8.90	0.85	3.86	10.96	0.85	10.96	14.79	Conc.3	5.00	57.34	8.55	62.36	97.68	28.14	23.12	97.68	23.12	36.52
Conc.5	2.00	19.12	2.85	6.22	0.74	4.04	13.04	0.74	13.04	10.23	Conc.4	8.00	70.81	10.56	71.26	98.53	32.00	34.08	98.53	34.08	51.31
Conc.6	3.00	24.64	3.67	5.46	0.06	6.04	10.42	0.06	10.42	9.41	Conc.5	10.00	89.93	13.41	77.48	99.27	36.04	47.12	99.27	47.12	61.54
Tails	0.00	556.08	82.92	17.06	0.67	57.92	42.47	0.67	42.47	29.04	Conc.6	13.00	114.57	17.08	82.94	99.33	42.08	57.53	99.33	57.53	70.96
TOTAL	13.00	670.65	100.00	100.00	100.00	100.00	100.00	100.00	100.00	100.00	Tails	13.00	670.65	100.00	100.00	100.00	100.00	100.00	100.00	100.00	

Table E.41: Flotation report for B14 of the Box-Behnken experiments.

TEST	B14							Feed:	Bornite -Malachite ore	
OBJECTIVE:	Box-Behnken Experiments							Feed:	Bornite -Malachite ore	
GRINDING CONDITIONS (Denver Mill):				FLOAT CONDITIONS: FLOATED BY: SK & MD						
MILL TYPE:	Rod Mill	ROD TYPE/Charge :		As is	CELL TYPE & VOLUME:			2 L	GAS: Air	
CHARGE (g):	~680	65 % solids		IMPELLER RPM:			1200	REPULP WATER: tap		
WATER:	to level (2L)				by air valve					
GRIND:	12 min					# of STROKES: Ro:	30/min			
		ml/g	g/Ton	STAGE	COND	FLOAT	pH	Eh	OBSERVATIONS	
REAGENTS					TIME	TIME				
Redox							7.89	280		
DETA (0.1%)		6	9						Slightly black with greenish tinge	
KAXanthe (0.1 %)		4	6.0	Cond.	2					
Cytec Hydroxamate		3 drps	34.0							
Pine oil		1 drp	1.5		0.5					
				Conc. 1			1	7.97		
DETA (0.1%)		6	9						Green froth	
KAXanthe (0.1 %)		4	6.0	Cond.	1					
Cytec Hydroxamate		3 drps	34.0							
Pine oil		1 drp	1.5		0.5					
				Conc. 2			2			
DETA (0.1%)		6	9						Pale green froth	
KAXanthe (0.1 %)		4	6.0	Cond.	1					
Cytec Hydroxamate		3 drps	34.0							
Pine oil		1 drp	1.5		0.5					
				Conc. 3			2			
DETA (0.5%)		6	9						Concentrates appear muddy	
KAXanthe (0.1 %)		4	6.0	Cond.	1					
Cytec Hydroxamate		3 drps	34.0							
Pine oil		1 drp	1.5		0.5					
				Conc. 4			3	8.17		
DETA (0.5%)		6	9							
KAXanthe (0.1 %)		4	6.0	Cond.	1					
Cytec Hydroxamate		3 drps	34.0							
Pine oil		1 drp	1.5		0.5					
				Conc. 5			3	8.21		
DETA (0.5%)		6	9							
KAXanthe (0.1 %)		4	6.0	Cond.	1					
Cytec Hydroxamate		3 drps	34.0							
Pine oil		1 drp	1.5		0.5					
				Conc. 6			4	8.26	254	

Table E.42: Flotation results spreadsheet for B14 of the Box-Behnken experiments.

GRADE									
	Time (Min)	Wt. (g)	Wt.%	Cu	S	Fe	C	Bo	Ma(C) (Non Bo) Cu
Conc.1	1.00	18.68	2.79	43.52	22.65	9.93	0.43	56.10	4.50
Conc.2	2.00	24.69	3.69	26.11	13.45	6.43	1.15	33.31	12.12
Conc.3	2.00	11.32	1.69	18.66	3.07	5.12	2.34	7.60	24.72
Conc.4	3.00	11.91	1.78	19.53	0.73	4.46	2.47	1.81	26.15
Conc.5	2.00	13.10	1.96	13.10	0.51	3.94	2.06	1.272	21.75
Conc.6	3.00	16.08	2.40	12.50	0.28	4.03	1.84	0.690	19.42
Tails	0.00	573.75	85.70	1.23	0.01	1.76	0.34	0.025	3.64
Calc. Head	13.00	669.51	100.00	4.45	1.22	2.37	0.52	3.02	5.47
									2.54

CUMULATIVE GRADES (%)									
	Time (Min)	Wt. (g)	Wt.%	Cu	S	Fe	C	Bo	Ma(C) (Non Bo) Cu
Conc.1	1.00	18.68	2.79	43.52	22.65	9.93	0.43	56.10	4.50
Conc.2	3.00	43.37	6.48	33.61	17.41	7.94	0.83	43.13	8.84
Conc.3	5.00	54.69	8.17	30.52	14.44	7.35	1.15	35.77	12.13
Conc.4	8.00	66.59	9.95	28.55	11.99	6.84	1.38	29.70	14.63
Conc.5	10.00	79.69	11.90	26.01	10.11	6.36	1.49	25.03	15.80
Conc.6	13.00	95.76	14.30	23.74	8.46	5.97	1.55	20.94	16.41
Tails	13.00	669.51	100.00	4.45	1.22	2.37	0.52	3.02	5.47
									2.54

RECOVERIES (%)									
	Time (Min)	Wt. (g)	Wt.%	Cu	S	Fe	C	Bo	Ma(C) (Non Bo) Cu
Conc.1	1.00	18.68	2.79	27.26	51.87	11.70	2.30	51.87	2.30
Conc.2	2.00	24.69	3.69	21.63	40.72	10.02	8.17	40.72	8.17
Conc.3	2.00	11.32	1.69	7.09	4.26	3.66	7.64	4.26	7.64
Conc.4	3.00	11.91	1.78	7.80	1.06	3.35	8.50	1.06	8.50
Conc.5	2.00	13.10	1.96	5.75	0.82	3.26	7.78	0.82	7.78
Conc.6	3.00	16.08	2.40	6.74	0.55	4.09	8.53	0.55	8.53
Tails	0.00	573.75	85.70	23.73	0.70	63.91	57.07	0.70	57.07
TOTAL	13.00	669.51	100.00	100.00	100.00	100.00	100.00	100.00	100.00

UNITS						
Cu	S	Fe	C	Bo	Ma(C)	(Non Bo-Ma) Cu
121.39	63.18	27.69	1.19	156.5	12.5	22.3
96.30	49.60	23.71	4.22	122.9	44.7	18.5
31.55	5.19	8.66	3.95	12.9	41.8	23.4
34.73	1.30	7.94	4.39	3.2	46.5	32.7
25.62	1.00	7.71	4.02	2.5	42.5	24.0
30.01	0.67	9.68	4.41	1.7	46.6	29.0
105.64	0.86	151.21	29.48	2.1	312.1	104.3
445.25	121.80	236.60	51.65	301.68	546.78	254.26

CUMULATIVE UNITS						
Cu	S	Fe	C	Bo	Ma(C)	(Non Bo-Ma) Cu
121.39	63.18	27.69	1.19	156.49	12.55	22.32
217.70	112.78	51.40	5.41	279.35	57.25	40.84
249.25	117.97	60.06	9.36	292.20	99.04	64.25
283.98	119.27	68.00	13.75	295.41	145.53	96.95
309.60	120.27	75.70	17.77	297.90	188.08	121.00
339.61	120.94	85.38	22.17	299.56	234.72	149.96
445.25	121.80	236.60	51.65	301.68	546.78	254.26

CUMULATIVE RECOVERIES (%)									
	Time (Min)	Wt. (g)	Wt.%	Cu	S	Fe	C	Bo	Ma(C) (Non Bo) Cu
Conc.1	0	0	0	0	0	0	0	0	0
Conc.2	1.00	18.68	2.79	27.26	51.87	11.70	2.30	51.87	2.30
Conc.3	3.00	43.37	6.48	48.89	92.60	21.72	10.47	92.60	10.47
Conc.4	5.00	54.69	8.17	55.98	96.86	25.38	18.11	96.86	18.11
Conc.5	8.00	66.59	9.95	63.78	97.92	28.74	26.62	97.92	26.62
Conc.6	10.00	79.69	11.90	69.53	98.75	32.00	34.40	98.75	34.40
Tails	13.00	95.76	14.30	76.27	99.30	36.09	42.93	99.30	42.93
									58.98
									100.00

Table E.43: Flotation report for B15 of the Box-Behnken experiments.

TEST	B15							Feed:	Bornite -Malachite ore			
OBJECTIVE:	Box-Behnken Experiments							Feed:	Bornite -Malachite ore			
GRINDING CONDITIONS (Denver Mill):				FLOAT CONDITIONS: FLOATED BY: SK & MD								
MILL TYPE:	Rod Mill	ROD TYPE/Charge :		As is	CELL TYPE & VOLUME:			2 L	GAS:			
CHARGE (g):	~680	65 % solids			IMPELLER RPM:			1200	REPULP WATER:			
WATER:	to level (2L)						by air valve					
GRIND:	12 min					# of STROKES: Ro:	30/min					
		ml/g	g/Ton	STAGE	COND	FLOAT	pH	Eh	OBSERVATIONS			
REAGENTS					TIME	TIME						
Redox							8.6	321				
DETA (0.1%)	6	9							Impeller was not placed correctly for Conc 1-3			
KAXanthe (0.1 %)	4	6.0	Cond.		2							
Cytec Hydroxamate	3 drps	34.0										
Pine oil	1 drp	1.5			0.5							
				Conc. 1			1	8.8				
DETA (0.1%)	6	9										
KAXanthe (0.1 %)	4	6.0	Cond.		1							
Cytec Hydroxamate	3 drps	34.0										
Pine oil	1 drp	1.5			0.5							
				Conc. 2			2	8.55				
DETA (0.1%)	6	9							Impeller speed was too high, and was corrected			
KAXanthe (0.1 %)	4	6.0	Cond.		1							
Cytec Hydroxamate	3 drps	34.0										
Pine oil	1 drp	1.5			0.5							
				Conc. 3			2	8.52				
DETA (0.5%)	6	9										
KAXanthe (0.1 %)	4	6.0	Cond.		1							
Cytec Hydroxamate	3 drps	34.0										
Pine oil	1 drp	1.5			0.5							
				Conc. 4			3	8.61				
DETA (0.5%)	6	9										
KAXanthe (0.1 %)	4	6.0	Cond.		1							
Cytec Hydroxamate	3 drps	34.0										
Pine oil	1 drp	1.5			0.5							
				Conc. 5			3	8.64				
DETA (0.5%)	6	9										
KAXanthe (0.1 %)	4	6.0	Cond.		1				NOTE : suspected pH meter error			
Cytec Hydroxamate	3 drps	34.0										
Pine oil	1 drp	1.5			0.5							
				Conc. 6			4	8.76	239			

Table E.44: Flotation results spreadsheet for B15 of the Box-Behnken experiments.

GRADE	Time (Min)	Wt. (g)	Wt.%	Cu	S	Fe	C	Bo	Ma(C)	(Non Bo) Cu
Conc.1	1.00	19.47	2.92	37.26	20.5	8.15	0.527	50.78	5.58	5.12
Conc.2	2.00	25.72	3.86	40.19	12.8	9.87	1.1	31.70	11.64	20.12
Conc.3	2.00	9.24	1.39	15.24	1.94	5.50	2.2	4.81	23.29	12.20
Conc.4	3.00	6.53	0.98	17.02	0.798	3.46	2.63	1.98	27.84	15.77
Conc.5	2.00	12.04	1.81	20.23	0.0385	4.12	3.23	0.095	34.19	20.17
Conc.6	3.00	15.16	2.27	15.73	0.0108	4.30	2.27	0.027	24.03	15.71
Tails	0.00	578.56	86.78	0.97	0.01	1.96	0.36	0.025	3.81	0.95
Calc. Head	13.00	666.72	100.00	4.58	1.14	2.60	0.54	2.82	5.68	2.80

CUMULATIVE GRADES (%)										
	Time (Min)	Wt. (g)	Wt.%	Cu	S	Fe	C	Bo	Ma(C)	(Non Bo) Cu
Conc.1	1.00	19.47	2.92	37.26	20.50	8.15	0.53	50.78	5.58	5.12
Conc.2	3.00	45.19	6.78	38.93	16.12	9.13	0.85	39.92	9.03	13.66
Conc.3	5.00	54.43	8.16	34.91	13.71	8.51	1.08	33.96	11.45	13.41
Conc.4	8.00	60.96	9.14	32.99	12.33	7.97	1.25	30.53	13.21	13.66
Conc.5	10.00	73.00	10.95	30.89	10.30	7.34	1.57	25.51	16.67	14.74
Conc.6	13.00	88.16	13.22	28.28	8.53	6.81	1.69	21.13	17.93	14.90
Tails	13.00	666.72	100.00	4.58	1.14	2.60	0.54	2.82	5.68	2.80

RECOVERIES (%)										
	Time (Min)	Wt. (g)	Wt.%	Cu	S	Fe	C	Bo	Ma(C)	(Non Bo) Cu
Conc.1	1.00	19.47	2.92	23.76	52.66	9.14	2.87	52.66	2.87	5.34
Conc.2	2.00	25.72	3.86	33.85	43.44	14.63	7.91	43.44	7.91	27.74
Conc.3	2.00	9.24	1.39	4.61	2.37	2.93	5.68	2.37	5.68	6.04
Conc.4	3.00	6.53	0.98	3.64	0.69	1.30	4.80	0.69	4.80	5.52
Conc.5	2.00	12.04	1.81	7.97	0.06	2.86	10.87	0.06	10.87	13.02
Conc.6	3.00	15.16	2.27	7.81	0.02	3.75	9.62	0.02	9.62	12.77
Tails	0.00	578.56	86.78	18.36	0.76	65.39	58.24	0.76	58.24	29.58
TOTAL	13.00	666.72	100.00	100.00	100.00	100.00	100.00	100.00	100.00	100.00

UNITS						
Cu	S	Fe	C	Bo	Ma(C)	(Non Bo-Ma) Cu
108.82	59.87	23.79	1.54	148.3	16.3	14.9
155.05	49.38	38.08	4.24	122.3	44.9	77.6
21.13	2.69	7.62	3.05	6.7	32.3	16.9
16.67	0.78	3.39	2.58	1.9	27.3	15.4
36.53	0.07	7.43	5.83	0.2	61.7	36.4
35.76	0.02	9.77	5.16	0.1	54.6	35.7
84.12	0.87	170.25	31.24	2.1	330.7	82.8
458.08	113.68	260.34	53.64	281.56	567.83	279.82

CUMULATIVE UNITS						
Cu	S	Fe	C	Bo	Ma(C)	(Non Bo-Ma) Cu
108.82	59.87	23.79	1.54	148.28	16.29	14.94
263.88	109.24	61.88	5.78	270.59	61.21	92.57
285.00	111.93	69.50	8.83	277.25	93.49	109.48
301.67	112.71	72.89	11.41	279.18	120.75	124.92
338.20	112.78	80.33	17.24	279.35	182.50	161.34
373.96	112.81	90.09	22.40	279.41	237.14	197.06
458.08	113.68	260.34	53.64	281.56	567.83	279.82

CUMULATIVE RECOVERIES (%)										
	Time (Min)	Wt. (g)	Wt.%	Cu	S	Fe	C	Bo	Ma(C)	(Non Bo) Cu
	0	0	0	0	0	0	0	0	0	0
Conc.1	1.00	19.47	2.92	23.76	52.66	9.14	2.87	52.66	2.87	5.34
Conc.2	3.00	45.19	6.78	57.60	96.10	23.77	10.78	96.10	10.78	33.08
Conc.3	5.00	54.43	8.16	62.22	98.47	26.70	16.46	98.47	16.46	39.12
Conc.4	8.00	60.96	9.14	65.86	99.15	28.00	21.27	99.15	21.27	44.64
Conc.5	10.00	73.00	10.95	73.83	99.22	30.85	32.14	99.22	32.14	57.66
Conc.6	13.00	88.16	13.22	81.64	99.24	34.61	41.76	99.24	41.76	70.42
Tails	13.00	666.72	100.00	100.00	100.00	100.00	100.00	100.00	100.00	100.00

Table E.45: Flotation report for BZ1 investigation of N-benzoyl.

TEST	BZ1									
OBJECTIVE:	N-Benzoyl Investigation					Feed:	Bornite -Malachite ore			
GRINDING CONDITIONS (Denver Mill):					FLOAT CONDITIONS:	FLOATED BY: SK & MD				
MILL TYPE:	Rod Mill	ROD TYPE/Charge :	As is			CELL TYPE & VOLUME:	2 L	GAS:	Air	
CHARGE (g):	680 g	65 % solids				IMPELLER RPM:	1200	REPULP WATER:	tap	
WATER:	to level (2L)					by air valve				
GRIND:	10 min				# of STROKES: Ro:	30/min				
		ml/g	g/Ton	STAGE	COND	FLOAT	pH	Eh	OBSERVATIONS	
REAGENTS					TIME	TIME				
Redox							7.89	259		
DETA (0.1%)	0	0							Not many particles being collected	
KAXanthe (0.1%)	8	12.0	Cond.		2				Only bornite	
N-Benzoyl	0.029g	34.0								
Pine oil	1	1.5			0.5					
			Conc. 1			1				
DETA (0.1%)	0	0							Very little bornite	
KAXanthe (0.1%)	8	12.0	Cond.		1				Poor frothing	
N-Benzoyl	0.029g	34.0								
Pine oil	1	1.5			0.5					
			Conc. 2			2				
DETA (0.1%)	0	0								
KAXanthe (0.1%)	8	12.0	Cond.		1					
N-Benzoyl	0.029g	34.0								
Pine oil	1	1.5			0.5					
			Conc. 3			2				
DETA (0.1%)	0	0								
KAXanthe (0.1%)	8	12.0	Cond.		1					
N-Benzoyl	0.029g	34.0								
Pine oil	1	1.5			0.5					
			Conc. 4			3				
DETA (0.1%)	0	0							Nothing coming...	
KAXanthe (0.1%)	8	12.0	Cond.		1					
N-Benzoyl	0.029g	34.0								
Pine oil	1	1.5			0.5					
			Conc. 5			3				
DETA (0.1%)	0	0							Very little was recovered.	
KAXanthe (0.1%)	8	12.0	Cond.		1					
N-Benzoyl	0.029g	34.0							Poor solubility ?	
Pine oil	1	1.5			0.5					
			Conc. 6			4	8.25	236	Very similar to collectorless test.	

Table E.46: Flotation results spreadsheet for BZ1 of the N-benzoyl investigation.

AA	Cu (%)		Fe (%)		UNITS		CUMULATIVE UNITS			
	Cu	Fe	Cu	Fe	S	C	Cu	Fe	S	C
Conc.1	57.53	11.14			117.95	22.84				
Conc.2	52.86	10.77			113.55	23.13				
Conc.3	43.31	11.11			23.58	6.05				
Conc.4	38.11	9.03			16.05	3.80				
Conc.5	26.40	7.16			8.97	2.43				
Conc.6	13.43	3.70			5.19	1.43				
Tails	2.53	2.07			238.12	194.82				
					523.43	254.51				

GRADE	Time (Min)	Wt. (g)	Wt.%	Cu	S	Fe	C	RECOVERIES (%)			
								Cu	S	Fe	C
Conc.1	1.00	13.63	2.05	57.53		11.14		Conc.1	22.53		8.98
Conc.2	2.00	14.28	2.15	52.86		10.77		Conc.2	21.69		9.09
Conc.3	2.00	3.62	0.54	43.31		11.11		Conc.3	4.51		2.38
Conc.4	3.00	2.8	0.42	38.11		9.03		Conc.4	3.07		1.49
Conc.5	3.00	2.26	0.34	26.40		7.16		Conc.5	1.71		0.96
Conc.6	4.00	2.57	0.39	13.43		3.70		Conc.6	0.99		0.56
Tails	0.00	625.66	94.11	2.53		2.07		Tails	45.49		76.55
Calc. Head	15.00	664.82	100.00	5.23		2.55		TOTAL	100.00		100.00

CUMULATIVE GRADES (%)					CUMULATIVE RECOVERIES (%)				
Wt. (%)	Cu	S	Fe	C	Cu	S	Fe	C	
	0	0	0	0					
Conc.1	2.05	57.532	11.143		Conc.1	22.53		8.98	
Conc.2	4.20	55.144	10.952		Conc.2	44.23		18.07	
Conc.3	4.74	53.786	10.970		Conc.3	48.73		20.44	
Conc.4	5.16	52.507	10.812		Conc.4	51.80		21.94	
Conc.5	5.50	50.895	10.586		Conc.5	53.52		22.89	
Conc.6	5.89	48.436	10.134		Conc.6	54.51		23.45	
Tails	100.00	5.234	2.545		Tails	100.00		100.00	

Table E.47: Flotation report for BZ2 of the N-Benzoyl investigation.

TEST	BZ2				FLOAT	pH	Eh	OBSERVATIONS		
OBJECTIVE:	N-Benzoyl Investigation				Feed:	Bornite -Malachite ore				
GRINDING CONDITIONS (Denver Mill):					FLOAT CONDITIONS:	FLOATED BY: SK & MD				
MILL TYPE:	Rod Mill	ROD TYPE/Charge :	As is		CELL TYPE & VOLUME:	2 L	GAS:	Air		
CHARGE (g):	680 g	65 % solids			IMPELLER RPM:	1200	REPULP WATER:	tap		
WATER:	to level (2L)				by air valve					
GRIND:	10 min					# of STROKES: Ro:	30/min			
	ml/g	g/Ton	STAGE	COND	FLOAT	pH	Eh	OBSERVATIONS		
REAGENTS			TIME		TIME					
Redox						7.84	310			
DETA (0.1%)	0	0						N-Benzoyl added in liquid form.		
KAXanthe (0.1%)	4	35.0	Cond.	2						
N-Benzoyl	0.58g	68.0								
Pine oil	1	1.5		0.5						
			Conc. 1			1				
DETA (0.1%)	0	0						Some bornite coming		
KAXanthe (0.1%)	4	35.0	Cond.	1						
N-Benzoyl	0.58g	68.0								
Pine oil	1	1.5		0.5						
			Conc. 2			2				
DETA (0.1%)	0	0						No malachite visible		
KAXanthe (0.1%)	4	35.0	Cond.	1						
N-Benzoyl	0.58g	68.0								
Pine oil	1	1.5		0.5						
			Conc. 3			2				
DETA (0.1%)	0	0						Slimes beginning to report to conc.		
KAXanthe (0.1%)	4	35.0	Cond.	1						
N-Benzoyl	0.58g	68.0								
Pine oil	1	1.5		0.5						
			Conc. 4			3				
DETA (0.1%)	0	0						More slimes.		
KAXanthe (0.1%)	4	35.0	Cond.	1						
N-Benzoyl	0.58g	68.0								
Pine oil	1	1.5		0.5						
			Conc. 5			3				
DETA (0.1%)	0	0						Even solubility didn't help recovery.		
KAXanthe (0.1%)	4	35.0	Cond.	1				Active towards slime/gangue		
N-Benzoyl	0.58g	68.0								
Pine oil	1	1.5		0.5						
			Conc. 6		4	8.16	274			
								Malachite responds !		
KAXanthe (0.1%)	0	0.0	Cond.	1				Very green		
Cytec Hydroxamate	3	34.0								
Pine oil	1	1.5	14.7	0.5						
			Conc. 7			3		More malachite		
KAXanthe (0.1%)	0	0.0	Cond.	1						
Cytec Hydroxamate	3	34.0								
Pine oil	1	1.5		0.5						
			Conc. 8			3				
KAXanthe (0.1%)	0	0.0	Cond.	1				Malachite still coming.		
Cytec Hydroxamate	3	34.0								
Pine oil	1	1.5		0.5						
			Conc. 9			3				

Table E.48: Flotation results spreadsheet for BZ2 of the N-Benzoyl investigation.

AA		UNITS				CUMULATIVE UNITS							
	Cu (%)	Fe (%)			Cu	Fe	S	C	Cu	Fe	S	C	
Conc.1	53.33	11.30			79.30	16.80			79.30	16.80			
Conc.2	48.24	50.04			88.13	31.41			167.42	108.21			
Conc.3	39.11	9.27			18.79	4.45			186.21	112.66			
Conc.4	27.93	8.11			10.73	3.11			196.94	115.78			
Conc.5	31.63	8.66			10.52	2.88			207.46	118.66			
Conc.6	31.80	9.44			23.36	6.93			230.83	125.59			
Conc.7	26.74	6.39			79.04	18.88			309.87	144.47			
Conc.8	9.12	3.16			48.56	16.82			358.42	161.29			
Conc.9	16.30	4.17			31.08	7.96			510.58	343.67			
Tails	1.43	2.06			121.08	174.42							
					510.58	343.67							
GRADE		RECOVERIES (%)				Cu S Fe C							
Time (Min)	Wt. (g)	Wt. %	Cu	S	Fe	C							
Conc.1	1.00	10.06	1.49	53.33		11.30	Conc.1	15.53		4.89			
Conc.2	2.00	12.36	1.83	48.24		50.04	Conc.2	17.26		26.60			
Conc.3	2.00	3.25	0.48	39.11		9.27	Conc.3	3.68		1.30			
Conc.4	3.00	2.6	0.38	27.93		8.11	Conc.4	2.10		0.91			
Conc.5	3.00	2.25	0.33	31.63		8.66	Conc.5	2.06		0.84			
Conc.6	4.00	4.97	0.73	31.80		9.44	Conc.6	4.58		2.02			
Conc.7	2.00	20	2.96	26.74		6.39	Conc.7	15.48		5.49			
Conc.8	2.00	36.02	5.32	9.12		3.16	Conc.8	9.51		4.89			
Conc.9	2.00	12.9	1.91	16.30		4.17	Conc.9	6.09		2.32			
Tails	0.00	572.17	84.57	1.43		2.06	Tails	23.71		50.75			
Calc. Head	21.00	676.58	100.00	5.11		3.44	TOTAL	100.00		100.00			
CUMULATIVE GRADES (%)		CUMULATIVE RECOVERIES (%)				Cu S Fe C							
	Wt. (%)	Cu	S	Fe	C								
Conc.1	1.49	53.331		11.301		Conc.1	15.53		4.89				
Conc.2	3.31	50.525		32.655		Conc.2	32.79		31.449				
Conc.3	3.79	49.079		29.694		Conc.3	36.47		32.78				
Conc.4	4.18	47.134		27.709		Conc.4	38.57		33.69				
Conc.5	4.51	45.991		26.304		Conc.5	40.63		34.53				
Conc.6	5.25	44.004		23.943		Conc.6	45.21		36.54				
Conc.7	8.20	37.781		17.615		Conc.7	60.69		42.04				
Conc.8	13.53	26.500		11.925		Conc.8	70.20		46.93				
Conc.9	15.43	33.086		22.270		Conc.9	76.29		49.25				
Tails	100.00	5.106		3.437		Tails	100.00		100.00				

Sample Calculations for Flotation Results :

This sample calculation is performed for test B1 of the Box-Behnken experiments. The calculations for the other flotation result reports are performed in the same fashion. To perform these calculations the following are required: concentrate weights; Cu and Fe metal assays; and the S and C assays.

Calculate weight percent for concentrate and tails:

$$\begin{aligned}\text{Wt \% (Conc 1)} &= (\text{Concentrate 1})\text{g} / (\text{Total weight})\text{g} \\ &= 2.98 \text{ g} / 669.44 \text{ g} = 0.45 \%\end{aligned}$$

This calculation is performed for each concentrate.

Calculate malachite and bornite grades:

$$\begin{aligned}\text{Grade (Malachite)} &= (\text{Carbon assay}) \times (\% \text{ C in Malachite}) \\ &= (0.419) \times (10.5856) = 4.44 \% \text{ Mal} \\ \text{Grade (Bornite)} &= (\text{Sulphur assay}) \times (\% \text{ S in Bornite}) \\ &= (23.6) \times (2.4769) = 58.45 \% \text{ Bornite}\end{aligned}$$

This calculation is performed for each concentrate.

Calculate metal and mineral units and cumulative units for each concentrate:

$$\begin{aligned}\text{Units (Metal)} &= (\text{Wt \%}) \times (\text{Metal Assay}) \\ &= (0.45 \%) \times (42.47\%) = 18.90 \text{ Cu units for Conc 1} \\ \text{Units (Mineral)} &= (\text{Wt \%}) \times (\text{Mineral Assay}) \\ &= (0.45 \%) \times (58.45 \% \text{ Bo}) = 26 \text{ Bo units for Conc 1}\end{aligned}$$

This calculation is performed for each concentrate for Cu, Fe, Ma and Bo. The cumulative metal units are also calculated.

Calculate metal and mineral grades for each concentrate

$$\begin{aligned}\text{Grade (\%)} &= (\text{Unit}) / \text{Wt \%} \\ &= (18.9) / (0.45) = 42.47 \% \text{ Cu for Conc 1}\end{aligned}$$

This calculation is repeated for each concentrate for Cu, Fe, Ma and Bo. The cumulative grades are also calculated.

$$\begin{aligned}\text{Head Grade (\%)} &= (\Sigma \text{ Units Conc 1- Tails}) / 100 \\ &= 497.44 / 100 = 4.97 \% \text{ Cu}\end{aligned}$$

$$\begin{aligned}\text{Final Cumulative Grade (\%)} &= (\text{Cumulative Units 1-6}) / \text{Wt \%} \\ &= (55.72) / (1.80) = 30.91 \% \text{ Cu}\end{aligned}$$

This calculation is performed for Cu, Fe, Ma, and Bo.

Calculate metal and mineral recoveries:

$$\begin{aligned}\text{Recovery} &= (\text{Concentrate Unit}) \times 100 / (\Sigma \text{ Units}) \\ &= (18.90) \times 100 / 497.44 = 3.80 \% \text{ Cu}\end{aligned}$$

This calculation is performed for each concentrate for Cu, Fe, Ma and Bo.

Final Cumulative Recovery (%) = (Σ Concentrate Recoveries)